Internationa Advanced School on Space Weather Modelling and Applications

18-29 October 2010 ICTP, Trieste, IT

DIRECT EFFECTS OF SOLAR RADIO WEATHER

M. MESSEROTTI[1,2,3]

[1] *INAF-Astronomical Observatory of Trieste, IT*

[2] *Department of Physics, University of Trieste, IT*

[3] *National Institute for Nuclear Physics, Trieste Division, IT*

SCHEME OF THE TALK

- DEFINING THE TERMINOLOGY
- EFFECTS ON GPS AND RADIO COMMUNICATIONS
- INTRODUCTION TO SOLAR RADIO ASTRONOMY
- SOLAR RFI OBSERVATION AND INTERPRETATION
- CONCLUSIONS

DIRECT EFFECTS OF SOLAR RADIO WEATHER

DEFINING THE TERMINOLOGY

SOLAR RADIO WEATHER

- THE SUN IS A SOURCE OF BROAD- AND NARROW-BAND RADIO EMISSIONS GENERATED BY COHERENT AND INCOHERENT PROCESSES

- SUCH RADIO EMISSION CAN INCREASE BY SEVERAL ORDERS OF MAGNITUDE UNDER PERTURBED SOLAR CONDITIONS

- **SOLAR RADIO WEATHER** REFERS TO THE PHYSICAL STATE OF THE SUN AS AN ENSAMBLE OF RADIO SOURCES

DIRECT EFFECTS OF SOLAR RADIO WEATHER

- SOLAR RADIO WEATHER SPANS FROM QUIET TO HIGHLY PERTURBED CONDITIONS, ACCORDING TO THE ORIGINATED LEVEL OF SOLAR RADIO NOISE
- TIME OF FLIGHT OF SOLAR EM EMISSIONS TO THE EARTH IS 8.3 MINUTES
- RADIO COMMUNICATION SYSTEMS (E.G. SATELLITE-BASED LOCALISATION, AVIATION, AND MOBILE COMMUNICATION SYSTEMS) ARE DIRECTLY INTERFERED UNDER SPECIFIC CONDITIONS WITH NO INTERMEDIATE PROCESS AND/OR AGENT

DIRECT EFFECTS OF SOLAR RADIO WEATHER

CHARACTERISTICS OF GPS SERVICES

Adapted from P.M. Kintner (Cornell University, USA; 2008)

STANDARD POSITIONING SERVICE

- POSITIONING AND TIMING SERVICE
- AVAILABLE ON A CONTINUOUS WORLDWIDE BASIS WITH NO CHARGE
- GPS L1 FREQUENCY (1.57542 GHz)
  1. **COARSE ACQUISITION** (C/A) CODE
  2. NAVIGATION DATA MESSAGE
- PREDICTABLE POSITION ACCURACY
  - 100 m (95%) HORIZONTALLY
  - 156 m (95%) VERTICALLY
- TIME TRANSFER ACCURACY TO UTC WITHIN 340 ns (95%)

PRECISE POSITIONING SERVICE

- HIGHLY ACCURATE MILITARY POSITIONING, VELOCITY AND TIMING SERVICE
- AVAILABLE ON A CONTINUOUS, WORLDWIDE BASIS TO U.S.-AUTHORISED USERS
- GPS L1 (1.57542 GHz) AND L2 (1.57542 GHz)
  - **P(Y)** CODE WITH ENCRYPTION
- PREDICTABLE POSITION ACCURACY
  - 22 m (95%) HORIZONTALLY
  - 27.7 m (95%) VERTICALLY
- TIME TRANSFER ACCURACY TO UTC WITHIN 200 ns (95%)

THE GPS SATELLITE CONSTELLATION

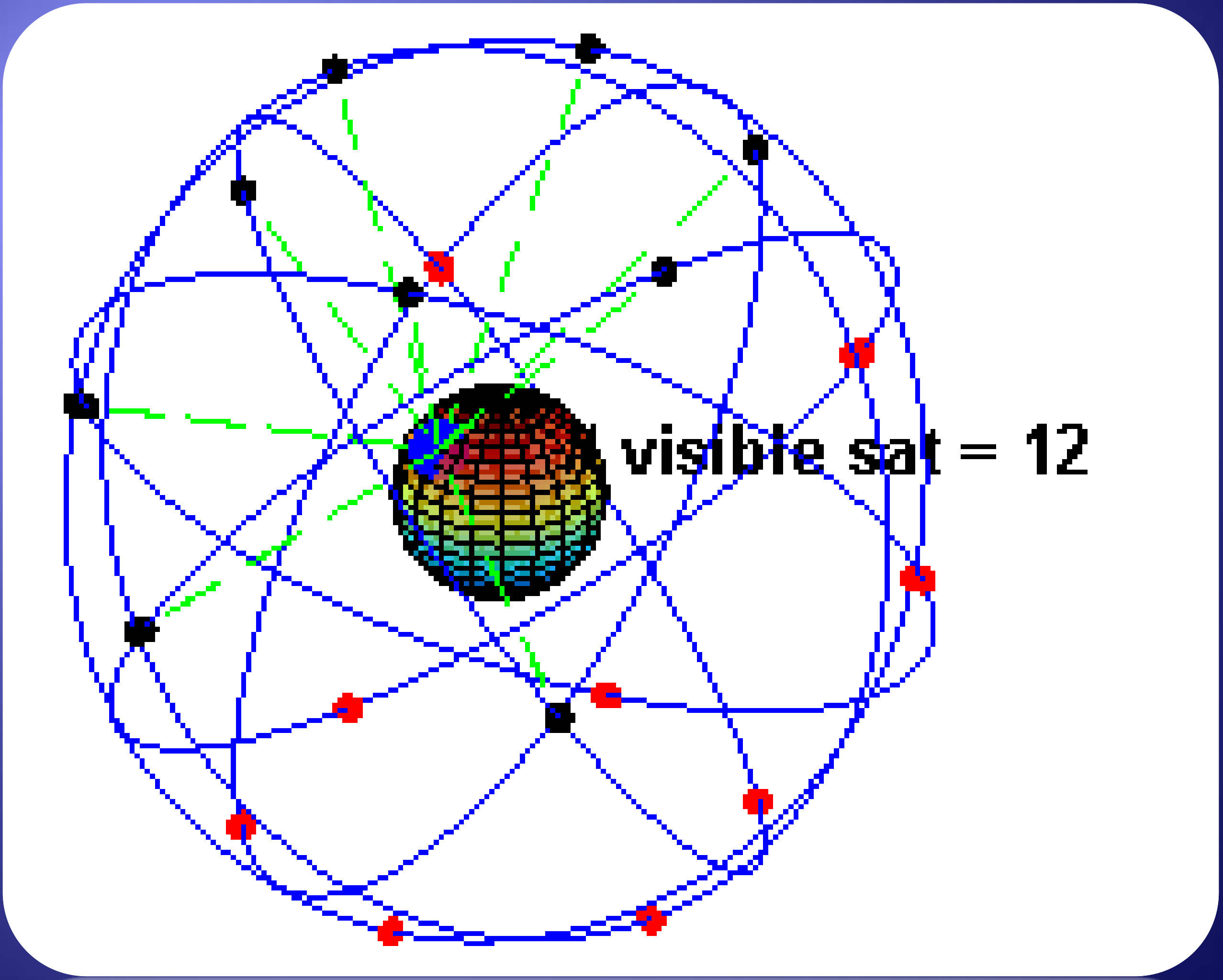

DIRECT EFFECTS OF SOLAR RADIO WEATHER

EFFECT OF SOLAR RADIO WEATHER ON GPS

RADIO QUIET SUN

- **VERY LOW SOLAR RADIO EMISSION LEVEL**
- GPS RADIO SIGNAL FROM SATELLITES
- **HIGH SIGNAL-TO-NOISE RATIO @ RECEIVER**
- <u>STANDARD POSITION ACCURACY</u>

RADIO ACTIVE SUN

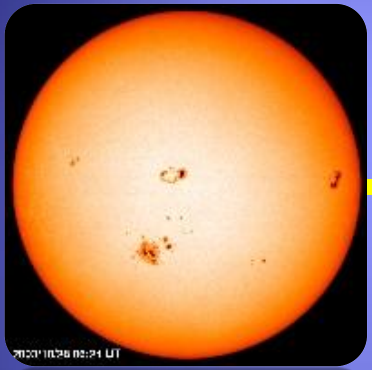

- **VERY HIGH SOLAR RADIO EMISSION LEVEL**
- GPS RADIO SIGNAL FROM SATELLITES
- **LOW SIGNAL-TO-NOISE RATIO @ RECEIVER**
- <u>HIGH POSITION ERROR TO TOTAL LOSS OF LOCK</u>
- <u>ALL SUNLIT EARTH HEMISPHERE AFFECTED</u>

DIRECT EFFECTS OF SOLAR RADIO WEATHER

EFFECT OF SOLAR RADIO WEATHER ON MOBILE COMMUNICATIONS

RADIO QUIET SUN

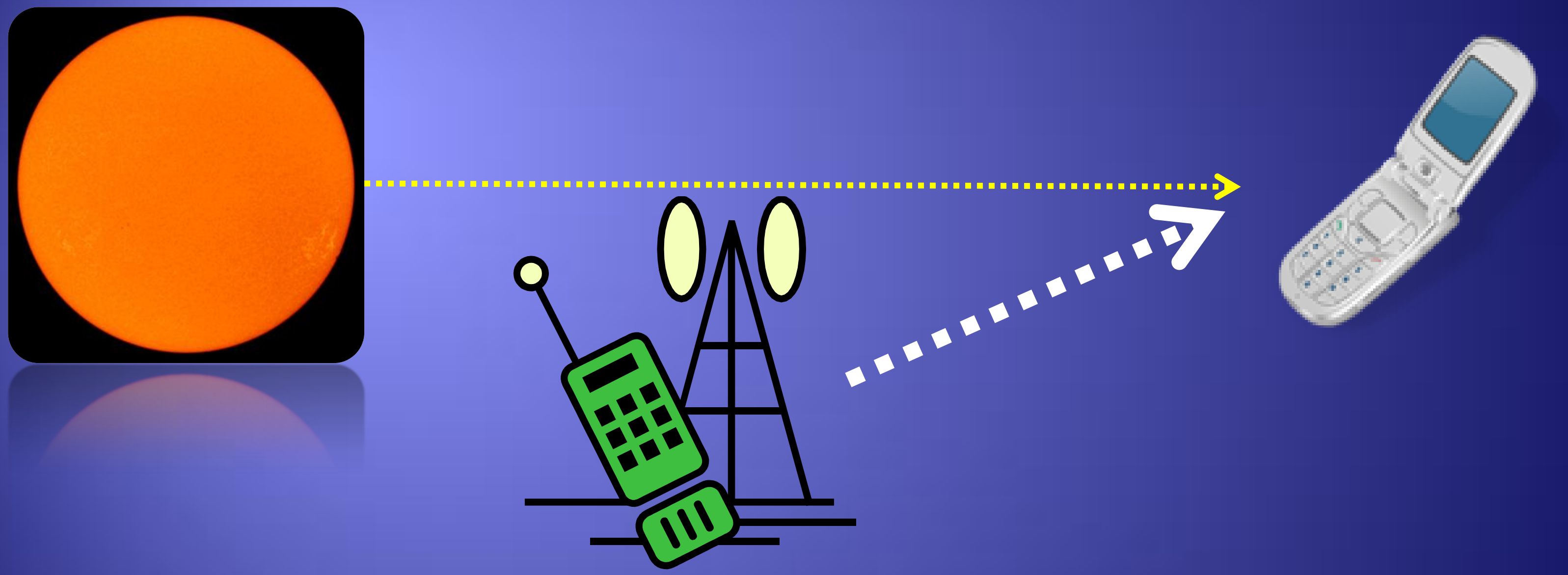

- **VERY LOW SOLAR RADIO EMISSION LEVEL**
- RADIO SIGNAL FROM CELL REPEATER
- **HIGH SIGNAL-TO-NOISE RATIO @ RECEIVER**
- <u>STANDARD COMMUNICATION QUALITY</u>
- <u>GEOMETRY KEY CONDITION</u>

RADIO ACTIVE SUN

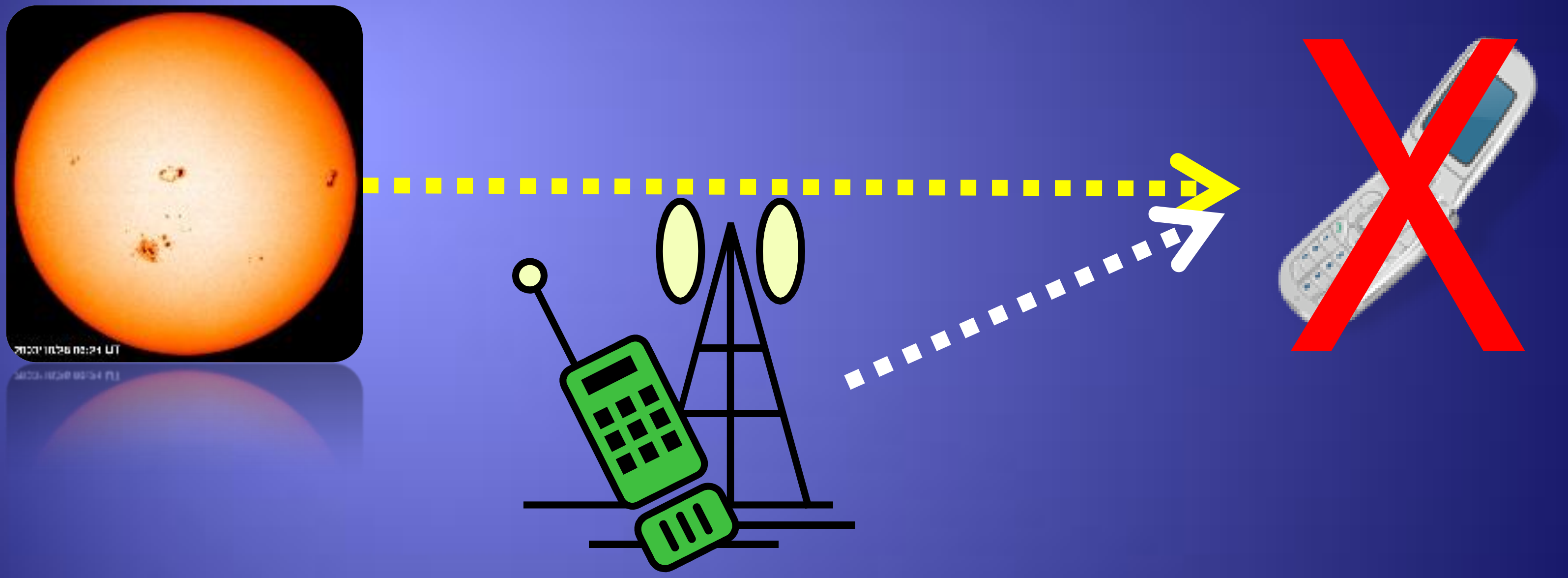

- **VERY HIGH SOLAR RADIO EMISSION LEVEL**
- RADIO SIGNAL FROM CELL REPEATER
- **LOW SIGNAL-TO-NOISE RATIO @ RECEIVER**
- <u>LOSS OF LOCK AND COMMUNICATION DROP</u>
- <u>GEOMETRY KEY CONDITION</u>

DIRECT EFFECTS OF SOLAR RADIO WEATHER

AN INTRODUCTION TO SOLAR RADIO ASTRONOMY

THE SOLAR RADIO PHENOMENOLOGY
Observations and Diagnostics

M. Messerotti

INAF-Trieste Astronomical Observatory, Trieste, Italy

and

Department of Physics, University of Trieste

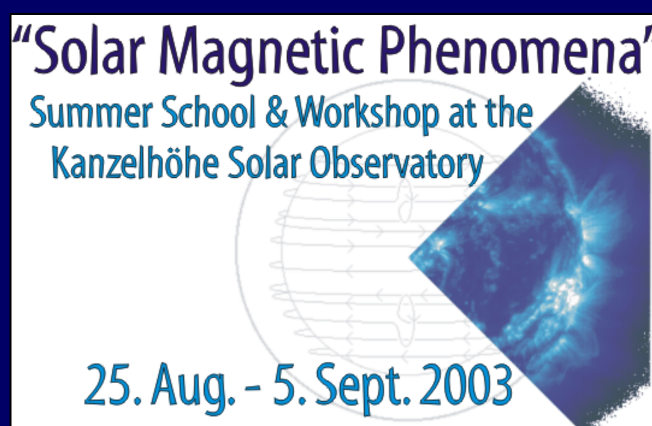

Scheme of the Lectures

- The Sun as an Active Star
- Solar Radio Astronomy: An Introduction
- Solar Activity as Driver of Geo-Effective Perturbations
- Space Weather Monitoring and Forecasting: A Scheme

Benz, A.O. 1993, “Plasma Astrophysics”, Kluwer Academic Publishers

Sawyer, C., Warwick, J.W., & Dennet, J.T. 1986, “Solar flare prediction”, Colorado Associated University Press

Messerotti, M., Zlobec, P., Padovan, S. 2000, The Trieste Near-Real-Time Coronal Surveillance Program: A Tool for Solar Activity Monitoring and Forecasting, Mem. S.A.It. (in press)

Messerotti, M. 2000, Solar-Terrestrial Activity Monitoring, in “The Dynamic Sun”, A. Hanslmeier and M. Messerotti (eds.), Kluwer Academic Publishers (in press)

Messerotti, M. 1999, The Dynamic Corona. Outline of observational features and radio diagnostics, in “Motion in the Solar Atmosphere”, A. Hanslmeier and M. Messerotti (eds.), Kluwer Academic Publishers, Astrophysics and Space Science Library 239, 139

Messerotti, M. et al. 1999, The solar surveillance program at the Kanzelhoehe Solar Observatory: new facilities for high speed digital imaging and dynamic event tracking, ESA WPP 155, 321

Messerotti, M. 1997, Probing the solar atmosphere through radiophysics, Kluwer Academic Publishers, Astrophysics and Space Science Library 494, 59

Messerotti, M. 1996, The role of non-imaging radio instruments in SOHO coordinated observations, in JOSO Annual Report 1995, M. Saniga (ed.), Astron. Inst. Slovak Acad. of Sciences, Tatranska Lomnica, 95

Messerotti, M. 1995, Radio and optical diagnostics of physical processes in the solar atmosphere: the key role of SOHO, in JOSO Annual Report 1994, M. Saniga (ed.), Astron. Inst. Slovak Acad. of Sciences, Tatranska Lomnica, 139

THE SUN
AS
AN ACTIVE STAR

The Sun as a Star

MAIN SEQUENCE YELLOW DWARF

- L 3.9 10^{26} W
- M 1.99 10^{30} kg
- R 6.96 10^{5} km
- T_e 5785 K

- Sp. type G2V
- Age 5 10^{9} years
- Phase stable H burning

- Variability on a second order scale

- Magneticity on a second order scale

The Sun as Physical System

COMPLEX SYSTEM made of
COUPLED MAGNETIZED PLASMAS
at different spatial scales and physical status

	T_e [K]	N_e [cm^{-3}]
• CORE	10^7	10^{19}
• RADIATIVE ZONE	10^6	10^{16}
• CONVECTIVE ZONE	10^5	10^{14}
• PHOTOSPHERE	10^3	10^{12}
• CHROMOSPHERE	10^4	10^{11}
• TRANSITION REGION	10^5	10^{10}
• CORONA	10^6	10^{09}
• SOLAR WIND	10^5	10^{01}

Solar Activity

COMPLEX of PHENOMENA

- **VARIABLE on**
  - spatial scale
  - time scale
  - energy scale
- **OCCURRING in**
  - photosphere — SUNSPOTS
  - chromosphere — FLARES
  - corona — CMEs
  - solar wind — FAST STREAMs
- **AS**
  - heating
  - particle acceleration
  - waves and shocks
  - emission of radiation
  - plasmoid formation
- **TRIGGERED by**
  - fluid motions
  - interacting magnetic fields

  at different spatial scales

Solar Activity Description

- **HUGE VARIETY OF PHENOMENA**

NEEDS

- **GLOBAL DESCRIPTION of REPRESENTATIVE ONES** via:

- **DIACHRONIC OBSERVATIONS** which produce:

- **TIME SERIES of INDEXES**, based on prominent observed features

TO GET

- **INSIGHTS ABOUT THE LONG-TERM GLOBAL BEHAVIOUR OF THE SUN AS A STAR**

- **INSIGHTS ABOUT THE SHORT-TERM LOCALIZED BEHAVIOUR OF THE SUN WHICH CAN BE GEO-EFFECTIVE**

THE SOLAR RADIATION SPECTRUM

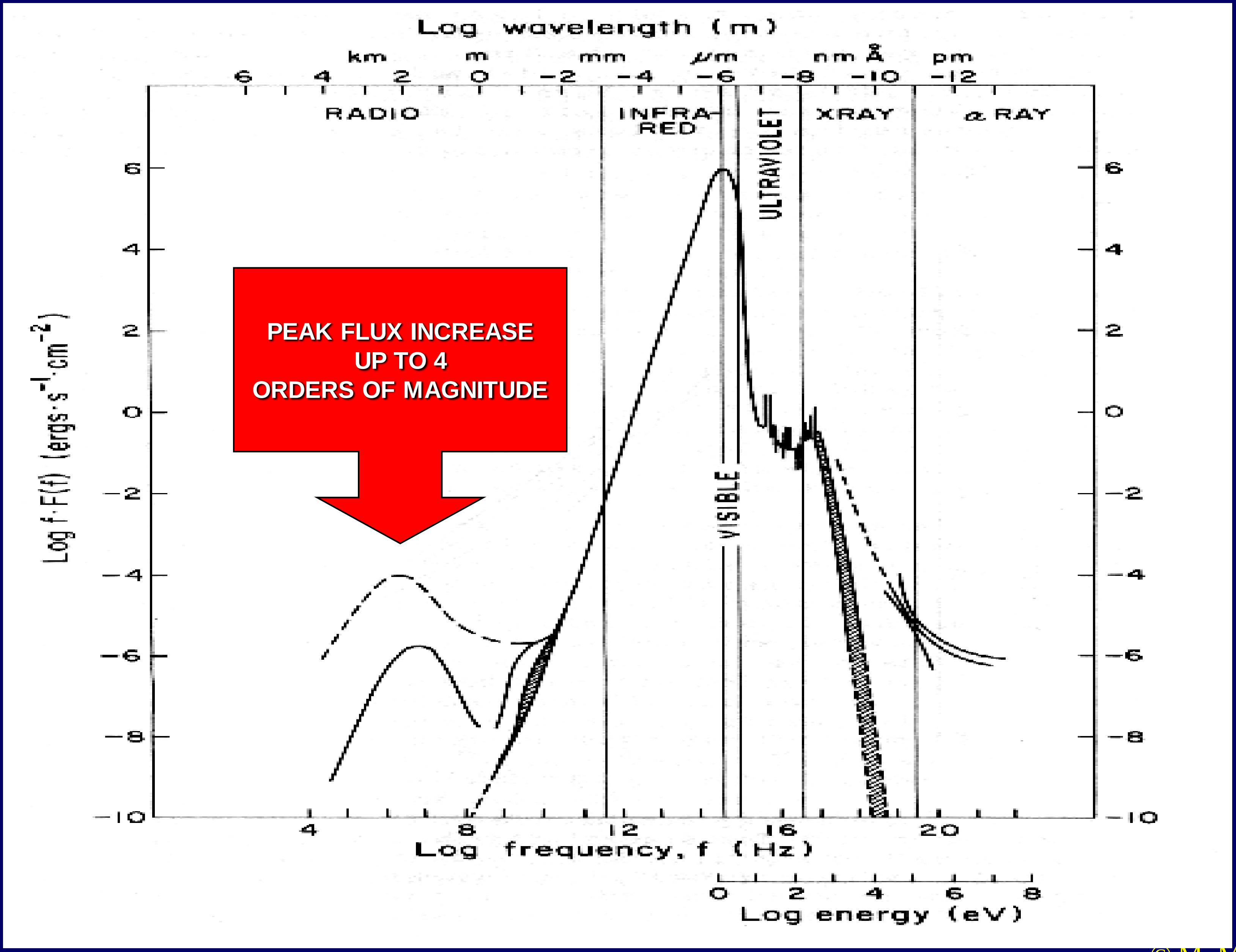

LOW AND HIGH SOLAR ACTIVITY

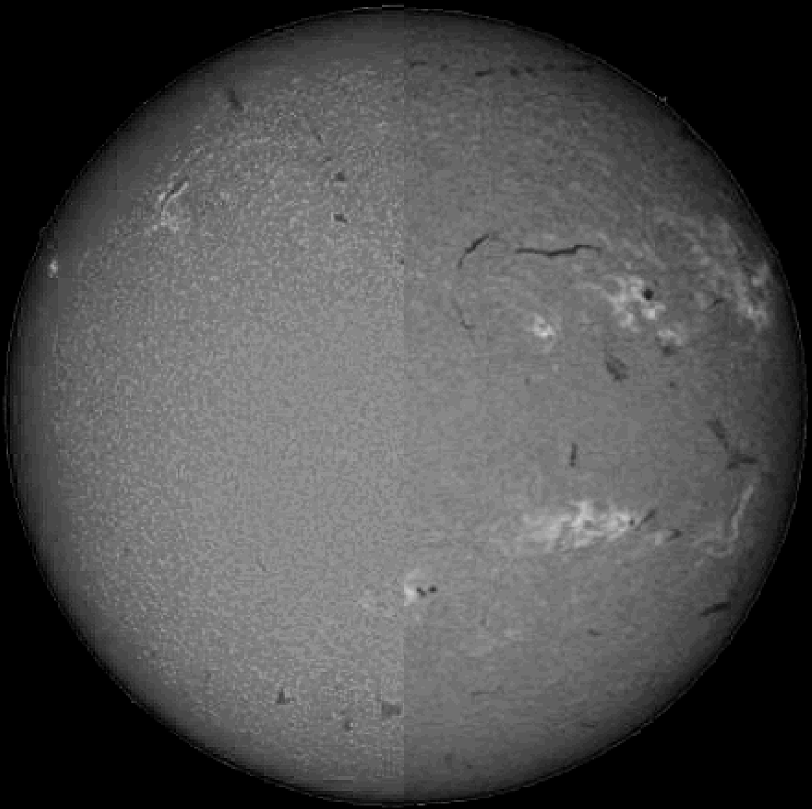

L H
H-alpha

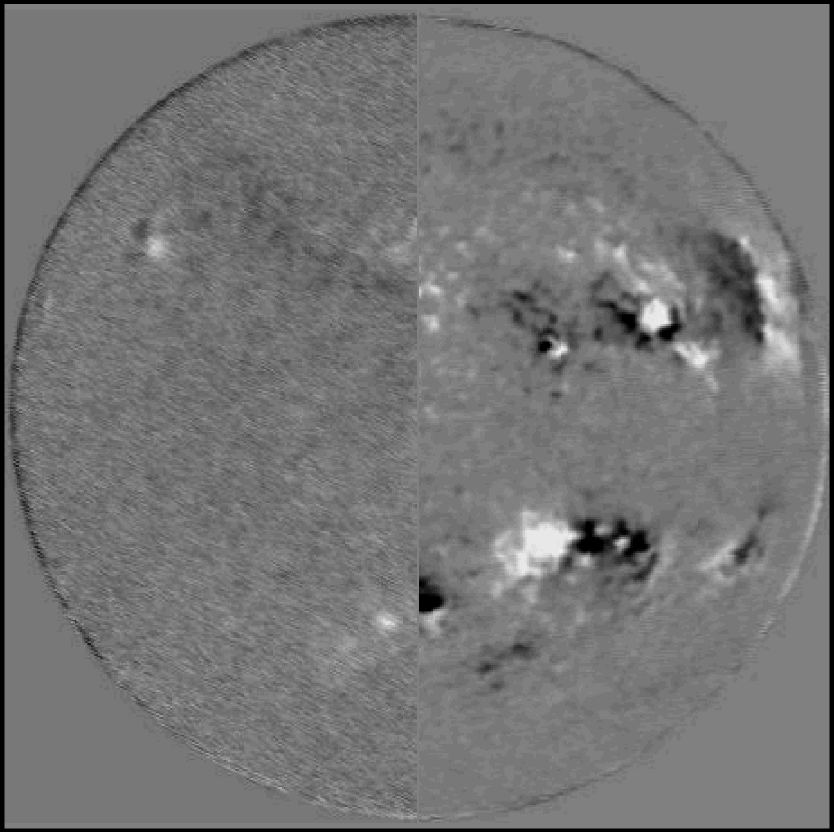

L H
M.F.

Images courtesy Kanzelhoehe Solar Observatory

ACTIVE REGION

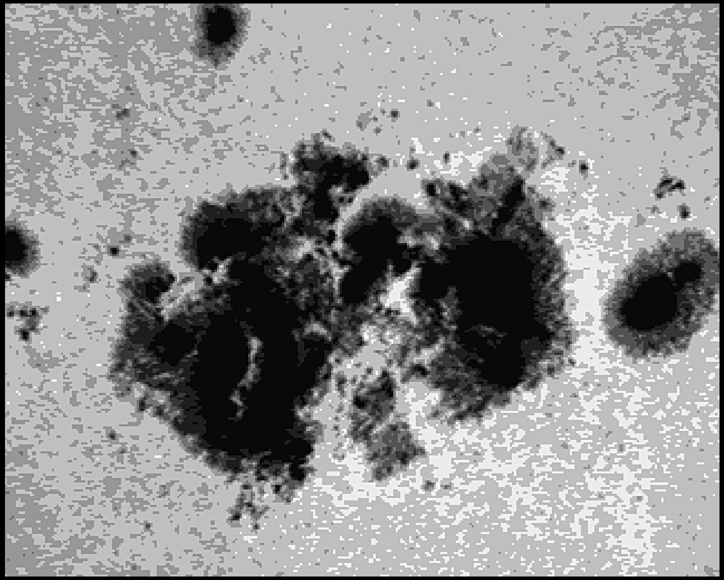

SUNSPOT GROUP

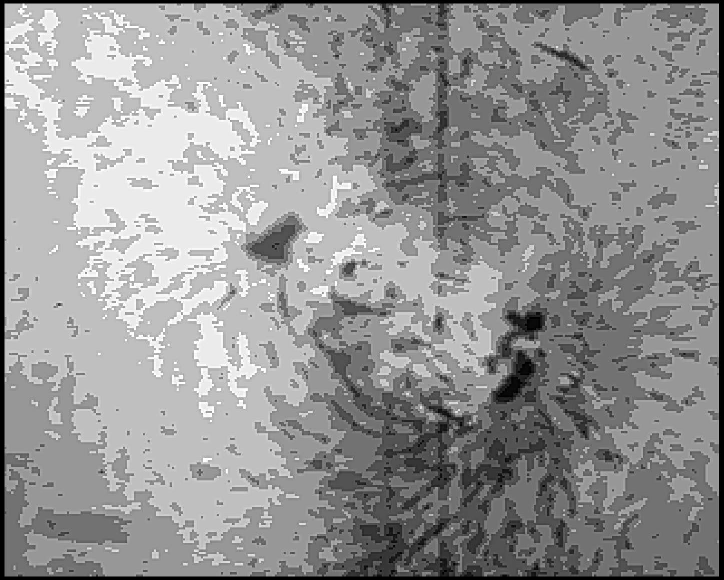

MAGNETIC FIELD

AR5395 - MARCH 1989

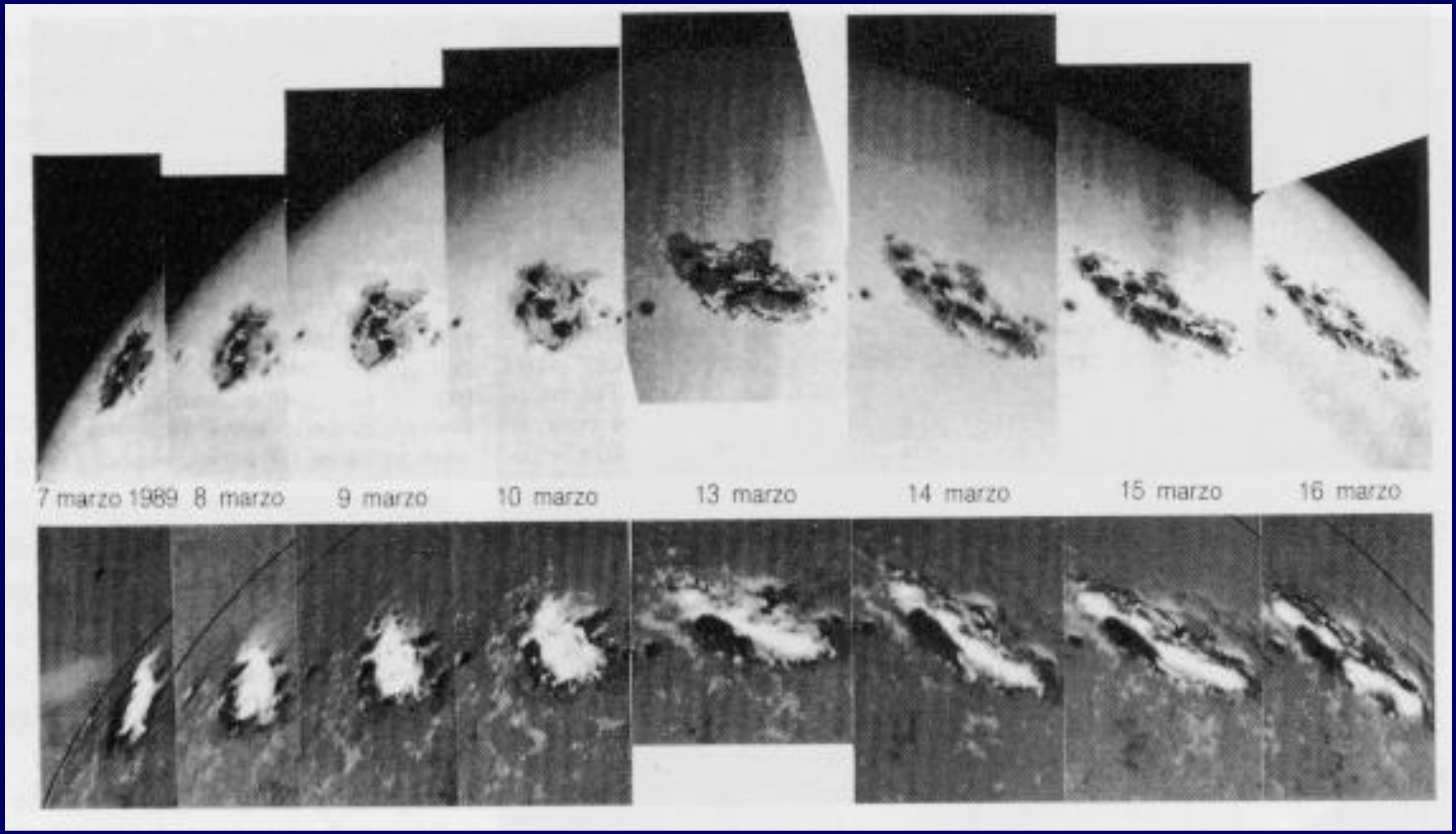

CHROMOSPHERE

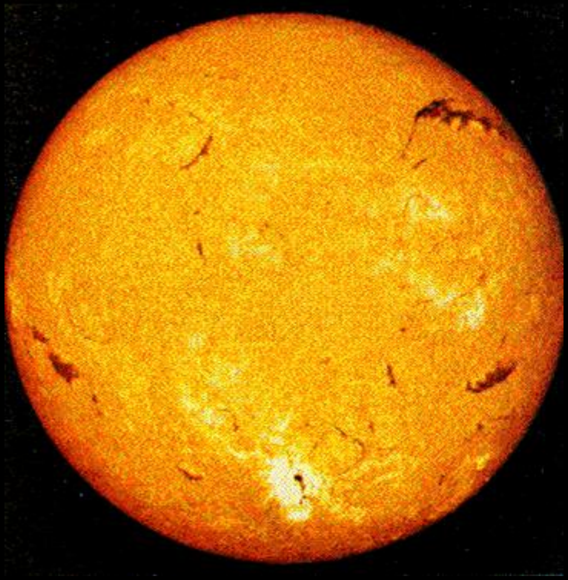

H-alpha

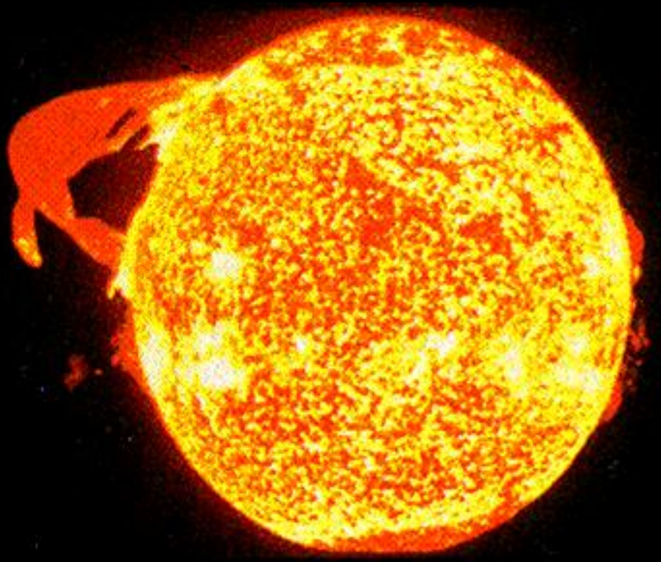

HeII

FLARE

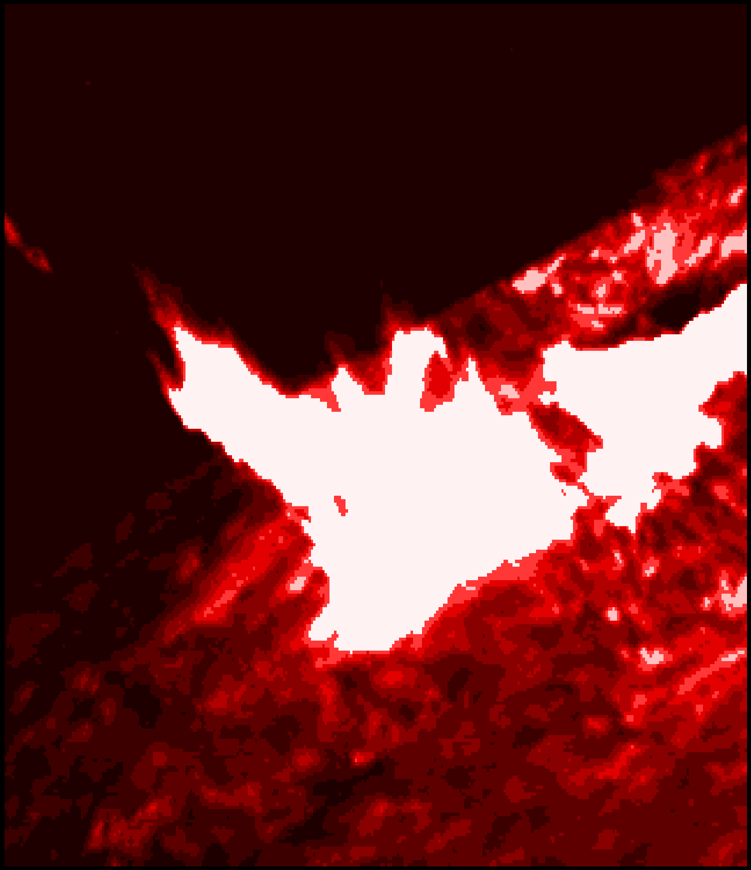

RADIO AND X CORONA

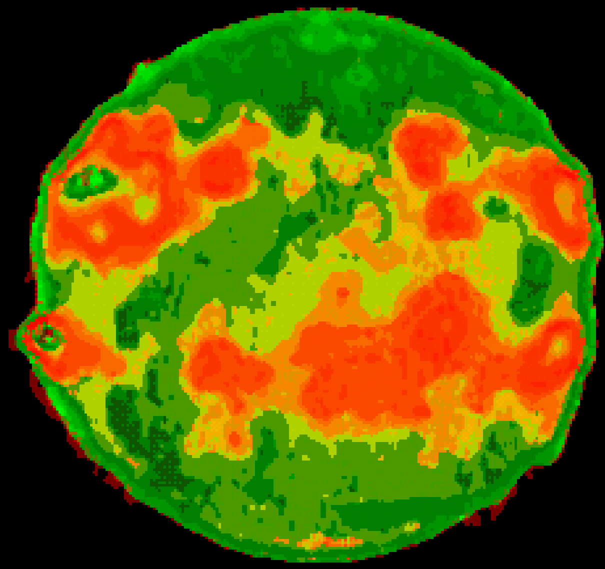

RADIO

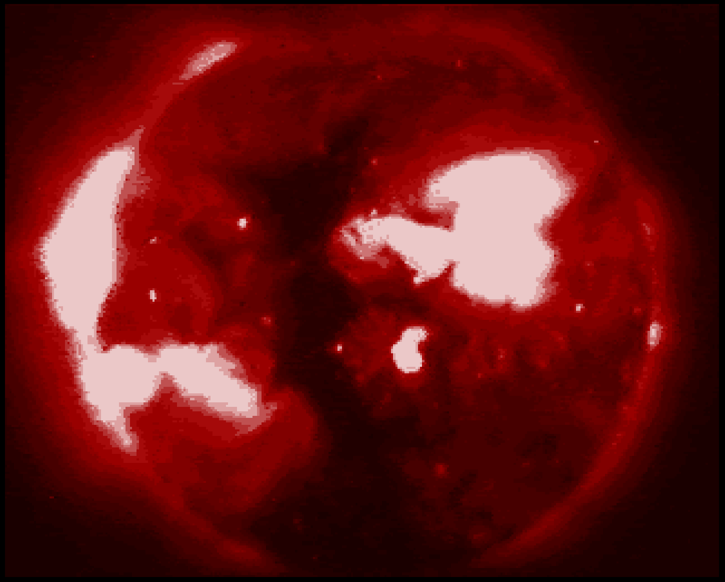

X

WHITE-LIGHT CORONA

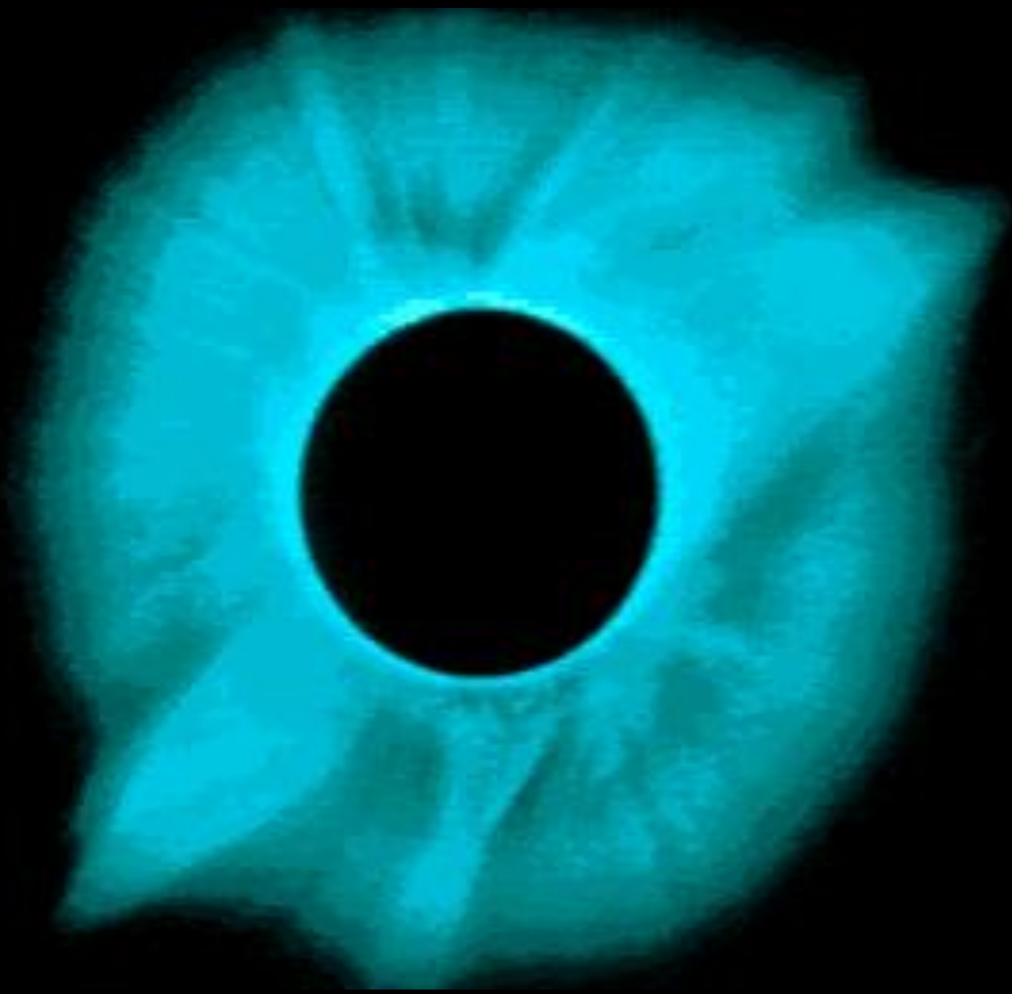

LARGE SCALE FEATURES OF THE SOLAR CORONA

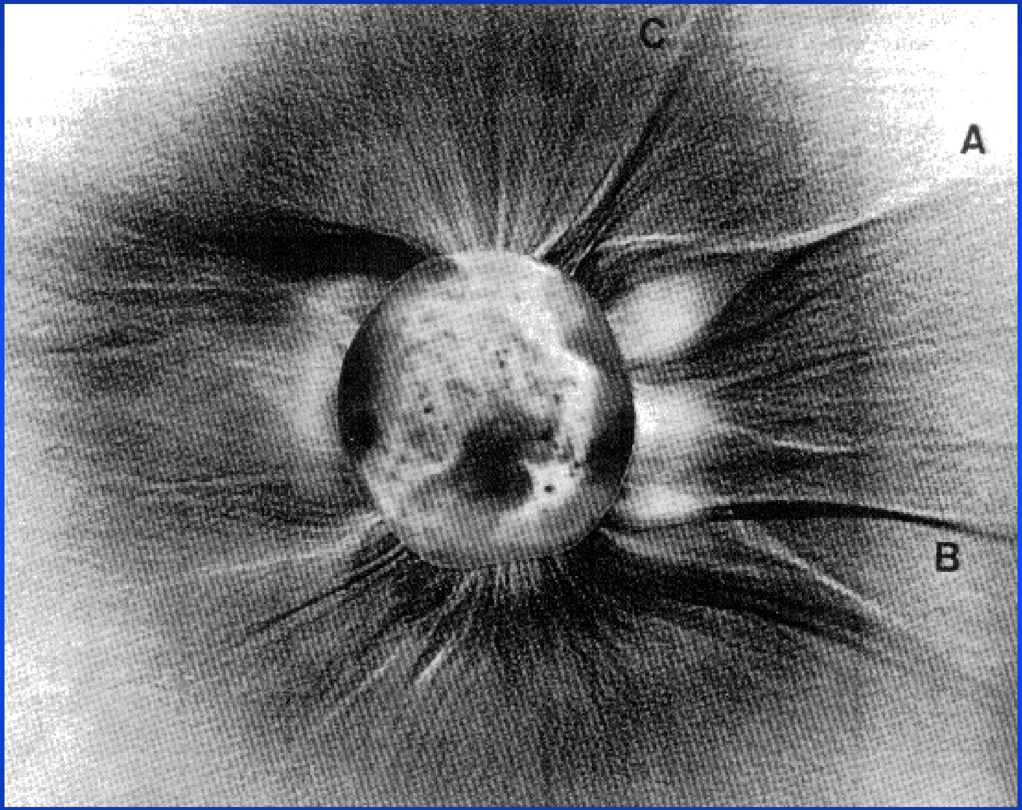

(A) Face-on streamer
(B) Streamer with tangential discontinuity
(C) Edge-on streamer
WL coronal eclipse picture (June 30, 1973) [Koutchmy, 1975]

SOLAR WIND

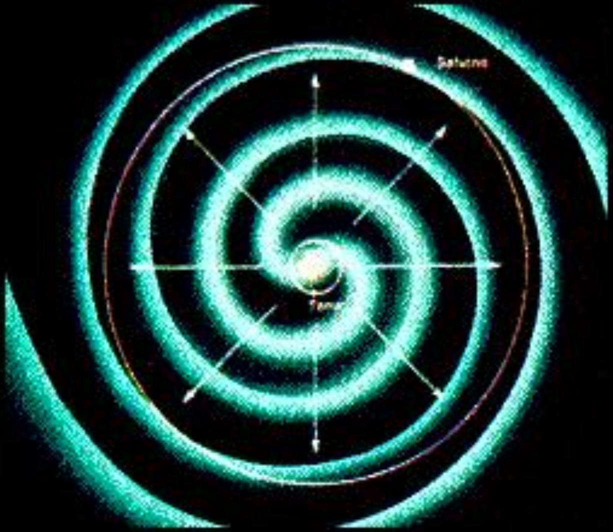

2-D

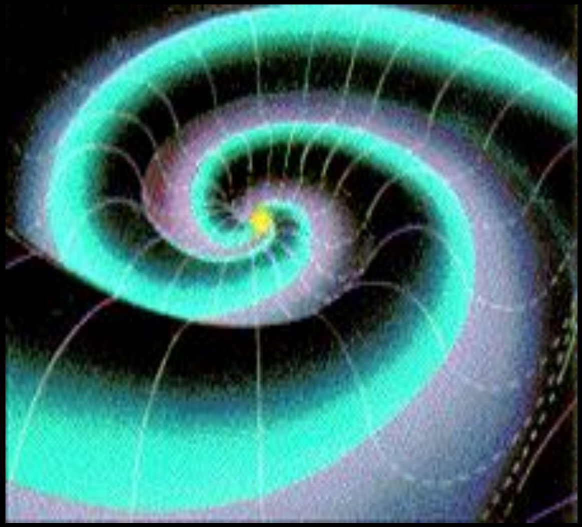

3-D

MULTIBAND OBSERVATIONS

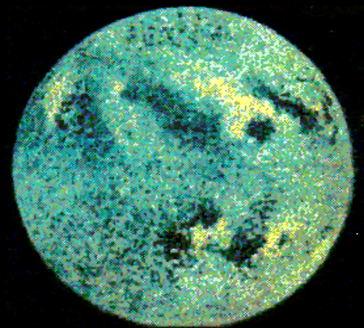

Magnetic Field

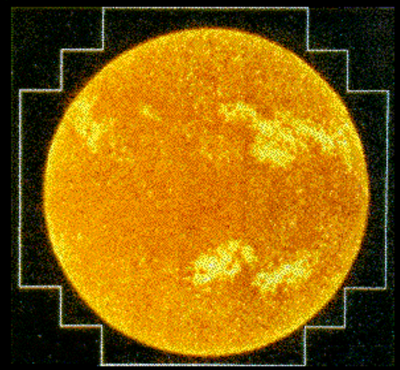

UV

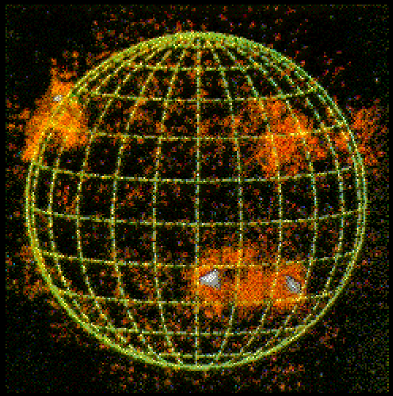

X

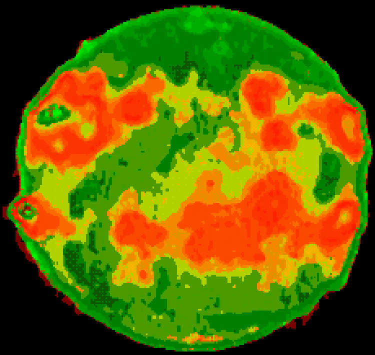

Radio

- **with ∞ Spectral Resolution**
- **with ∞ Spectral Coverage**
- **with ∞ Spatial Resolution**
- **with ∞ Temporal Resolution**

are a MUST for SELF-CONSISTENT MODELLING !

SPACE-BASED MULTIBAND OBSERVATIONS FROM SOHO

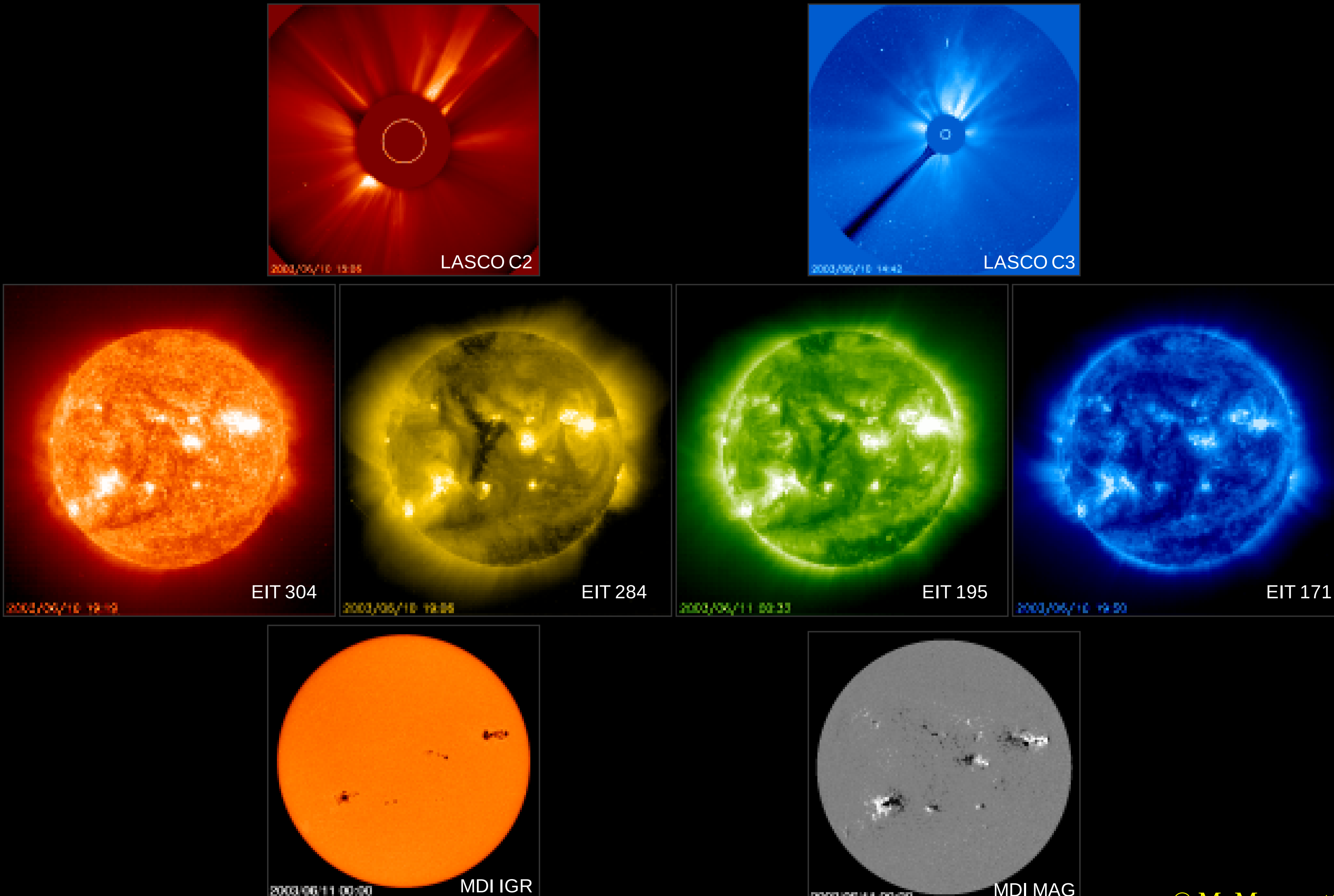

M.M. (GURU?...) MEDITATIONS about SUN MODELLING

- No self-consistent, global models of the Sun exist yet capable to cope with the multiscale phenomenology we observe

- Only varieties of partial models relevant to limited domains in the {space:time:wavelength}-hyperspace do exist

  e.g. “I have a nice dynamo mechanism”, “I have seen a flare”, “I observed 20 CME’s”, and so on…

- Most existing models do not fit at the interface of their respective domains

  e.g. I will ignore the environment outside my modelling domain to simplify my work and get convergence ;-)

- The higher the level of detail, the more difficult the relevant modelling

AND ? ...

WE MUST NOT FEEL DISCOURAGED, AS

TO DATE, IN A GALILEAN MEANING ;-) , THE SUN IS THE ASTROPHYSICAL OBJECT MOST DIFFICULT TO BE MODELLED

NEVERTHELESS ...

NEVER WE MUST BE TOO MUCH HAPPY WITH OUR MODELS OR INTERPRETATIONS, EVEN IN CASE THEY ARE A SIGNIFICANT IMPROVEMENT WITH RESPECT TO THE PREVIOUS WORKS OTHERWISE WE RISK TO MISS THE OVERALL SCENARIO :

TILES ARE FUNDAMENTAL BUT ARE FUNCTIONAL TO THE COMPLETE MOSAIC !

AN INTRODUCTION TO SOLAR RADIO ASTRONOMY

- **RADIO WAVES IN THE SOLAR PLASMA**
  - Propagation of radio waves in the solar corona
  - Radio emission processes

- **SYNOPSIS OF SOLAR RADIO INSTRUMENTS**

- **THE FREQUENCY-DENSITY-HEIGHT RELATION**
  - **Coronal density models**
  - Effects of density inhomogeneities on radio wave propagation
  - **The coronal plasma frequency**
  - **The coronal gyrofrequency**
  - Estimated altitude of flare-related radio emissions

- **Plasma diagnostics from radio signatures of particle beams**

- **SYNOPSIS OF SOLAR RADIO EVENTS**

- **The radio sun through imaging radio instruments**

PROPAGATION OF RADIO WAVES IN THE SOLAR CORONA

RADIO EMISSION OBSERVABLES

- Radio domain ⇒ Rayleigh-Jeans approximation $h\nu \ll k_B T$

- Specific Intensity: $\mathcal{I}_\nu = k_B T_B \nu^2 / c^2$ T_B Brightness Temperature

- Source Function: $\mathcal{S}_\nu = k_B T_{\mathrm{eff}} \nu^2 / c^2$ T_{eff} Effective Temperature

- Spatially unresolved observations [S_ν] = [sfu]

  1 solar flux unit (sfu) = 10^{-22} W m^{-2} Hz^{-1}

- Imaging instruments are characterized by an angular resolution determined by the antenna beam solid angle Ω_{bm}.

  The measured quantity is the Flux density per beam:

$$\langle S_\nu \rangle_{bm} = k_B \langle T_B \rangle_{bm} \nu^2 \Omega_{bm} / c^2$$

  with $\langle T_B \rangle_{bm}$ the mean brightness temperature over the beam Ω_{bm}.

RADIO EMISSION SOURCES

- For an **optically thick** source, which emits incoherent radiation

$$T_B = T_{\mathrm{eff}}$$

with T_{eff} kinetic temperature if the source is in thermal equilibrium or mean energy of emitting electrons otherwise

- For an **optically thin** source

$$T_B \approx \tau_\nu T_{\mathrm{eff}}$$

with τ_ν the **optical depth**

The microphysics of the specific emission mechanism is embodied in the **absorption coefficient** κ_ν through $\tau_\nu = \int \kappa_\nu \, dl$

For coherent emission one can have $T_B \gg T_{\mathrm{eff}}$

Radio Flux Density and Polarization

- The **Flux density S** for one polarization is related to T_b by

$$S = k\nu^2/c^2 \int T_b \, d\Omega,$$

where dΩ is a differential solid angle and the integral is over the projected area of the source.

- The **Circular Polarization (CP) degree** is

$$r_c = (T_{b,x} - T_{b,o})/(T_{b,x} + T_{b,o}),$$

and is therefore related to the brightness temperature not to S, which is an integrated observable (!)

It is related to the magnetic field polarity at the source

THE ELECTROMAGNETIC MODES

- Coronal plasma ~ cold magnetized plasma

- It behaves like a birefringent medium

- A radio wave is splitted into two components with different velocity and polarization: the ordinary (o) mode and the extraordinary (x) mode, but the (z) and whistler modes can propagate as well.

- The magnetoionic theory can describe the propagation of the above modes

- The x- and o-modes can propagate from the source to ∞

- The z- and whistler modes are prevented by stopbands in the refractive index

THE QC APPROXIMATIONS

- Let us define $X = (\nu_{pe}/\nu)^2$ and $Y = \nu_{Be}/\nu$ where ν is the frequency of the wave, ν_{pe} the electron plasma frequency and ν_{pe} the electron cyclotron frequency

- When $Y \sin^2\theta/2(1-X)\cos\theta \ll 1$ with θ angle between the em wave normal and the magnetic field vector, the QUASICIRCULAR APPROXIMATION holds

- The propagation of the x- and o-modes is adequately described by the QC approximation in many cases of interest

- The radiation is very nearly circularly polarized

- The observables are the TOTAL INTENSITY (Stokes I) and the CIRCULARLY POLARIZED RADIATION (Stokes V) parameters

THE QT APPROXIMATIONS

- When $Y \sin^2 \theta / 2(1-X) \cos\theta >> 1$ with θ angle between the em wave normal and the magnetic field vector, the QUASITRANSVERSE APPROXIMATION holds

- The radiation is linearly polarized at the source

- Faraday rotation is very large in the coronal medium and differential Faraday rotation across typical receiver bandwidths and/or the differential Faraday rotation from the front to back of an optically thin source washes out the linear polarization completely

- No linearly polarized solar radio emission was observed to date

MODE COUPLING

Propagation effects can modify the observed polarization

- WEAK MODE COUPLING The magnetoionic theory prevails and the wave modes propagate independently

  When the wave cross a QT region (the longitudinal component of the magnetic field changes sign), the SENSE OF CP REVERSES

- STRONG MODE COUPLING The magnetoionic theory breaks down and the magnetoionic modes are no longer independent

  When the wave cross a QT region, the x- and o-modes couples, and the SENSE OF CP REMAINS UNCHANGED.

Under certain conditions, mode coupling can play a role in DEPOLARIZING the radiation.

RADIO EMISSION PROCESSES

(e.g. Bastian et al., 1998)

PHYSICAL NATURE OF SOLAR RADIO EMISSIONS

- In the (mm-m) wavelenght range solar radio emissions are:

  - **incoherent radiation** generated by continuous processes

  - **coherent radiation** generated by nonlinear resonant processes involving the

    - electron plasma frequency

      $$f_{pe}(R) = 8973 \cdot 10^{-6} \sqrt{N_e(R)} \ \mathrm{MHz}$$

    - electron gyrofrequency

      $$f_{ce}^{s} = s \cdot f_{ce} = s \cdot (2.80 \cdot B)\,\mathrm{MHz} \qquad (s = 1, 2, 3, \ldots)$$

    - harmonics of the above

  - no emission or absorption spectral lines from atomic or molecular transitions observed

  - radio recombination lines from ions in the mm-cm band are undetectable due to the extreme pressure broadening

DIRECT EM EMISSION PROCESSES 1

- THERMAL FREE-FREE EMISSION (Bremsstrahlung)
  Individual electrons are deflected in the Coulomb field of ions
  (Unpolarized em waves - Occurs almost everywhere) !!

- INCOHERENT GYRORESONANCE and
  GYROSYNCHROTRON EMISSION
  Gyration of electrons around magnetic field lines prevails over
  collisions (gyroresonance – non-relativistic,
  gyrosynchrotron – mildly relativistic,
  synchrotron – highly relativistic electrons)
  (Polarized em waves in x-mode - Dominates at mm-cm wavelengths) !!

  Various possibilities:
  - gyroresonance radiation from thermal electrons
  - gyrosynchrotron radiation from thermal electrons
  - gyrosynchrotron radiation from power-law electrons
  - synchrotron radiation from power-law electrons
  - Razin-Tsytovich: suppression of gyrosynchrotron emission at low f

DIRECT EMISSION PROCESSES 2

- ELECTRON CYCLOTRON MASER

Radiation is amplified by the MASER at frequencies near the electron-cyclotron frequency and its low-harmonics.

To operate the MASER requires:

a) a population inversion in the electron distribution as compared with the equilibrium (the pump for the MASER);

b) a relatively strong magnetic field or low-density plasma so that the electron-cyclotron frequency is somewhat larger than the electron plasma frequency.

The free energy is directly converted into coherent em radiation.

Invoked to explain high brightness temperature, spiky emissions.

INDIRECT EM EMISSION PROCESSES

- PLASMA RADIATION

It is a coherent mechanism involving:

1. the generation of plasma waves at the electron plasma frequency or its second harmonics via various plasma instabilities, i.e. wave growth in an unstable plasma configuration where a source of free energy exists (i.e. higher number of degrees of freedom in the plasma;
   e.g. an injected nonthermal particle beam which originate
   Langmuir waves via a beam-plasma instability or
   a loss-cone distribution of electrons which excites
   upper hybrid waves and Bernstein modes)

2. the conversion of such longitudinal plasma waves into transverse em waves via various cohalescence/scattering processes (Polarized in the o-mode) !!

ELECTRON BEAM INSTABILITIES

(e.g. Omura et al., 2001)

ELECTRON BEAMS IN SPACE PLASMAS

- ARE FORMED IN VARIOUS PROCESSES
  - Particle reflection at shocks
  - Inductive electric field
  - Parallel electric field of kinetic Alfvèn waves
- CAUSE
  - strong electrostatic instabilities, which lead to the diffusion excitation of:
    - Langmuir waves
    - Ion acoustic waves
    - Electrostatic solitary waves
- Electrons diffuse in velocity space and are observed as a diffused or flat-top distribution function

LINEAR DISPERSION RELATION 1

- Few species of electrons and ions drifting along a static magnetic field

- Particle distribution funtions are defined in 3-D velocity space

- By integrating the velocity distribution function with 2 velocity components perpendicular to the magnetic field, we obtain a reduced velocity distribution function of the parallel velocity component v

- Each distribution function forms a Maxwellian

$$f_s(v) = \frac{n_s}{\sqrt{2\pi} V_{ts}} \exp\left(-\frac{(v - V_{ds})^2}{2V_{ts}^2}\right)$$

where V_{te} – thermal velocity and V_{de} – drift velocity

LINEAR DISPERSION RELATION 2

- The kinetic description of the beam-plasma instability is given by the dispersion relations derived from

- the Vlasov equation for species "s"

$$\frac{\partial f_s}{\partial t} + \boldsymbol{v} \cdot \frac{\partial f_s}{\partial \boldsymbol{x}} + \frac{q_s}{m_s}\boldsymbol{E} \cdot \frac{\partial f_s}{\partial \boldsymbol{v}} = 0$$

- the Poisson equation

$$\nabla \cdot \boldsymbol{E} = -\frac{1}{\epsilon_o}\sum_s q_s n_s$$

where E – parallel electric field

LINEAR DISPERSION RELATION 3

- Vlasov equations are linearized and reduced to those relevant to an unmagnetized plasma

- By applying the Fourier and Laplace transforms to the Vlasov and Poisson equations in space and time, it is obtained the DISPERSION RELATION of electrostatic waves with wave vectors parallel to the static magnetic field

$$D(k,\omega) = 1 - \sum_s \frac{\Pi_s^2}{k^2} \int_L \frac{\mathrm{d}g_s/\mathrm{d}v}{v - \omega/k} \mathrm{d}v$$

where Π_s – plasma frequency of species "s"
g_s - normalized unperturbed velocity distribution function f_s/n_s at $t=0$

- Solutions of the dispersion relation are NORMAL MODES

LINEAR DISPERSION RELATION 4

- The wavenumber k is assumed to be positive

- The frequency is complex $\omega = \omega_r + i\gamma$

- The integration over the velocity is taken along the Landau contour

- When the thermal velocity is comparable to the phase velocity, the dispersion relation yields a finite imaginary part

$$D_r(k,\omega) + i\, D_i(k,\omega) = 0$$

- If $|\gamma| << |\omega_r|$ an approximate GROWTH RATE is

$$\gamma = -\frac{D_i(k,\omega_r)}{\partial D_r(k,\omega_r)/\partial \omega_r}$$

LINEAR DISPERSION RELATION 5

- An INSTABILITY $(\gamma > 0)$ due to the imaginary part of D_i is called a RESISTIVE INSTABILITY

- When the thermal velocities are small enough

$$\frac{\omega}{k} - V_{ds} >> kV_{ts}$$

the dispersion relation is simplified as

$$1 = \sum_s \frac{\Pi_s^2}{(\omega - kV_{ds})^2}$$

- This dispersion relation has no imaginary part

- An INSTABILITY due to a positive γ in such a case is called a REACTIVE INSTABILITY

REACTIVE INSTABILITIES

- Bunching of particles at particular wave phases is important
- BI-STREAM INSTABILITY by two cold electron beams of approximately equal densities
- BUNEMAN INSTABILITY by a single electron population with a finite drift velocity with respect to the background ions
- The maximum growth rate is comparable to the frequency of the total plasma frequency
- The wave mode with the maximum growth rate grows to a large level to form large potentials that can trap the whole electron population

RESISTIVE INSTABILITIES 1

- In resistive instabilities of random phase the resistence acts in a negative way: amplification (negative absorption) carries the intensities of particular wave modes to very high levels and leads to COHERENT EMISSION, which can directly escape if electromagnetic or before must be converted into em transverse waves

- The maximum growth rate depends on the density of the electron beams and the thermal velocities of the background electrons and ions

- The gradient of the velocity distribution function at the phase velocity of a growing wave determines the growth rate

RESISTIVE INSTABILITIES 2

- The wave with the maximum growth rate grows from a thermal noise level to a level that traps the resonant electrons and effectively diffuses the electron beams

- When the growth rate is small enough that the wave spectra are broad with random phases, the quasi-linear diffusion takes place and make the velocity distribution function marginally stable

WEAK BEAM-PLASMA INSTABILITY

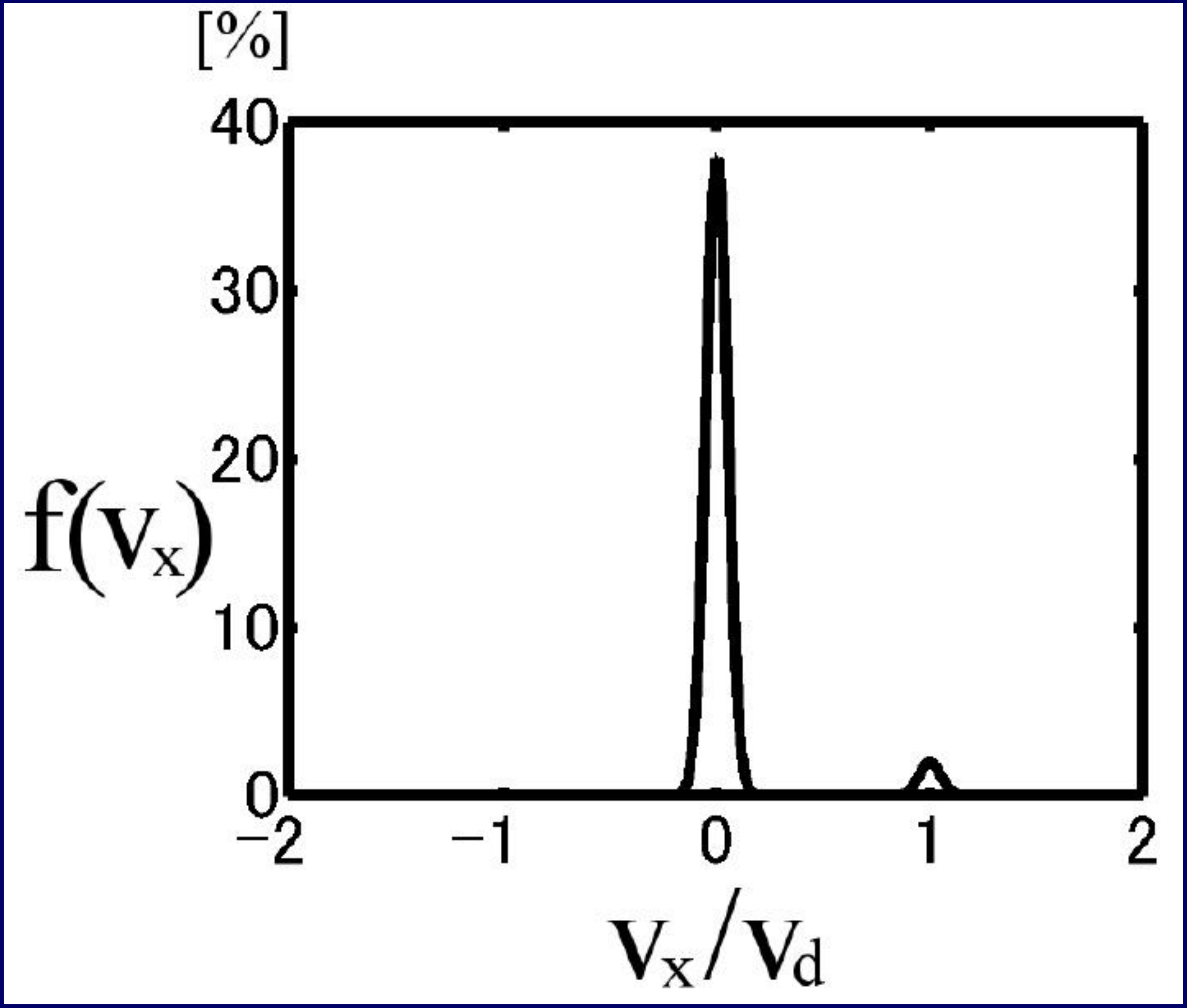

- V_d/V_{te}=2.0
- V_d/V_{tb}=2.0
- N_b/N_T=0.005

Type III burst
$N_b/N_T=10^{-6}$

NONLINEAR PARTICLES TRAPPING 1

- When an electron beam instability saturates after a sufficient growth time $(\gamma_{max} t > 1)$, most of the electrons forming the beam are trapped by coherent electrostatic potentials formed by the dominant wave mode with the maximum growth rate

- The trajectories of the trapped electrons are described by the equations of motion under a wave with wavenumber k, frequency ω and wave amplitude E_w

$$\frac{\mathrm{d}v}{\mathrm{d}t} = \frac{q}{m} E_w \sin\left(kx - \omega t + \zeta_o\right) \qquad \frac{\mathrm{d}x}{\mathrm{d}t} = v$$

- Taking a reference frame moving with the wave phase velocity as a variable of the velocity

$$\theta = k(v - \frac{\omega}{k}) = kv - \omega$$

NONLINEAR PARTICLES TRAPPING 2

- Defining a phase $\zeta = kx - \omega t + \zeta_o + \pi$ for a positive charge $(q > 0)$
- Defining a phase $\zeta = kx - \omega t + \zeta_o$ for a negative charge $(q < 0)$
- We obtain the equation of a pendulum

$$\frac{\mathrm{d}\theta}{\mathrm{d}t} = -\omega_t^2 \sin\zeta \qquad \frac{\mathrm{d}\zeta}{\mathrm{d}t} = \theta$$

with the trapping frequency

$$\omega_t = \sqrt{\frac{k|q|E_w}{m}}$$

NONLINEAR PARTICLES TRAPPING 3

- Integrating the above equations, it is obtained the equation of a particle trajectory in (θ, ζ) :

$$\theta^2 = 2\omega_t^2 \cos\zeta + C$$

where C is a constant corresponding to a specific trajectory.

- Particles oscillate around a stable equilibrium point at $(\theta, \zeta) = (0, 0)$ with the trapping frequency

- The saddle point of resonant particles trajectories is located at $(\theta, \zeta) = (0, \pm\pi)$ which gives the separatrix of the trapping region

- The maximum value of θ of the trapping region is given by $kV_t = 2\omega_t$ where V_t is called the trapping velocity

NONLINEAR PARTICLES TRAPPING 4

- In the presence of electrostatic waves, the velocity distribution function of the electron beam becomes flat over the range

$$V_r - V_t < v < V_r + V_t$$

- Resonant electrons are diffused over the velocity range

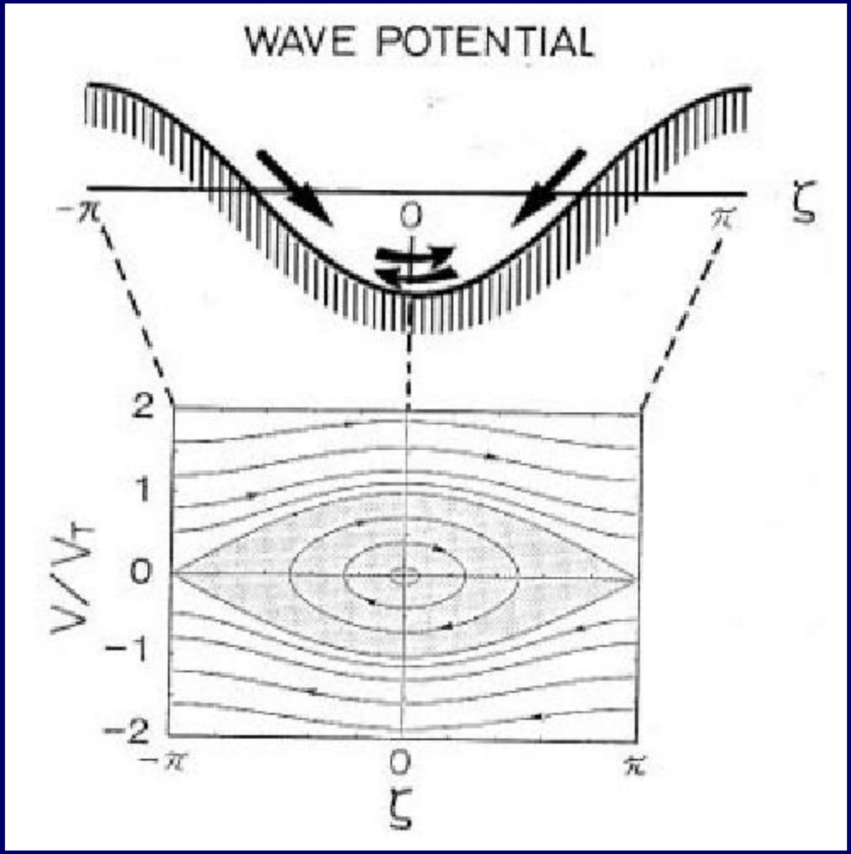

NONLINEAR PARTICLES TRAPPING 5

PIC Simulation

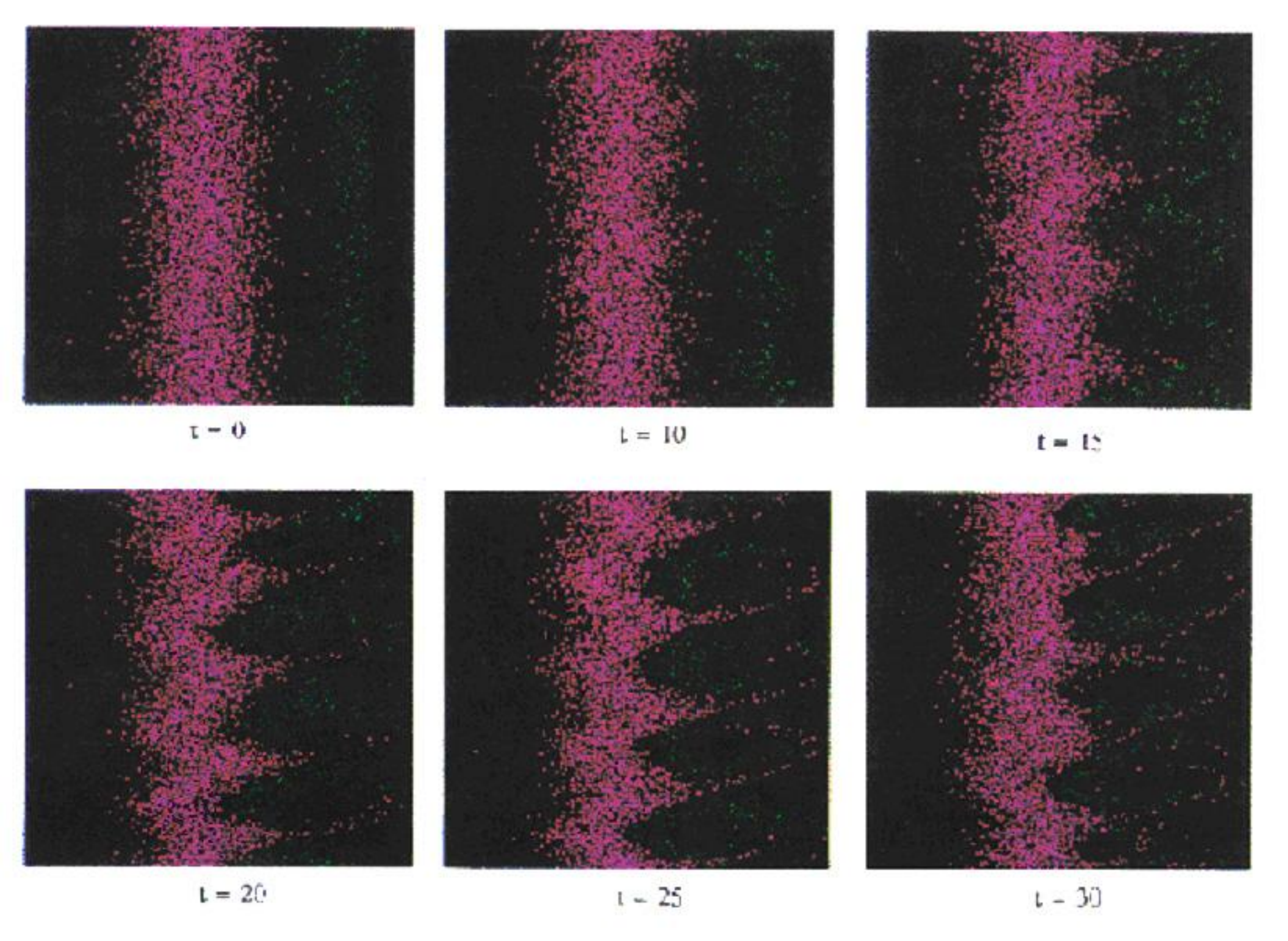

CONVERSION INTO EM WAVES

Langmuir waves are converted into transverse em waves near the local plasma frequency f_{pe} or its second harmonic ($2\,f_{pe}$) according to different processes.

- Fundamental emission (f_{pe})

    - IP type III bursts (in-situ observations)

A Langmuir wave decays into a daughter Langmuir wave and an ion-sound wave $L \Rightarrow L' + S$, which coalesces with another Langmuir wave into a radio wave $L + S \Rightarrow T$.

    - Coronal type III bursts (?)

- Harmonic emission ($2\,f_{pe}$)

Two Langmuir waves with frequency f_{pe} coalesce $L + L' \Rightarrow T$

FREQUENCY AND MOMENTUM MATCHING

To get a reasonable efficiency in the conversion process, it must be assured

- Frequency matching $\omega_t = \omega_L + \omega_3$

e.g. For fundamental radiation $\omega_t \approx \omega_L \approx \omega_{pe}$ and hence ω_3 must be small (low-frequency wave)

- Momentum matching $\mathbf{k}_t = \mathbf{k}_L + \mathbf{k}_3$,

e.g. As $|\mathbf{k}_t| << |\mathbf{k}_L|$ it must be $\mathbf{k}_3 \approx -\mathbf{k}_L$

Three possible processes:

1. Scattering by the electric field by thermal ions
2. Scattering by low-frequency waves (ion-sound, lower-hybrid)
3. Direct conversion by high gradient density inhomogeneities

SYNOPSIS OF
SOLAR RADIO INSTRUMENTS

SOLAR RADIO INSTRUMENTS

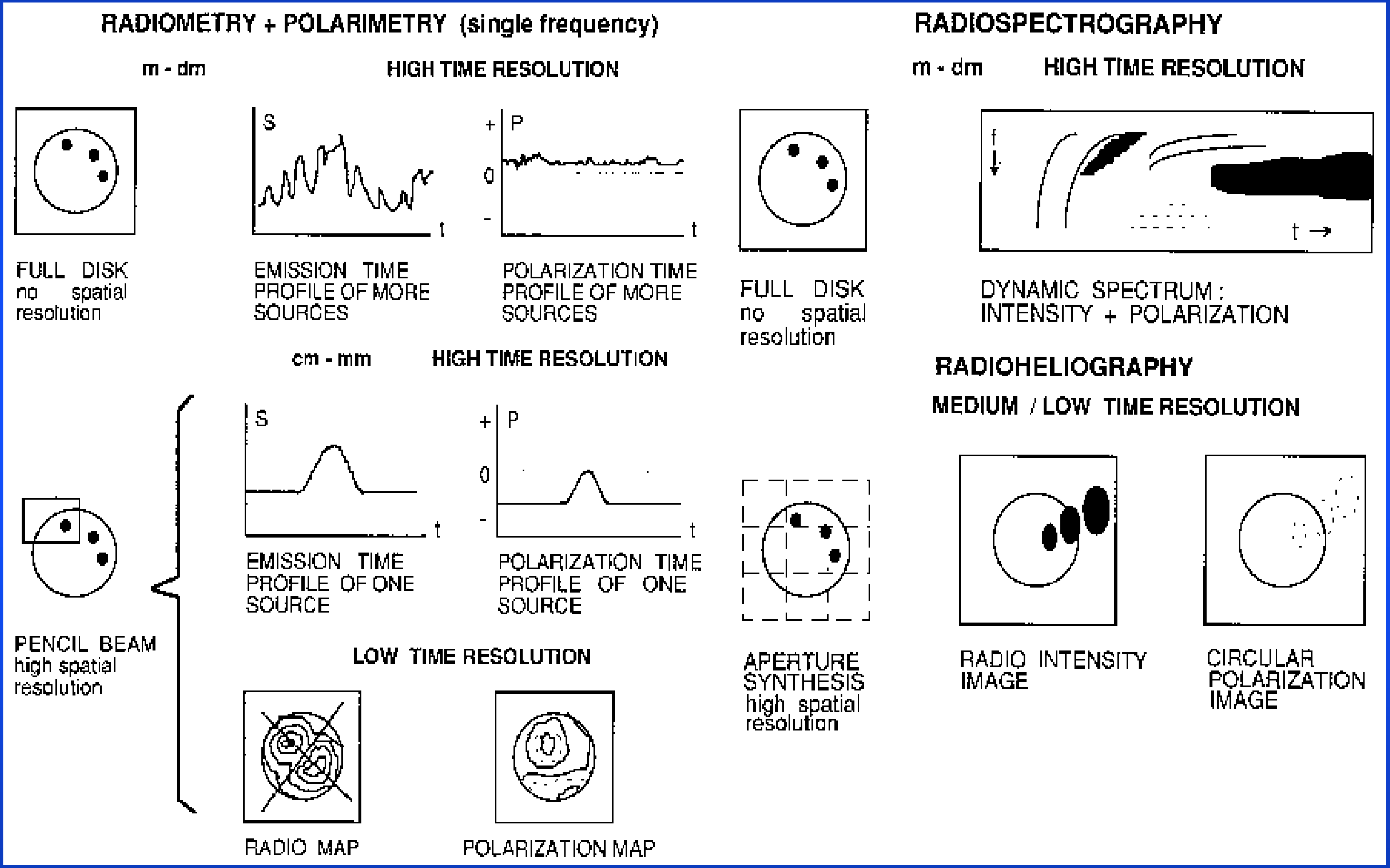

WAVELENGTH COVERAGE

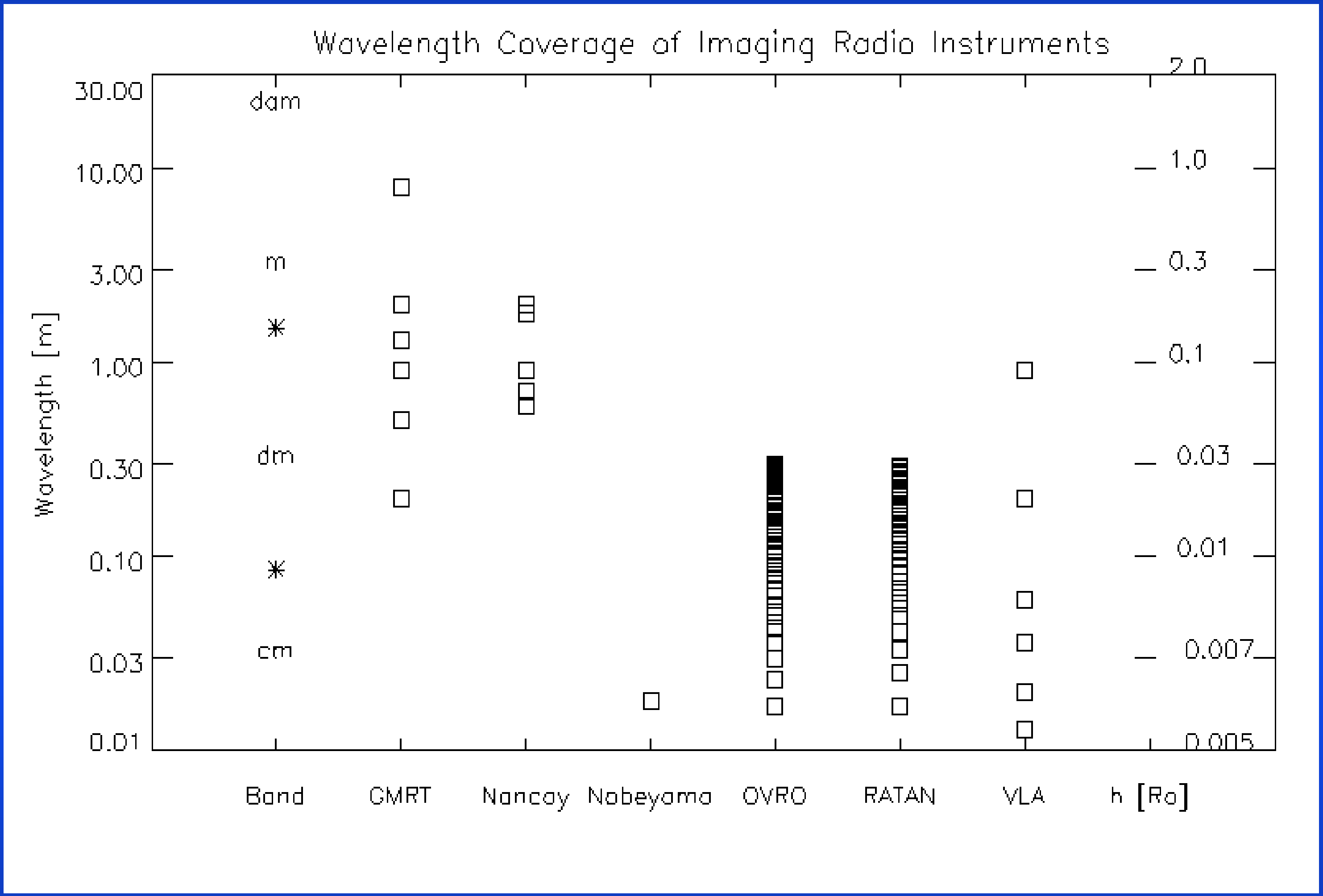

The Local Plasma Frequency and Radio Wave Propagation

The local plasma frequency $f_p = f_p(R,\theta,\varphi)$

- is a nonlinear functional of the plasma electron density N_e
- is a nonlinear functional of the radial distance R
- determines propagative and non-propagative conditions:
    - $f_{wave} > f_p$ propagation
    - $f_{wave} = f_p$ reflection
      (vanishing refraction index $\mu^2=1-(f_p/f_{wave})^2=0$)
    - $f_{wave} < f_p$ absorption (imaginary refraction index)

THE FREQUENCY-DENSITY-HEIGHT RELATION

Characterization of the Solar Atmosphere

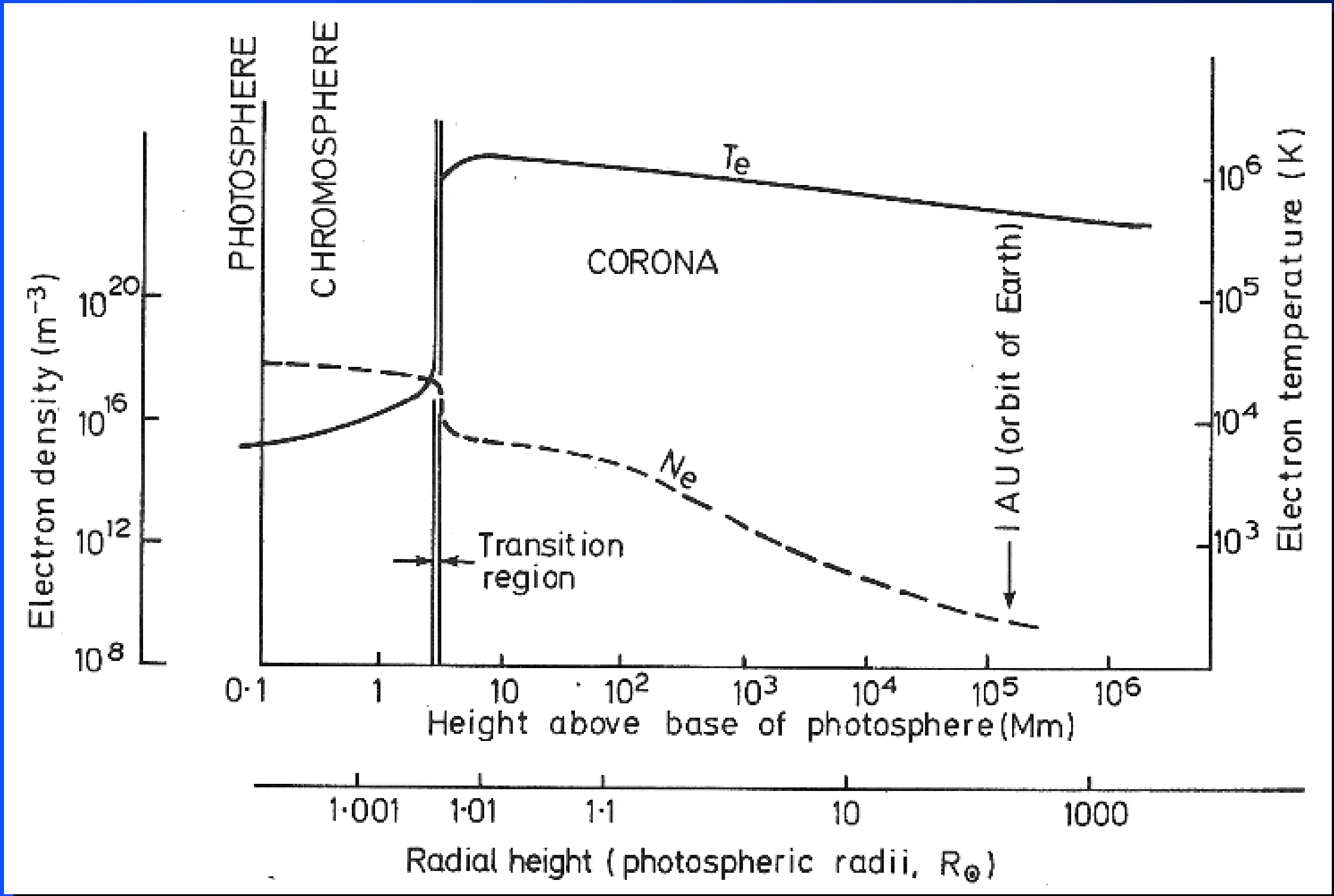

McLean & Labrum (1985)

Coronal Plasma Frequency

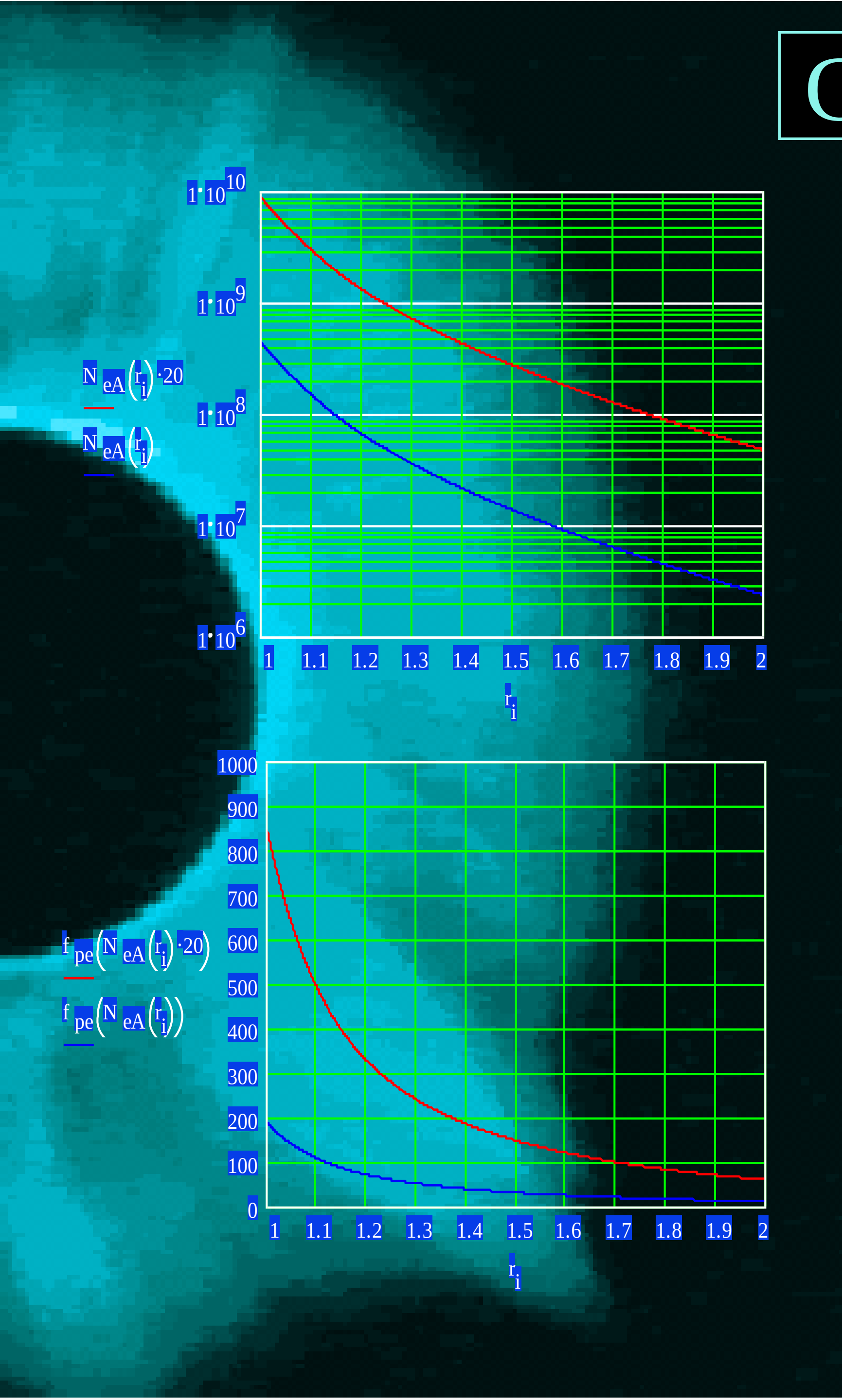

Coronal Density Model (Allen, 1947)

$$N_{eA}(r) := \left(1.55\cdot 10^{8}\cdot r^{-6} + 2.99\cdot 10^{8}\cdot r^{-16}\right)$$

Electron Plasma Frequency [MHz]

$$f_{pe}(N_e) := 8973\cdot 10^{-6}\cdot\sqrt{N_e}$$

Coronal Radio Diagnostic

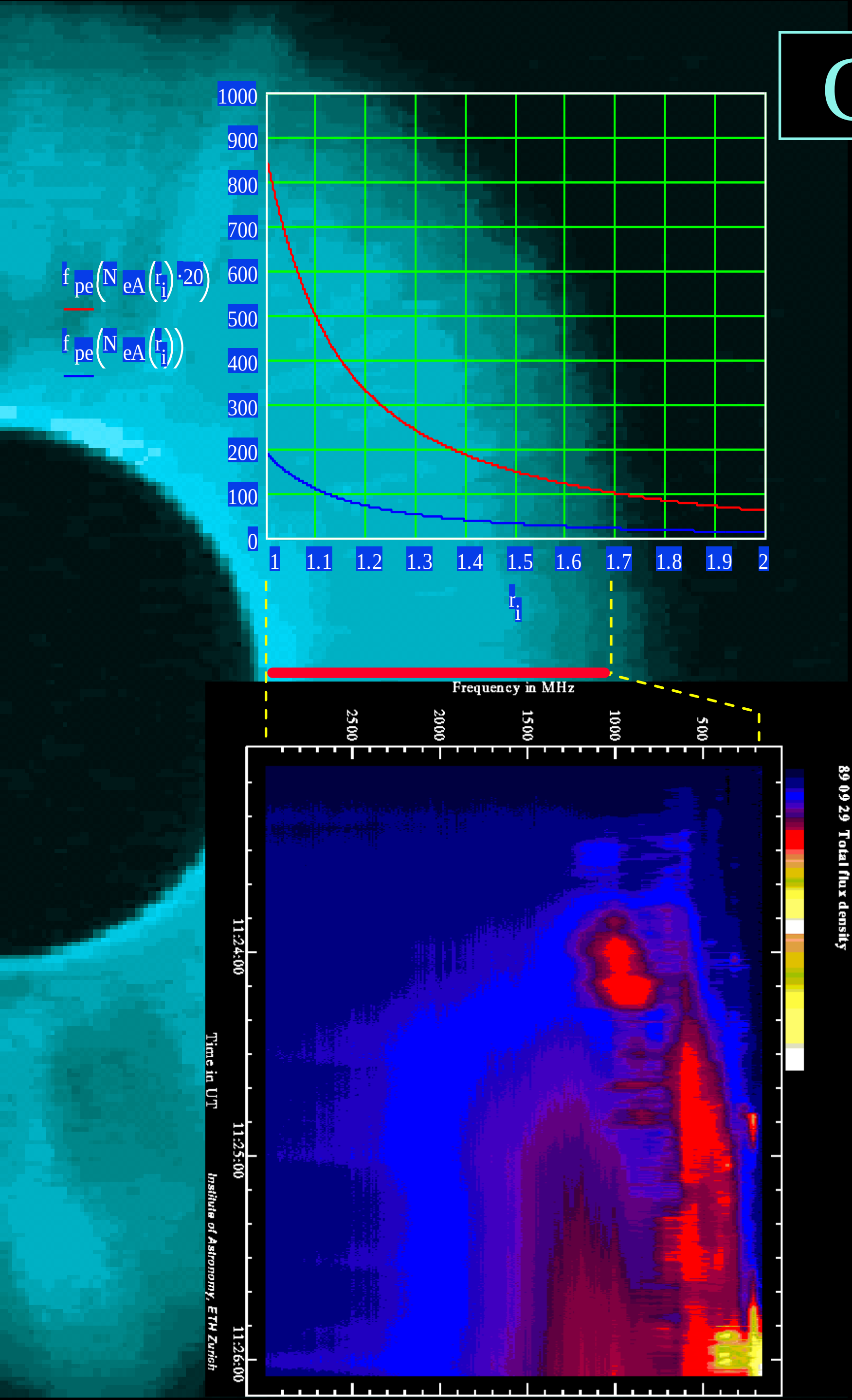

$f_{pe} = f_{pe}(\, N_e \,)$

$N_e = N_e(\, r \,)$

$f_{pe} = f_{pe}(\, r \,)$

EM Waves with frequency f propagate if and only if

$f \geq f_{pe}(r)$

i.e. are emitted by the layer at radial distance r

Radio Spectrum

$S = S\,(\, f \,,\, t \,)$

RADIO SIGNATURES OF PARTICLE BEAMS

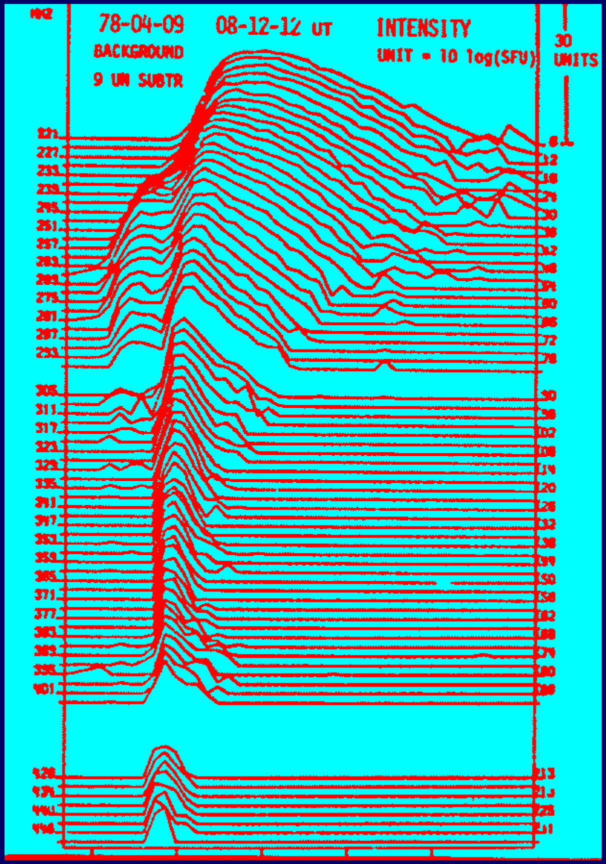

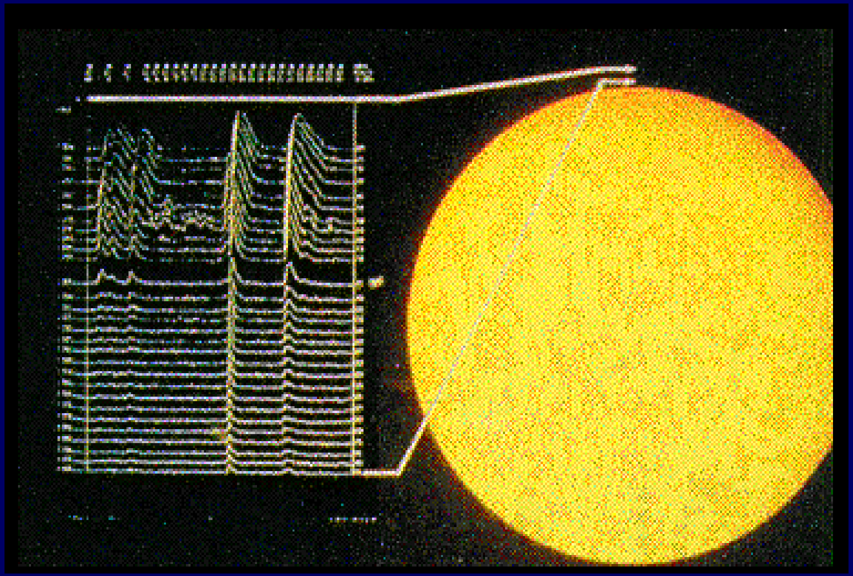

TYPE III RADIO BURST

CORONAL DENSITY MODELS

UNPERTURBED SOLAR ATMOSPHERE
BASIC MODEL

- Two-components plasma with uniform distribution of kinetic temperature:
  1) chromosphere with $T = 2 \times 10^4$ K
  2) corona with $T = 2 \times 10^6$ K

  with a net separation at $h = 10^4$ km above the photosphere, i.e. at R = 1.0144 solar radii from Sun's center

- Spherical symmetry for the electron density distribution as a function of the radial distance R: $N_e(R, \vartheta, \varphi) \equiv N_e(R)$ which assumes different forms in the two different plasma regimes

UNPERTURBED SOLAR ATMOSPHERE
MODEL ELECTRON DENSITY FOR THE CHROMOSPHERE

- ISOTHERMAL CHROMOSPHERE
- $h \in [5 \cdot 10^2\,\mathrm{km},\ 10^4\,\mathrm{km}]$
- R $\in$ $[1.0007\,R_\odot, 1.0144\,R_\odot]$
- exponential function (Zheleznyakov, 1970):

$$N_e(R) = 5.7 \cdot 10^{11} \exp\{-535.92\,[R - (1 + 718.39 \cdot 10^{-6})]\}\ \mathrm{cm}^{-3}$$

UNPERTURBED SOLAR ATMOSPHERE

MODEL ELECTRON DENSITY FOR THE INNER CORONA

- ISOTHERMAL CORONA
- $R \in (1.0144\, R_\odot, 3\, R_\odot]$
- power-law function (Allen, 1947; Baumbach, 1937):

$$N_e(R) = 10^8\, (1.55\, R^{-6} + 2.99\, R^{-16})\ \mathrm{cm}^{-3}$$

- power-law function from K corona (Newkirk, 1961):

$$N_e(R) = N_0 \cdot 10^{\frac{4.32}{R}}\ \mathrm{cm}^{-3} \qquad N_0 = 4.2 \cdot 10^4$$

- non-spherical, axisymmetric model (Saito et al., 1977):

$$N_e(R) = (1.36 \cdot 10^6\, R^{-2.14} + 1.68 \cdot 10^8\, R^{-6.13})\ \mathrm{cm}^{-3}$$

which fits better the observed quiet corona

MORE REFINED, RECENT MODELS EXIST (e.g. Clette, 1997)

UNPERTURBED SOLAR ATMOSPHERE
MODEL ELECTRON DENSITY
FOR THE OUTER CORONA

- PLASMA REGIME TYPICAL OF SOLAR WIND WHICH FEEDS THE IPM AT SUPERSONIC VELOCITIES

- conservation of particle flux with increasing R $\Rightarrow$

- inverse power-law dependence on R as R^{-2}

- model from optical eclipse observations (Blackwell and Petford, 1966):

$$N_e(R) = 1.46 \cdot 10^6 \, R^{-2.3} \ \mathrm{cm}^{-3}$$

CHARACTERIZATION OF SOLAR ACTIVITY FEATURES

Solar Activity Features	
Attribute	Interpretation
Radial location	Layer of occurrence
Surface location	Heliographical coordinates
Morphology	Form factor
Topology	Structural factor
Lifetime	Observational persistence
Time evolution	Temporal modifications
Energetics	Involved energy release
Radiation	Enhanced emission of radiation

LARGE-SCALE PLASMA FEATURES

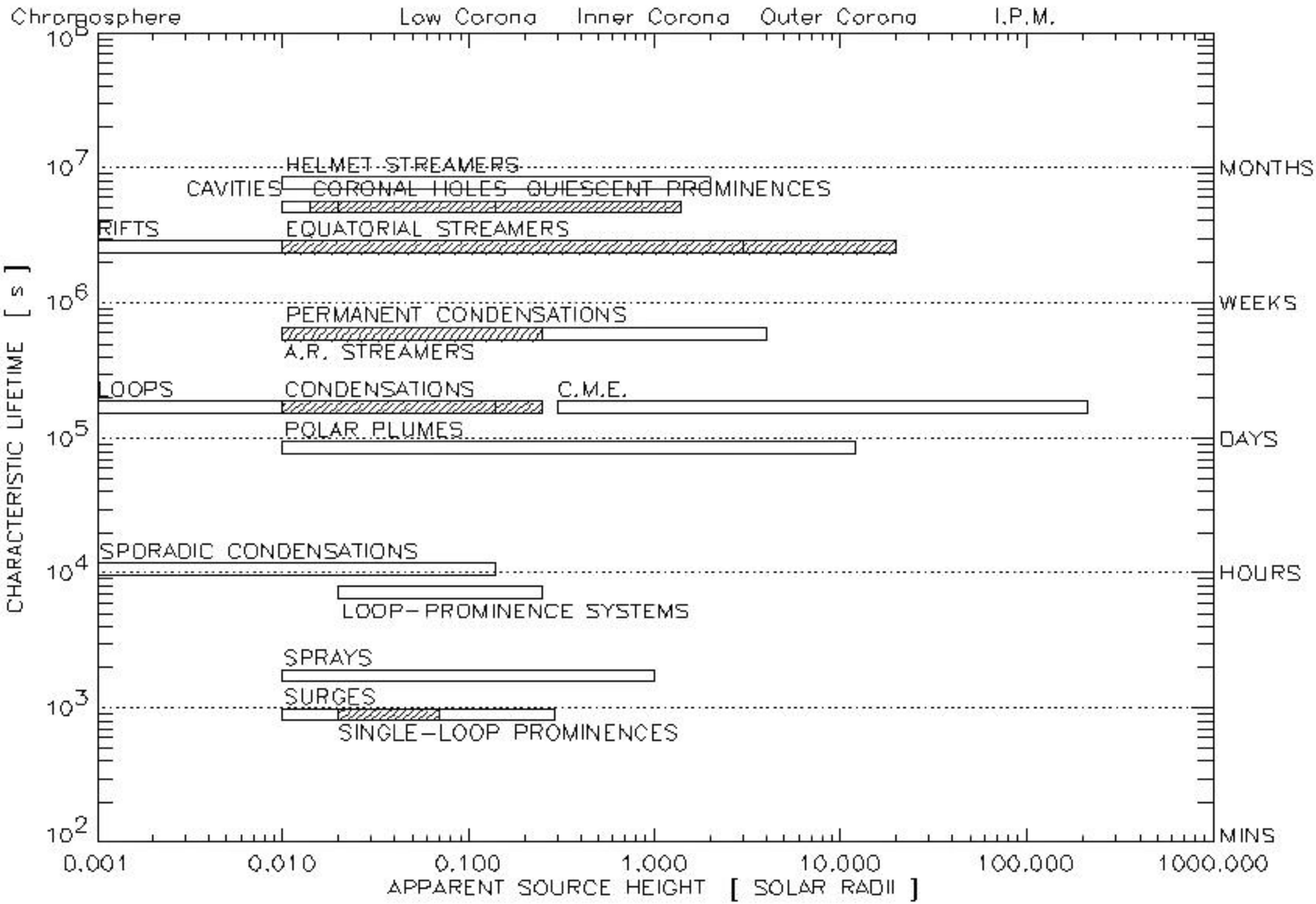

PERTURBED SOLAR ATMOSPHERE

MODEL ELECTRON DENSITY FOR THE ACTIVE INNER CORONA

- Coronal plasma above Active Regions
- Coronal structures, e.g. Streamers
- Coronal density model derived from observed quiet K corona
- Multiplicative factor ranging from 2 to 20
  - Quiet corona: {Newkirk x 1 } or {Saito x 1 }
  - Coronal structure: {Newkirk x 20} or {Saito x 20}

SUMMARY OF ELECTRON DENSITY MODELS
FOR THE CORONA AND THE IPM

Density model (Equation)	R_{min} $[R_\odot]$	R_{max} $[R_\odot]$	N_e^{max} [cm^{-3}]	N_e^{min} [cm^{-3}]	f_{pe}^{max} [MHz]	f_{pe}^{min} [MHz]
Zheleznyakov (2)	1.0144	1.0129	$3.88 \cdot 10^{11}$	$8.19 \cdot 10^{08}$	5588	257
Baumbach-Allen (3)	1.0172	2.5	$3.67 \cdot 10^{08}$	$6.35 \cdot 10^{05}$	172	7
Newkirk $\times$ 1 (4)	"	"	$7.42 \cdot 10^{08}$	$2.25 \cdot 10^{06}$	244	13
Saito $\times$ 1 (5)	"	"	$1.53 \cdot 10^{08}$	$8 \cdot 10^{05}$	111	8
Blackwell-Petford (6)	3	30	$1.17 \cdot 10^{05}$	584.7	3	0.22
" (6)	50	214.9	181	6.3	0.12	0.02
Newkirk $\times$ 20 (4)	1.0172	2.5	$1.48 \cdot 10^{10}$	$4.49 \cdot 10^{05}$	1093	60
Saito $\times$ 20 (5)	"	"	$3 \cdot 10^{09}$	$1.6 \cdot 10^{07}$	496	36

AVERAGE SOURCE HEIGHT FOR SOLAR RADIO EMISSIONS

WITH THE DUE CAUTIONS AND ADOPTING THE PROPER CORRECTIONS WHEN MODELLING, WE CAN SAY THAT SOLAR RADIO EMISSIONS OCCUR IN THE FOLLOWING BANDS ACCORDING TO THE LOCATION OF THE SOURCE:

- mm chromosphere to low corona
- cm low corona
- m inner corona
- dam outer corona
- hm IPM
- km IPM to 1 AU

ELECTRON DENSITY MODEL
(UNPERTURBED CORONA)
(Newkirk, 1961)

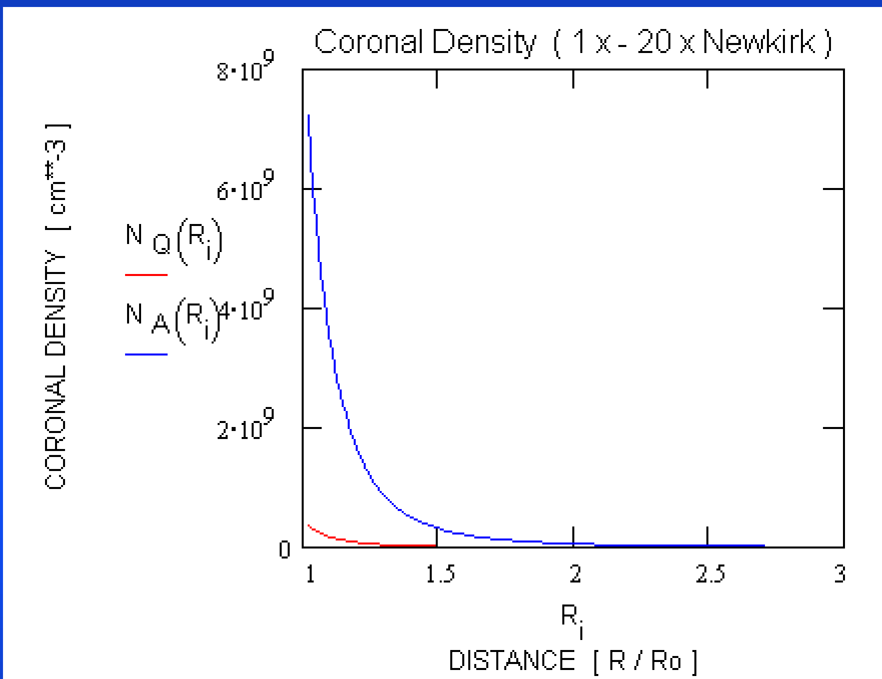

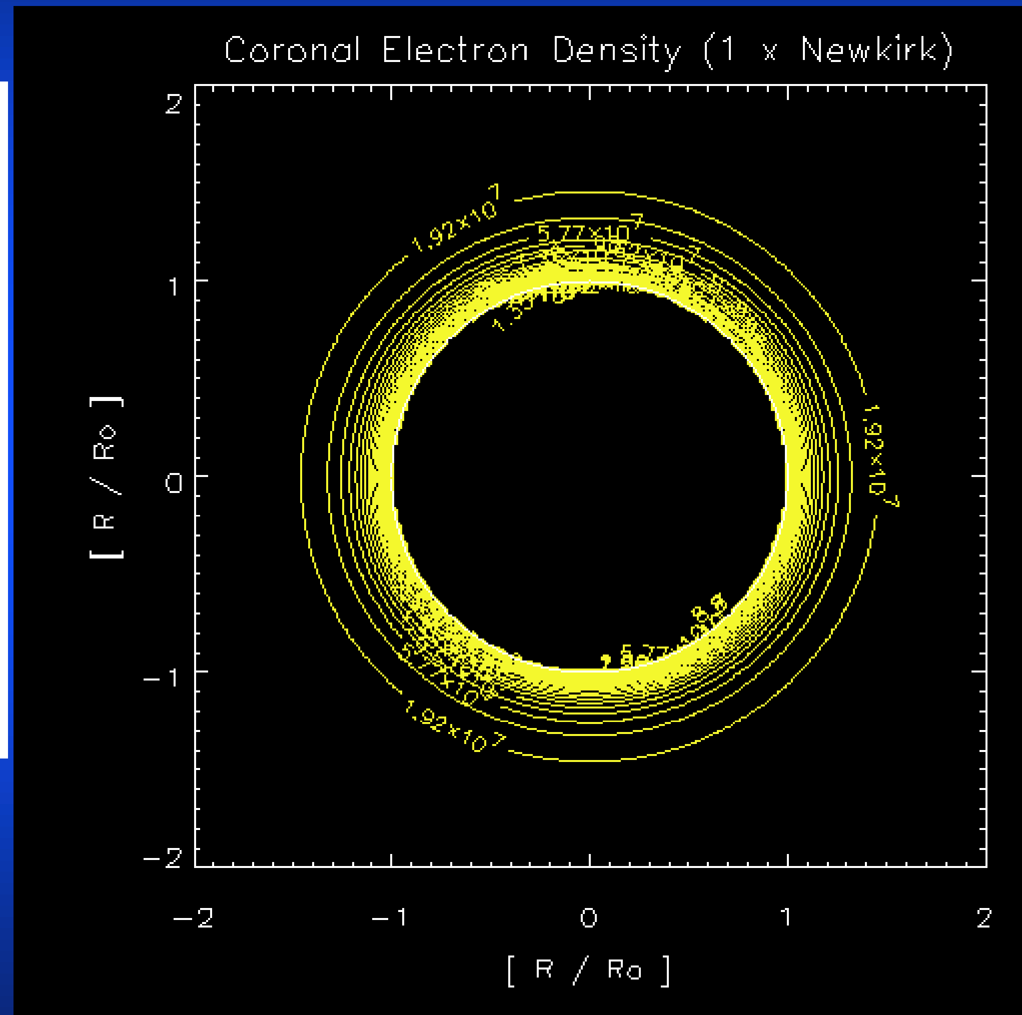

$N_0 := 2.1 \cdot 10^4$

$$N_Q(R) := N_0 \cdot 10^{\frac{4.32}{R}}$$

$N_A(R) := n \cdot N_Q(R)$

$n := 20$

ELECTRON DENSITY MODEL: UNPERTURBED CORONA
(Newkirk, 1961)

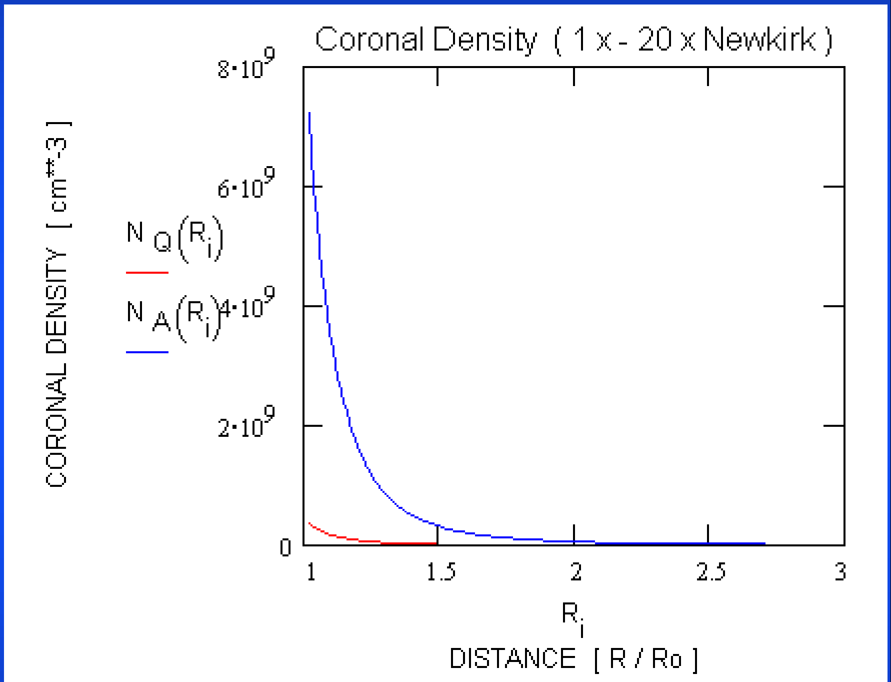

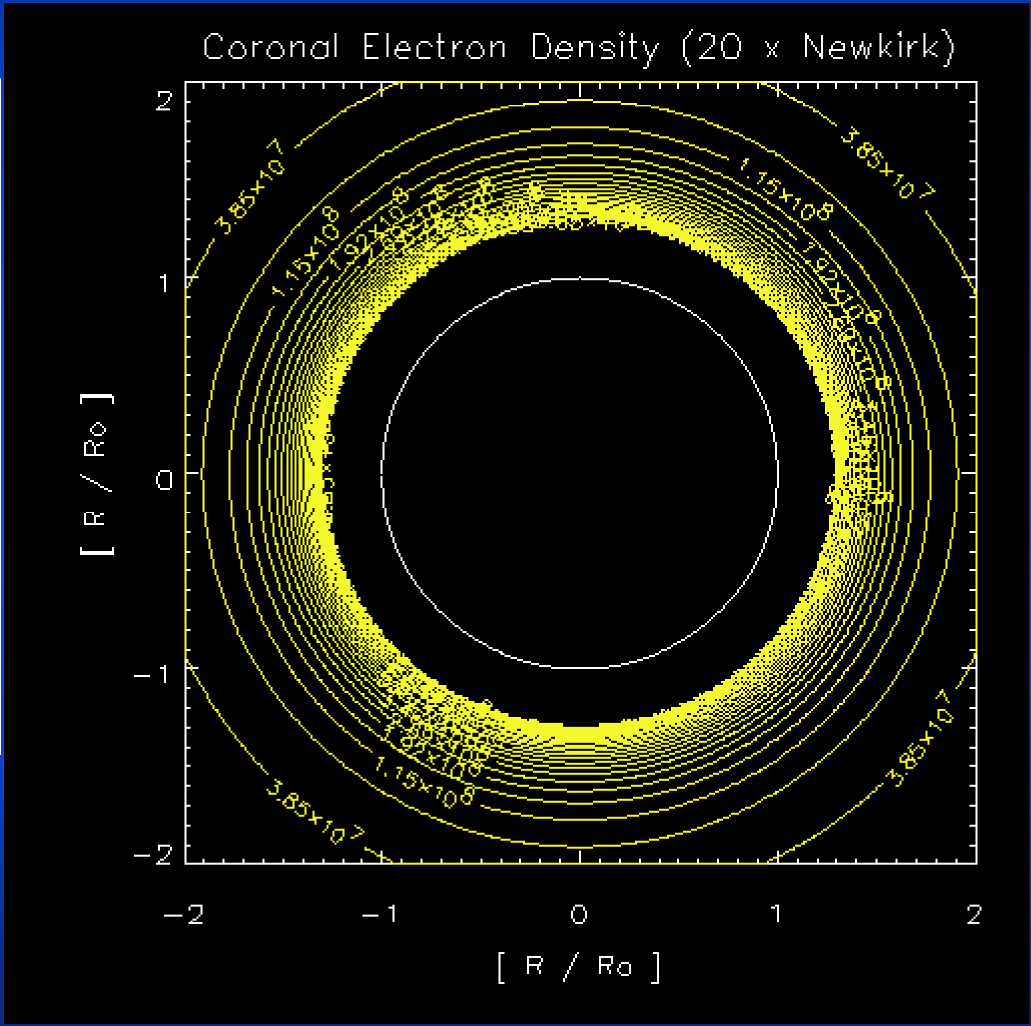

$N_A(R) := n \cdot N_Q(R)$ $n := 20$

ELECTRON DENSITY MODEL: CORONAL CONDENSATION (Newkirk, 1961)

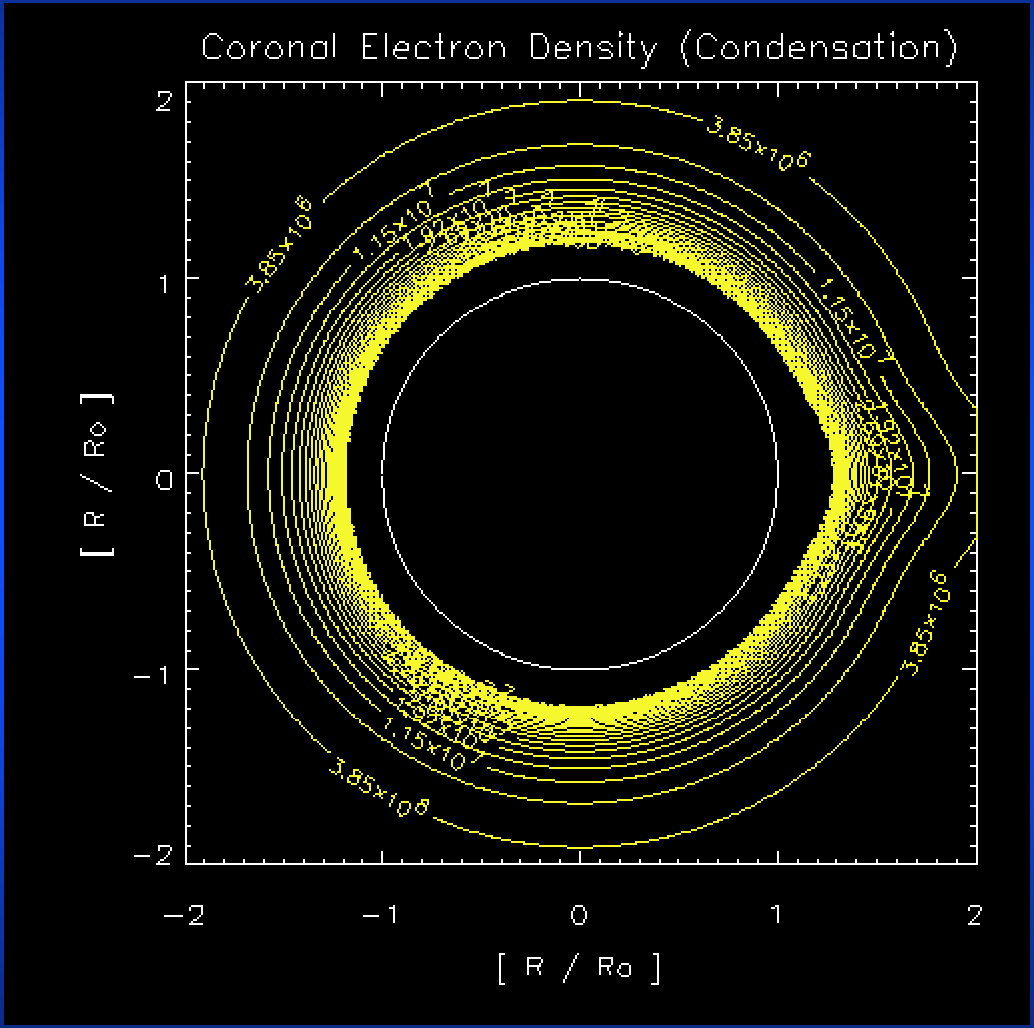

$$N_C(R,x,y) := N_Q(R)\cdot\left[1 + 0.97\cdot\exp\left[-\frac{(y-R)^2+(x)^2}{2\cdot(0.235)^2}\right]\right]$$

ELECTRON DENSITY MODEL: SMOOTH STREAMER
(Itkina and Levin, 1992)

$$N_{IL}(R,\theta,R_0,\theta_s,\Delta\theta,A_1,A_2,M) := N_Q(R)\cdot\left(1 + A_1\cdot \exp\left(-q(R,\theta,R_0,\theta_s,\Delta\theta)^2\right)\right)\cdot\left(1 + A_2\cdot\cos\left(M\cdot q(R,\theta,R_0,\theta_s,\Delta\theta)\right)^2\right)$$

$$q(R,\theta,R_0,\theta_s,\Delta\theta) := \frac{R}{R_0}\cdot\frac{\theta-\theta_s}{\Delta\theta}$$

$R_0 := 1.2$ radial distance of the sou

$\theta_s := \frac{\pi}{2}$ heliocentric longitude of streamer

$\Delta\theta := \frac{\pi}{6}$ streamer width in longit

streamer intensity fibers number fibers int

$A_1 := 5$ $M := 0$ $A_2 := 0$ SMOOTH STREAME

SMOOTH STREAMER: DENSITY CONTOURS
(Itkina and Levin, 1992)

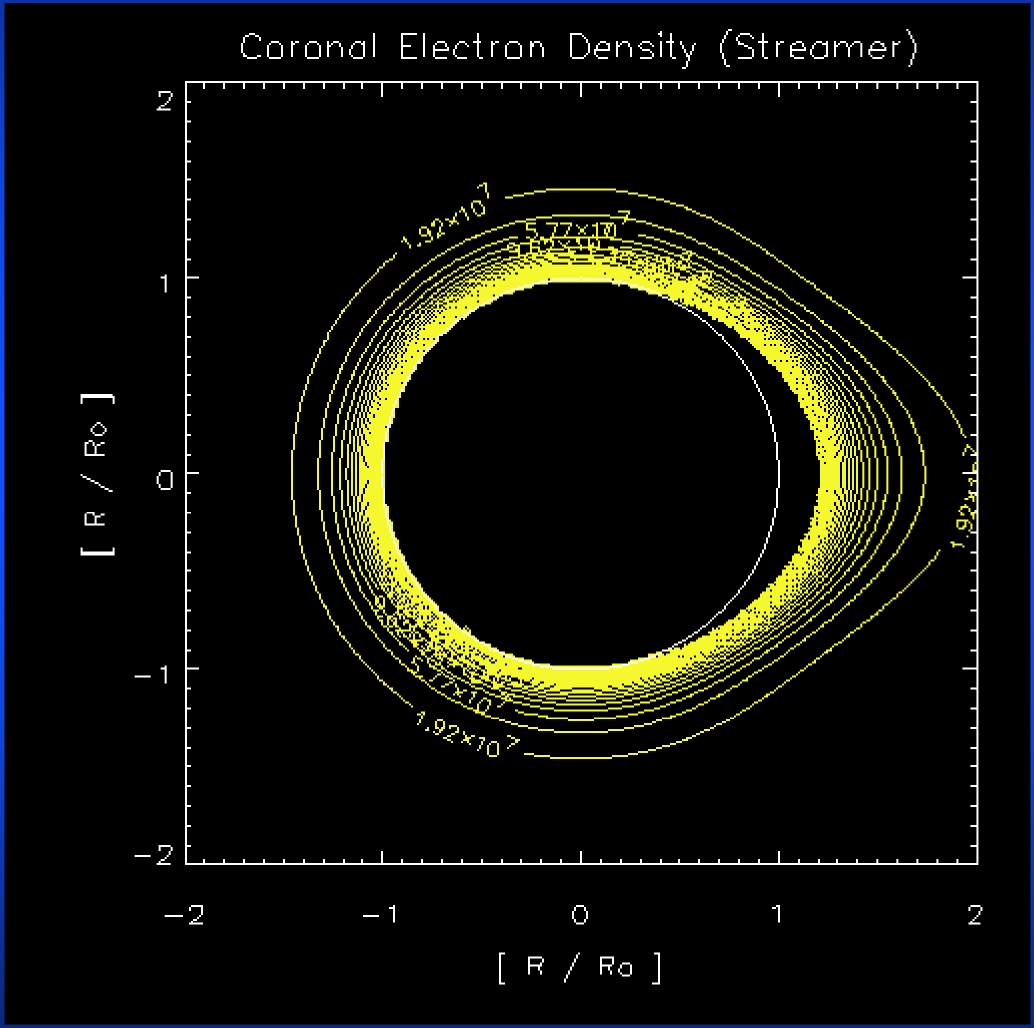

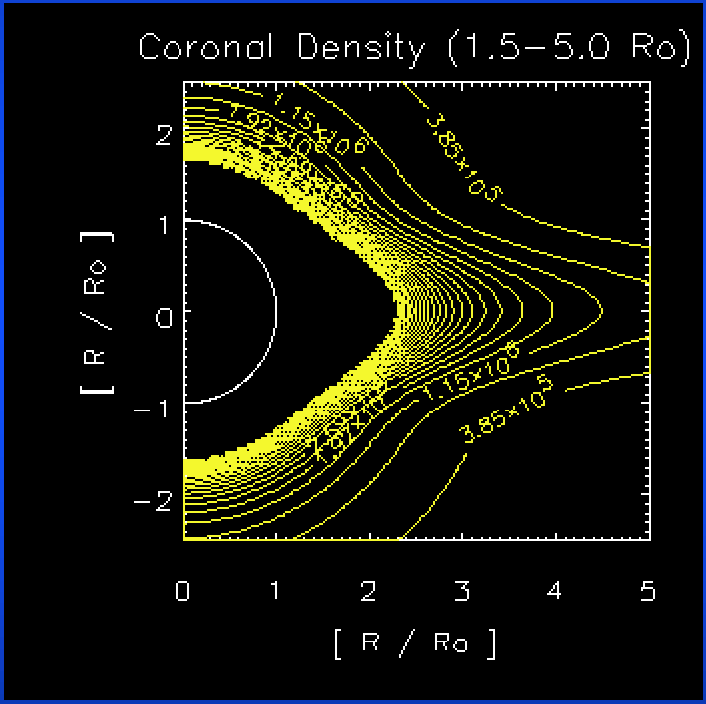

SMOOTH STREAMER: DENSITY PROFILES
(Itkina and Levin, 1992)

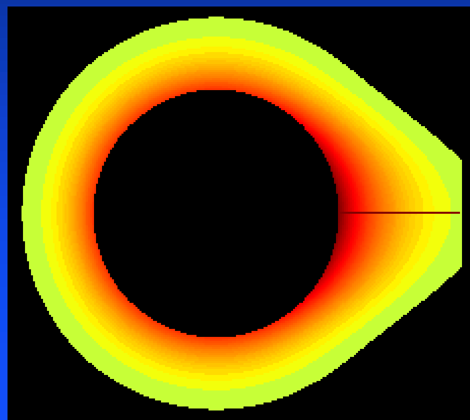

Radial profile

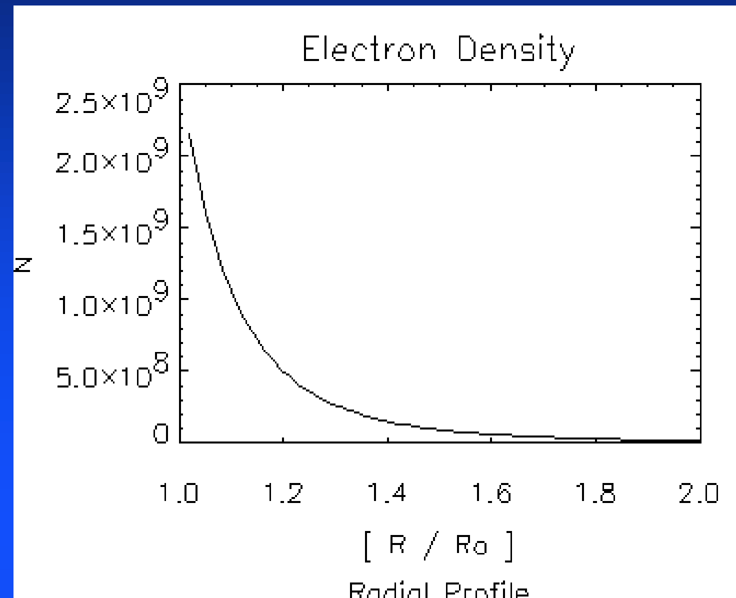

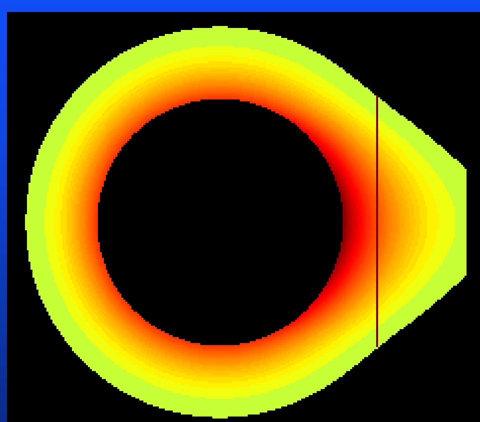

Transverse profile

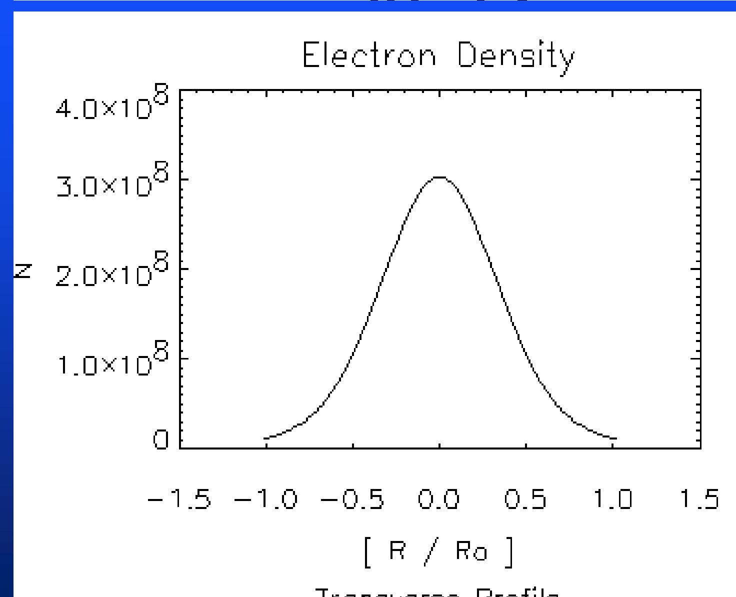

FINE-SCALE PLASMA FEATURES

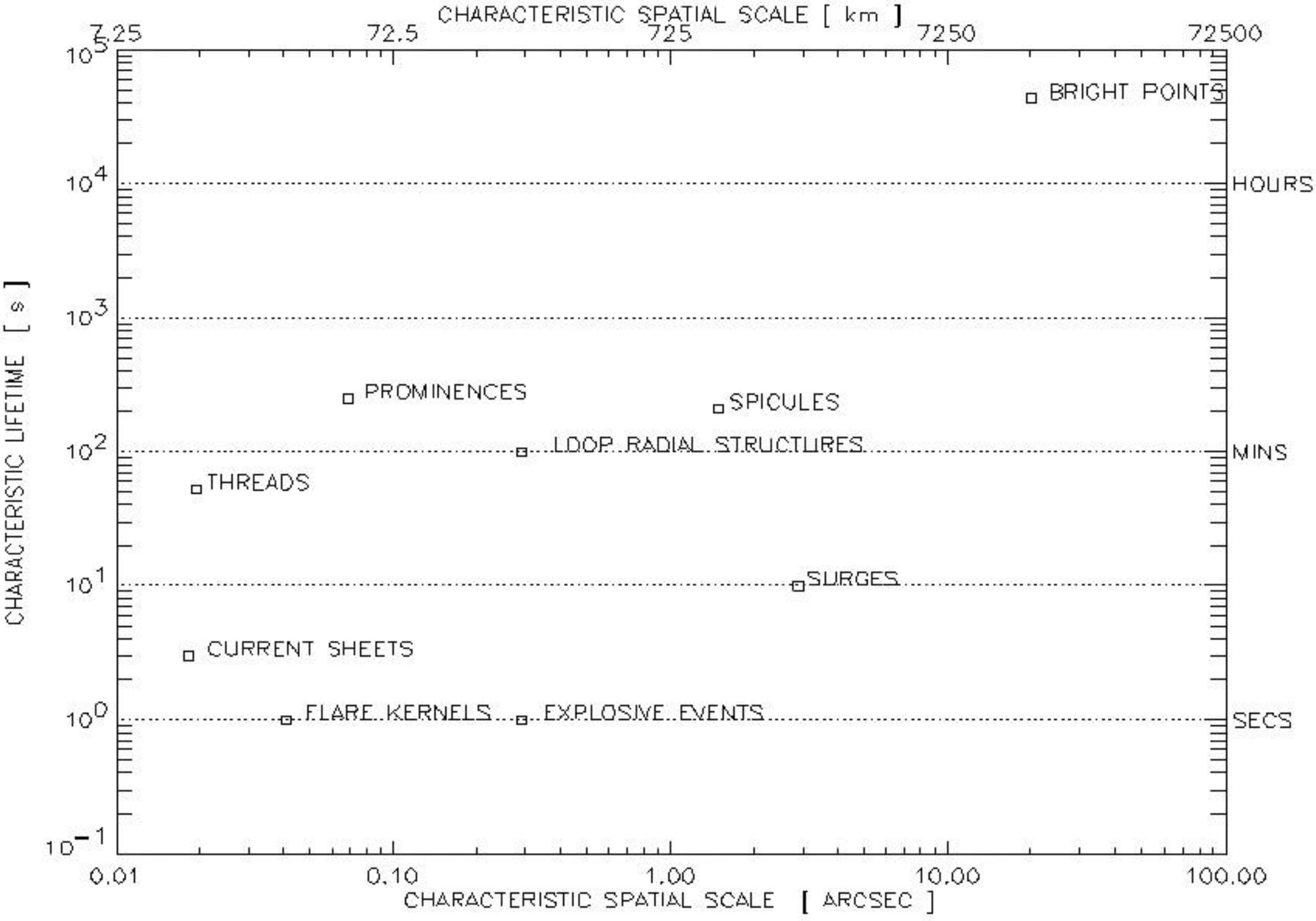

ELECTRON DENSITY MODEL: STREAMER + FIBERS
(Itkina and Levin, 1992)

$$N_{IL}(R,\theta,R_0,\theta_s,\Delta\theta,A_1,A_2,M) := N_Q(R)\cdot\left(1 + A_1\cdot\exp\left(-q(R,\theta,R_0,\theta_s,\Delta\theta)^2\right)\right)\cdot\left(1 + A_2\cdot\cos\left(M\cdot q(R,\theta,R_0,\theta_s,\Delta\theta)\right)^2\right)$$

$$q(R,\theta,R_0,\theta_s,\Delta\theta) := \frac{R}{R_0}\cdot\frac{\theta - \theta_s}{\Delta\theta}$$

$R_0 := 1.2$ radial distance of the sou

$\theta_s := \frac{\pi}{2}$ heliocentric longitude of streamer

$\Delta\theta := \frac{\pi}{6}$ streamer width in longit

streamer intensity fibers number fibers int

$A_1 := 5$ $M := 12$ $A_2 := 1$ STREAMER WITH SMALL SCA
STRATIFICATION

STREAMER + FIBERS: DENSITY CONTOURS
(Itkina and Levin, 1992)

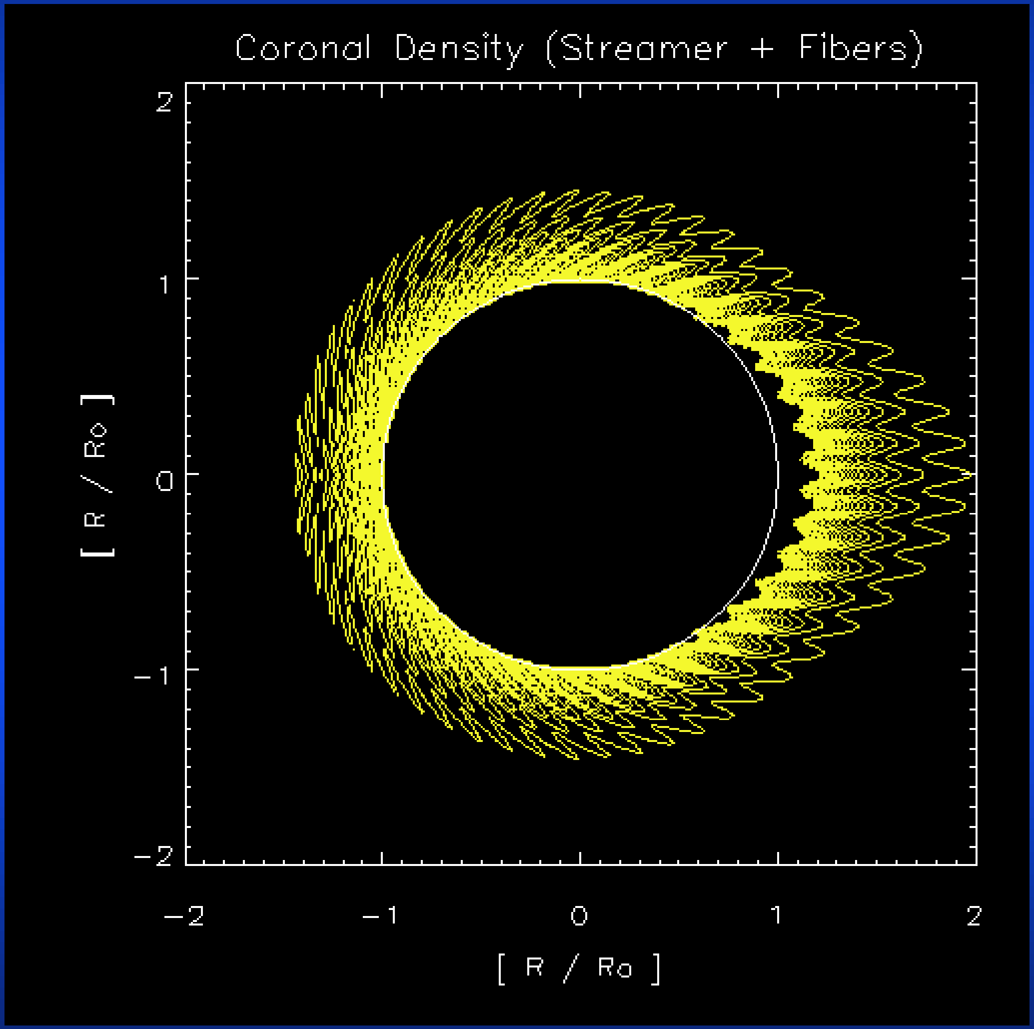

STREAMER + FIBERS: RADIAL DENSITY PROFILES
(Itkina and Levin, 1992)

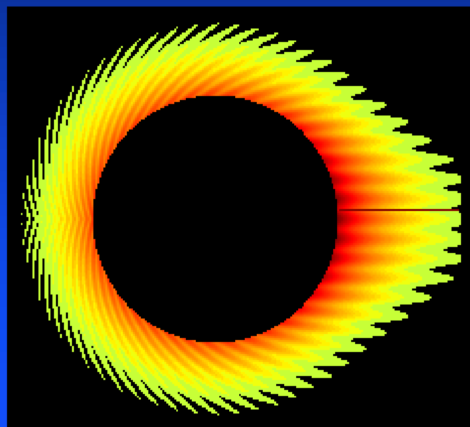

Radial profile off-fiber

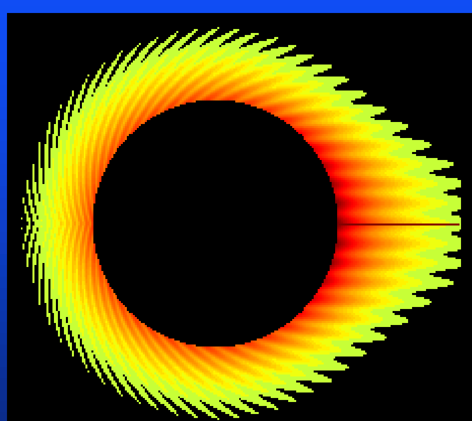

Radial profile in-fiber

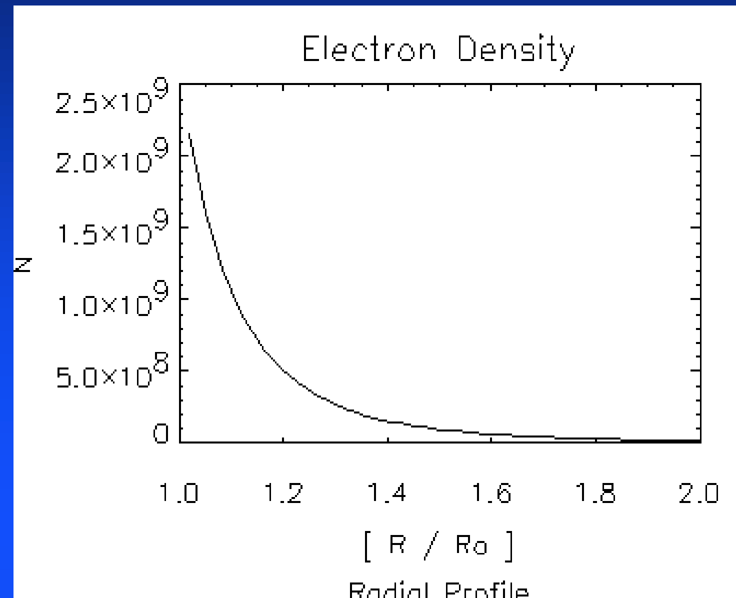

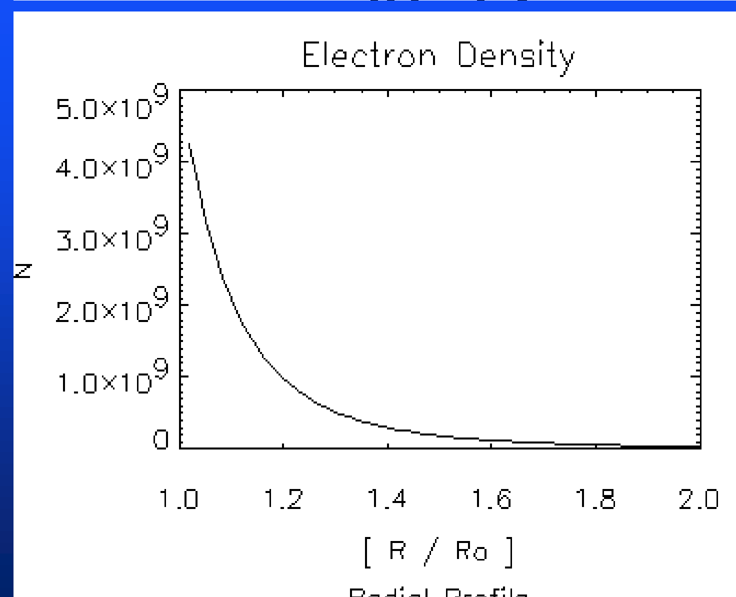

STREAMER + FIBERS: TRANSVERSE DENSITY PROFILE (Itkina and Levin, 1992)

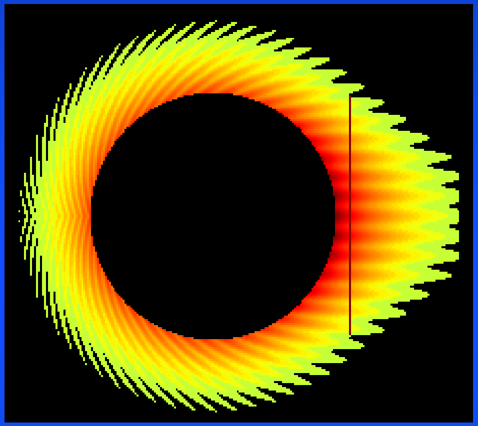

Transverse profile

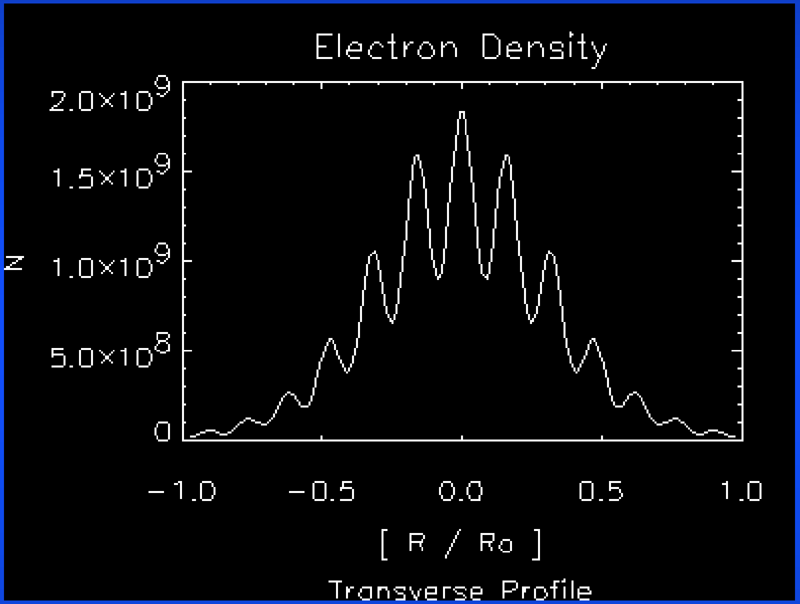

EFFECTS OF DENSITY INHOMOGENEITIES ON RADIO WAVE PROPAGATION

Refraction of Radio Waves on Large-Scale Coronal Structures

$$n = (1 - \omega_p{}^2 / \omega^2)^{1/2}$$

$$\bar{v}_g = cn\hat{k}$$

$$\frac{d\bar{x}}{ds} = \hat{k}$$

$$\frac{d(n\hat{k})}{ds} = \frac{\partial n}{\partial \bar{x}}$$

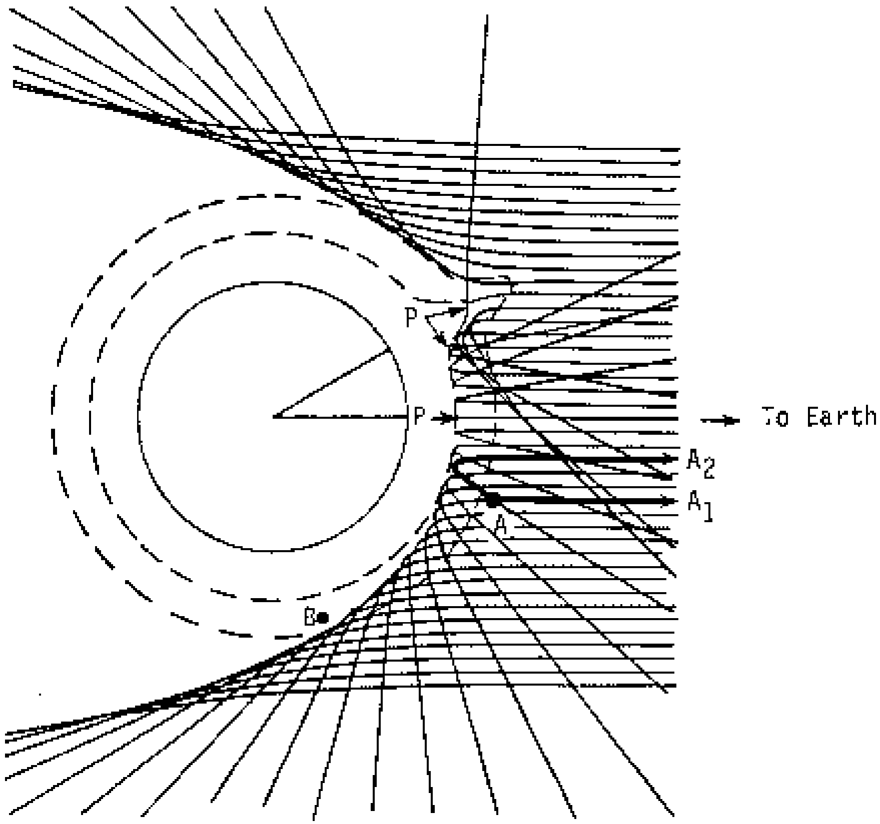

McLean and Melrose (1985)

Refraction makes the radiation more directive

Refraction and Scattering of Radio Waves on Random Coronal Inhomogeneities

$$\langle \delta^2 \rangle^{1/2} = 0.94 (f_p / f)^2 (\varepsilon^2 / h)^{1/2} (\delta s)^{1/2}$$

R.M.S. ANGULAR DEVIATION

$\varepsilon \to$ *r.m.s. relative fluctuation* $\Delta N_e / N_e$

$h \to$ *correlation coefficient of fluctuations*

Steinberg et al. (1971)

$\varepsilon = 10^{-2} \; h = 5 \cdot 10^{-5} R_o$

Riddle (1974)

$\varepsilon = 0.02 \; h = 5 \cdot 10^{-4}$

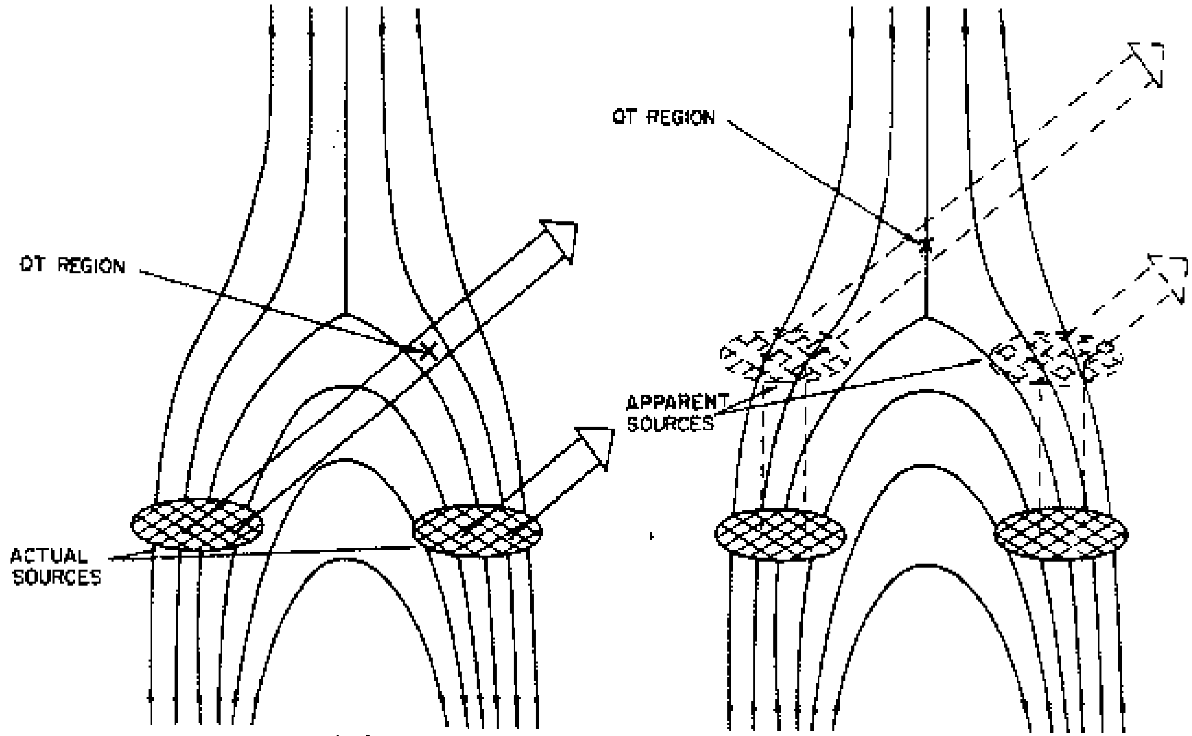

Melrose, 1973; Elgaroy, 1977

Scattering makes the radiation less directive and increases the apparent source size. Bastian (1994) has pointed out that angular broadening is relevant to frequencies of several GHz or more and limits the angular resolution at which compact sources can be imaged,

Reflection of Radio Waves on Ordered Coronal Structures (Fibers)

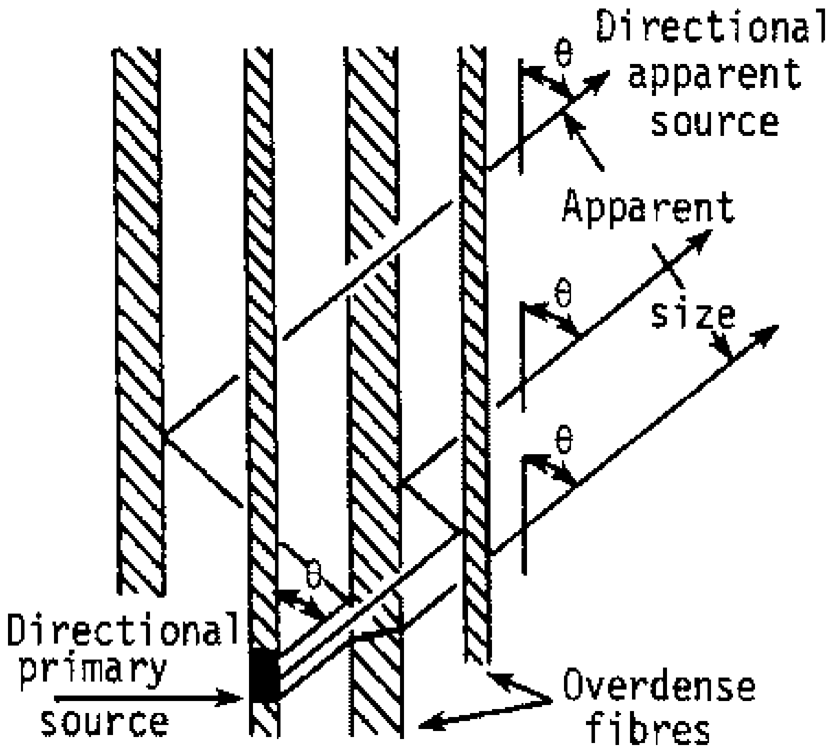

Bougeret and Steinberg (1977)

Reflection maintains the directivity and increases the apparent source size

THE CORONAL PLASMA FREQUENCY

CORONAL PLASMA FREQUENCY: RADIAL PROFILE
(Newkirk x 1 and Newkirk x 20)

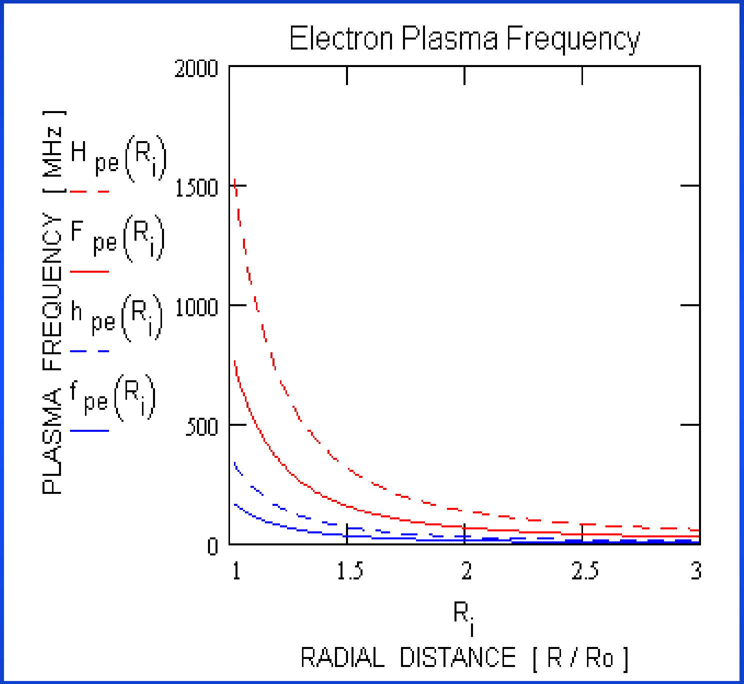

$$f_{pe}(R) := 8.98 \cdot 10^{3} \cdot \sqrt{N_Q(R)} \cdot 10^{-6}$$

$$F_{pe}(R) := 8.98 \cdot 10^{3} \cdot \sqrt{N_A(R)} \cdot 10^{-6}$$

CORONAL PLASMA FREQUENCY:
FREQUENCY CONTOURS
(Newkirk x 1 and Newkirk x 20)

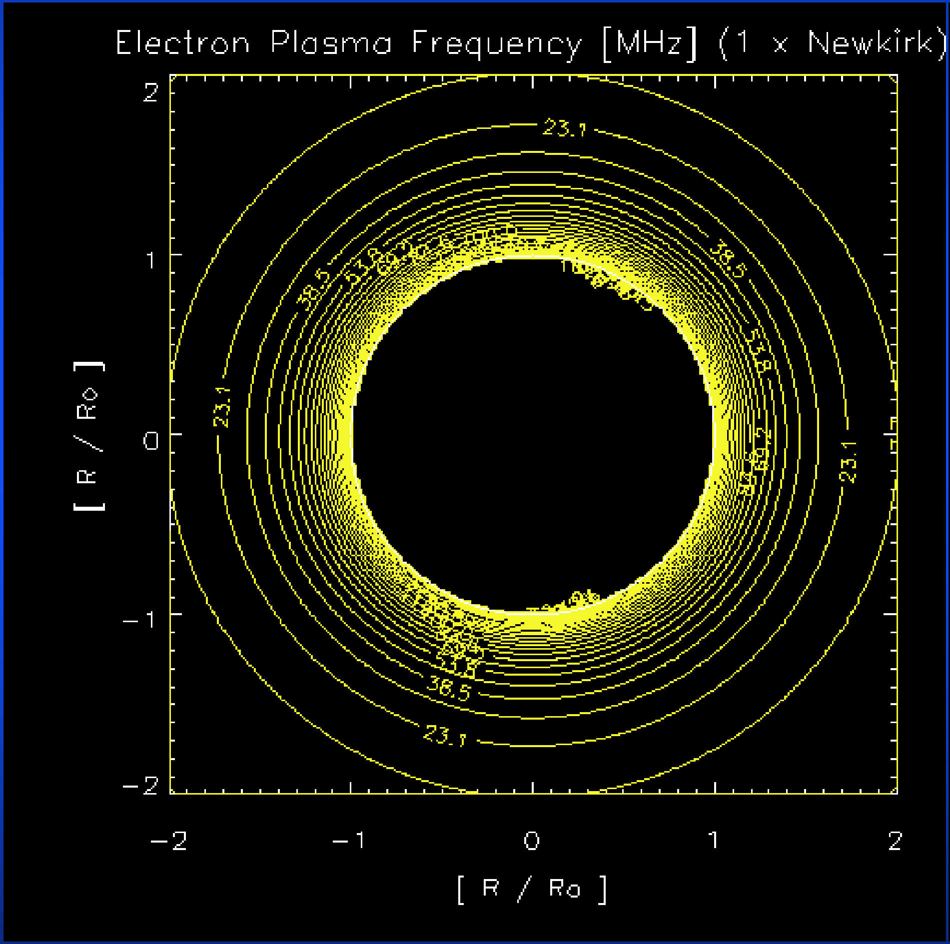

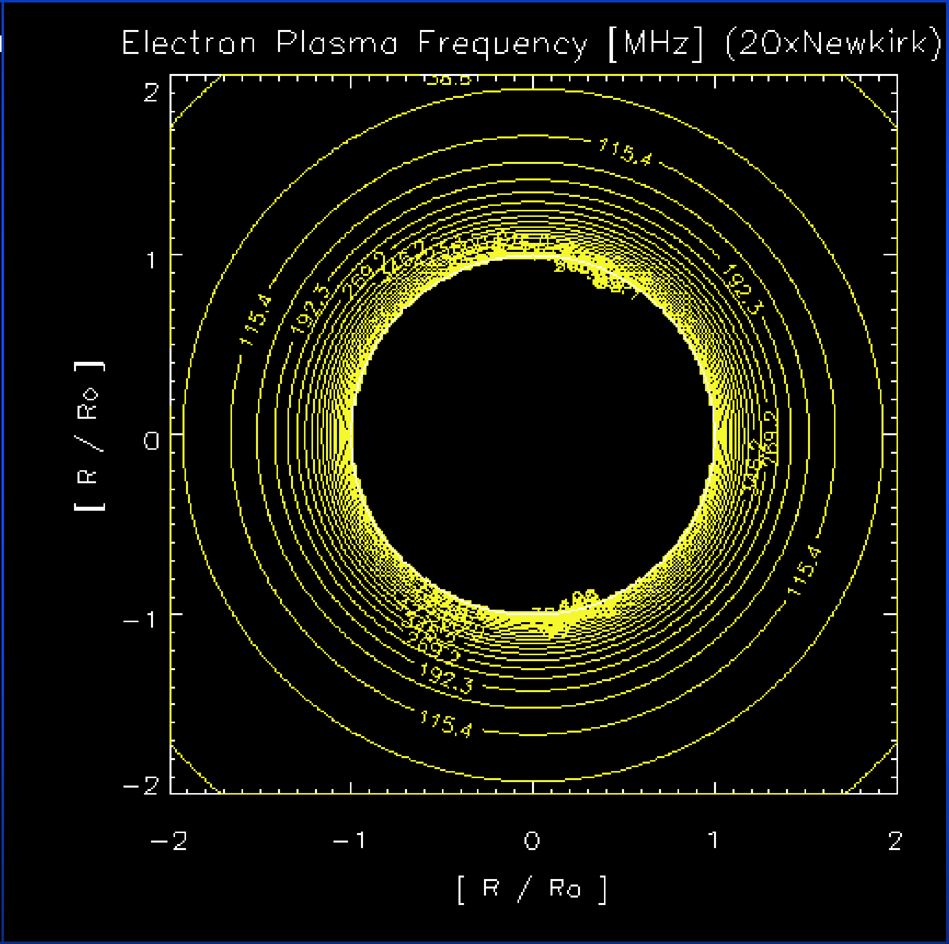

CORONAL PLASMA FREQUENCY:
FREQUENCY CONTOURS
(Coronal Condensation)

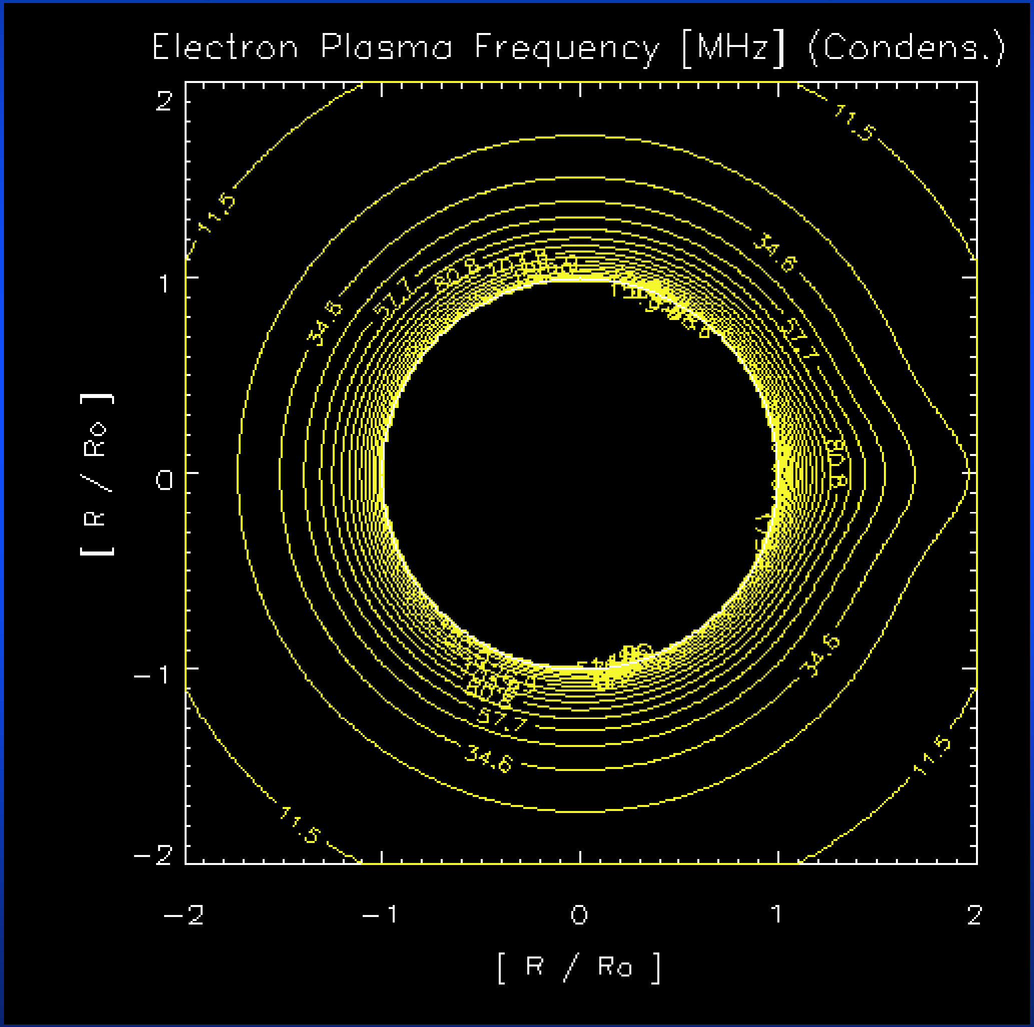

CORONAL PLASMA FREQUENCY:
FREQUENCY CONTOURS
(Smooth Streamer and Streamer with Fibers)

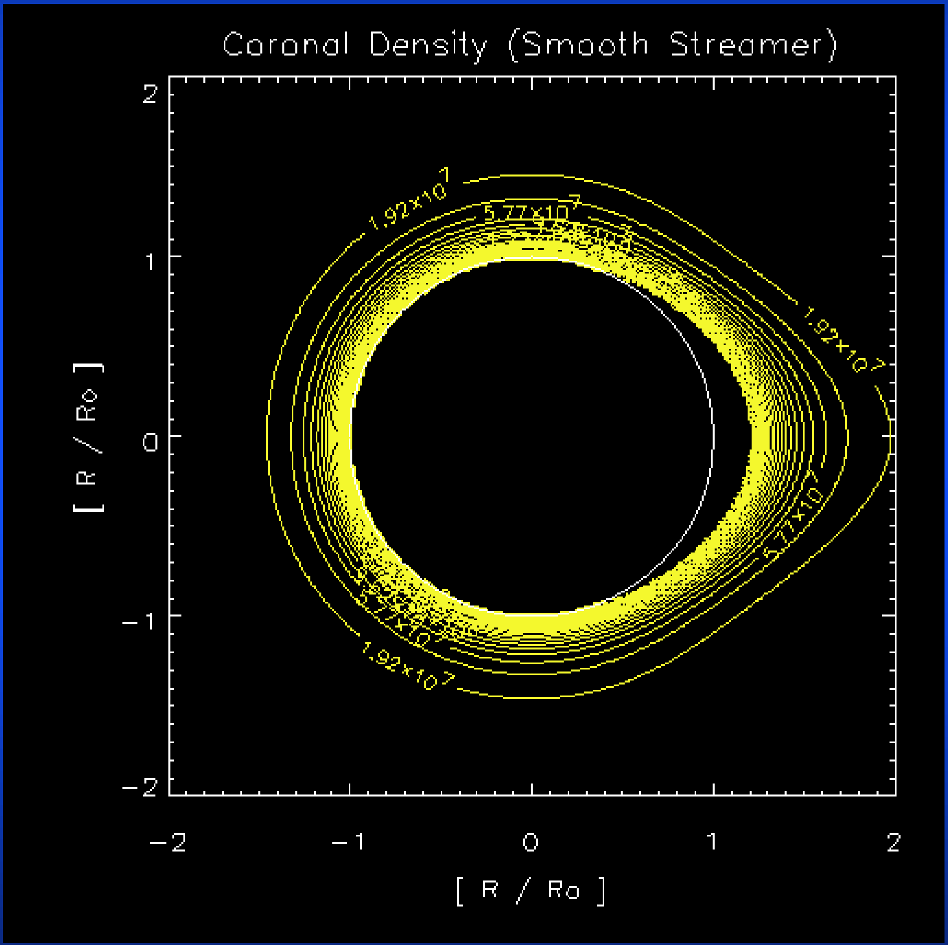

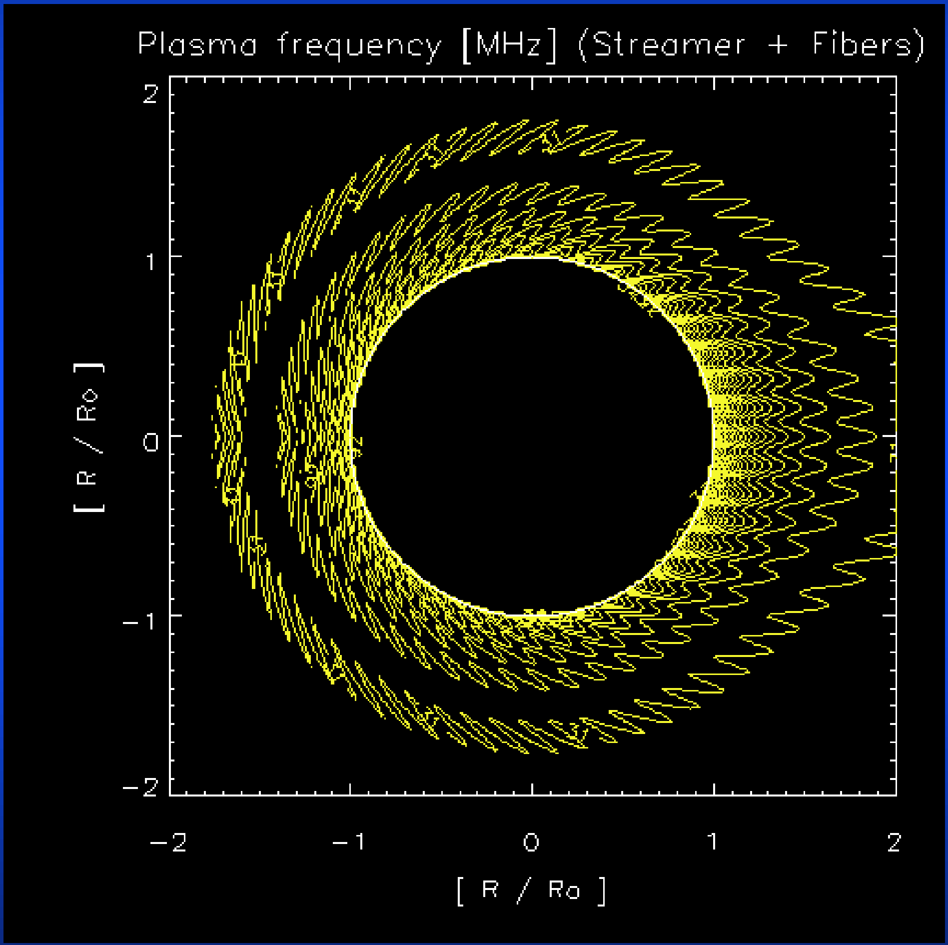

THE CORONAL GYROFREQUENCY

CORONAL MAGNETIC FIELD ABOVE AR
(Dulk and McLean, 1978)

$B_{ar}(R) := 0.5 \cdot (R - 1)^{-1.5}\ G$ (1.02<= R <=1(

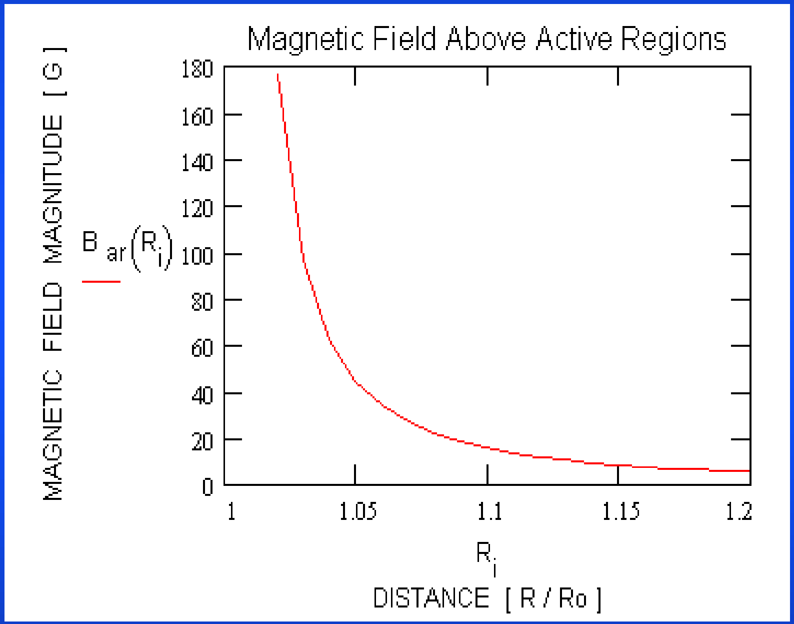

CORONAL GYROFREQUENCY: RADIAL PROFILE
(assuming the Dulk and McLean model)

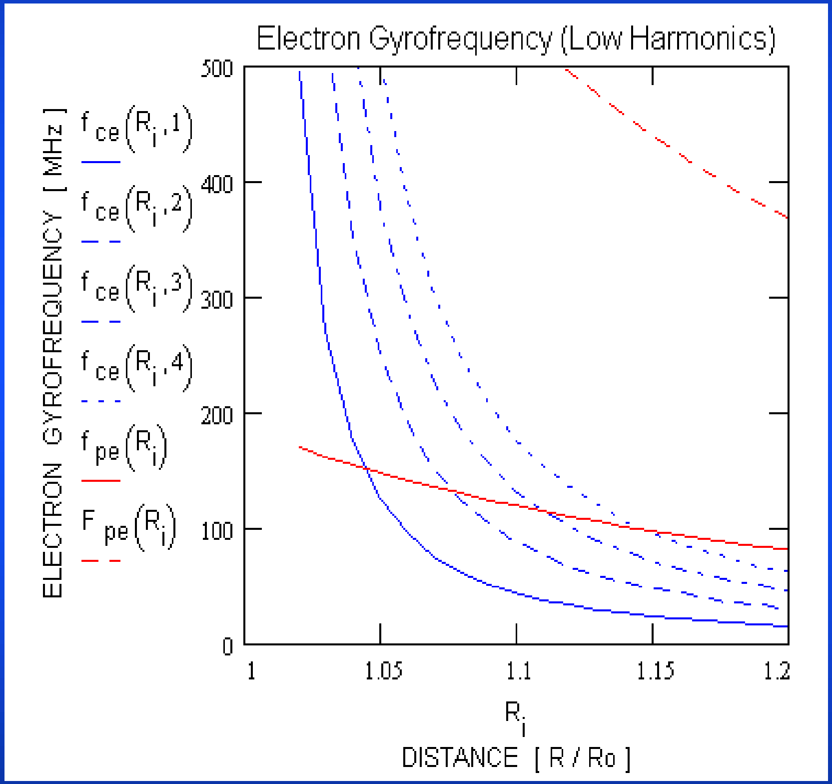

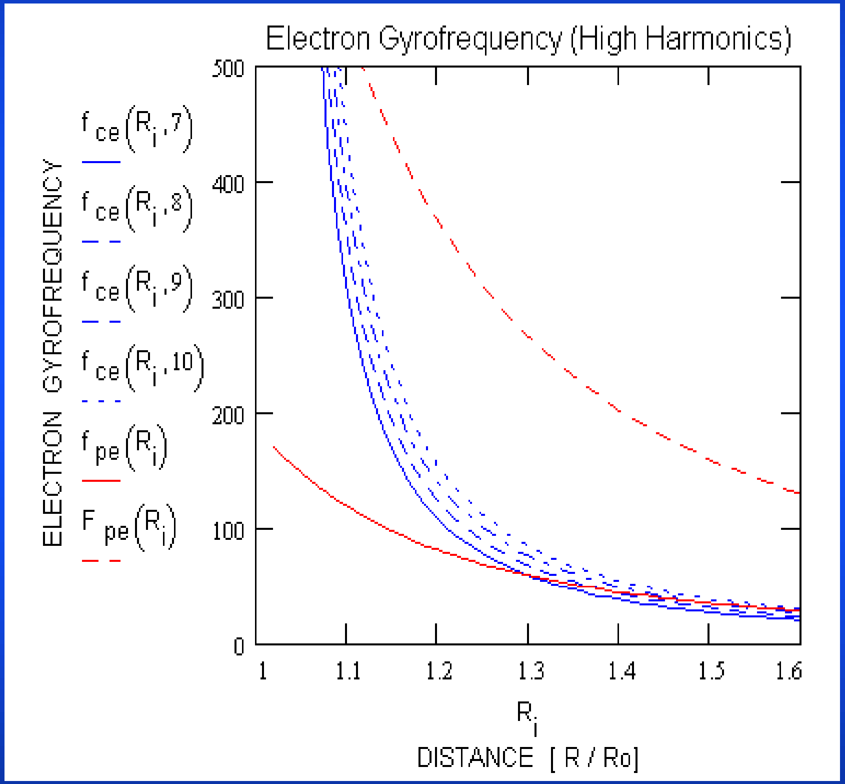

Low-order Harmonics $f_{ce}(R,s) := 2.80 \cdot B_{ar}(R) \cdot s$ **Higher-order Harmonics**

ESTIMATED ALTITUDE OF FLARE-RELATED RADIO EMISSIONS

ALTITUDE OF FLARE-RELATED RADIO EMISSIONS (Dulk, 1986)

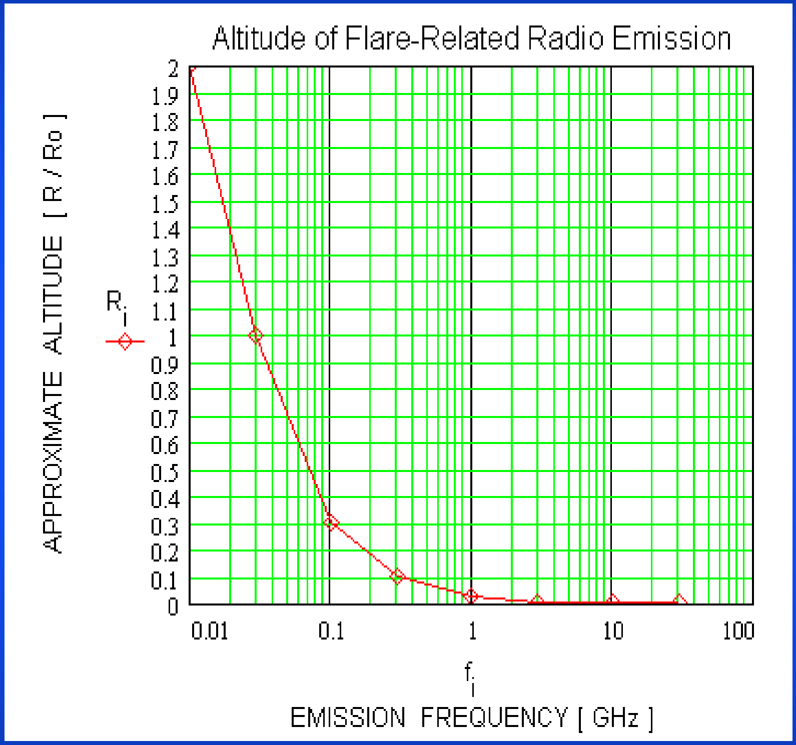

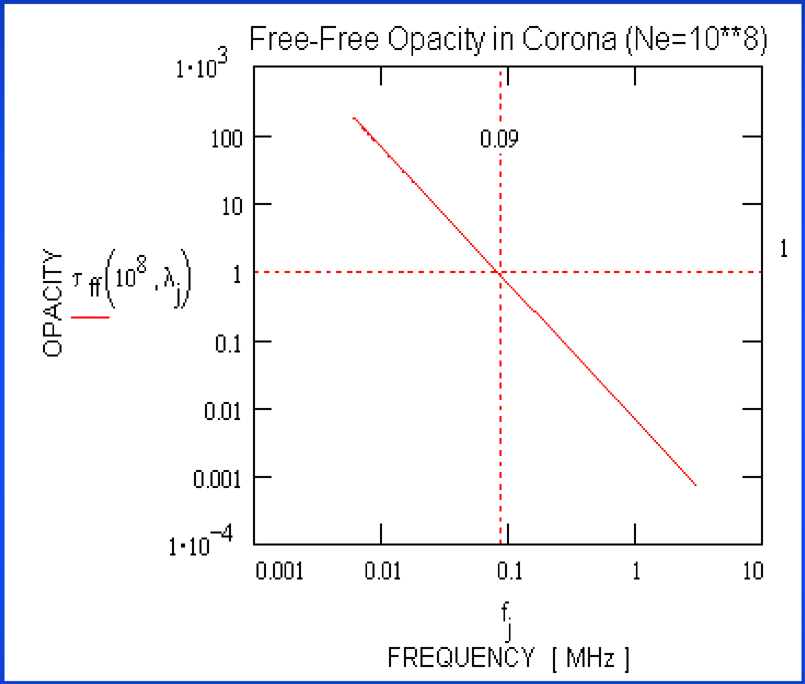

$$\tau_{ff} = \kappa_{ff}\ \lambda^2\ H\ N_e^{\ 2} = 7.5\cdot10^{-22}\ \lambda^2\ N_e^{\ 2} \quad (H = 5\cdot10^9\ cm)$$

Approximate Altitude

Free-free Opacity

PLASMA DIAGNOSTICS FROM RADIO SIGNATURES OF PARTICLE BEAMS

RADIO SIGNATURES OF BEAMS

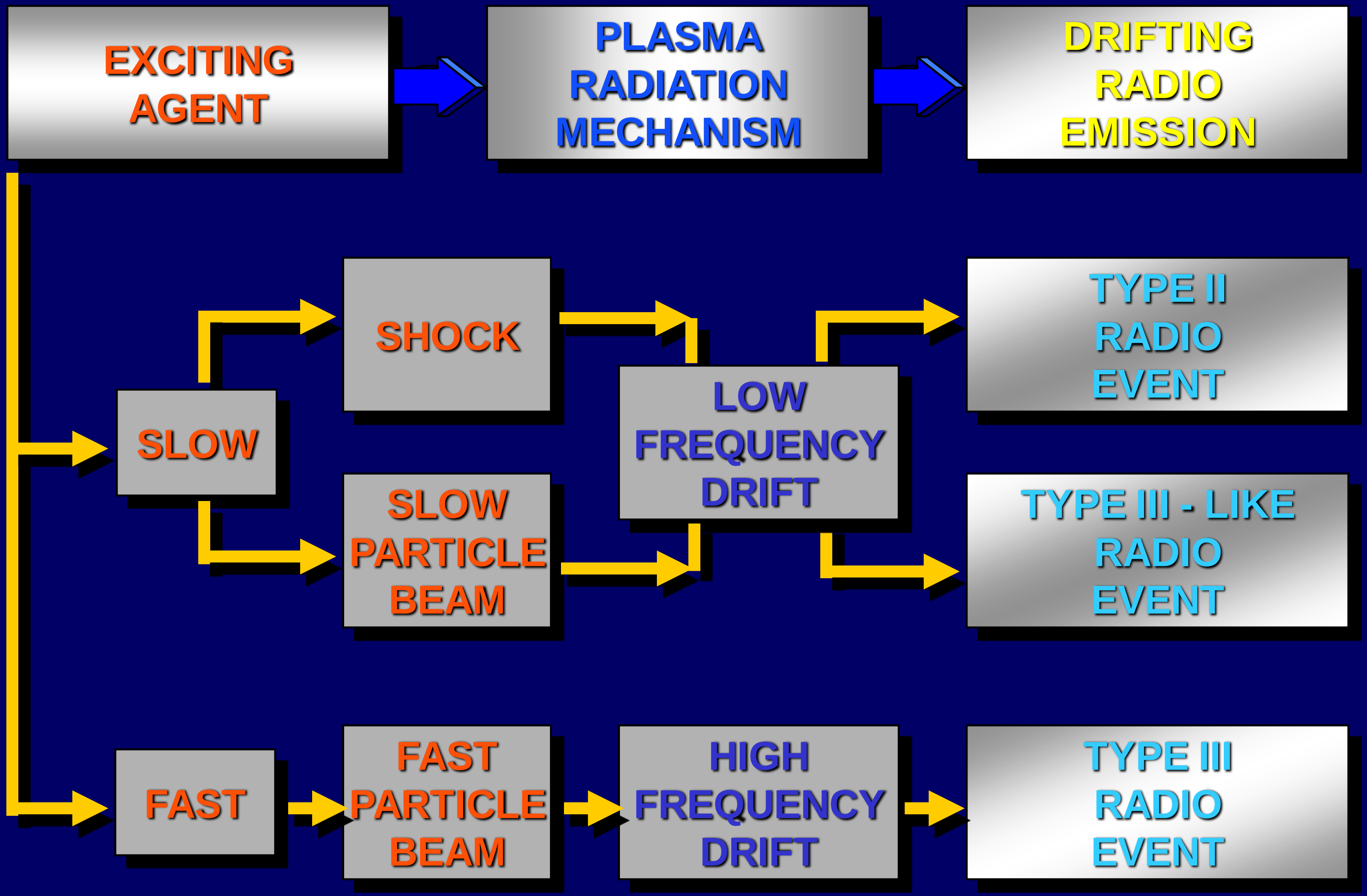

BEAM FORMATION AND DIAGNOSTICS

BEAM FORMATION

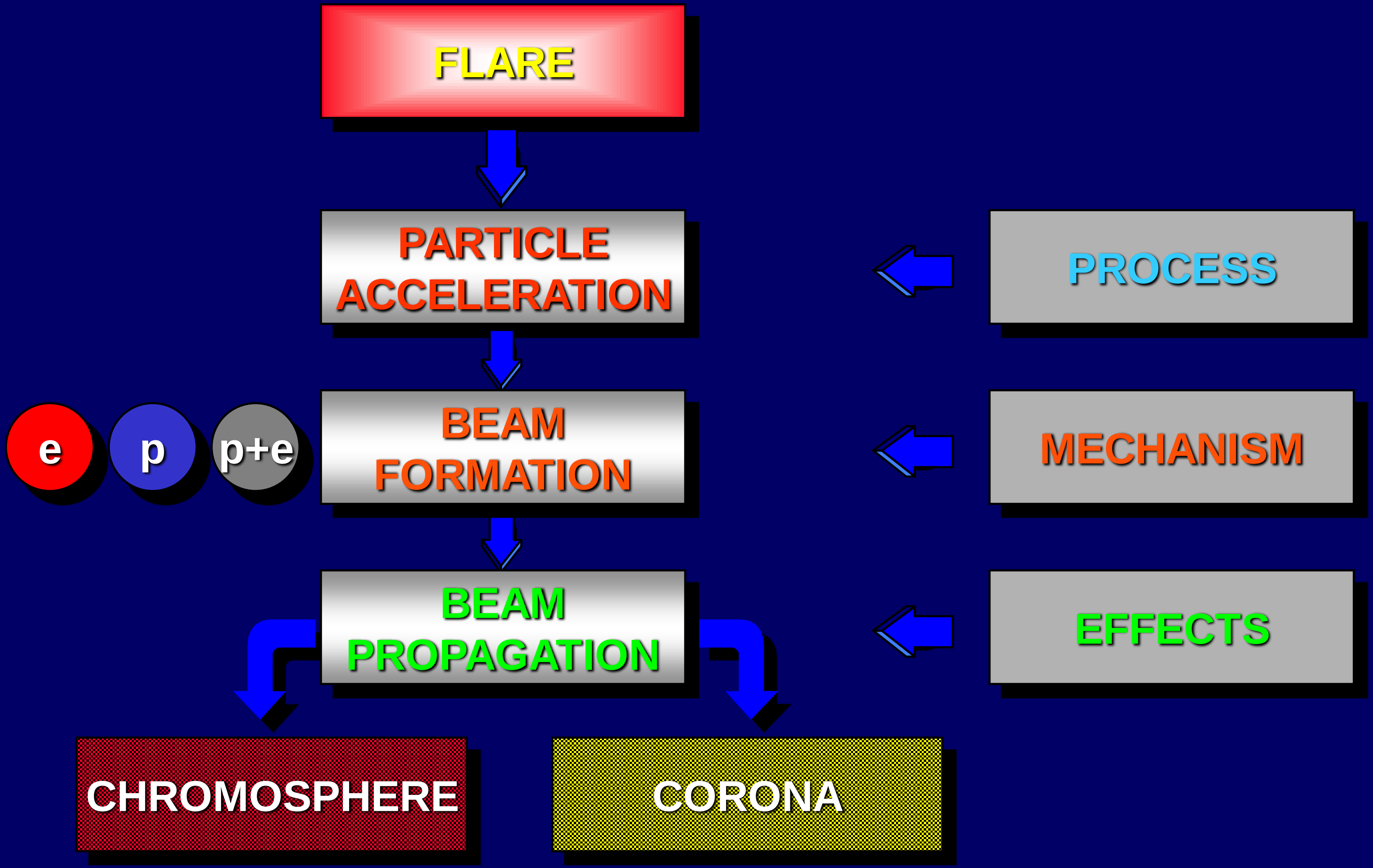

BEAM SIGNATURES

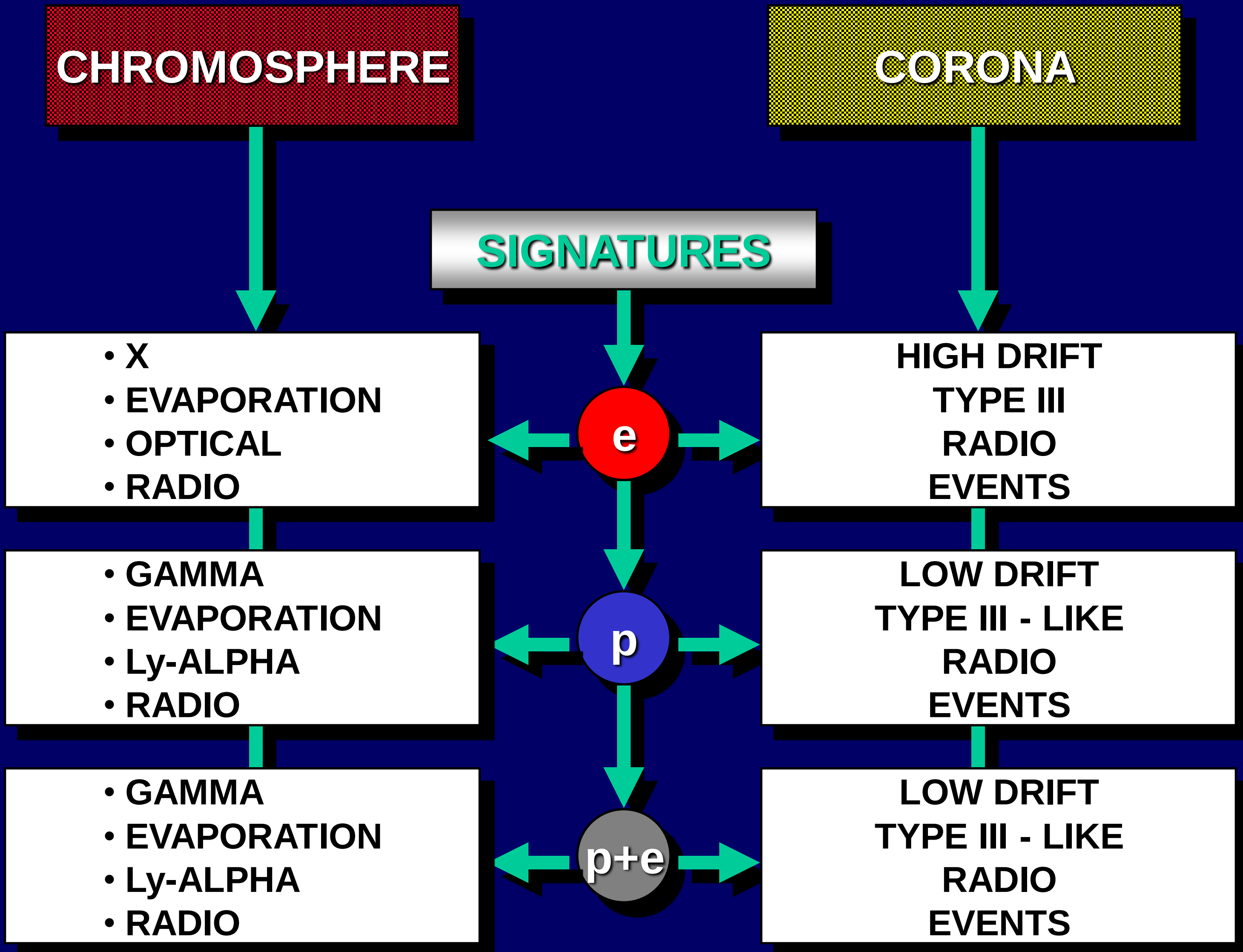

POSSIBLE BEAM DIAGNOSTICS

PARTICLE ACCELERATION	BEAM FORMATION	BEAM PROPAGATION	BEAM RADIATION
Turbulent Electric Fields [H line profiles]	Particle Detection in the IP Medium [In Situ Measures]	3-D Density Map in Streamers [Ly-alpha intensity]	LF Ion-Sound Turbulence [H line profiles]
Reconnecting Magnetic Fields [XUV line profiles]		MHD-Waves in the Solar Wind [Radio Sounding]	Temperatures NT Velocities [X-UV line profiles]
Shock-Wave Propagation [UV line intensities]			Coronal Plasmoids [Ly-alpha profiles]
			Impact Polarization [H-alpha line]
			NT Emission [Ly-alpha line]

BEAM PHYSICS THROUGH SOHO

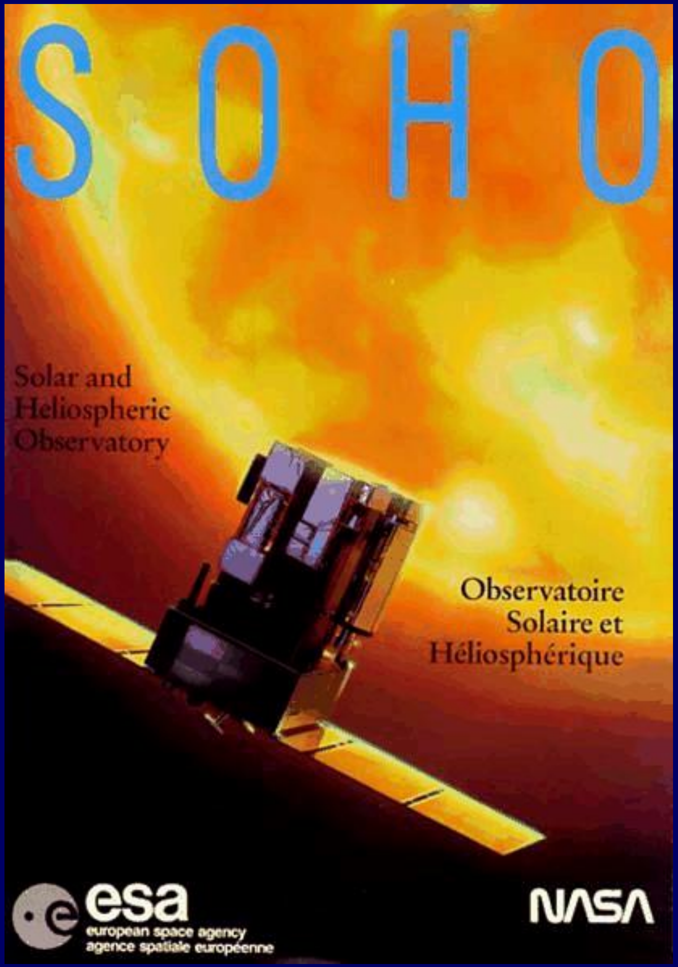

UVCS
Coronal T, n, V

SUMER
Chromo/Corona Plasma Flow

SWAN
Mass Flux in Solar Wind

CELIAS
Energetics and Composition

COSTEP
Suprathermal Particles

ERNE
Energetic Particles

SCHEME OF THE
PLASMA RADIATION MECHANISM

PLASMA RADIATION MECHANISM

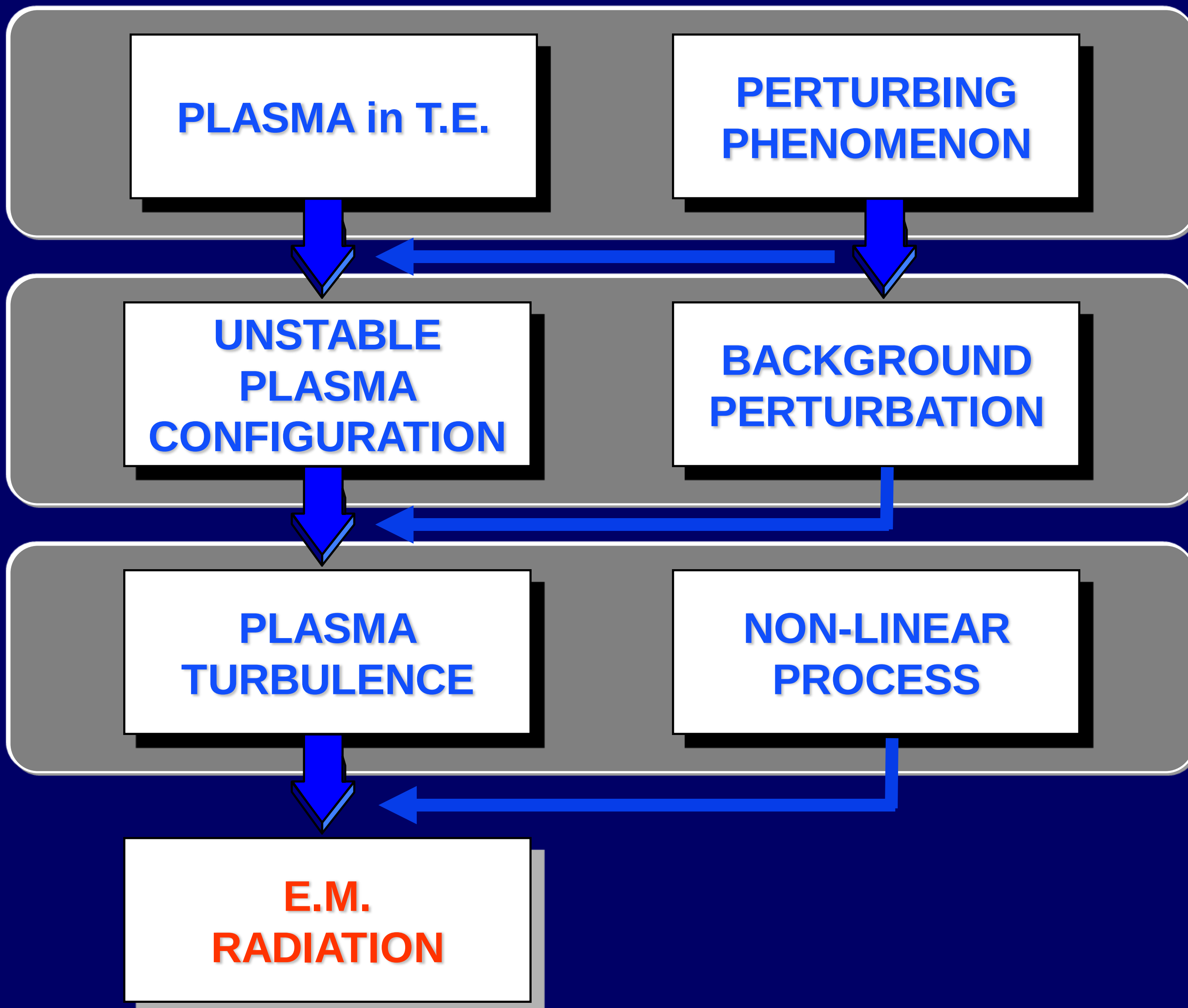

RADIO SIGNATURES
IN
THE DYNAMIC SPECTRUM

RADIO SIGNATURES OF PARTICLE BEAMS

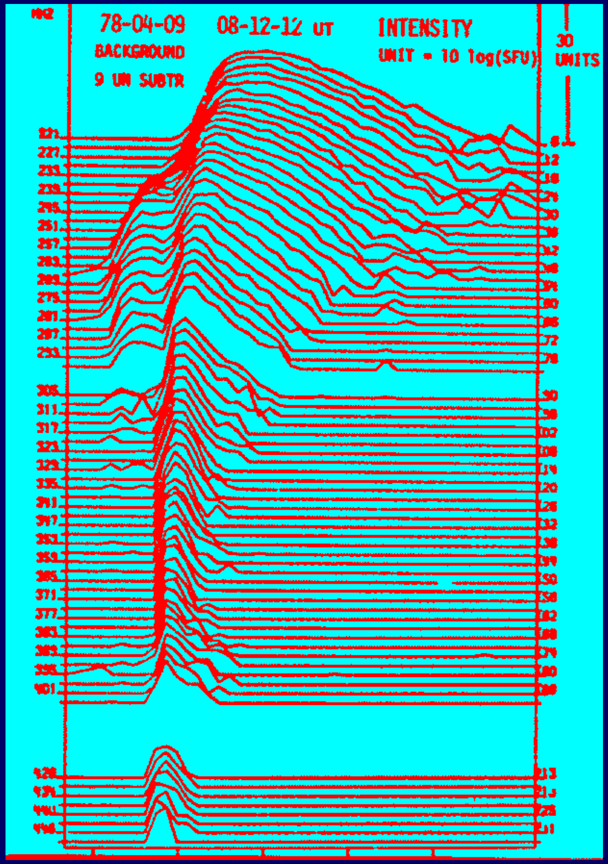

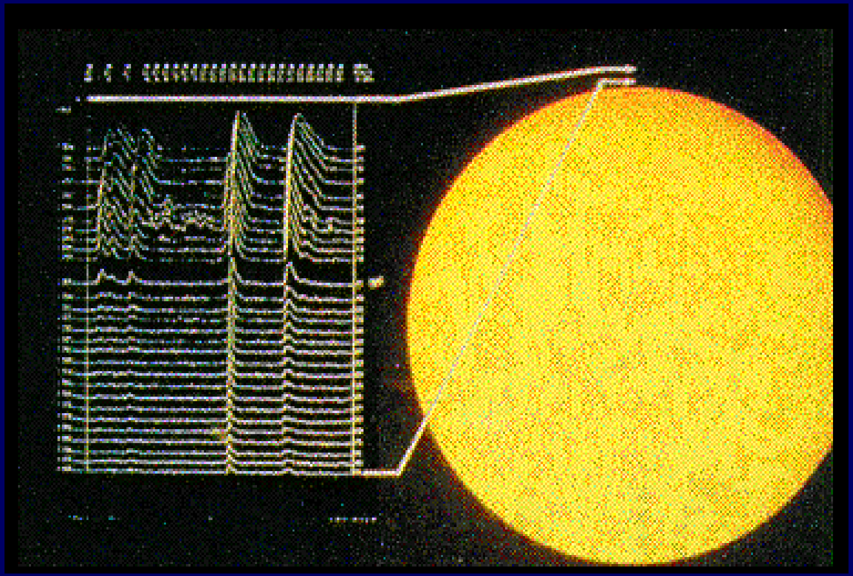

TYPE III RADIO BURST

Characteristic Parameters [t] of a Radio Spectrum

Total Duration

$$\Delta t_{tot} = t_{END} - t_{START}$$

Instantaneous Duration

$$\Delta t_{ist} = \Delta t(f)$$

Instant. Duration Evolution

$$\frac{\partial \Delta t_{ist}}{\partial f}$$

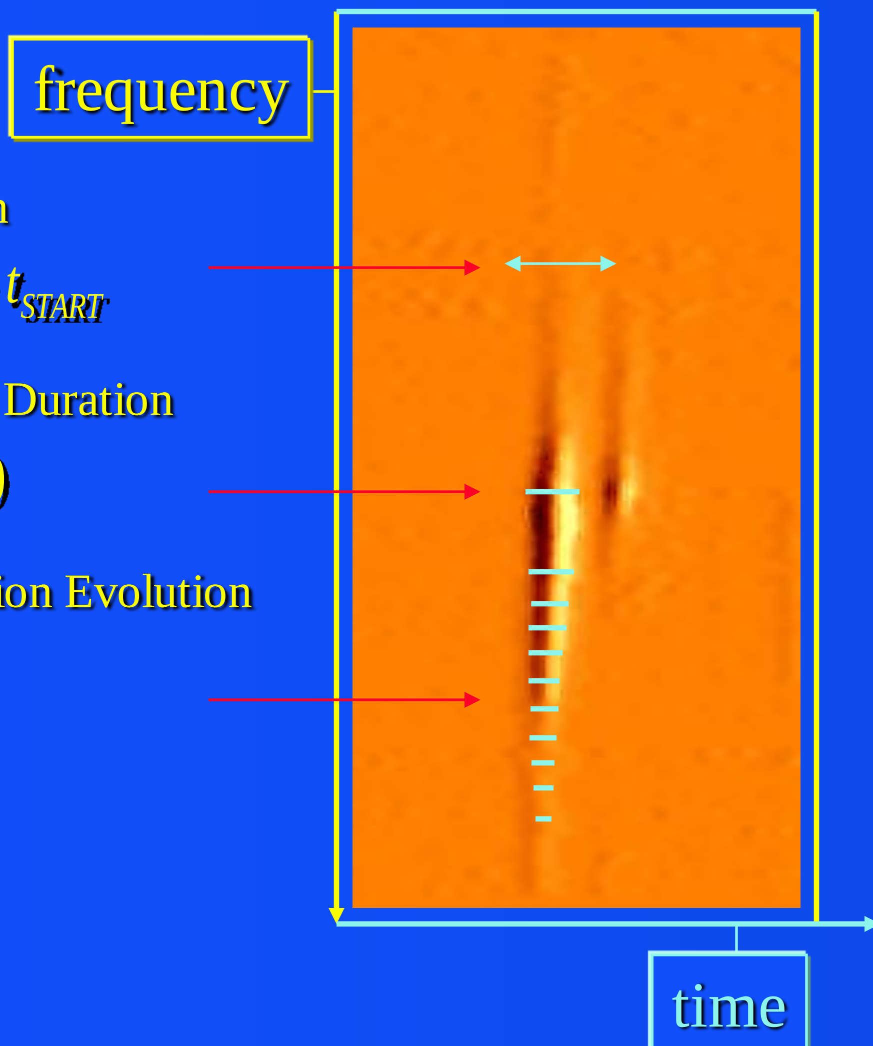

Total Duration

Process(es)

- global geometry
- global energetics
- global evolution

Instantaneous Duration

Perturbed Layer

- local geometry
- local energetics
- local process(es)

Instant. Duration Evolution

- Exciting Agent Dynamics
- Density Model Along Trajectory
- Local process(es) Along Trajectory
- Propagation Effects in Medium

Characteristic Parameters [t @ f]
of a Radio Spectrum

frequency

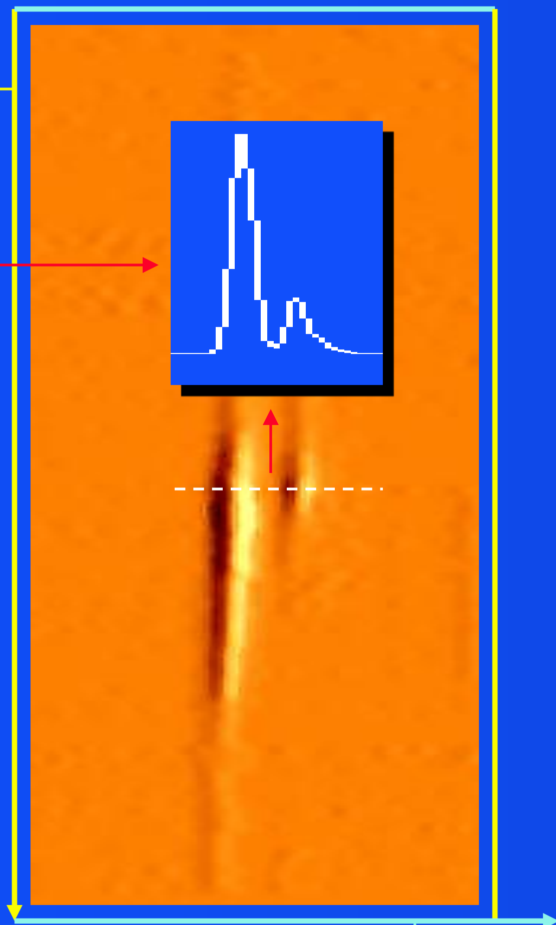

time

Flux Density Time Profile @ f

$$S_f = S_f(t)$$

Polarization Time Profile @ f

$$P_f = \frac{S_f^L(t) - S_f^R(t)}{S_f^L(t) + S_f^R(t)} = P_f(t)$$

Modes Delay Evolution

$$\delta \dot{t}_{LR} = \frac{\partial t_{LR}}{\partial t} \qquad \frac{\partial t_{LR}}{\partial f}$$

Flux Density Time Profile @ f

Perturbed layer
- response of the layer
- evolution of the instability
- diagnostic of process

Polarization Time Profile @ f

Perturbed Layer
- local geometry
- local magnetic field
- local propagation effects

Modes Delay Evolution

- Density Model Along Trajectory
- Propagation Effects Along Trajectory
- Local process(es) Along Trajectory
- Propagation Effects in Medium

Characteristic Parameters [f] of a Radio Spectrum

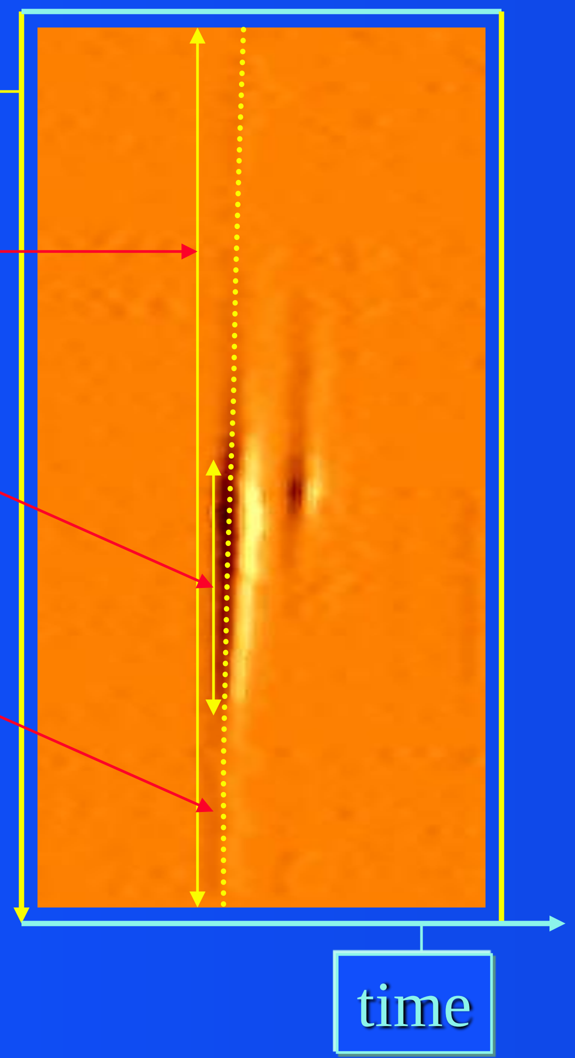

Maximum Bandwidth

$$\Delta f_{\max} = f_{MAX} - f_{MIN}$$

Instantaneous Bandwidth

$$\Delta f_{ist} = \Delta f(t)$$

Frequency Drift

$$\dot{f} = \frac{\partial f}{\partial t}$$

Frequency Drift Evolution

$$\ddot{f} = \frac{\partial^2 f}{\partial t^2}$$

Maximum Bandwidth

Perturbed Region

- global geometry
- density model
- process(es)

Instantaneous Bandwidth

Perturbed Layer

- local geometry
- local density
- local process(es)

Frequency Drift

- Exciting Agent Dynamics
- Density Model Along Trajectory
- Local process(es) Along Trajectory
- Propagation Effects in Medium

Frequency Drift Evolution

- Instability Evolution
- Density Model Along Trajectory
- Local process(es) Along Trajectory
- Propagation Effects in Medium

Characteristic Parameters [E] of a Radio Spectrum

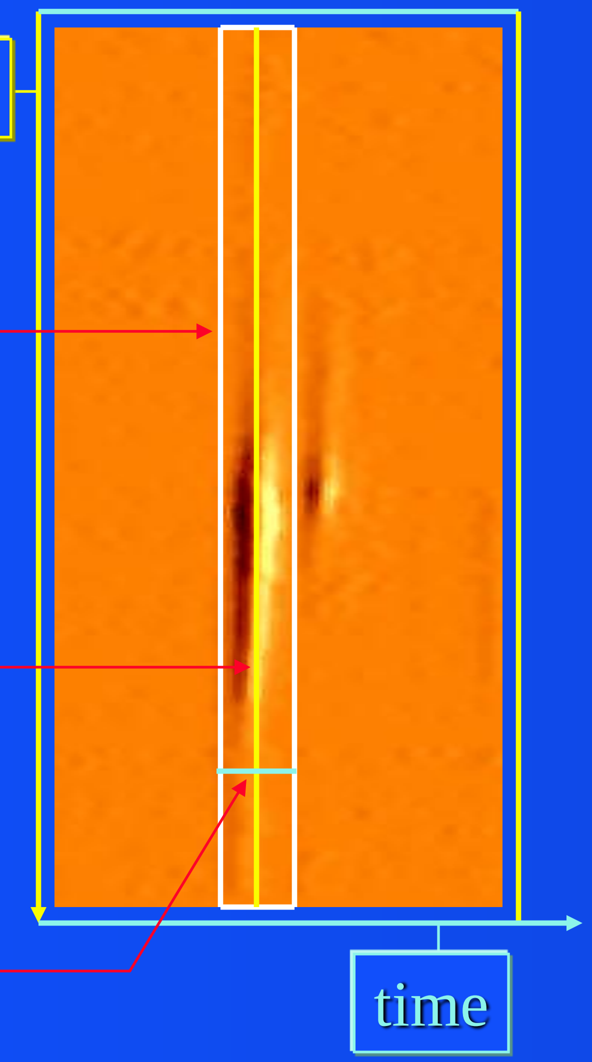

Total Power Density

$$P_{TOT} = \int_{f_{MIN}}^{f_{MAX}} \int_{t_{MIN}}^{t_{MAX}} S(t, f)\, dt\, d f$$

Spectral Power Density [t]

$$P_t = \int_{f_{MIN}}^{f_{MAX}} S(t, f)\, d f$$

Spectral Power Density [f]

$$P_f = \int_{t_{MIN}}^{t_{MAX}} S(t, f)\, dt$$

Total Power Density

Global Energetics of Region
- process(es) energetics
- source model
- instability character

Spectral Power Density [t]

Instantaneous Energetics of Layers
- global response of layers at time t
- local process(es)

Spectral Power Density [f]

Energetics of Single Layer
- response of single layer at frequency f
- process in layer

ADVANCED RADIO DIAGNOSTICS

3D Reconstruction of Type III Exciters Trajectories

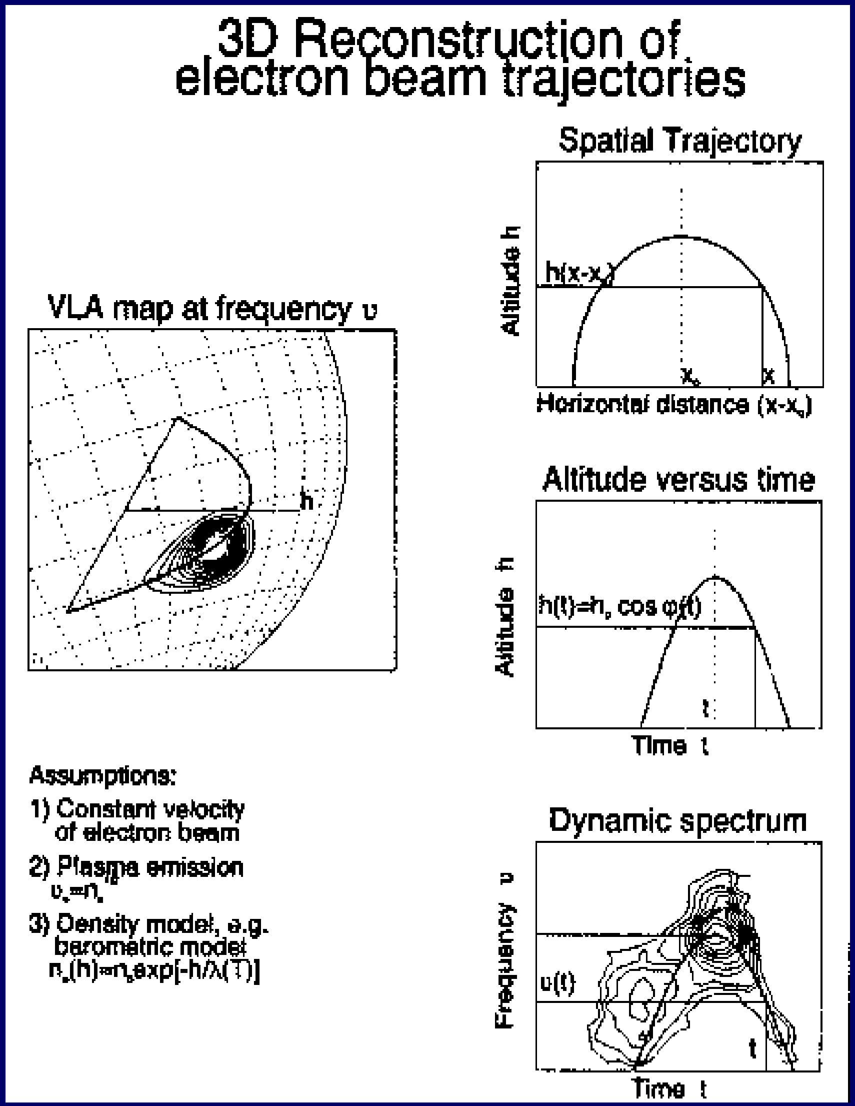

High space resolution radio data

+

Radio dynamic spectra

3D trajectories of electron beams

Tracing of magnetic field lines

3D model of coronal structures

Aschwanden (1992)

Tracing Magnetic Structures in Radio and X

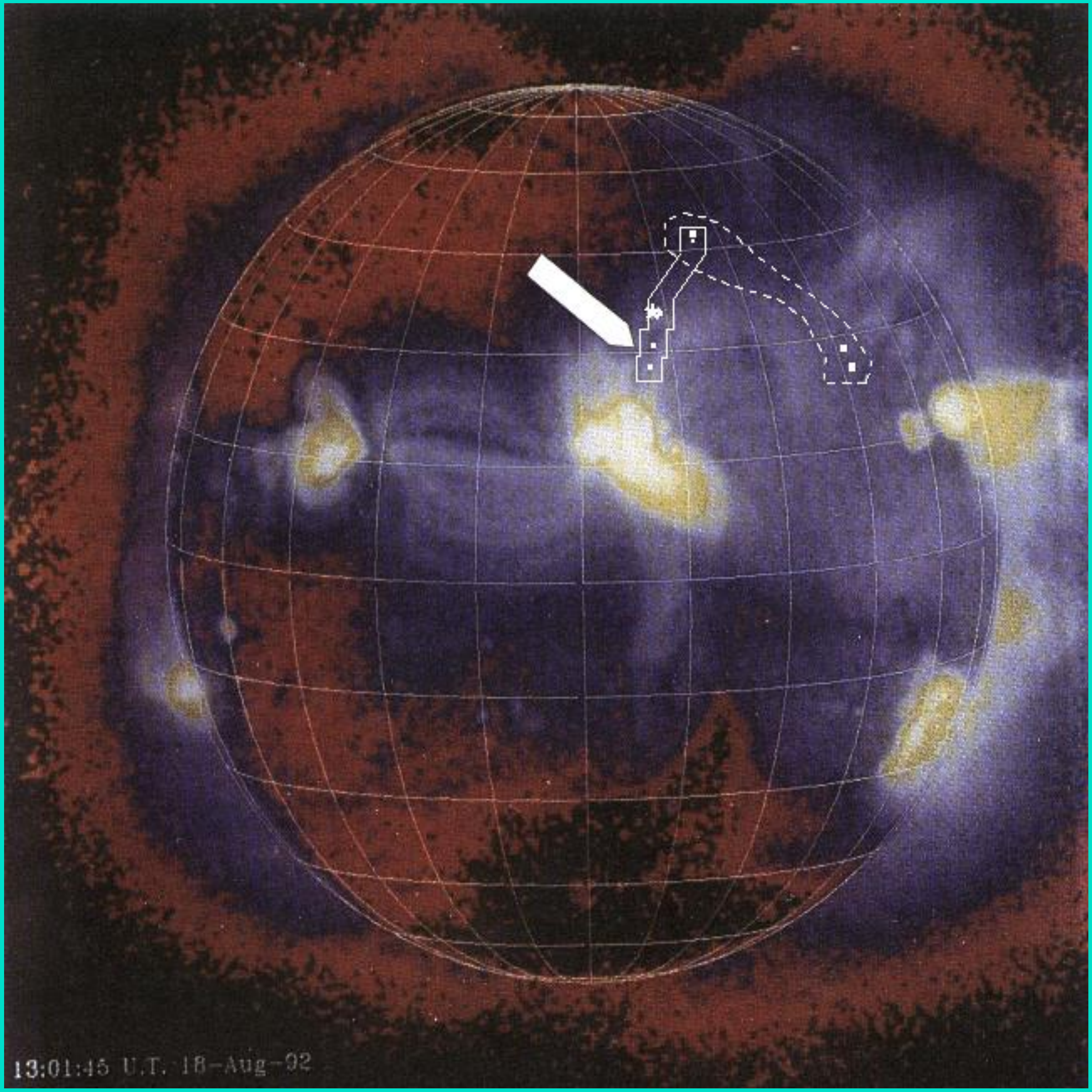

Nancay Multifrequency Radioheliograph (435-169 MHz)
+
Yohkoh Soft X-Ray

Pick et al. (1994)

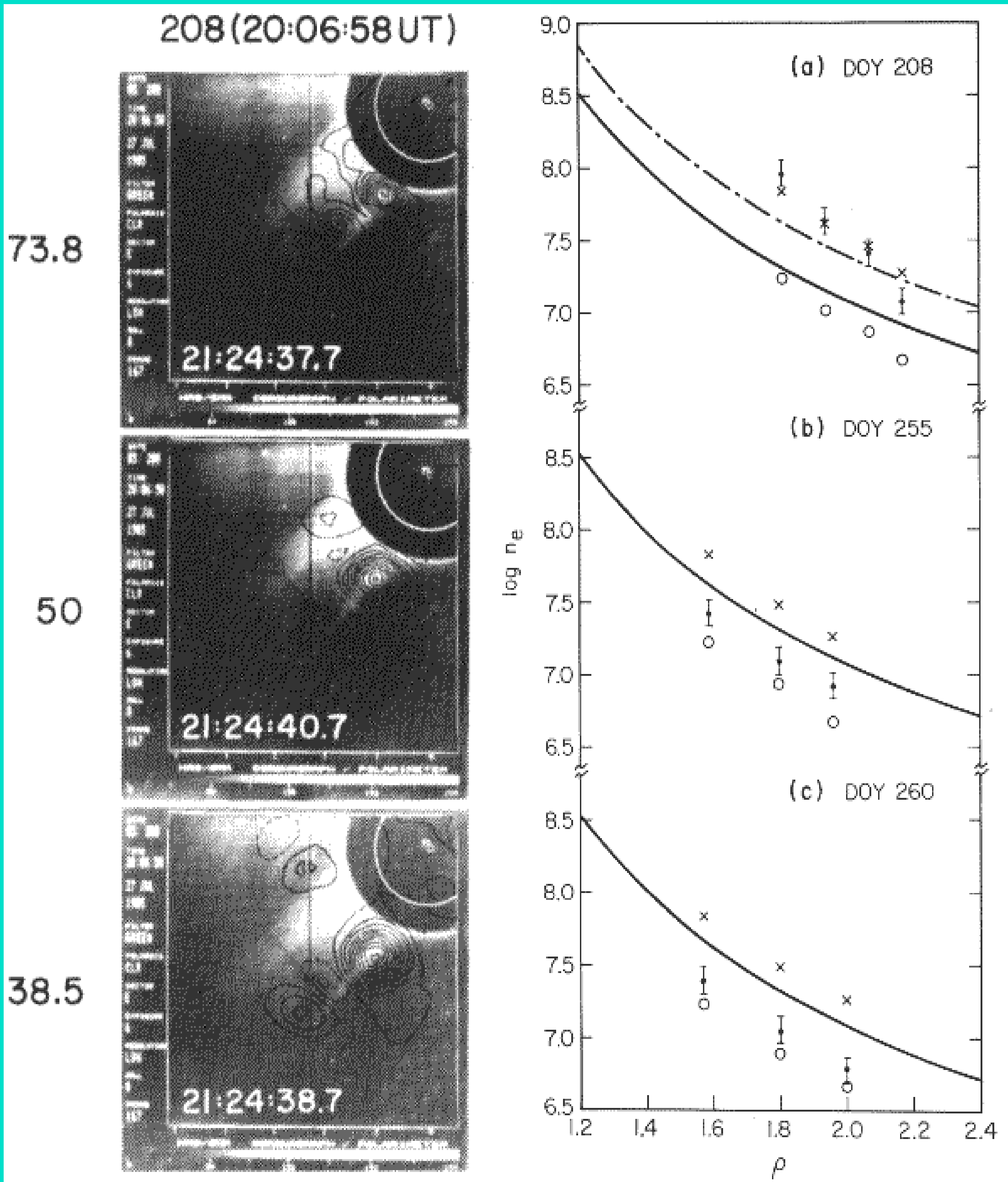

Tracing Electron Density in Streamer Radio and WL

Clark Lake Multifrequency Radioheliograph (73.8-38.5 MHz)
+
SMM-C/P

Gopalswamy et al. (1987)

PLASMA THEORY OF OBSERVED RADIO EMISSION

MODELING TIME PROFILE OF TYPE III RADIO BURSTS

A Step Towards
Self-Consistent Coronal Diagnostics

DIRECT GENERATION OF EM WAVES BY A ROTATING BEAM

CYCLOTRON RADIATION

- Distribution function of energetic electrons (*rotating beam*)

$$f(v) = \frac{n_b}{2\pi v_{\perp 0}} \delta(v_\parallel - v_s)\, \delta(v_\perp - v_{\perp 0})$$

- n_b beam density
- $v_\parallel, v_\perp$ longitudinal and transverse particle velocity component
- v_s streaming velocity of the beam

- EM waves excited at high cyclotron harmonics

$$\Rightarrow \text{QT propagation} \Rightarrow t_0 \sim \frac{l}{c}$$

- t_0 time of wave-beam interaction (enhancement time)
- l transverse size of beam
- c velocity of light

$\rightarrow$ $l = const.$ **at each coronal level** $\Rightarrow$ $t_0 \approx const.$

$\rightarrow$ ASSUME:

- excitation described in terms of linear theory
- transverse propagation
- $\omega_{pe}^2 << s^2 \omega_{he}^2$ with ω_{pe} electron plasma frequency; s cyclotron harmonic number; ω_{he} electron cyclotron frequency
- $\frac{v_\perp^2}{c^2} << 1$

- Energy density of electromagnetic waves

$$W = W_0 \exp(\delta\, t_0)$$

- W_0 initial (thermal) energy level of waves
- δ growth rate
- t_0 time of wave-beam interaction

- Growth rates for the (e) and (o) modes

$$\delta_e \sim \omega \left[\frac{{\omega_b}^2 \gamma {v_\perp}^2}{8\pi s^2 {\omega_{he}}^2 c^2 \left(e s v_\perp / 2c \right)^{2(s-1)} \left(s-1 \right)^{1-2s}} \right]^{1/3}$$

$$\delta_o \sim \omega \left[\frac{{\omega_b}^2 \gamma {v_\parallel}^2}{2\pi s^3 {\omega_{he}}^2 c^2 \left(e v_\perp / 2c \right)^{2s}} \right]^{1/3}$$

- frequency of radiation
- ${\omega_b}^2 = \dfrac{4\pi e^2 n_b}{m}$ n_b - beam density
- $\gamma = \left(1 - \dfrac{v^2}{c^2} \right)^{1/2}$

$\rightarrow \omega = \omega_0$ (fixed frequency): $\delta = \delta(n_b, E_{b\perp})$

but $\Delta t_{burst}\big|_{\omega=\omega_0} \sim 1\,s \quad \Rightarrow \quad \Delta E_b\big|_{path} \rightarrow 0 \quad \Rightarrow \quad \delta = \delta(n_b)$

the growth rate of em waves is determined by beam density.

- Beam density at a given height in corona

$$n_b = \frac{C}{t^2\, S} \exp\left(- \frac{b^2}{t^2} \right)$$

- $C = \dfrac{2\, N_0\, x_0}{\Delta v^2}$ $\quad N_0$ total number of particles in the beam
- $b = \dfrac{x_0}{\Delta v}$ $\quad \Delta v$ spread in velocities of the initial distribution

  (when $\Delta v \sim v_s$, $\rightarrow$ travel time of beam to reach level)
- S beam cross-section

- Energy density of electromagnetic waves

$$W \approx W_0 \exp\left[\delta\,(n_b)\,t_0\right] = W_0 \exp\left\{ a_{e,o} \left[\frac{C}{t^2} \exp\left(-\frac{b^2}{t^2} \right) \right]^{1/3} \right\}$$

$$a_e = \omega\, t_0 \left[\frac{e^2 \gamma\, v_\perp{}^2}{2ms^2 \omega_{he}{}^2 c^2 S} \left(\frac{esv_\perp}{2\,c} \right)^{2(s-1)} (s-1)^{1-2s} \right]^{1/3}$$

$$a_o = \omega\, t_0 \left[\frac{2\,e^2 \gamma\, v_\parallel{}^2}{ms^3 \omega_{he}{}^2 c^2 S} \left(\frac{e v_\perp}{2\,c} \right)^{2s} \right]^{1/3}$$

- Estimation of em waves enhancement $\Gamma = \exp(\delta \; t_0)$ required for generation of observed emission

Spectral energy density of the waves: $W_k = W_{0k} \; \Gamma$

Thermal fluctuations: $W_{0k} = k \, T$

Observed emission intensity: I ~ 10 erg/cm^2/s

Corresponding waves' energy density: $W \sim \dfrac{4 \pi I}{c} \sim 10^{-9}$ erg/cm^2

and spectral energy density: $W_k \sim \dfrac{W}{4 \pi k^3} \sim 10^{-6}$ erg

For $T \sim 10^6 \; K$, $W_{0k} \sim 10^{-10} \; erg$ $\Rightarrow$ $\Gamma \sim 10^4$

- Coronal and Beam Parameters in computed time profiles

Initial distance from heating region	$x_0 \sim 10^{10}\ cm$
Characteristic velocities	$v_{\parallel} \sim v_{\perp} \sim v_s \sim 10^{10}\ cm/s$
Beam density	$n_b \sim 10\ cm^{-3}$
Beam cross-section	$S \sim 10^{19}\ cm^2$
Total number of beam particles	$N_0 \sim S \cdot x_0 \sim 10^{30}$
Characteristic frequencies	$\omega \sim \mathrm{s}\omega_{\mathrm{he}} \sim \omega_{pe} \sim 10^9\ s^{-1}$
Cyclotron harmonic number	~ 10
↓	
Travel time of beam to reach	$b \sim x_0 / v_s \sim 1\,s$
*	$C \sim 10^{20}\ s^2 / cm^3$
*	$a \sim 10^{-5}\ cm$ (1,2)

(1) assuming the enhancement time $t_0 \sim 0.01\,s$ and hence the enhancement length much shorter than the beam transverse size.

(2) it can be shown by inference from observations that, as a first approximation, the parameter *a* and hence the enhancement of em waves at a given cyclotron harmonic is independent of the ambient plasma density.

COMPUTED TIME PROFILES

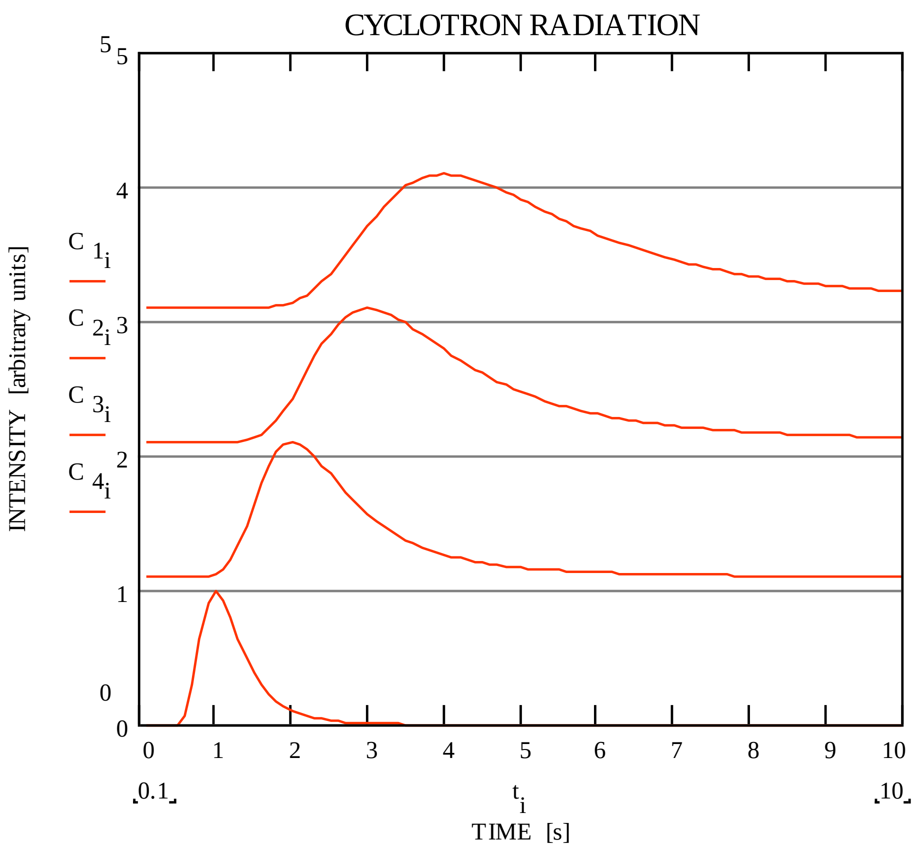

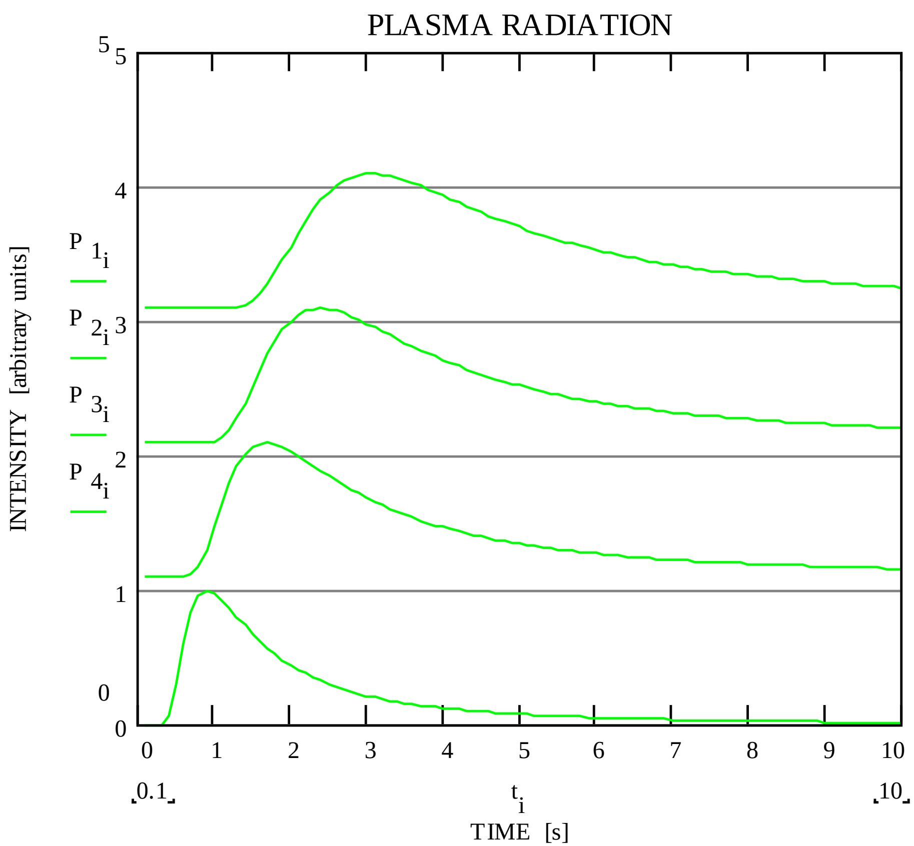

SYNOPSIS OF SOLAR RADIO EVENTS

Spectrum of Quiet Sun at Sunspot Minimum

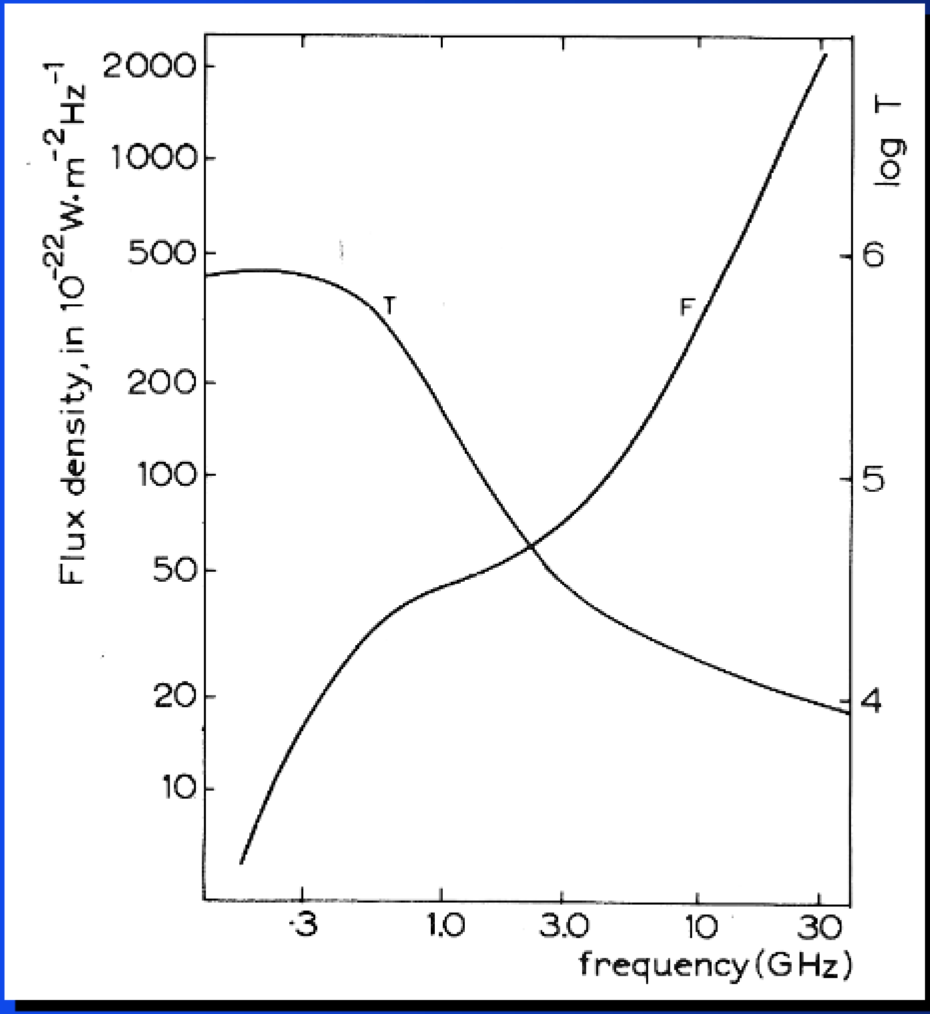

Bruzek & Durrant (1977)

S-COMPONENT Characteristics

	S-COMPONENT
Duration	14 days (1/2 rotation)
T_b	10^6 K (corona); <10^6 K (chromosphere)
Circular polarization	random; core (2' arc) @ 3-15 cm with CP up to 30% (x) (LSH)
Occurrence frequency range	37 GHz - 170 MHz
Bandwidth	
Frequency drift (Speed)	
Emission mechanism	thermal + cyclotron
Source size	2' - 4' (37 Ghz) 10' (170 MHz)
Source height	chromosphere @ f > 3 Ghz corona @ f < 3 GHz
Magnetic topology	closed
Associated phenomena	sunspots

RADIO INDEX @ 2800 MHz (10.7 cm) ≡ SUNSPOT NUMBER

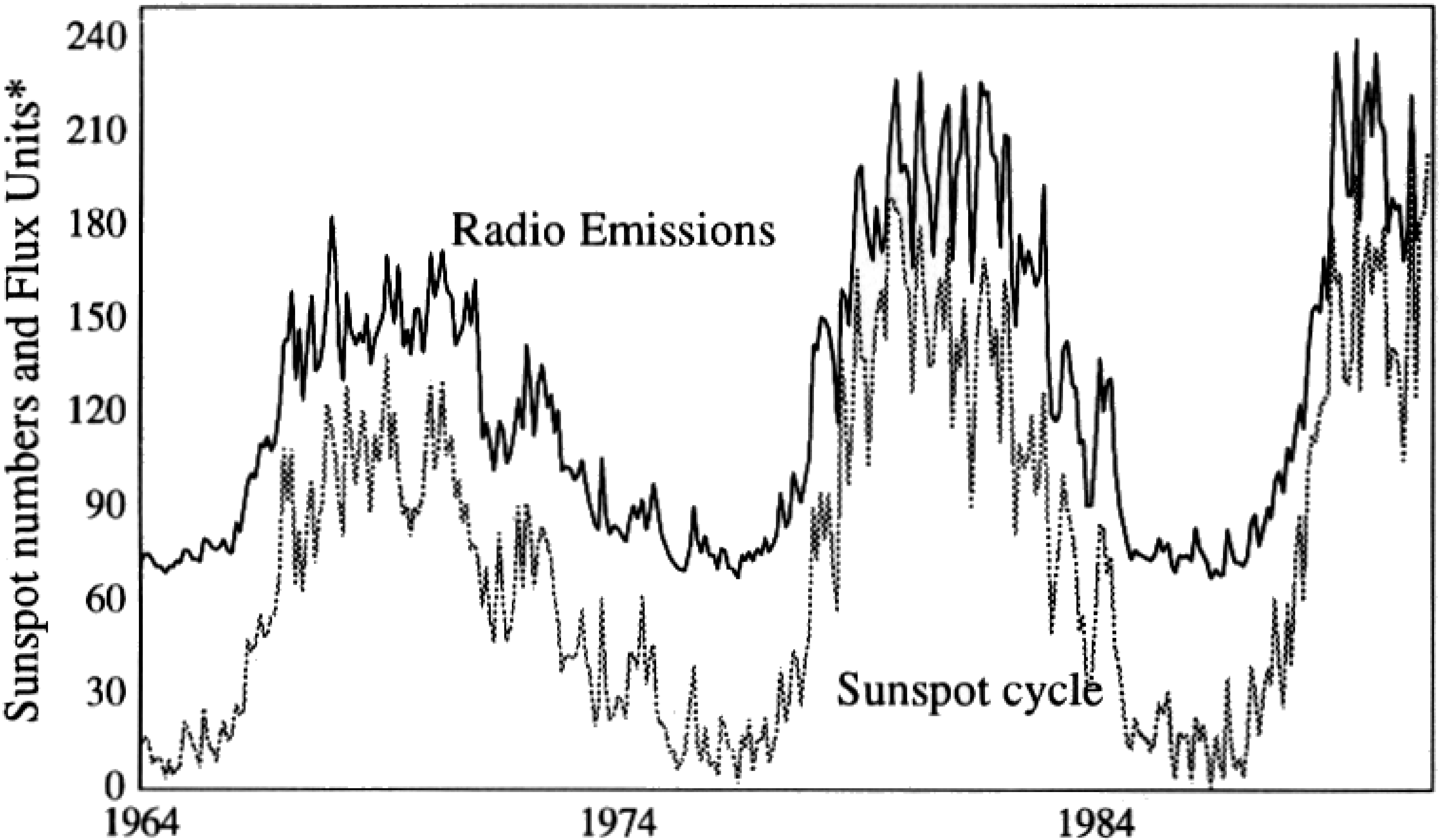

NOISE STORM Continuum + Type I Bursts

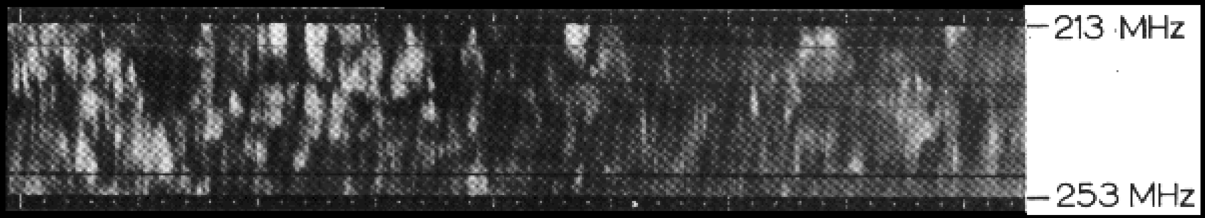

NOISE STORM WITH BACKGROUND CONTINUUM SUBTRACTED
[May 5, 1971; 0717 UT; Dwingeloo] (Bruzek & Durrant, 1977)

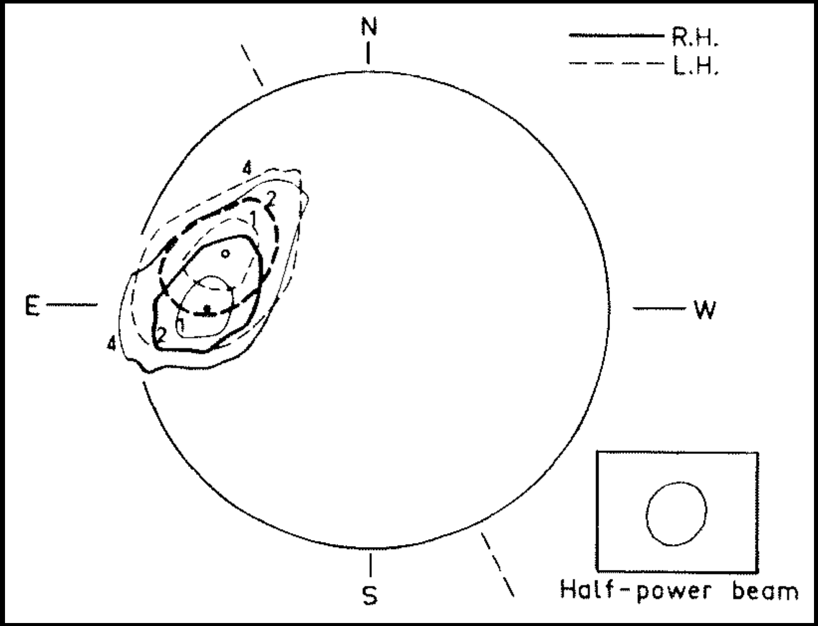

RH AND LH RADIO SOURCES OF A NOISE STORM
[October 21, 1968; 60% RH; sep. 3′ arc; size 6′x6′; pol. o-mode LSH; 80 MHz; Culgoora]

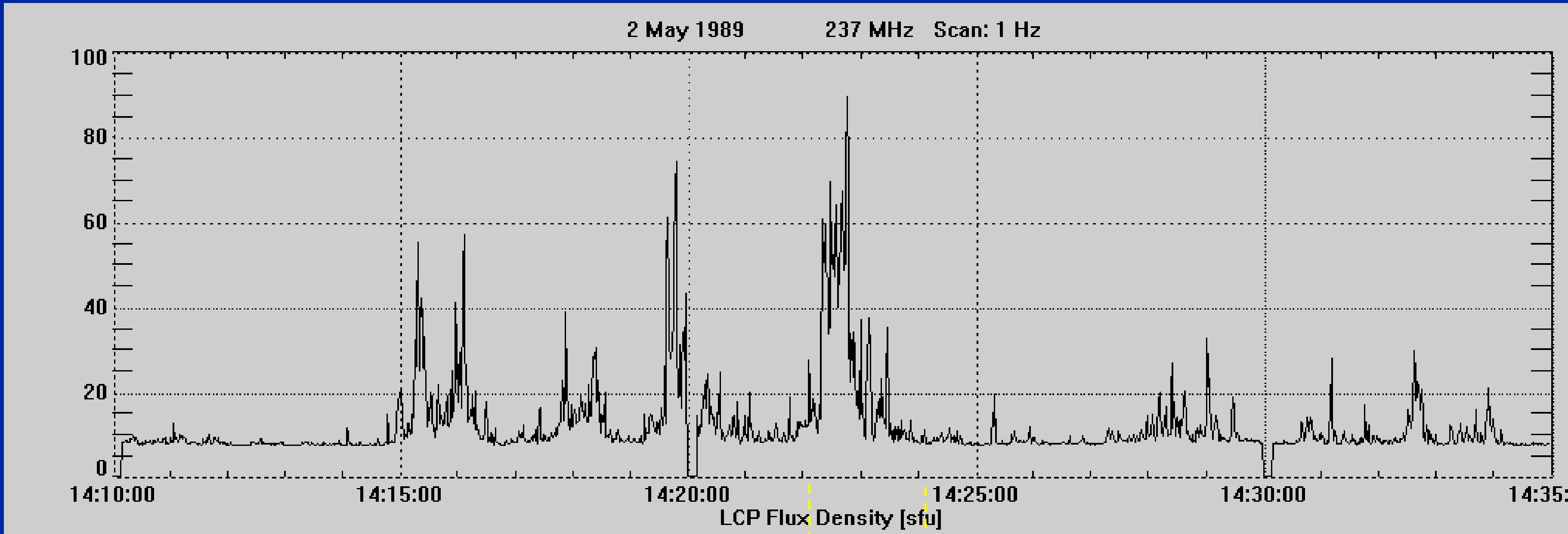

Type I Bursts

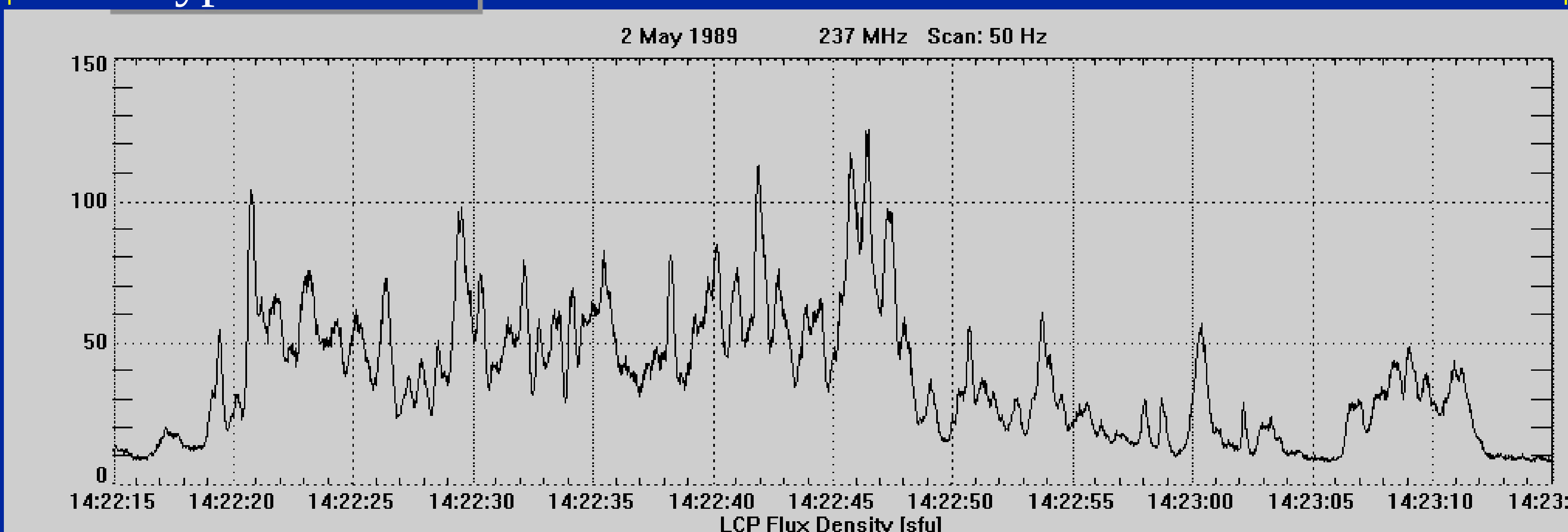

TYPE II BURST

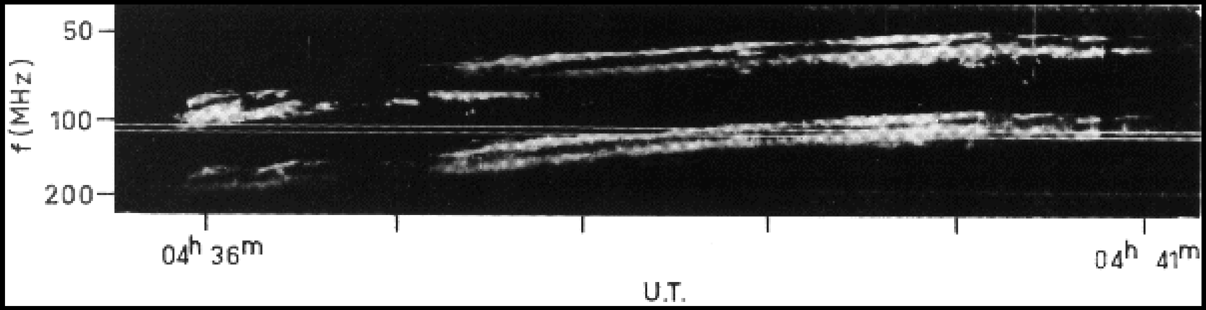

HARMONIC AND SPLIT BAND STRUCTURE OF A TYPE II BURST

[Culgoora] (Dulk, 1970; Bruzek & Durrant, 1977)

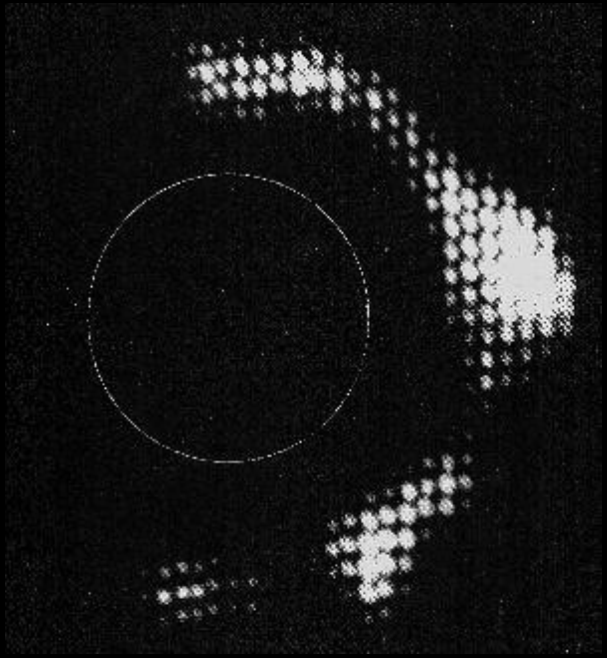

RADIO HELIOGRAM OF A TYPE II BURST SOURCE

[March 30, 1969; 80 MHz; Culgoora] (Smerd, 1970; Bruzek & Durrant, 1977)

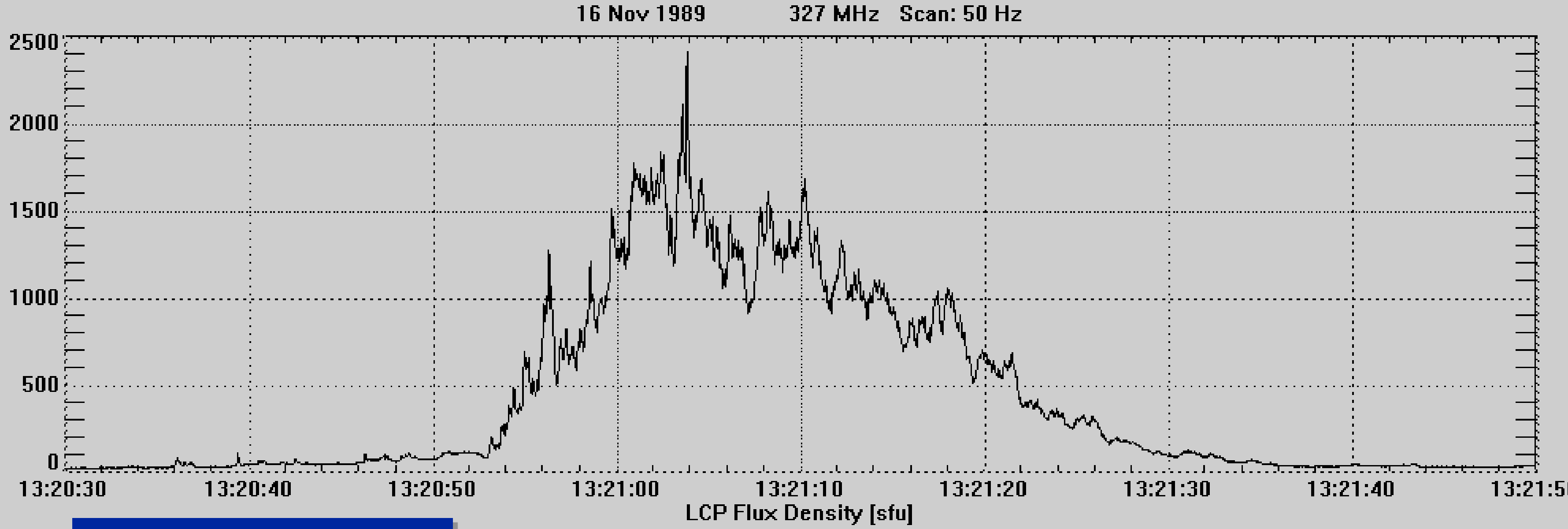

Type II Burst

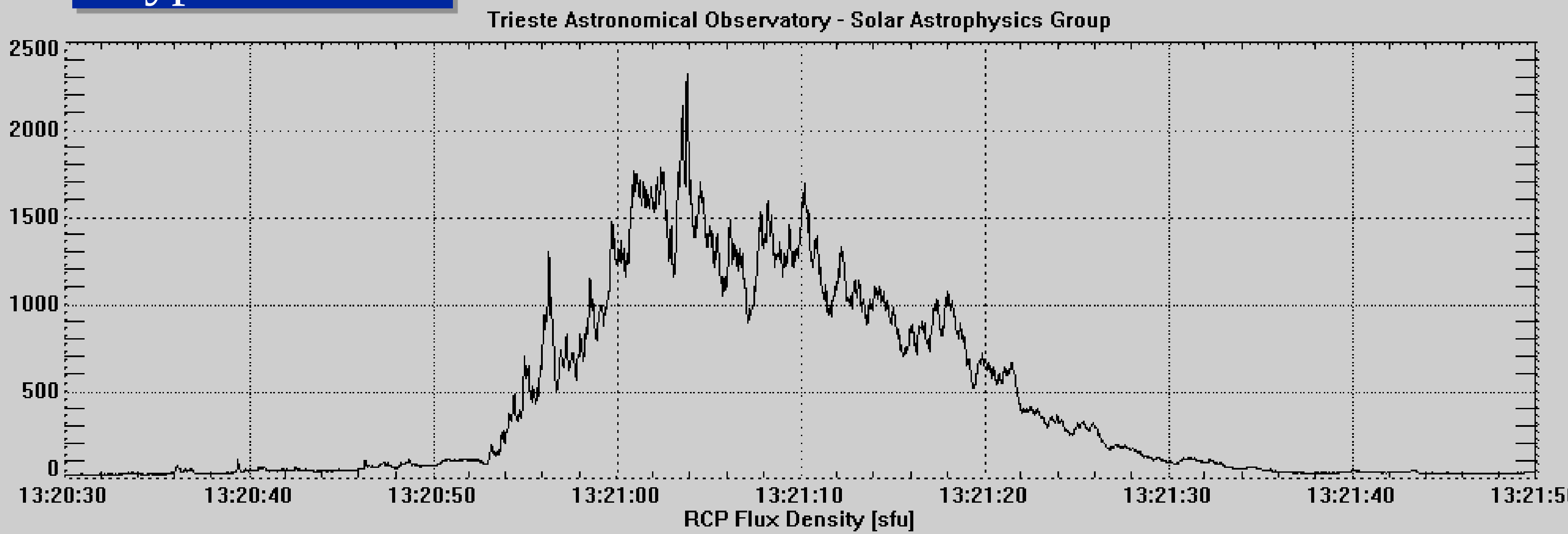

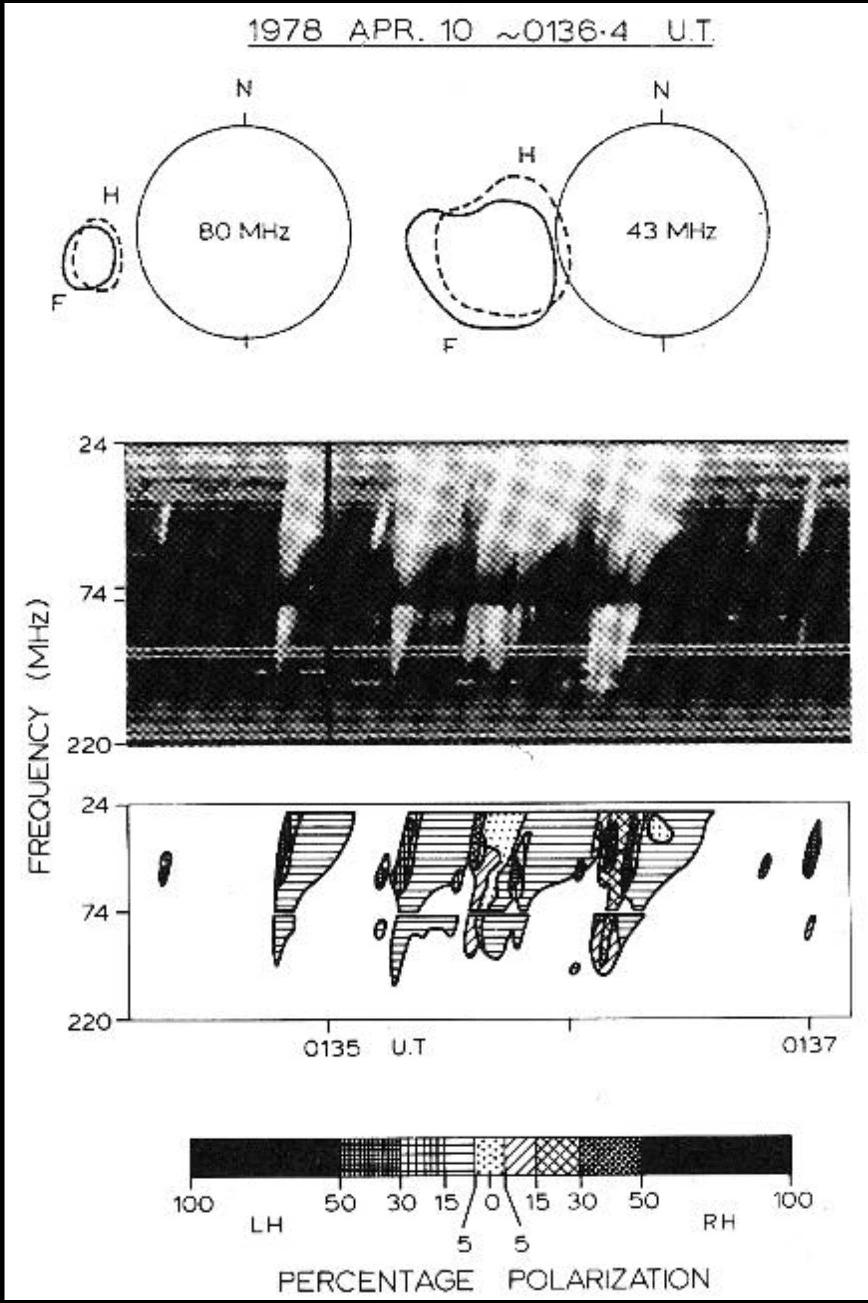

TYPE III BURST

GROUP OF TYPE III BURSTS
[April 10, 1978; 43 and 80 MHz; Culgoora]
(DS80; McLean & Labrum, 1985)

Blips

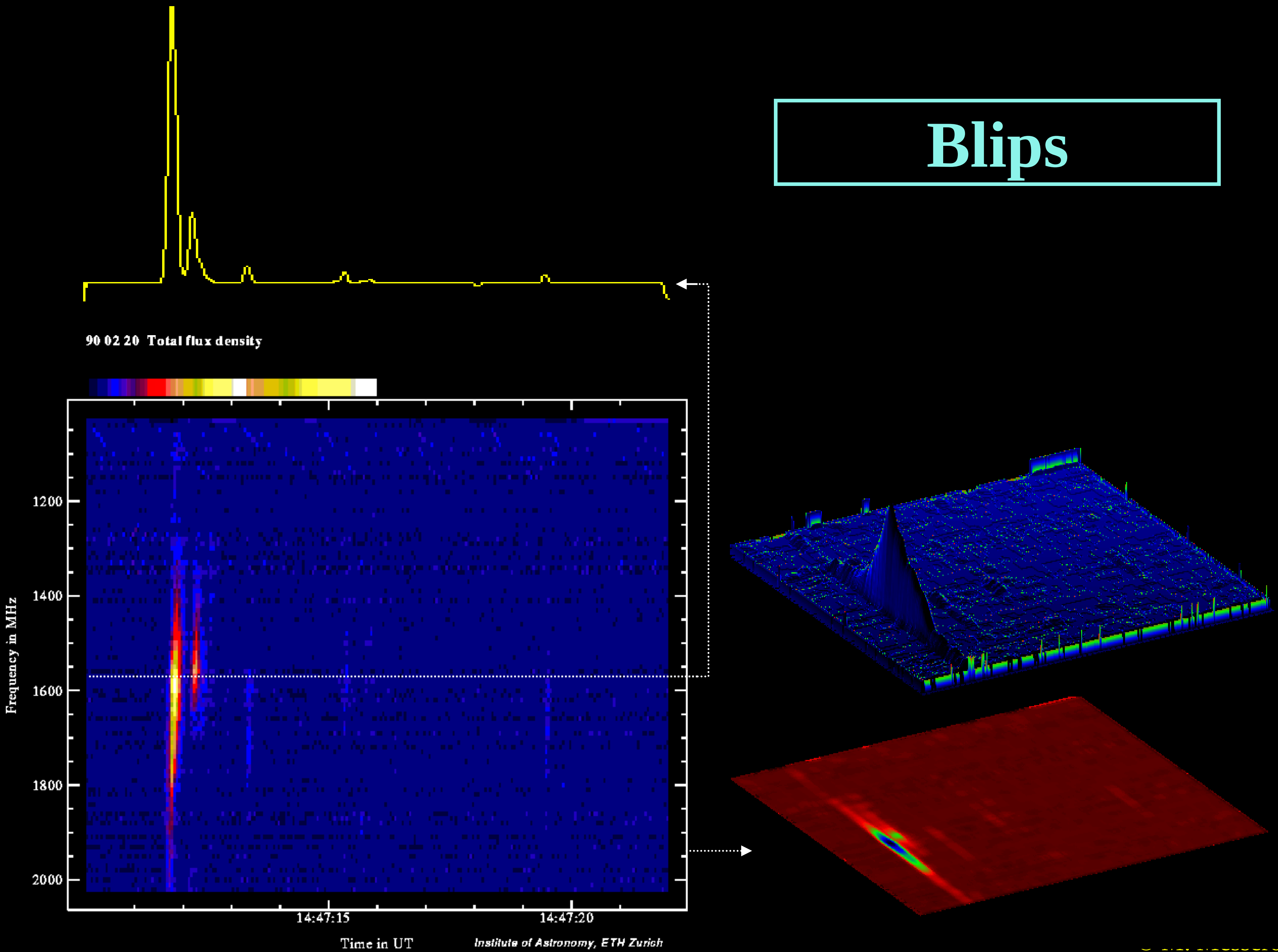

90 02 20 Total flux density
1200
1400
1600
1800
2000
Frequency in MHz
14:47:15
14:47:20
Time in UT
Institute of Astronomy, ETH Zurich

Type III Bursts

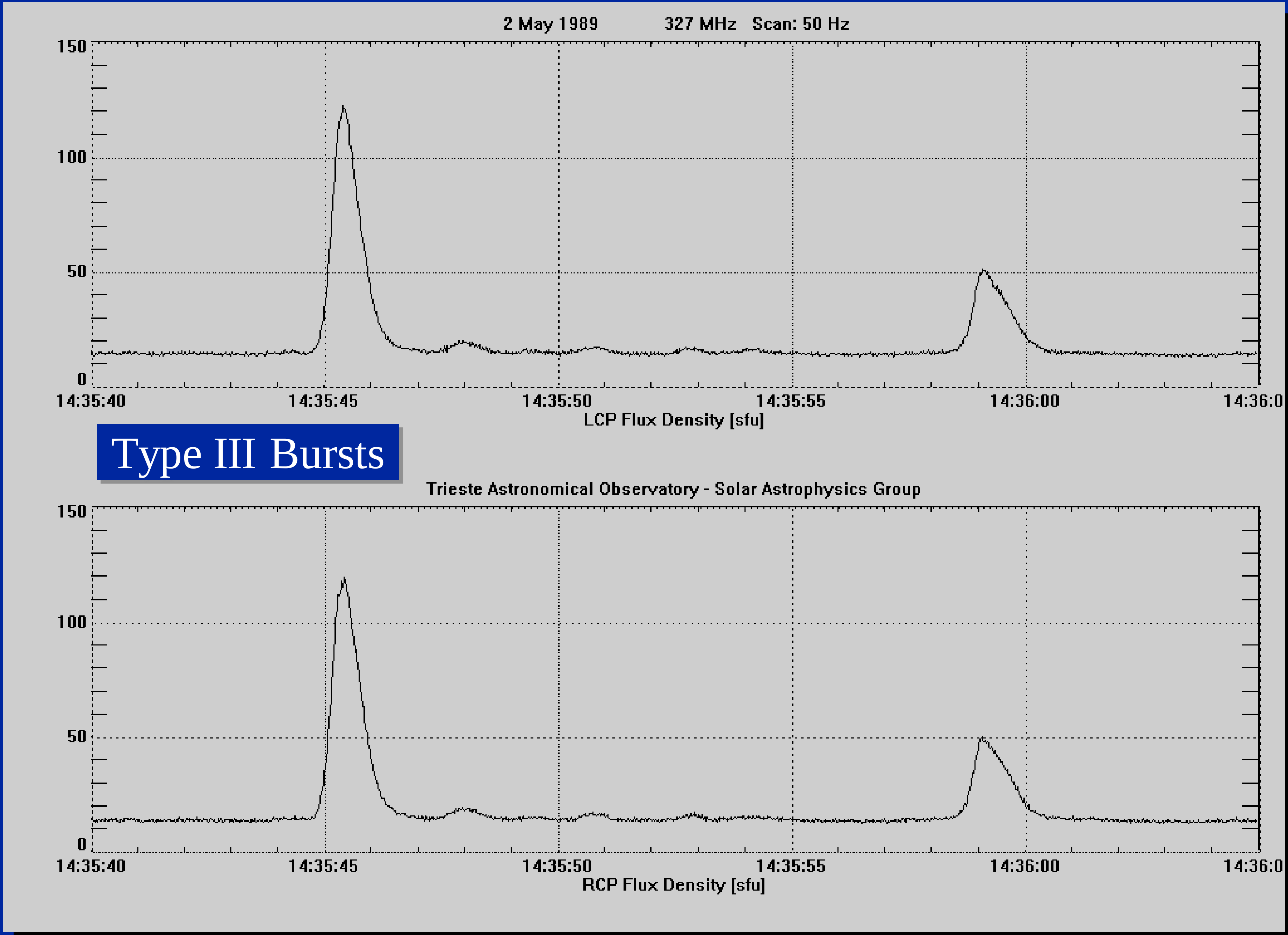

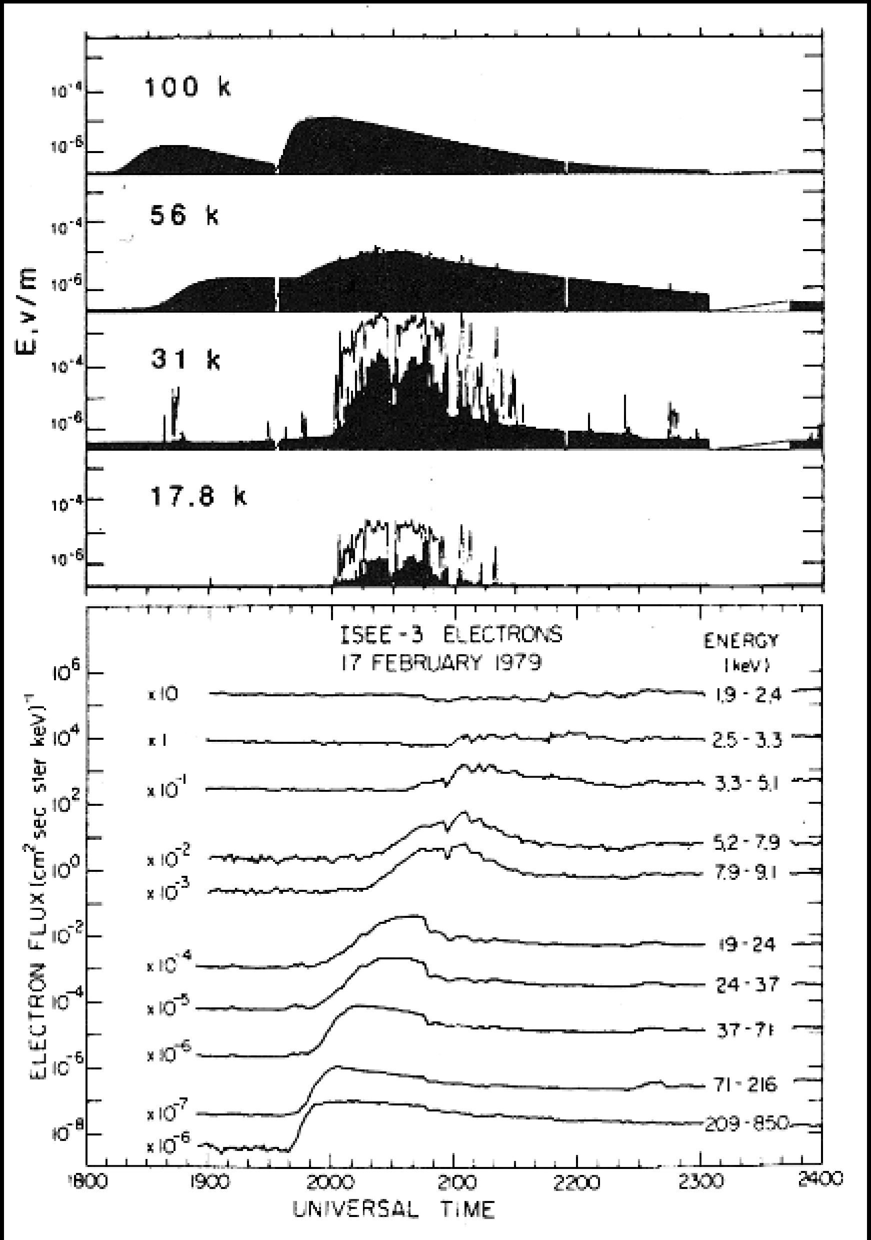

IP TYPE III BURST

ELECTRIC FIELD INTENSITY AND ELECTRON FLUXES MEASURED ON ISEE-3

- 100 kHz & 56.2 kHz > Type III bursts
- 31.1 kHz & 17.8 kHz > Plasma waves
- Electron flux in the range 2-200 keV (Lin et al., 1981; McLean & Labrum, 1985)

TYPE U BURST

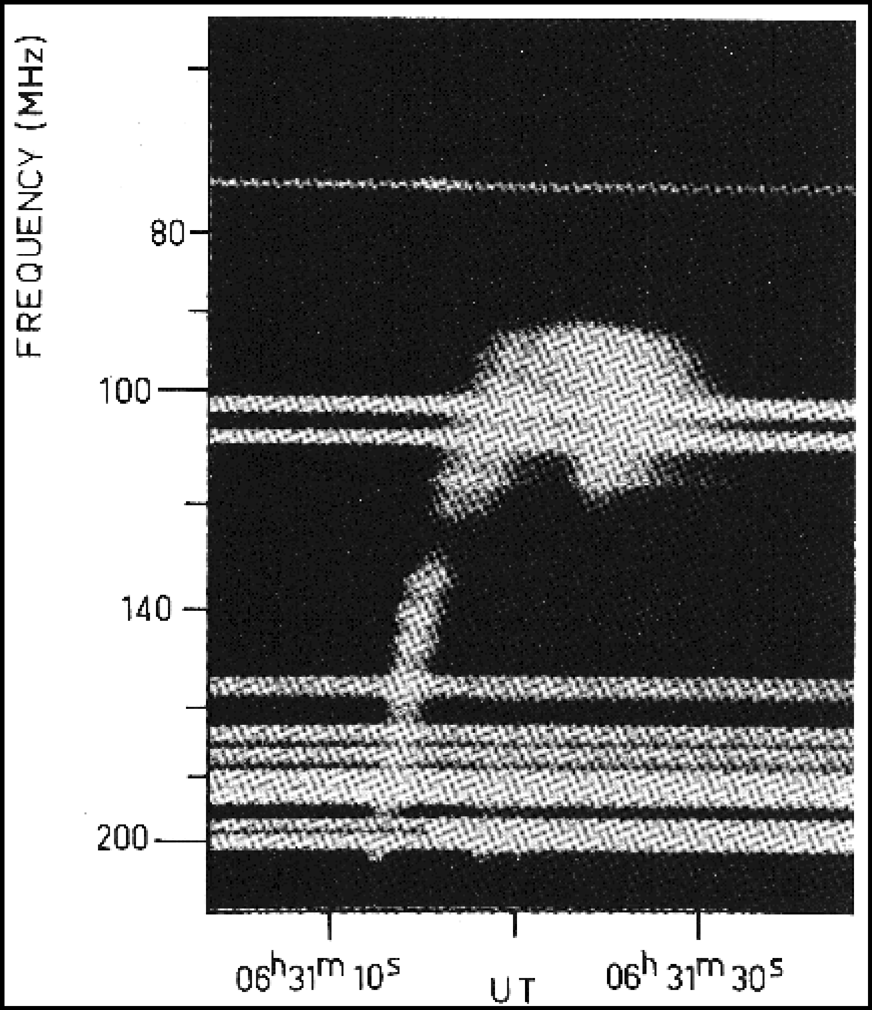

DYNAMIC SPECTROGRAM OF A TYPE U BURST
[Culgoora] (Stewart, 1975; Bruzek & Durrant, 1977)

TYPE IV BURST

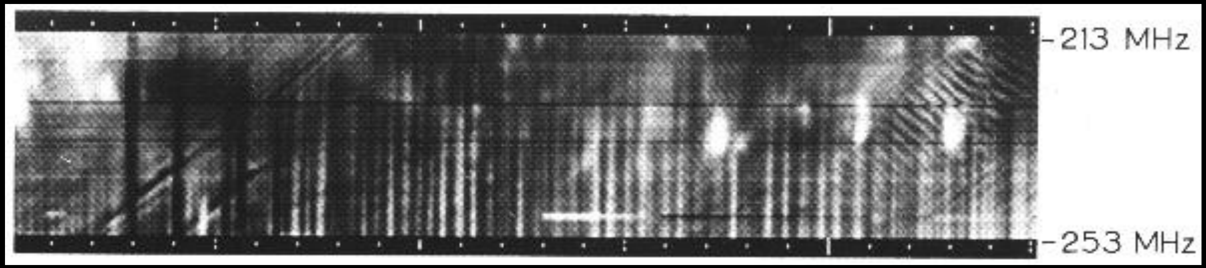

FINE STRUCTURES IN THE TYPE IV CONTINUUM

- broad-band short-lived absorptions
- pulsating structure
- zebra pattern
- fibres

[June 29, 1971; Dwingeloo] (Fokker in Bruzek & Durrant, 1977)

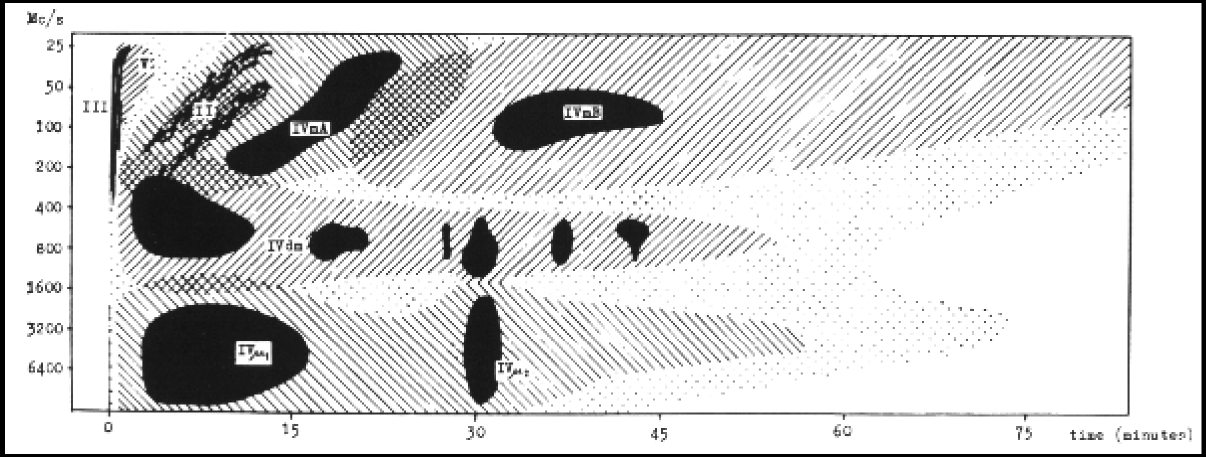

SCHEMATIC SPECTRAL DIAGRAM OF A TYPE VI BURST

(Fokker in Bruzek & Durrant, 1977)

MOVING TYPE IV BURST

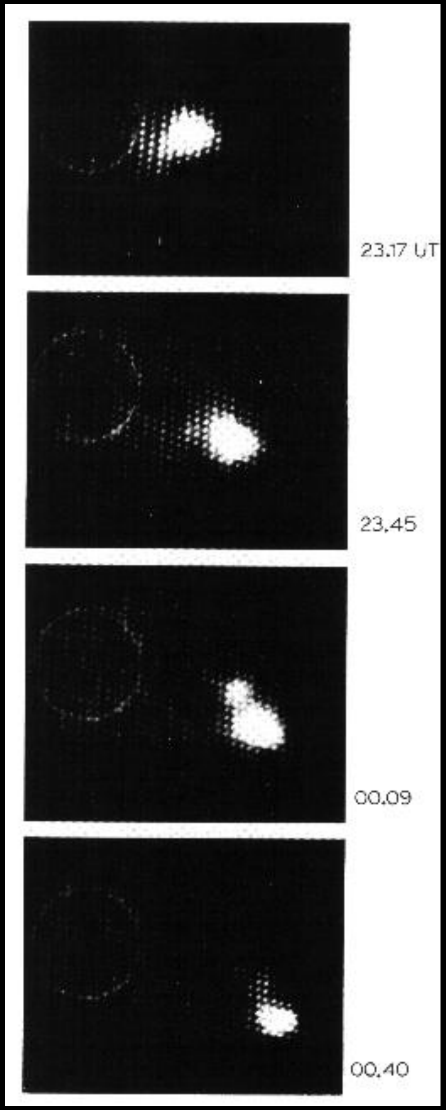

RADIOHELIOGRAM OF A MOVING TYPE IV BURST

[March 1, 1969; 80 MHz; Culgoora] (Riddle, 1970; Bruzek & Durrant, 1977)

Type IV Burst

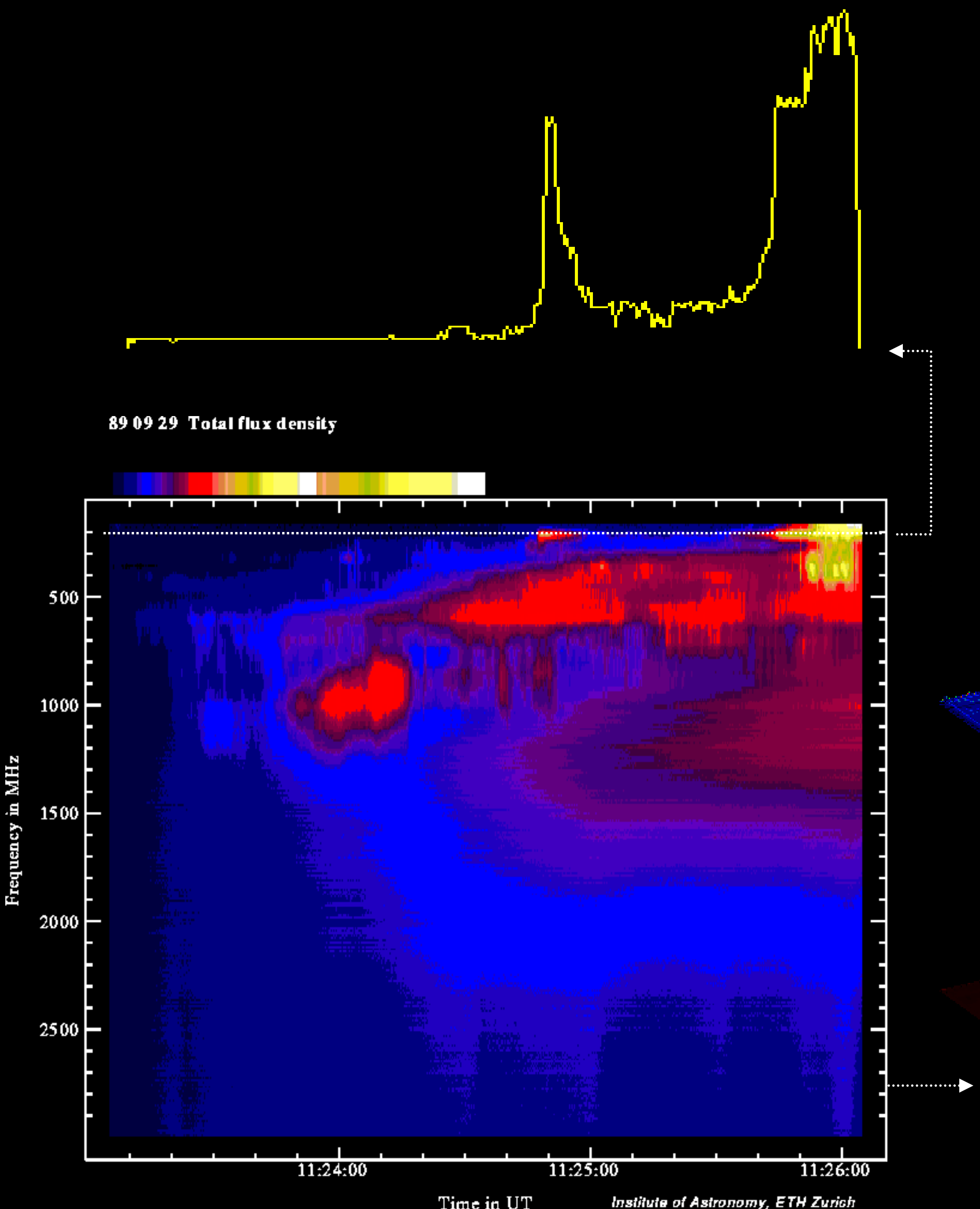

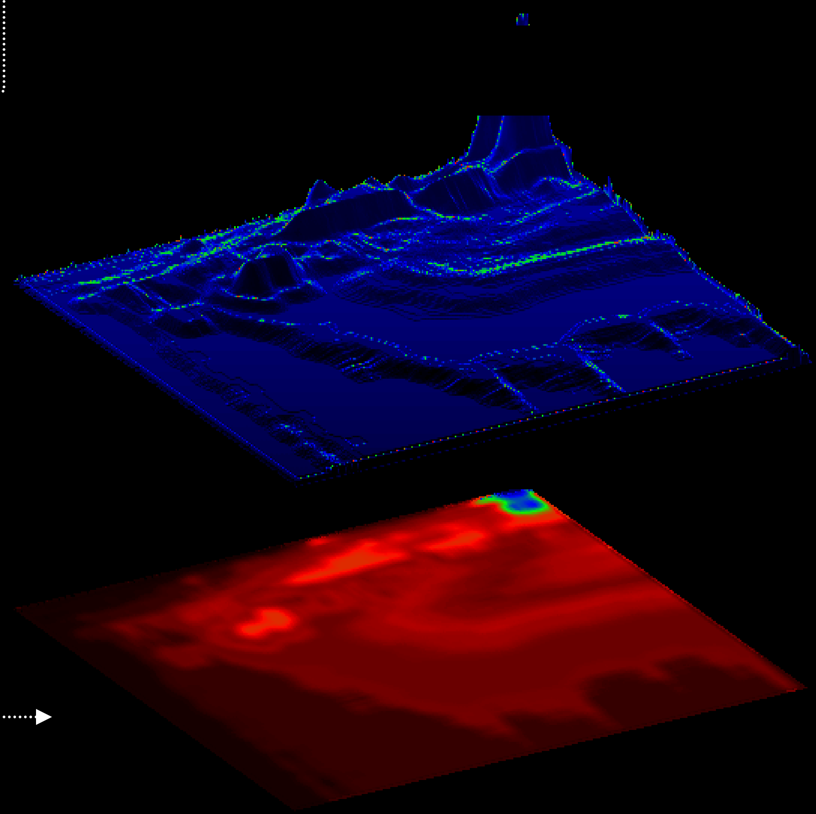

Type IV Burst

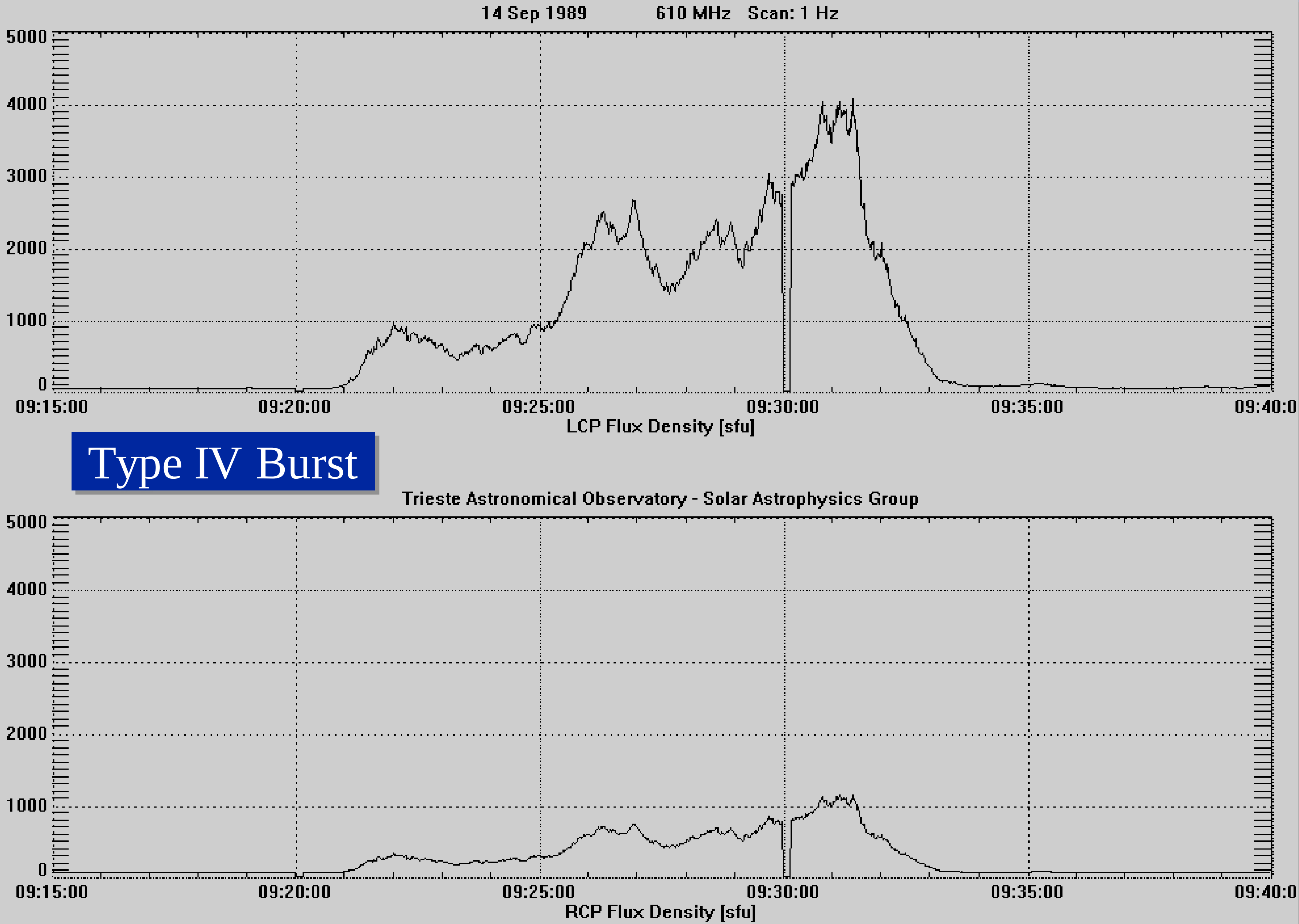

Spikes

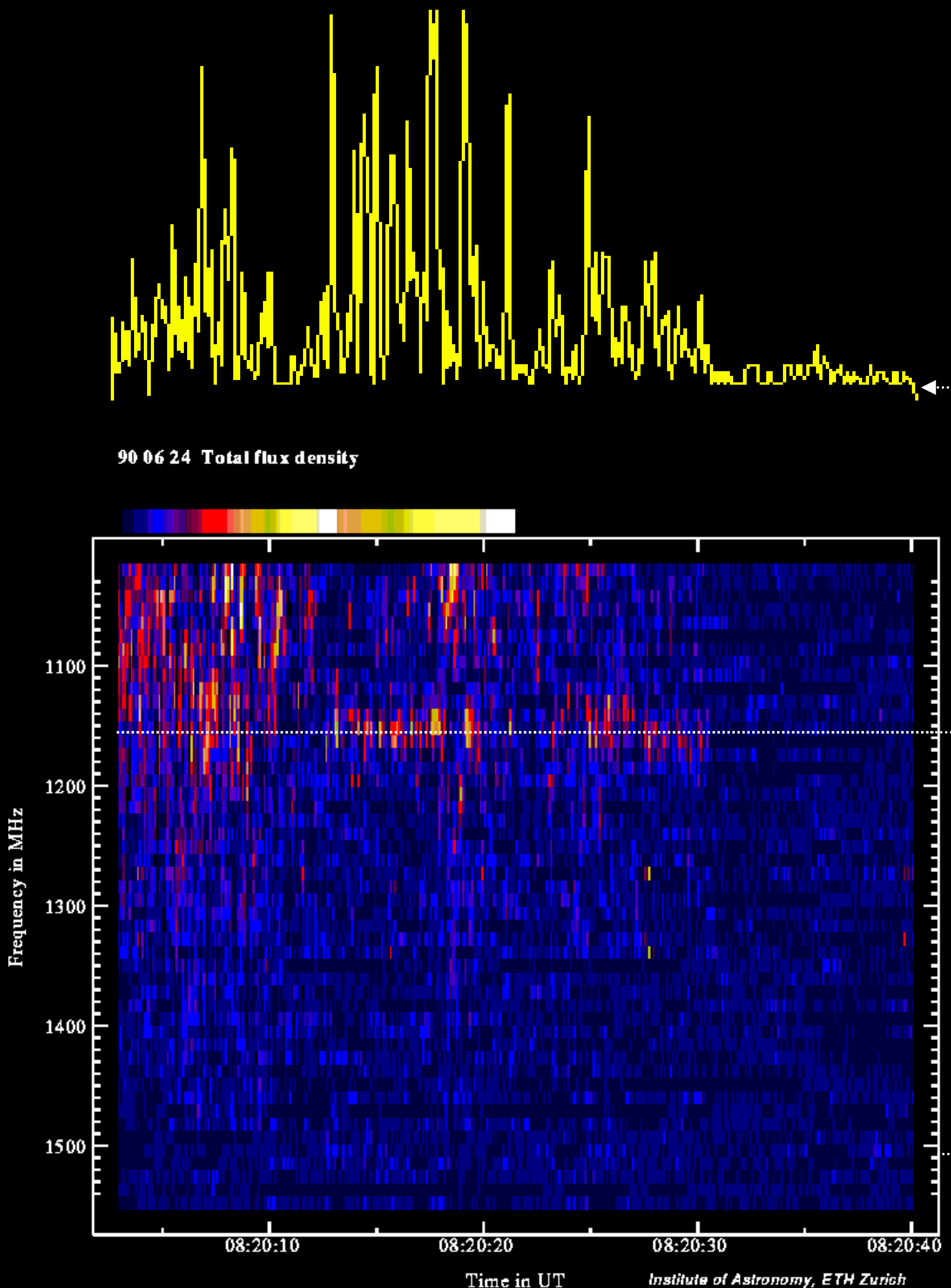
90 06 24 Total flux density
1100
1200
1300
1400
1500
Frequency in MHz
08:20:10
08:20:20
08:20:30
08:20:40
Time in UT
Institute of Astronomy, ETH Zurich

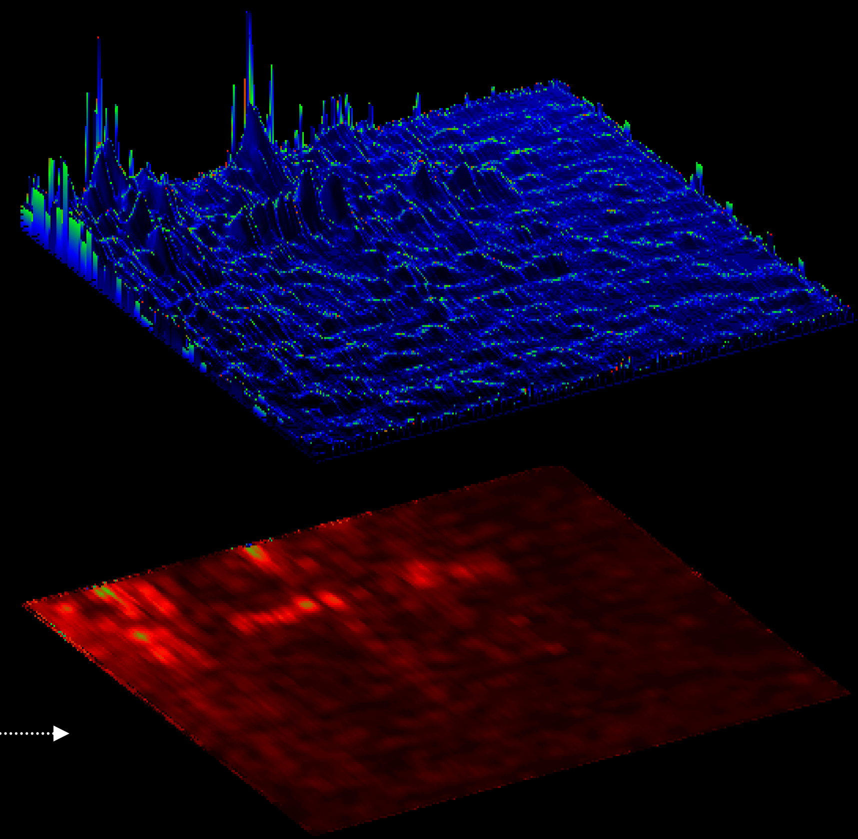

Spikes

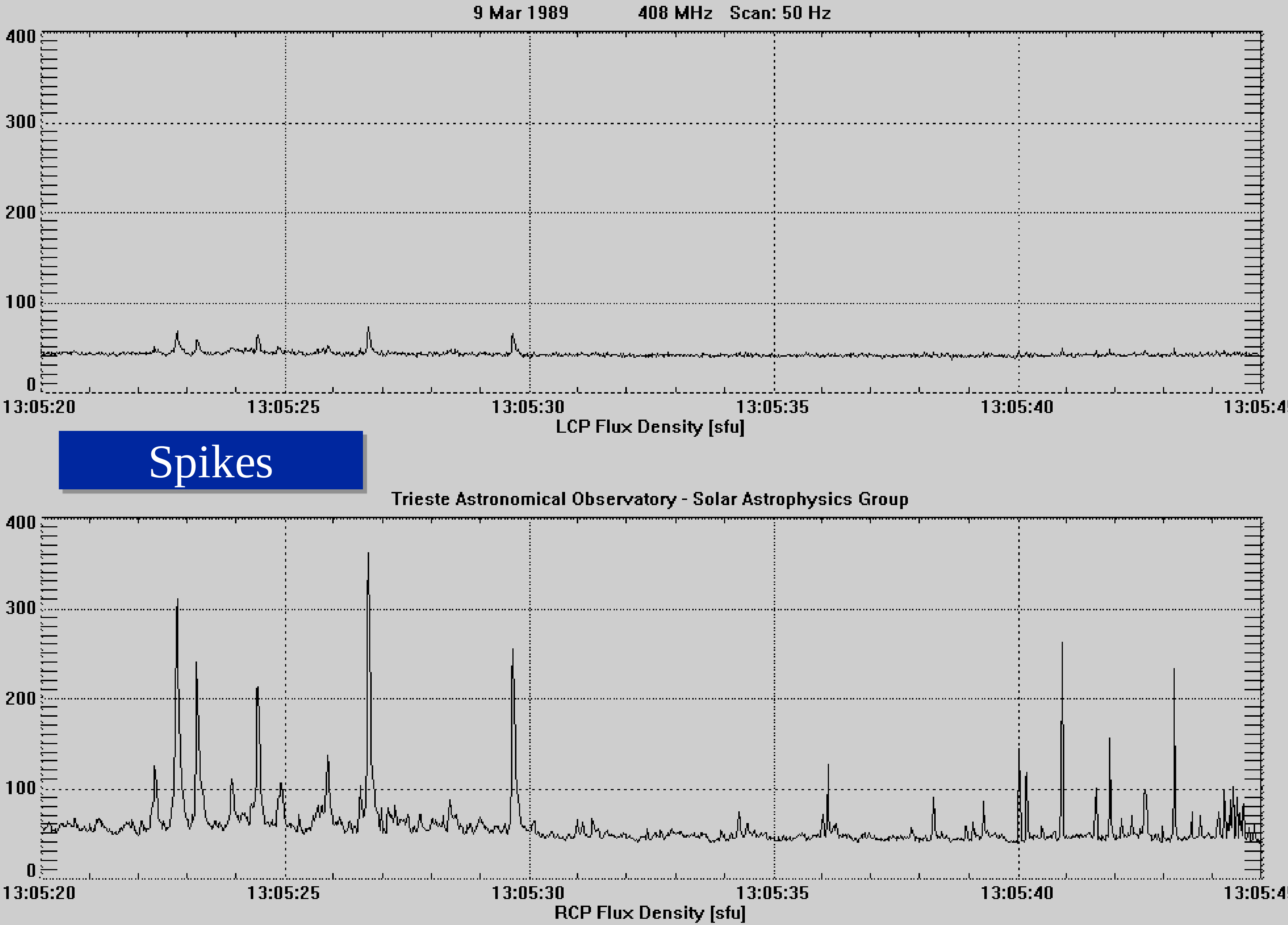

9 Mar 1989
408 MHz Scan: 50 Hz
400
300
200
100
0
13:05:20
13:05:25
13:05:30
13:05:35
13:05:40
13:05:4
LCP Flux Density [sfu]
Trieste Astronomical Observatory - Solar Astrophysics Group
400
300
200
100
0
13:05:20
13:05:25
13:05:30
13:05:35
13:05:40
13:05:4
RCP Flux Density [sfu]

Pulsations

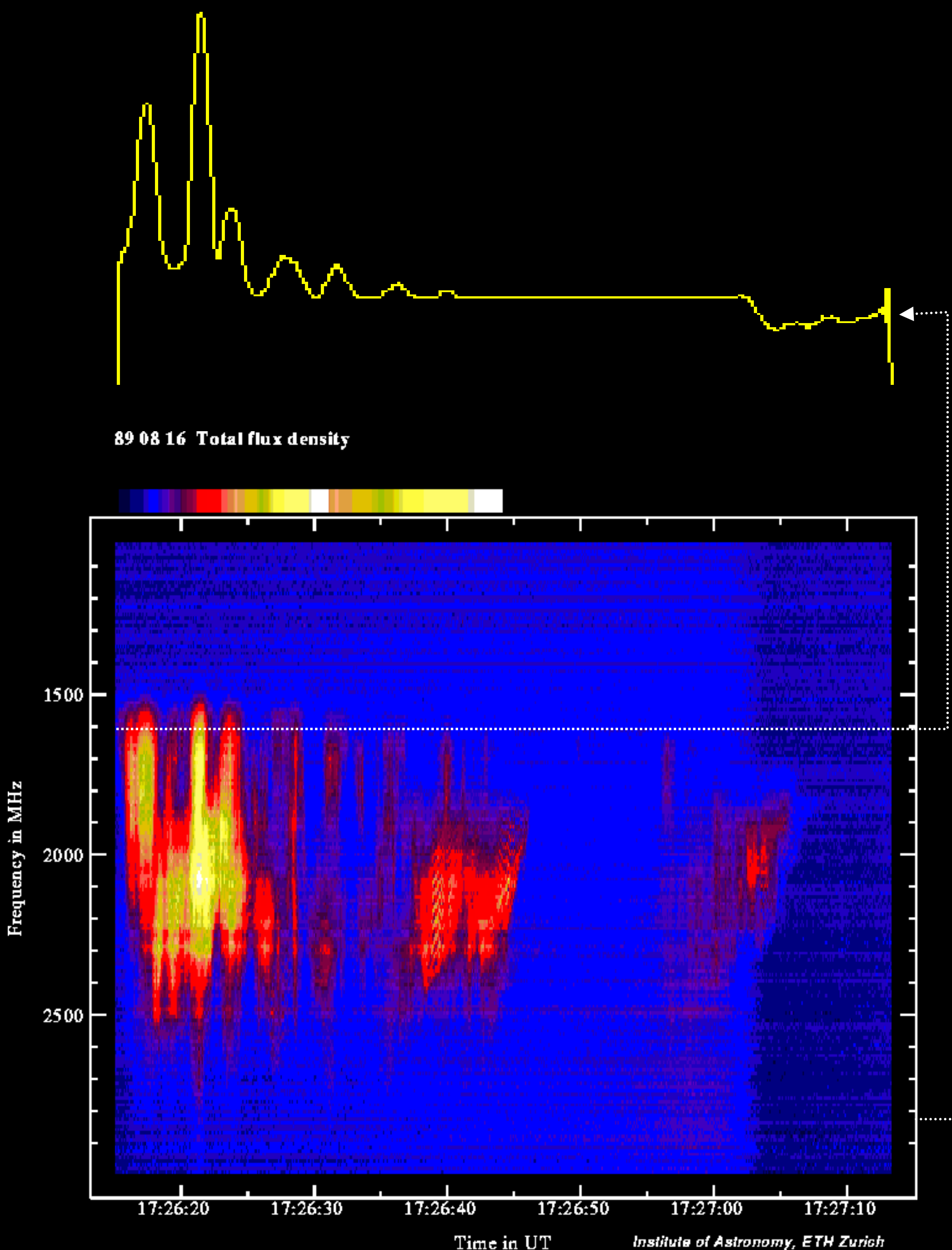
89 08 16 Total flux density
1500
2000
2500
Frequency in MHz
17:26:20
17:26:30
17:26:40
17:26:50
17:27:00
17:27:10
Time in UT
Institute of Astronomy, ETH Zurich

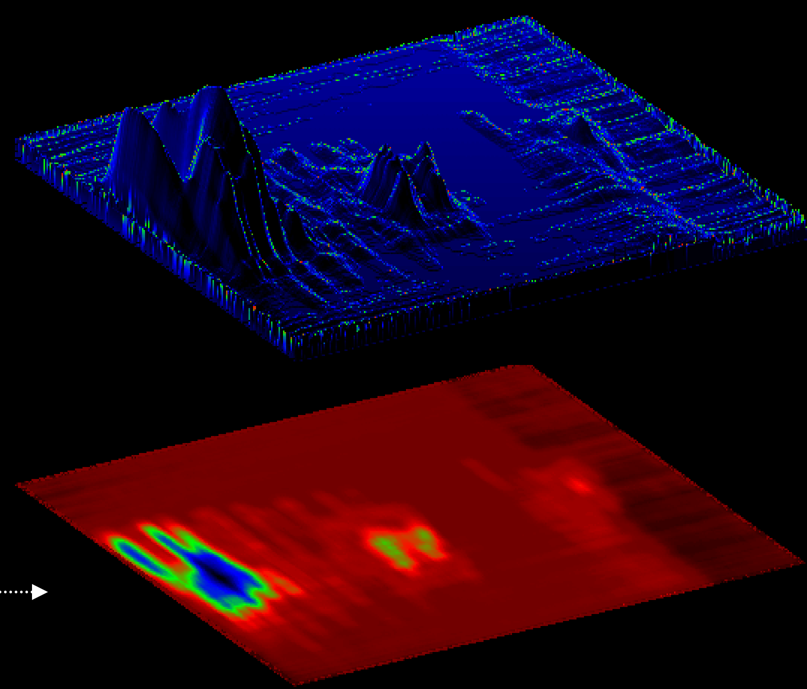

Pulsations

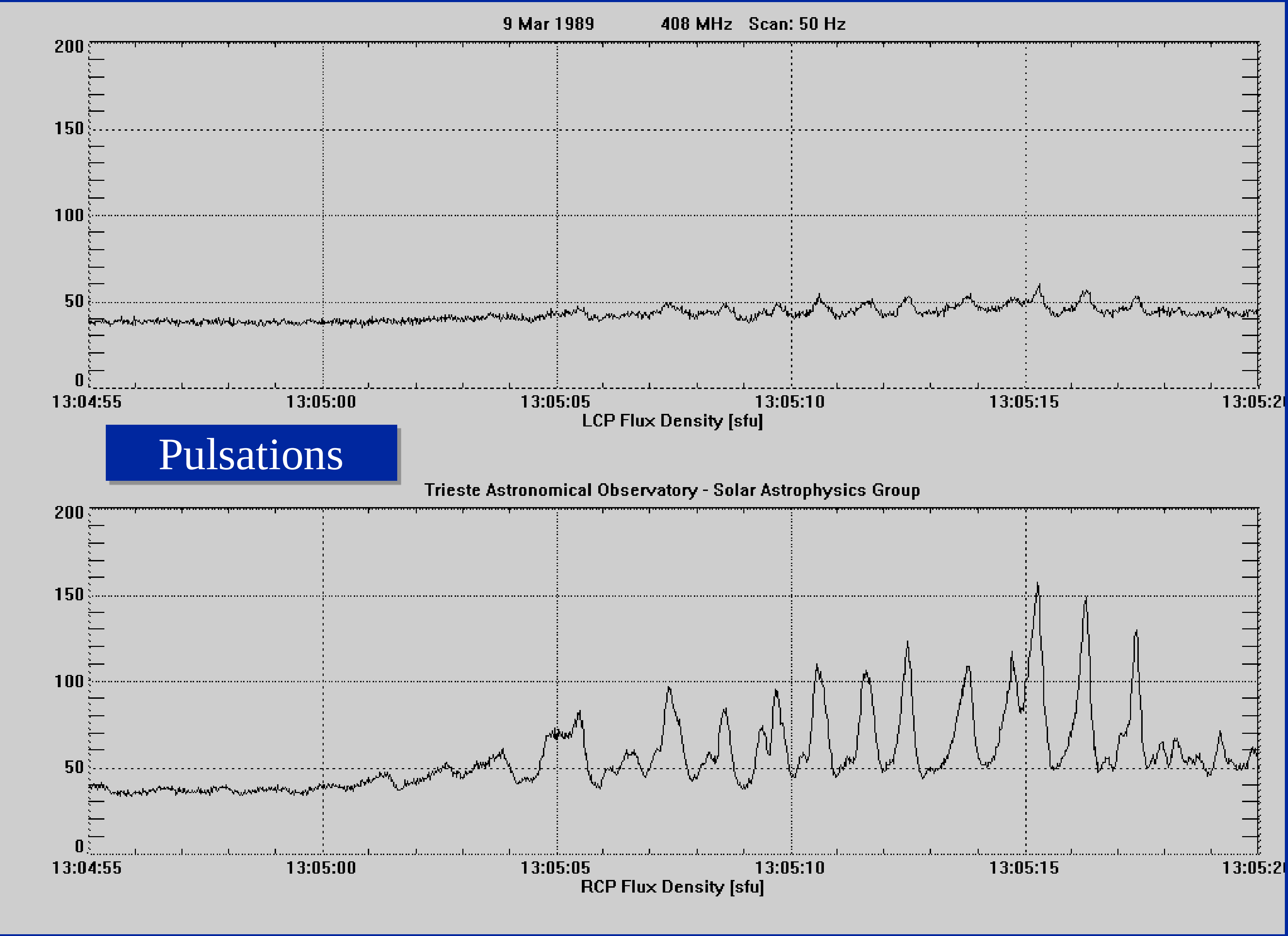

9 Mar 1989
408 MHz
Scan: 50 Hz
200
150
100
50
0
13:04:55
13:05:00
13:05:05
13:05:10
13:05:15
13:05:20
LCP Flux Density [sfu]
Trieste Astronomical Observatory - Solar Astrophysics Group
RCP Flux Density [sfu]

TYPE V BURST

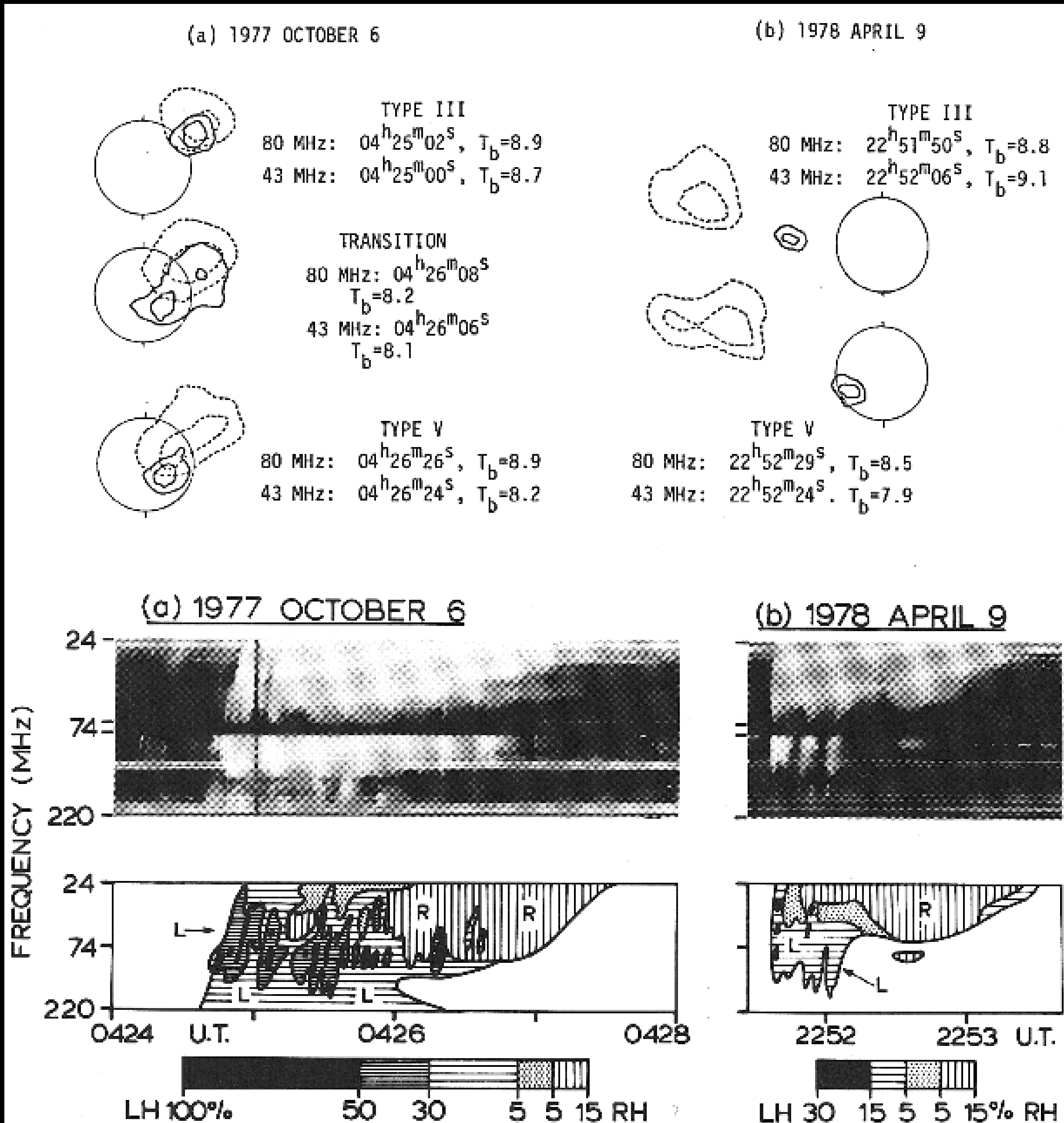

TYPE III-V BURSTS
[43 and 80 MHz; Culgoora]
(DSG; McLean & Labrum, 1985)

THE RADIO SUN THROUGH
IMAGING RADIO INSTRUMENTS

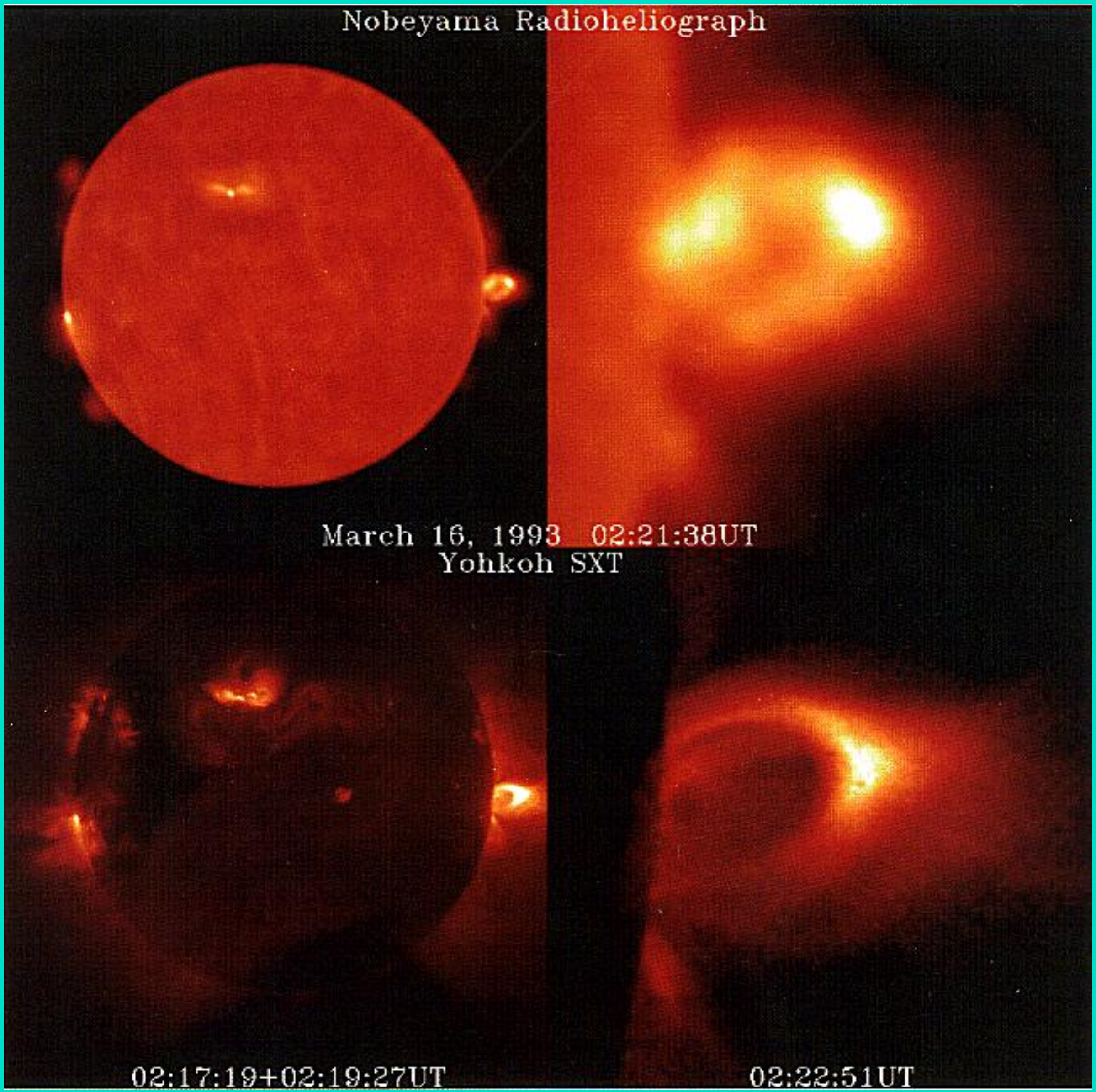

Coronal Loop in Radio (1.7 cm) and Soft X-Rays

Nobeyama Radioheliograph (17 GHz)
+
Yohkoh Soft X-Ray

NRG (1994)

Coronal Features in Radio at 20 cm and 91 cm (VLA)

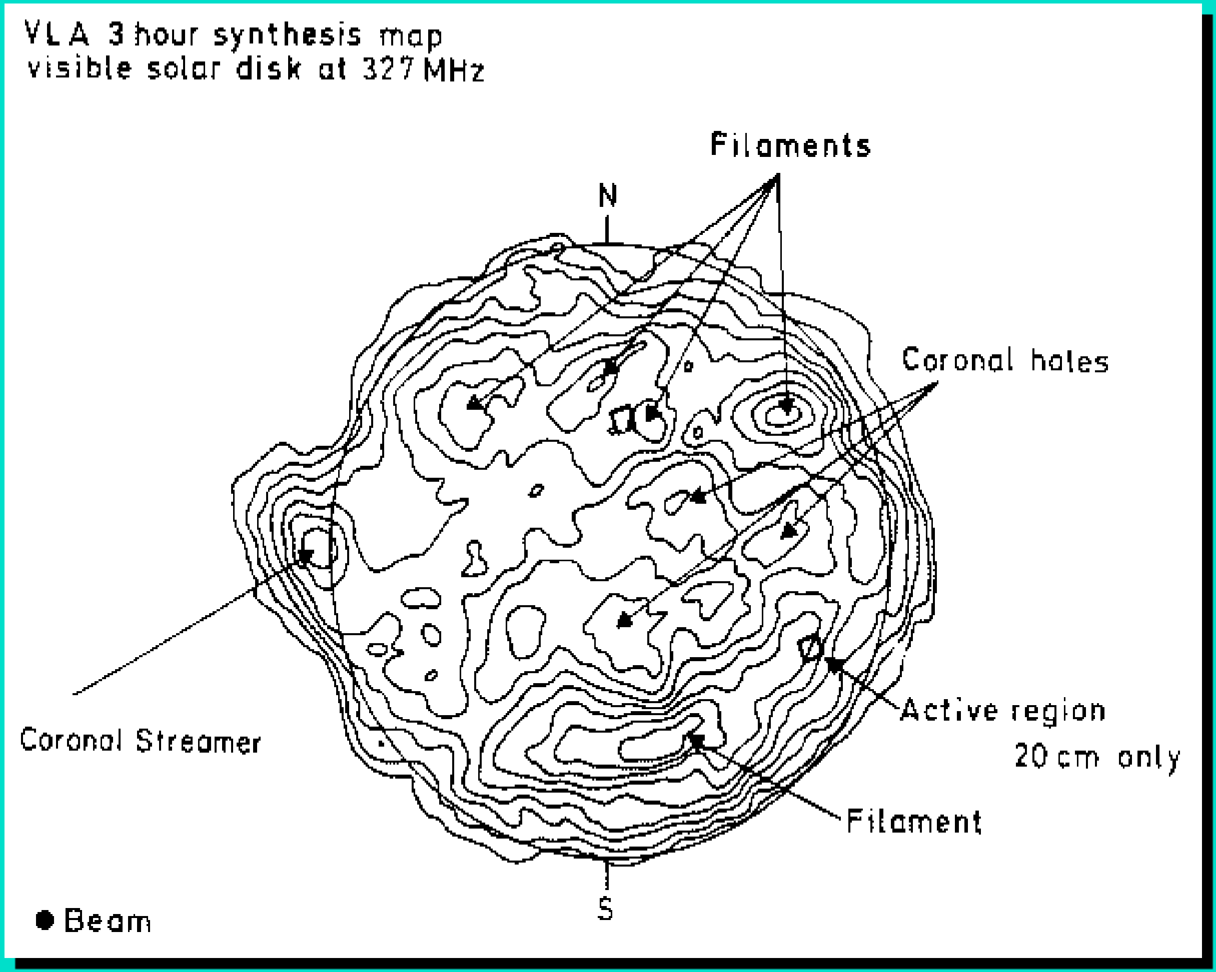

Lang (1992)

Coronal Features in Radio at 1.7 m (Nancay) and 4.1 m (CLRO)

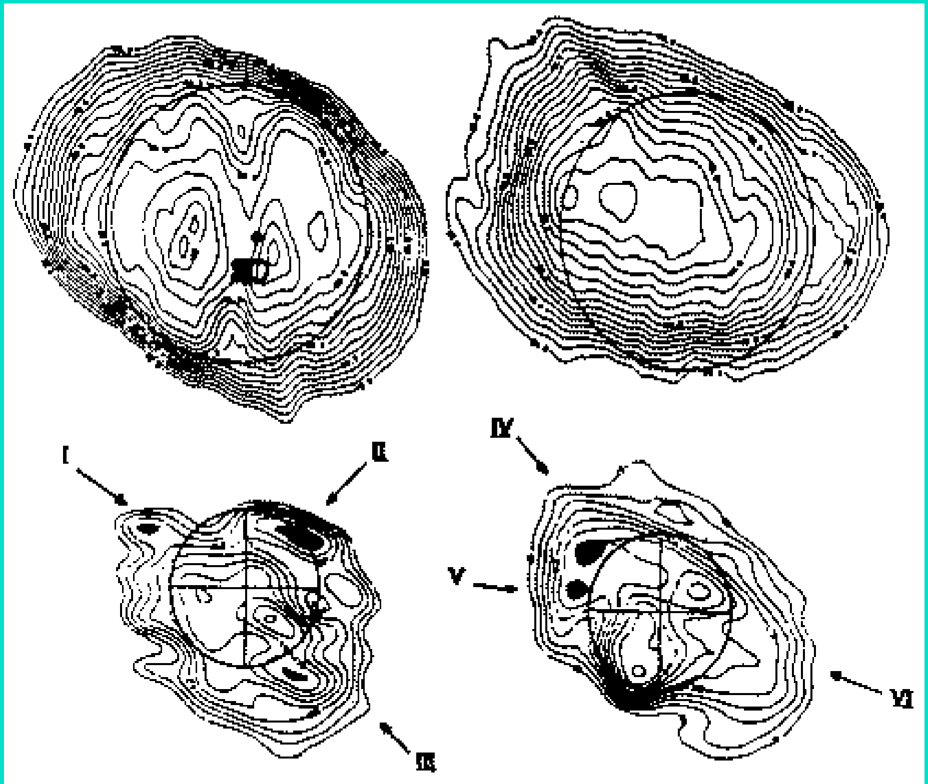

Kundu (1992)

Coronal Features in Radio at 70 cm and 1.8 m (Nancay)

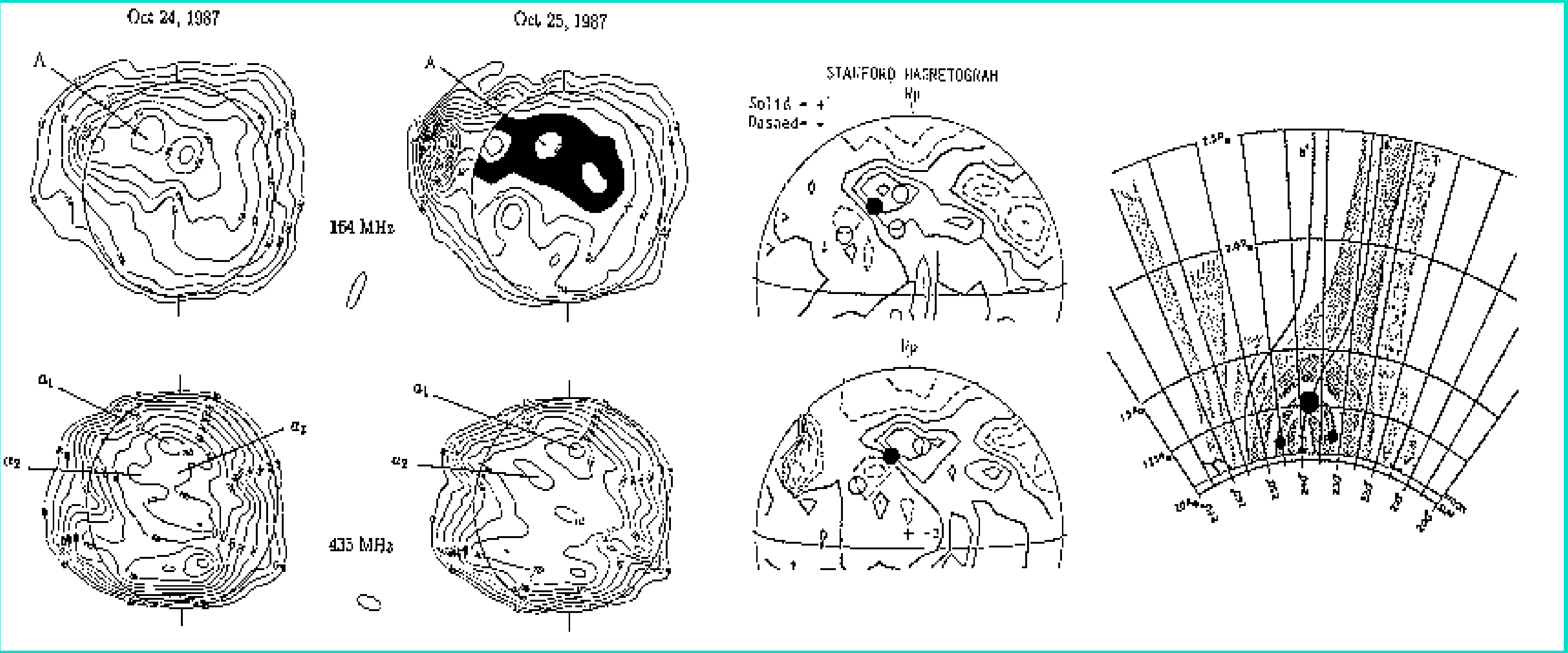

Lantos and Alissandrakis (1992)

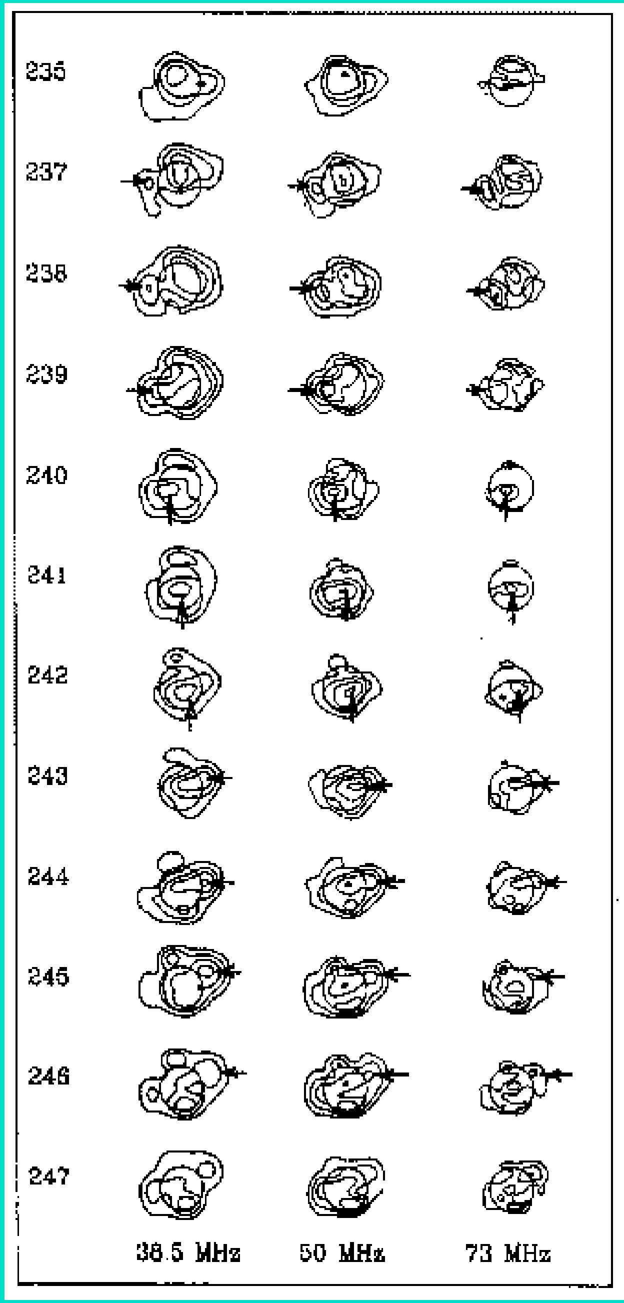

Coronal Features in Radio at 4 m, 6 m and 7.8 m (CLRO)

Rotation of streamers:

•Model of geometry
•Computation of Ray-Tracing Images

Results:

•Density profiles ~ 5 x Saito
•Background ~ 0.1 x Saito (scattering?)

Schmal et al. (1992)

THE SOLAR ACTIVITY AS DRIVER OF GEO-EFFECTIVE PERTURBATIONS

COUPLING IN THE SUN-EARTH SYSTEM

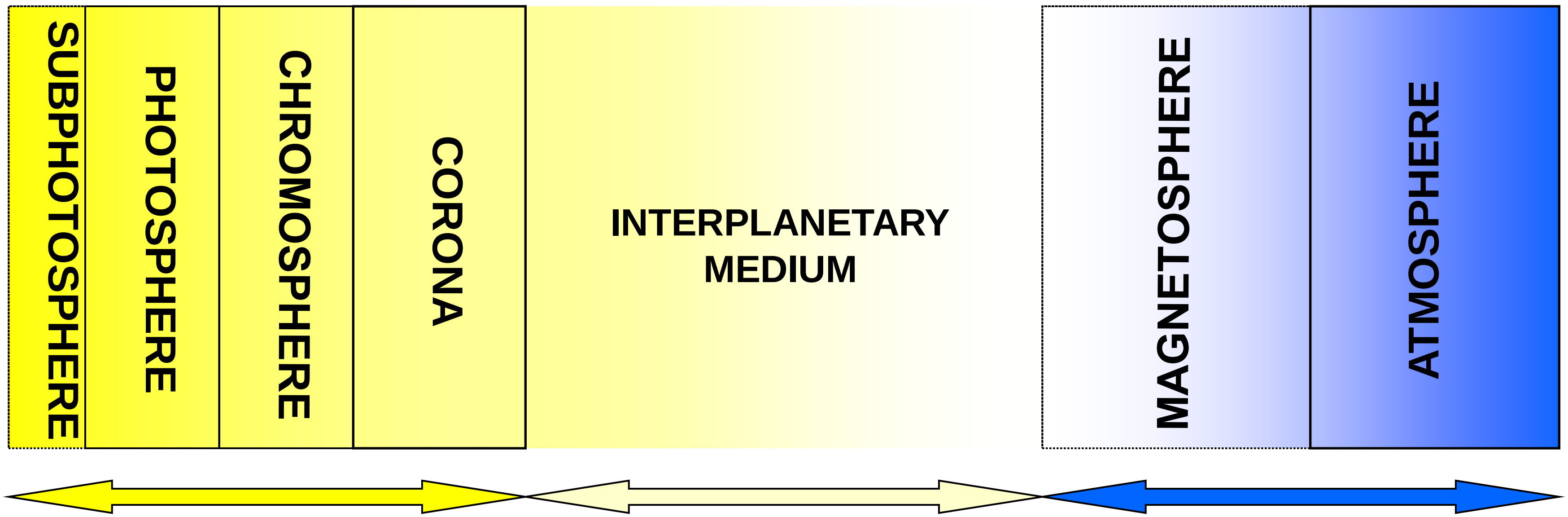

SUN	INTERPLANETARY SPACE	EARTH ENVIRONMENT
Radiated Power $3.82\ 10^{23}$ kW		1.36 kW/m^2
Total SW Mass Flow 10^6 tons/s		
Energy in SW $4.1\ 10^{20}$ W		10^{13} W / 30 R_E
Energy in CME $7\ 10^{18}$ W		$1.73\ 10^{17}$ W

CHARACTER OF THE MAGNETIC FIELD

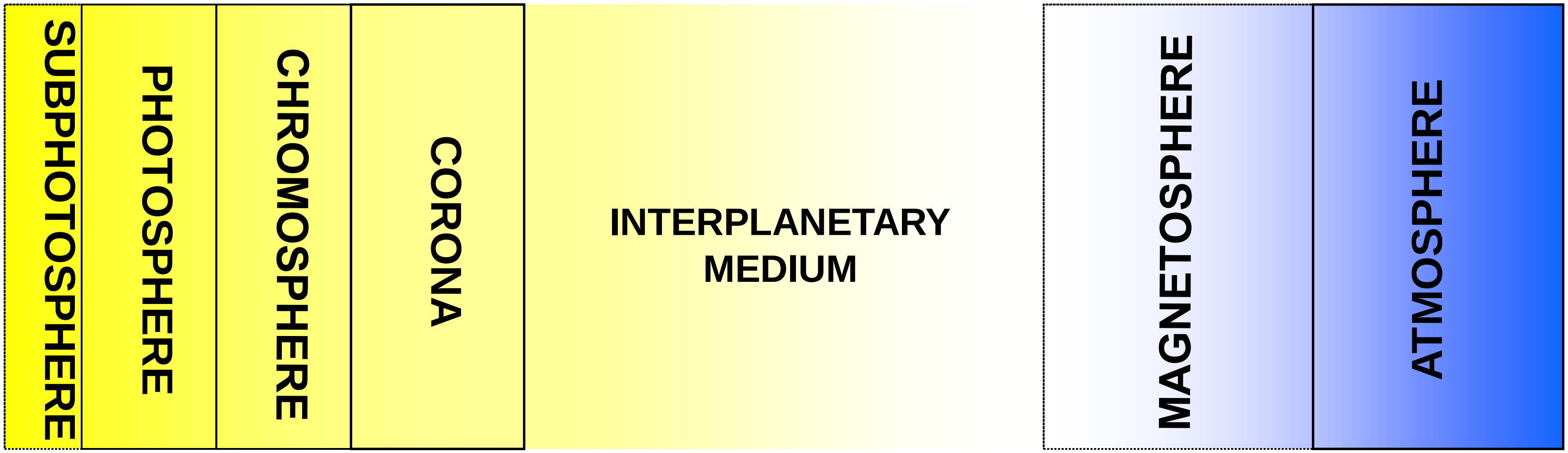

DIPOLAR RADIAL SECTORED DIPOLAR
AZIMUTHAL WARPED ASYMMETRIC
MAGNETIC FIELD

SOLAR DRIVERS OF IPM & EARTH PERTURBATIONS

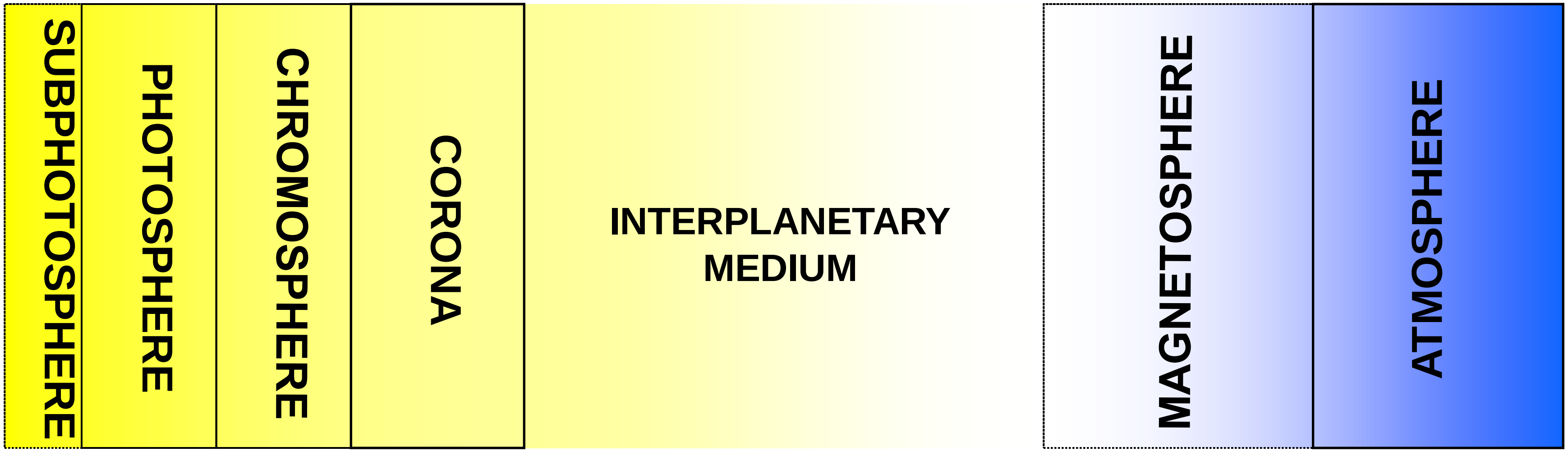

Fluid motions

Sunspots

e.g.

Flares — γ, X, UV — SID

p, e — PCA

Prominences — CME

Filaments

Condensations

Streamers — Slow SW

Recurrent & n.-rec.

Coronal Holes — Fast SW — Geomagnetic Storms

INDICATIVE TIMING OF S-T PERTURBATIONS

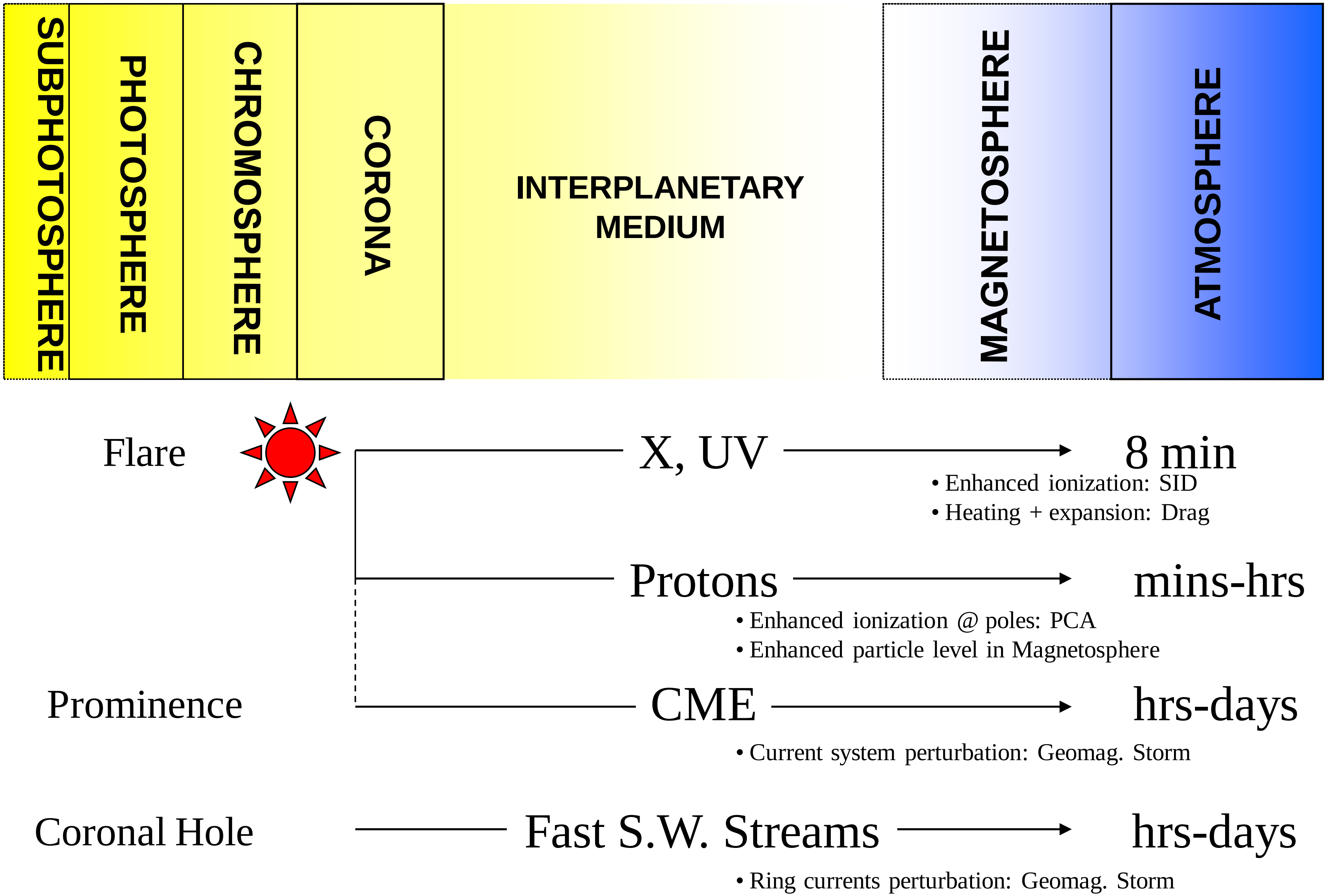

A SCHEME FOR SPACE WEATHER MONITORING

Solar-Terrestrial Environment

PHYSICAL CONDITIONS

- defined as SPACE WEATHER
- strongly affected by SOLAR ACTIVITY but
- HIGHLY NONLINEARLY COUPLED with it
- QUITE COMPLEX TO FORECAST

SPACE WEATHER
Alerts and Forecasts Scheme

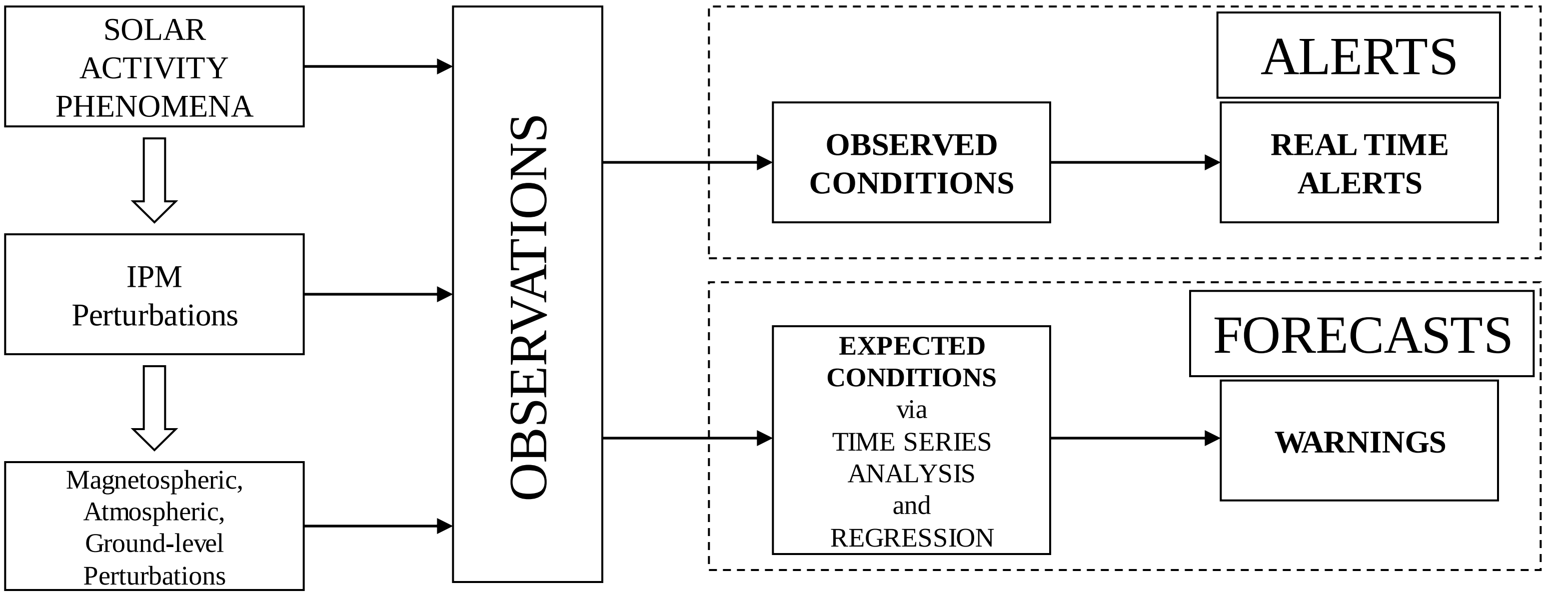

SPACE WEATHER
Solar Surveillance and Alerting Program at Kanzelhöhe Solar Observatory

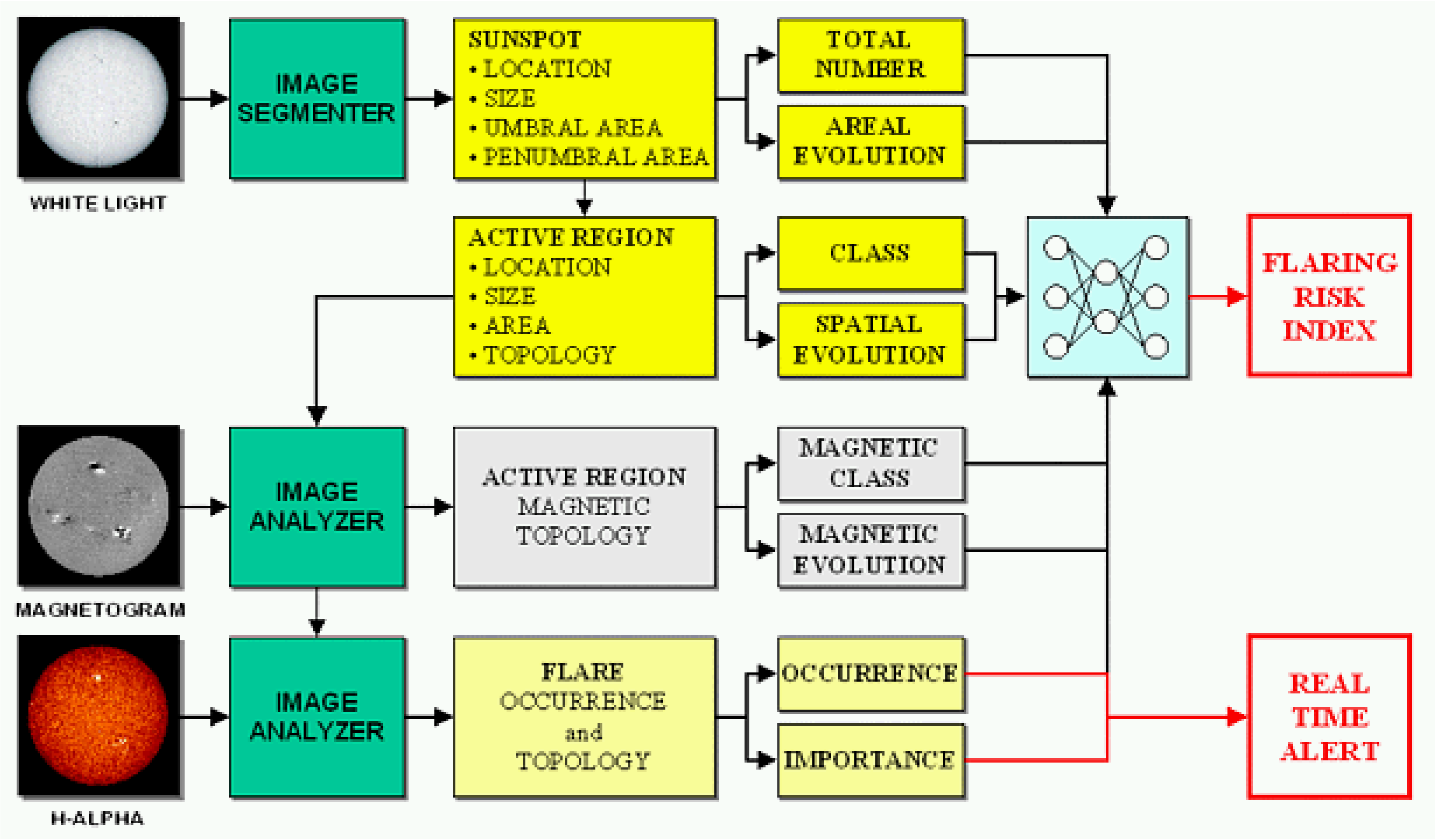

SOLAR FLARE

- **Magnetic reconnection** occurs and result in:
  - **Plasma heating**
    - T~10^4 K in chromosphere
    - T~10^7 K in corona
  - **Particle acceleration** (20 keV - 1 GeV)
  - **Total energy** in largest events ~10^{25} J
  - **Transient e.m. radiation**
    - from γ to Radio (thermal)
    - HXR (< 0.1 nm) (non-thermal)
    - Radio by en. Particles (non-thermal)

FLARE MODEL

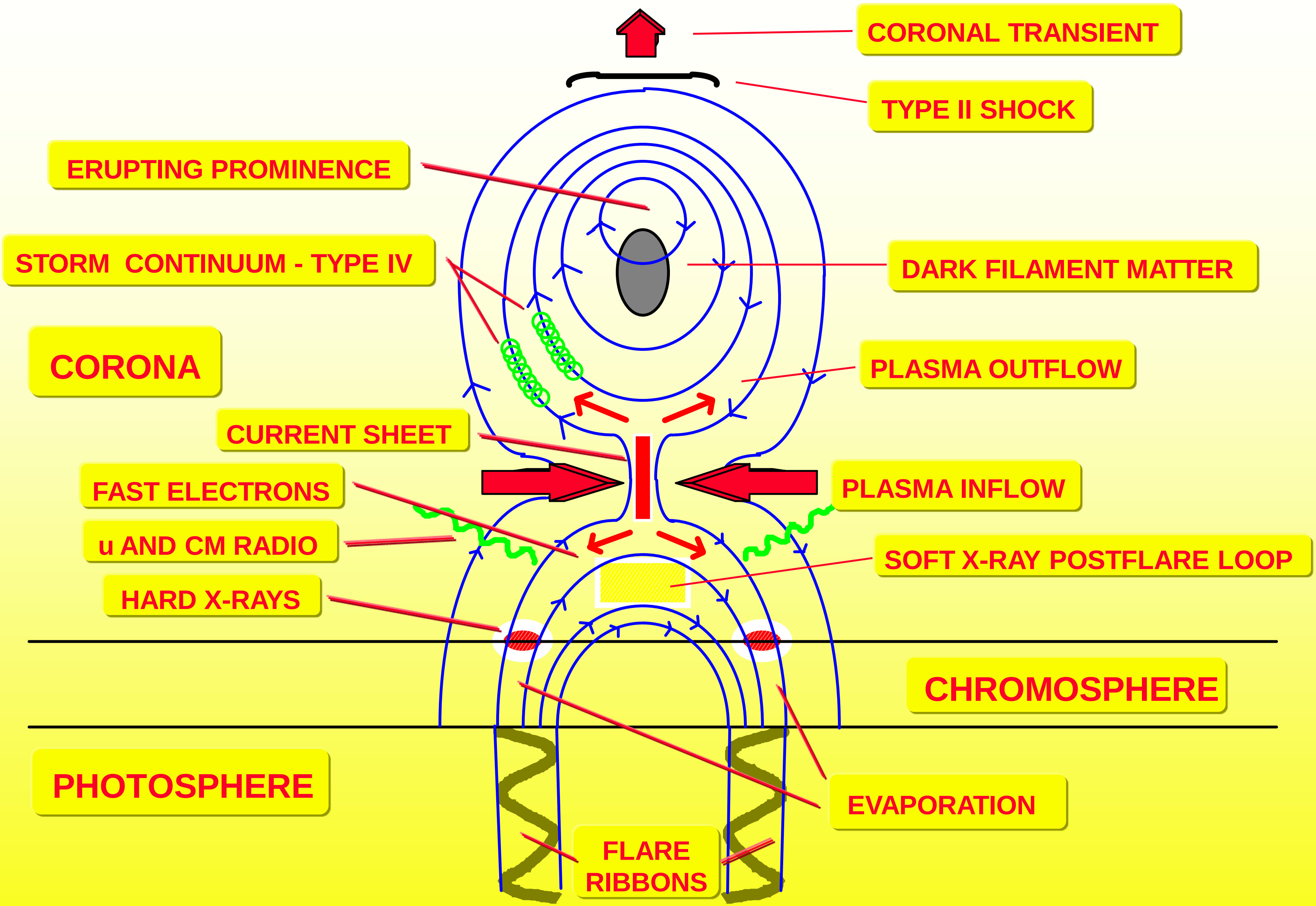
CORONAL TRANSIENT
TYPE II SHOCK
ERUPTING PROMINENCE
STORM CONTINUUM - TYPE IV
DARK FILAMENT MATTER
CORONA
PLASMA OUTFLOW
CURRENT SHEET
FAST ELECTRONS
PLASMA INFLOW
u AND CM RADIO
SOFT X-RAY POSTFLARE LOOP
HARD X-RAYS
CHROMOSPHERE
PHOTOSPHERE
EVAPORATION
FLARE
RIBBONS

Timing of Flare-Related Events

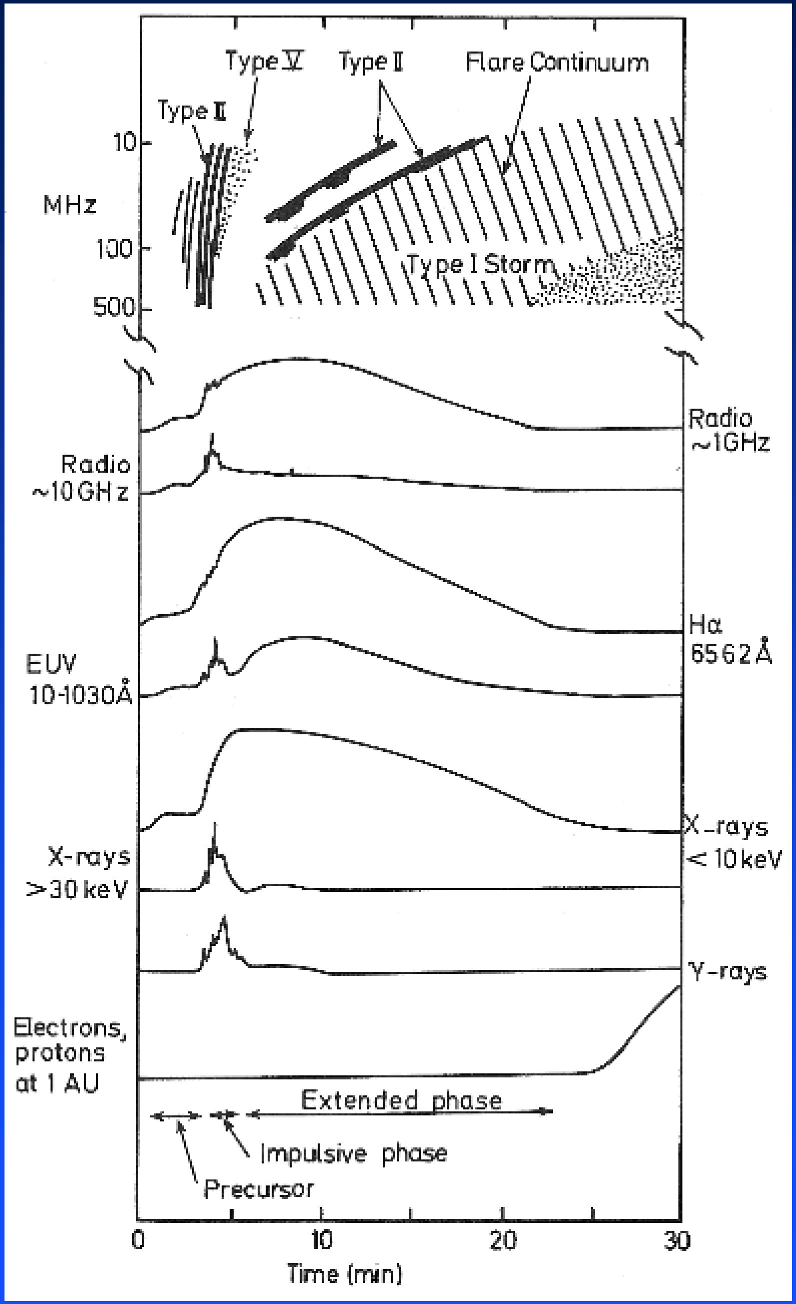

McLean & Labrum (1985)

Typical Timing of Solar Radio Bursts with Respect to Flares

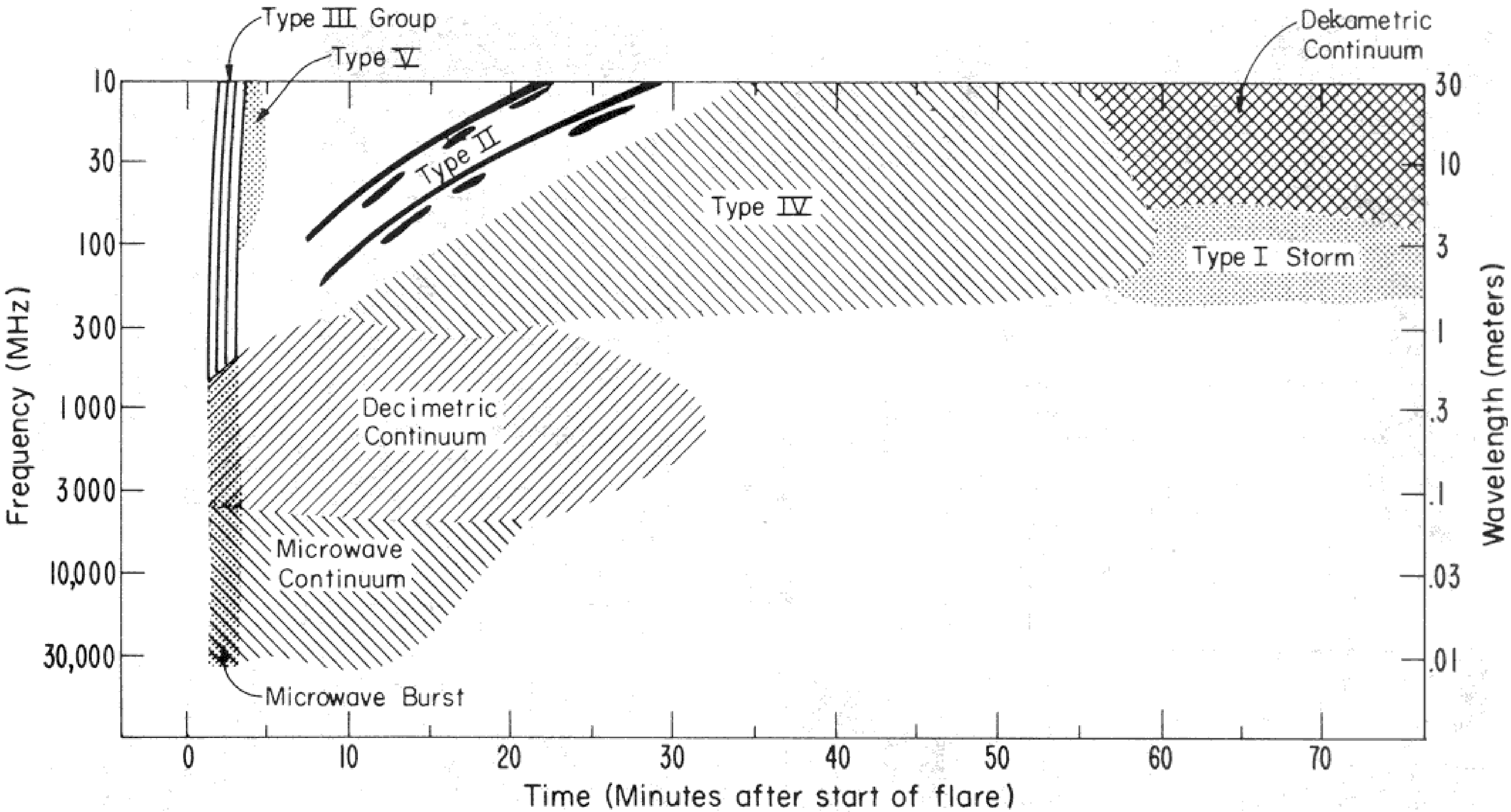

Synopsis of Flare-Reated Solar Radio Events

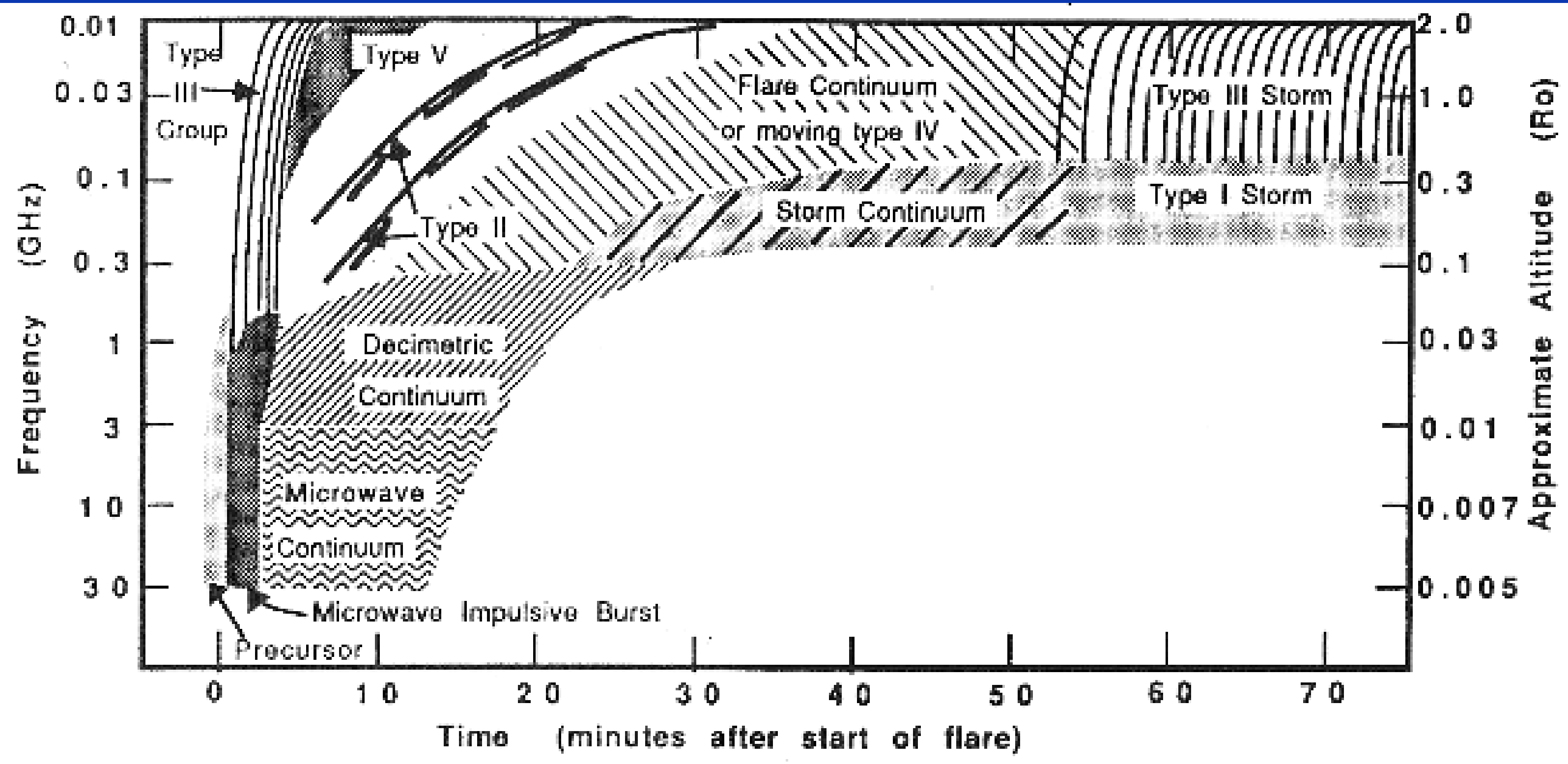

Dulk (1994)

Solar Radio Burst Classifications

TYPE	CHARACTERISTICS	DURATION	FREQUENCY RANGE	ASSOCIATED PHENOMENA
I	Short, narrow-band bursts Usually in large numbers with underlying continuum.	Burst: 1 second. Storm: hrs.- days	80-200 MHz	Active regions eruptive prominences.
II	Slow drifting bursts. Often accompanied by second harmonic	5-30 minutes	Fundamental: 20-150 MHz.	Flares, proton emission, mag-netonetohydro-dynamic shock waves
III	Fast drifting bursts. Can occur singularly, in groups,or storms. Can be accompanied by second harmonic.	Burst: 1-3 seconds. Group: 1-5 min.	10 kHz-1 GHz	Active regions, flares.
IV	Stationary Type IV Broad-band continua emission with fine structure.	Hours - days.	20 - >1000 MHz.	Flares, proton
	Moving Type IV Broad-band, slow drifting, smooth continua.	30 min.-2 hrs.	20-400 MHz.	Eruptive prominences Magnetohydro-dynamic shock waves
	Flare Continua: Broad-band, smooth continua.	3-45 min.	25-200 MHz	Flares, proton Emission
V	Smooth, short lived continua Follow some type III bursts. Never occur in isolation.	1-3 min.	10-200 MHz.	Same as type III bursts.

SPACE WEATHER
SEC Alerts and Warnings

CATEGORY TYPE	THRESHOLD	ALERT	WARNING
Radio			
245 MHz burst	peak flux $\geq$ 100 s.f.u.	*	
245 MHz noise storm	peak flux > 5 times background	*	
10 cm burst	peak flux $\geq$ 100% above background	*	
Type II event	any	*	
Type IV event	any	*	
Particle			
Electron Event	peak flux 10^3 pfu @ > 2 MeV	*	
Suspected Proton Flare	peak flux 10 p.f.u. @ > 10 MeV	*	
P10 Proton event	peak flux 10 p.f.u. @ > 10 MeV	*	*
P100 Proton event	peak flux 100 p.f.u. @ >100 MeV	*	*
SST Radiation Alert	$\geq 0.1^{-4}$ sievert/hour ($\geq$ 10 millirems/hour)	*	*
X-ray			
M5	peak flux $\geq 5*10^{-5}$ W m^{-2}	*	
X1	peak flux $\geq 1*10^{-4}$ W m^{-2}	*	
Geomagnetic			
A Index $\geq$ 20	running $A_B \geq 20$	*	*
A Index $\geq$ 30	running $A_B \geq 30$	*	*
A Index $\geq$ 50	running $A_B \geq 50$	*	*
K Index = 4	$K_B = 4$	*	
K Index = 5	$K_B = 5$	*	
K Index $\geq$ 6	$K_B \geq 6$	*	
Atmospheric disturbance			
Stratwarm	stratospheric warming conditions	*	

- Sievert (Sv): effective (equivalent) dose of radiation received by a living organism 1 Sv = 100 rem

- particle flux unit (p.f.u.) [cm^{-2} s^{-1} sr^{-1}]

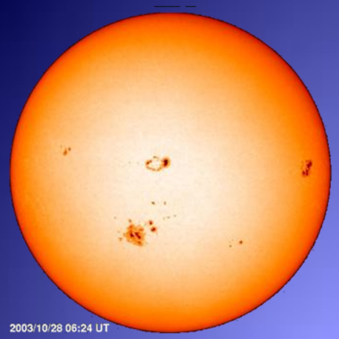

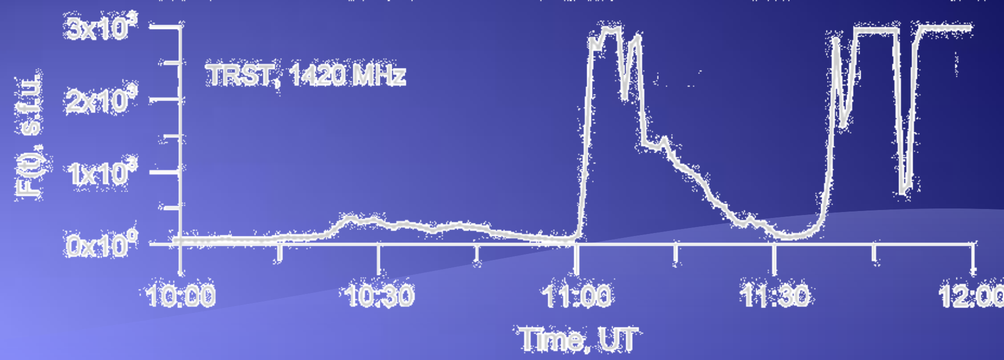

SUN-ORIGINATED RADIO FREQUENCY INTERFERENCES

M. Messerotti[1,2,3]

[1] INAF-Astronomical Observatory of Trieste, IT

[2] Department of Physics, University of Trieste, IT

[3] NATO RTO SCI-229 ET

OUTLINE OF THE TALK

- SRBs in the SSA framework
- Monitoring SRBs for Space Weather
- Effects of SRBs on Wireless Systems
- Effects of SRBs on GPS Systems
- Schematic of an operational service
- Roadmap to the development
- Conclusions

CHARACTERISATION OF THE SPACE ENVIRONMENT

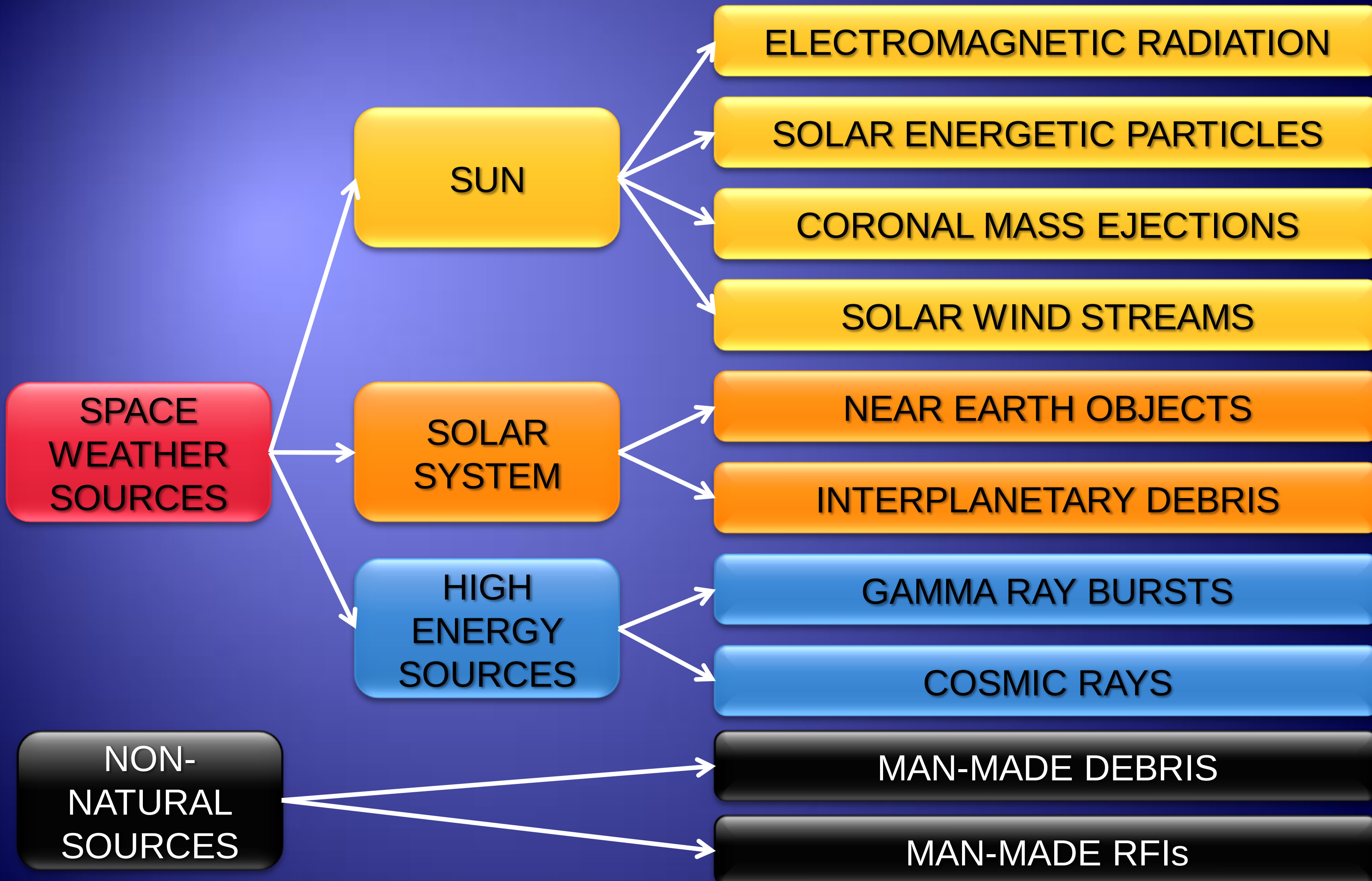

NATO Wide Information Exchange Scenario

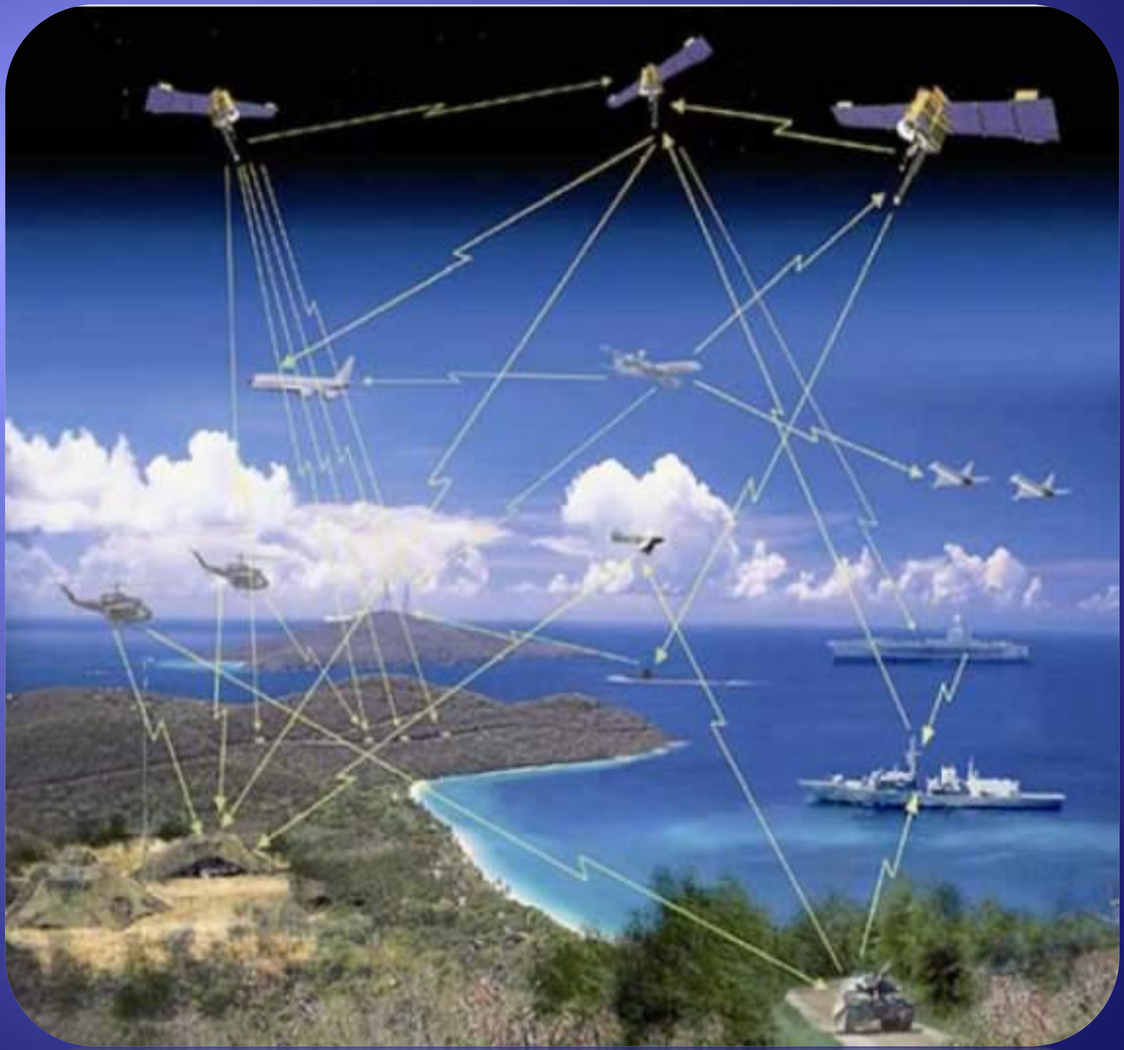

From
NATO RTO
Pamphlet

Global Satcom Outage Regions

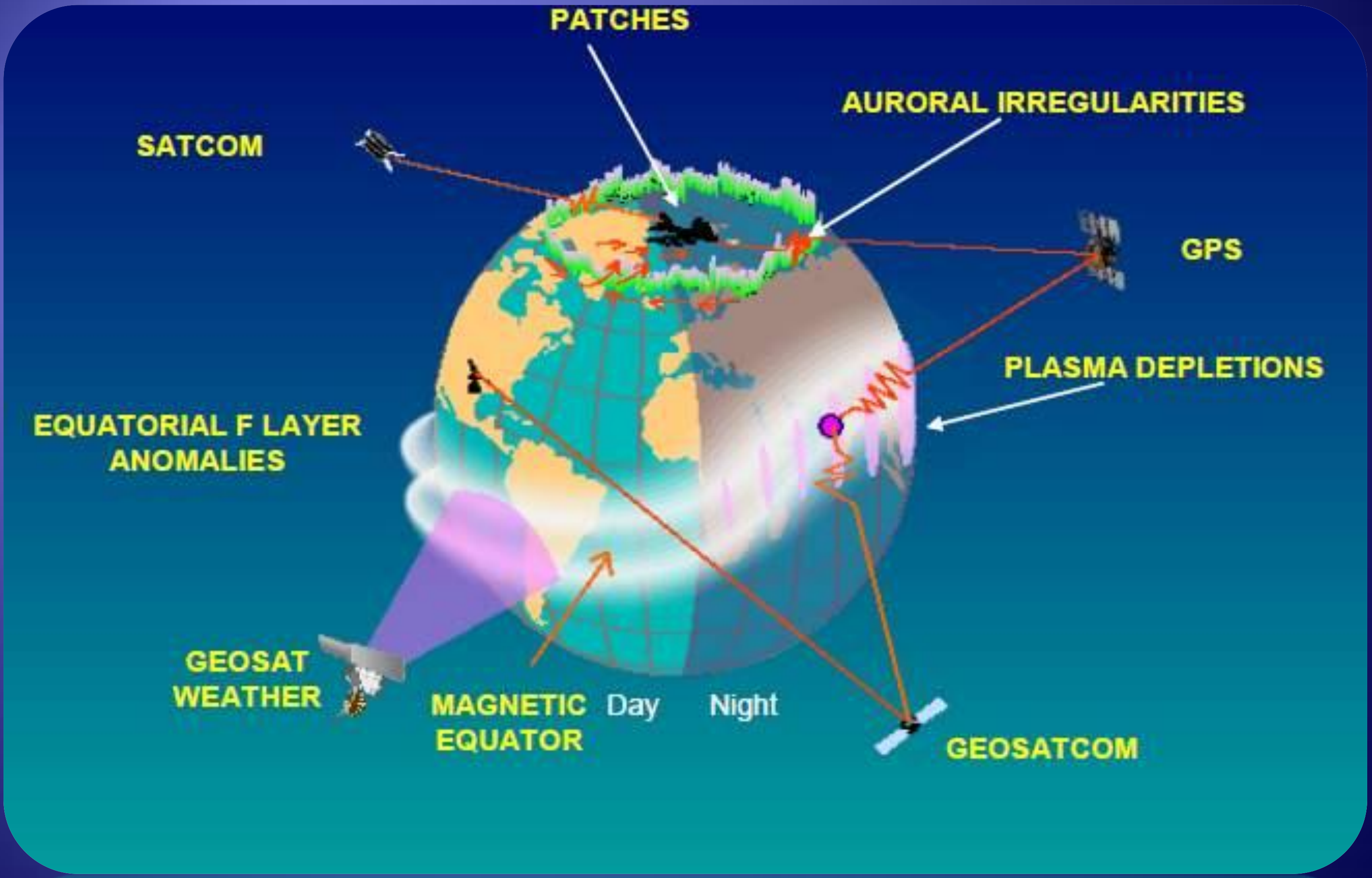

Courtesy H.C. Carlson

SSA Information Integrated into a Single Integrated Space Picture

(Hand & France, 2008)

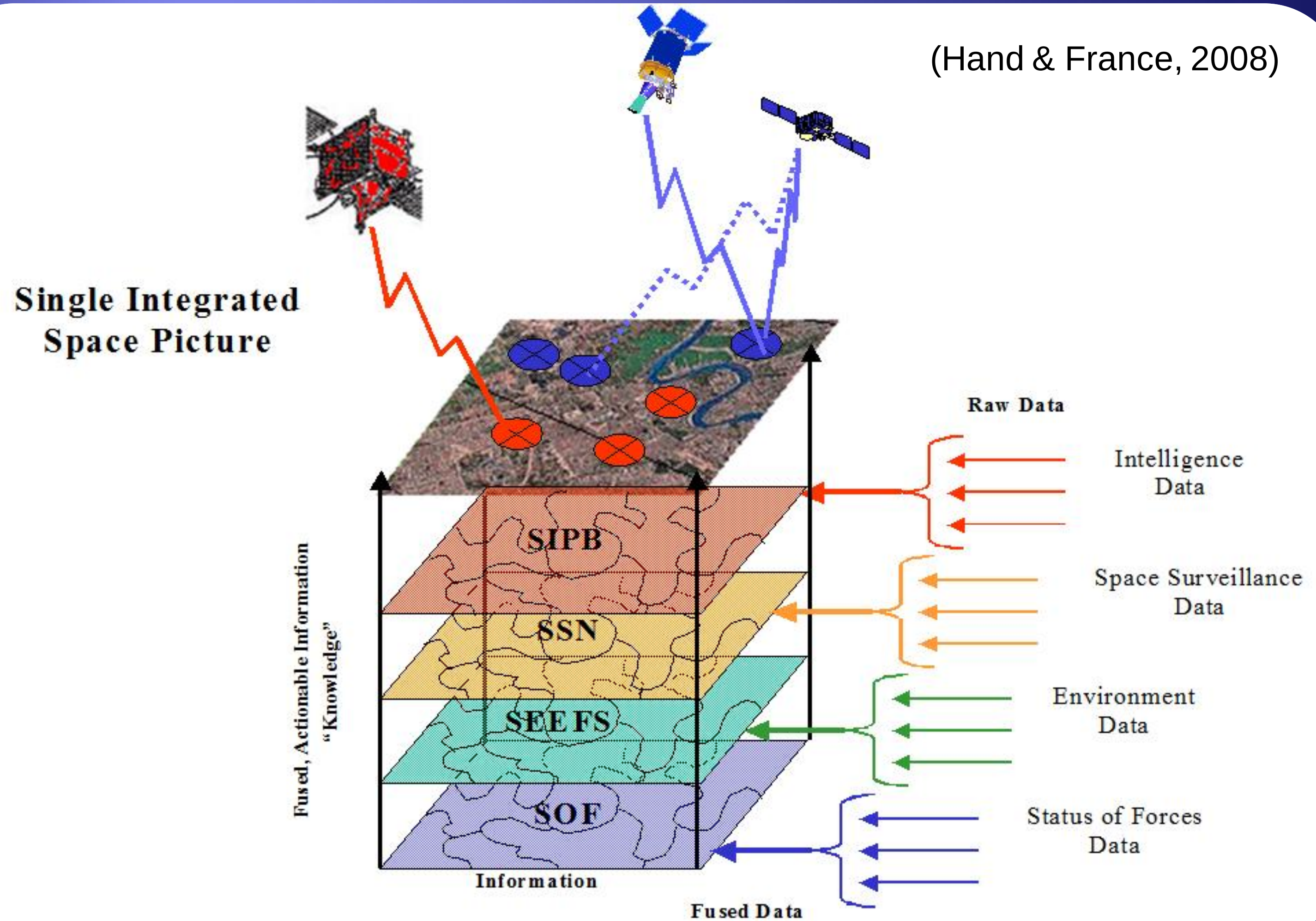

DIVERSITY OF RISK ASSESSMENT

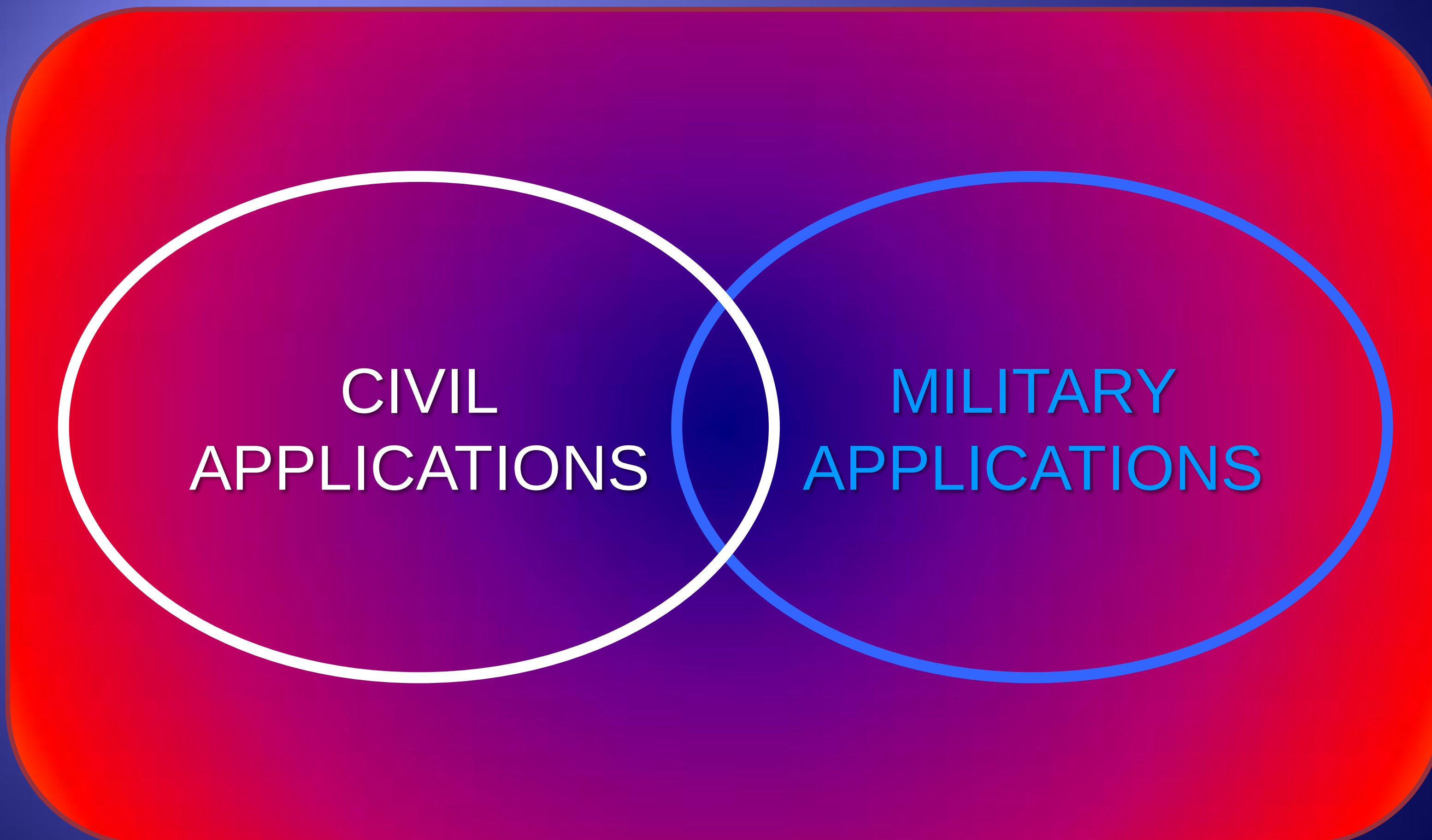

The Sun as a Radio Noise Source

- The Sun is a radio source
  - non-directional
  - broad band
- Solar radio noise can
  - increase by several orders of magnitude during outbursts
  - persist at high levels for minutes to hours
- Enhanced solar radio noise can perturb
  - HF communications
  - Mobile communications
  - Global Navigation Satellite Systems (GPS, GNSS)
  - Radars
  - WAAS
  - SATCOM

→ **DIRECT GEOEFFECT**

Systems Affected by Solar RFI

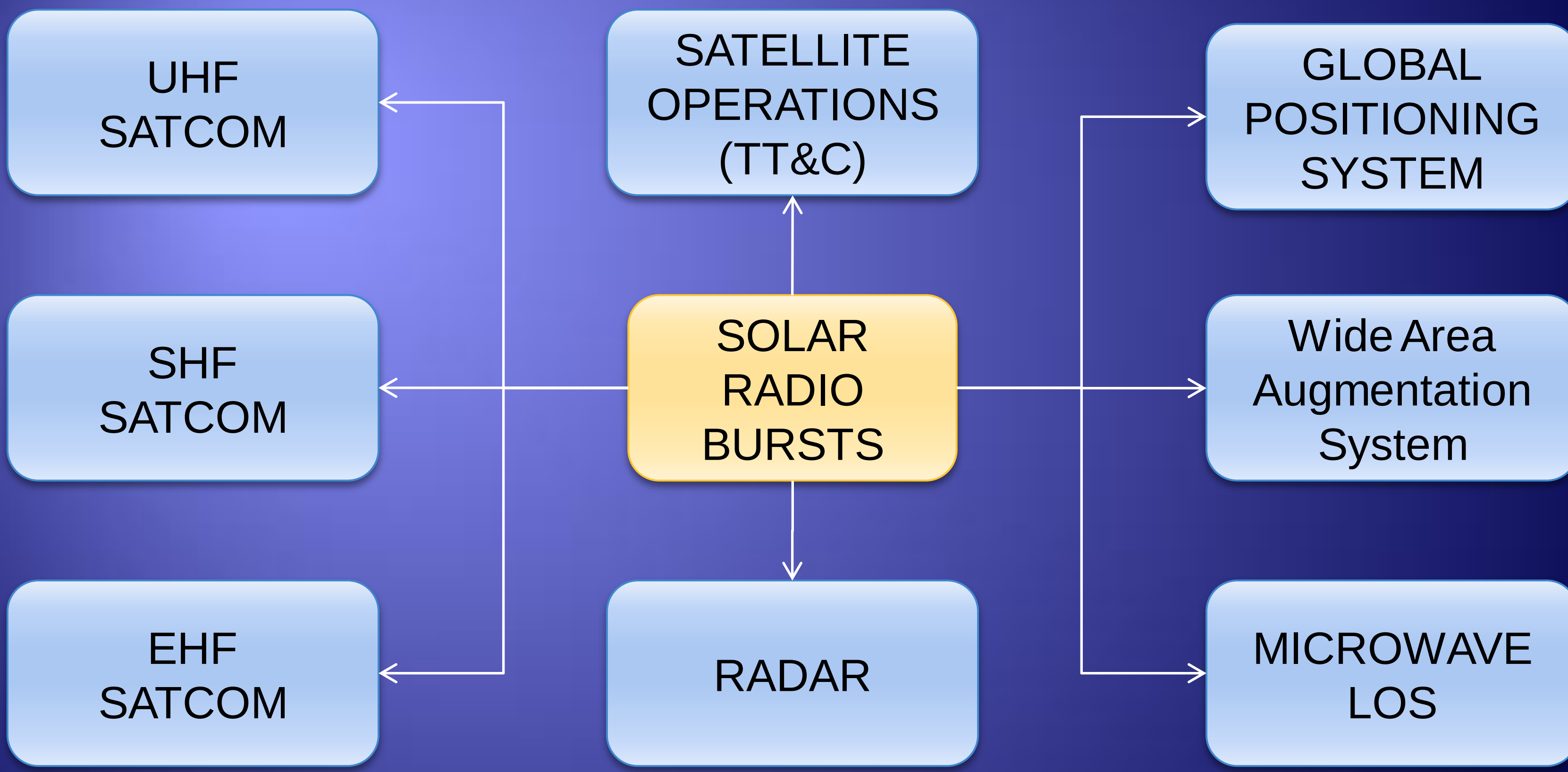

Ref. Chairman of the Joint Chief of Staff CJCSM 3320.02B (2008)

SSA Environmental Effects Fusion System (SEEFS) for Solar RFIs

UNCLASSIFIED

Solar Radio Burst Effects Receiver View - Mock-A Network: SATCOM-MOCK-A	Valid Time Mon Aug 30 14:17:25 2004Z	Data Age N/A	NOWCAST WATCH

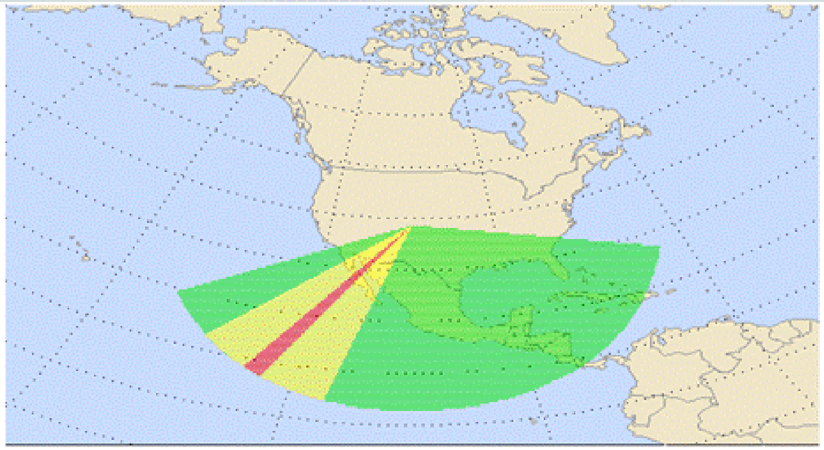

SCOPE VIEW RECEIVER VIEW

Solar Burst RFI Vulnerability Time:

30/1358 to 30/1410Z ENDED

Site Location:
Lat: 38.83
Lon: -104.82

Operating Frequency	Causative Lobe	Potential Solar RFI |SNR|	Vulnerability Dimensions: Azimuth	Elevation	Range
20000 MHz	Main	14.0	213.6 to 218.6	53.4 to 58.4	NA
	Side 1	11.0	198.1 to 232.1	37.9 to 71.9	NA
	Side 2	LTT	NA	NA	NA
	Rear	LTT	NA	NA	NA
500 MHz	Main	31.0	213.6 to 218.6	53.4 to 58.4	NA
	Side 1	LTT	NA	NA	NA
	Side 2	LTT	NA	NA	NA
	Rear	LTT	NA	NA	NA

Potential Solar RFI Levels
- Severe
- Moderate
- None
- MISG
- LTT = |SNR| Less than threshold

GLOBAL VIEW | TEXT SUMMARY | SOLAR DATA | FEEDBACK FORM | STATUS MATRIX | Last 5 Runs = 30/1406 30/1405 30/1404 29/2349 29/2249

UNCLASSIFIED

ARCHIVE | Product Generation Time: Mon Aug 30 14:17:25 2004 | Update Interval: 1800 min or less | HELP

(Hand & France, 2008)

USAF
RSTN Radio Solar Telescope Network

- 4 Stations
  (Trieste, IT; 1969-1972)
- Radio Interference Measurement Set (RIMS) [8 frequencies]
- Solar Radio Spectrograph (SRS)

Monitoring SRBs for Space Weather

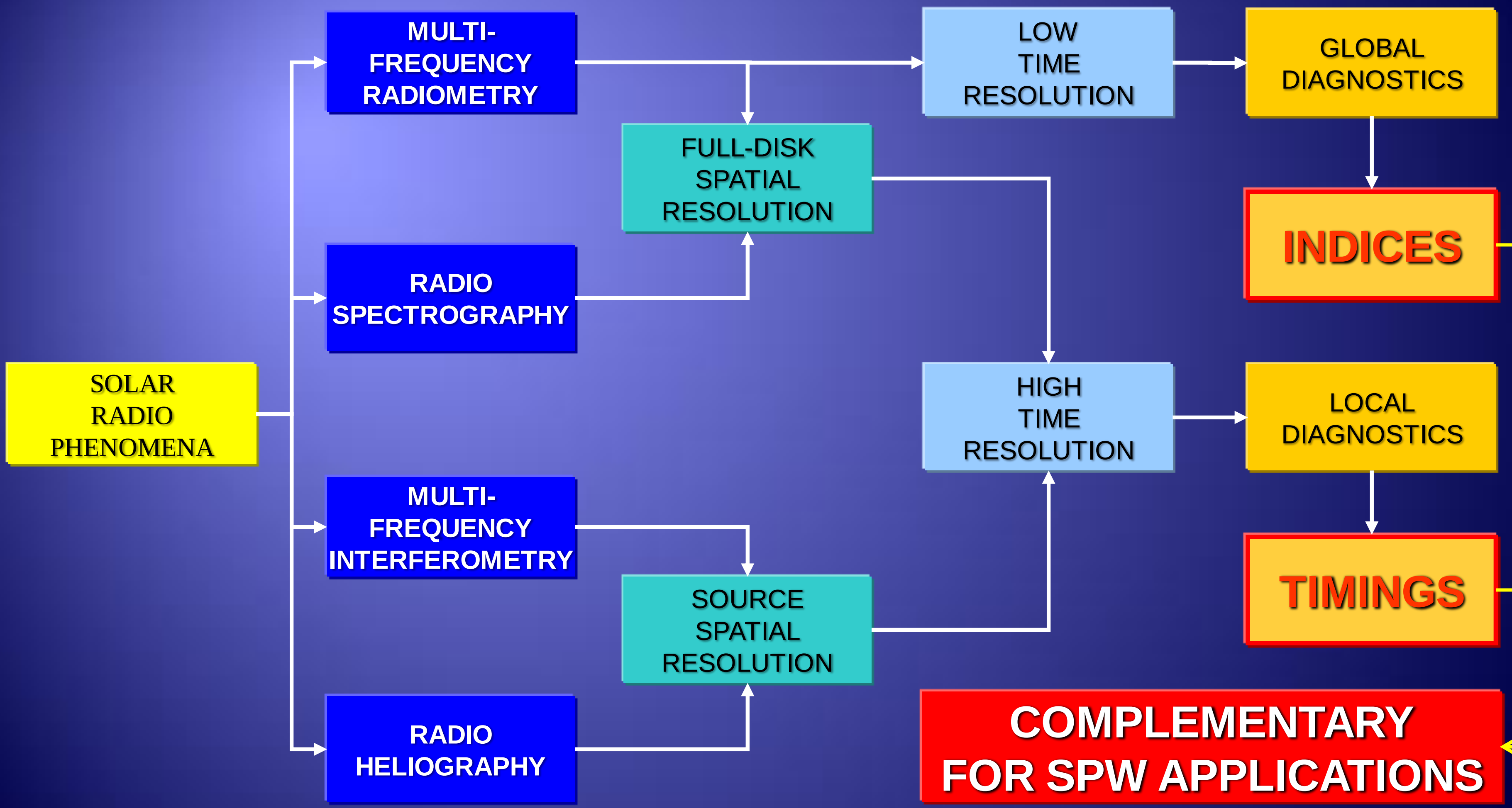

Effects of SRBs on Wireless Systems

- Bala et al. (2002):
  - For a cellular base station operating at 900 MHz , the equivalent solar flux (thermal noise=solar noise level) $F_{eq} \sim 960$ SFU $\rightarrow$ more than twice the thermal noise power.
  - For a base station operating at 2.4 GHz, $F_{eq} \sim 6{,}000$ SFU.
  - The bit error rate (ber) changes rapidly with the S/N power ratio. (0.75 dB change $\rightarrow$ 10x in ber).
  - Assuming an SRB effectivity threshold of 1,000 SFU, the statistics over 4 decades indicates a probability of interference every 10-20 days on average per year, modulated by the solar cycle.
- Lanzerotti et al. (2002); Nita et al. (2004)

Effects of SRBs on GPS Systems

- Cerruti et al. (2006):
  - **Observed** reduced carrier-to-noise ratio in sunlit GPS receivers over the duration of SRB (8,700 SFU RHCP $\rightarrow$ 2.3 dB loss; 2005.09.07)
  - Estimated L1 C/N_0 fade of 3 dB and L2 C/N_0 fade of 5.2 dB for commonly used GPS antennas with a gain of 4 dBic, from a SRB of 10,000 SFU
  - SRB are a potential threat to life-critical systems based on a Global Navigation Satellite System (GNSS): a 80,000 SFU SRB can determine a 12 dB fade at L1 and a 26.2 dB fade on the L2 channel $\rightarrow$ loss of lock in semi-codeless receivers.
- Possibly 4,000-12,000 SFU Chen et al. (2005)

Powerful solar radio bursts as a global and free tool for testing satellite broadband radio systems, including GPS–GLONASS–GALILEO (Afraimovich et al., JASTP 70, 1985, 2008)

- Investigated failures in the global positioning system (GPS) performance produced by solar radio bursts with unprecedented radio flux density during the X6.5 and X3.4 solar flares on 6 and 13 December 2006, respectively
- Significant experimental evidence was found that high-precision GPS positioning on the Earth's entire sunlit side was partially disrupted for more than 10–15min on 6 and 13 December 2006

GPS Failures on 28 October 2003

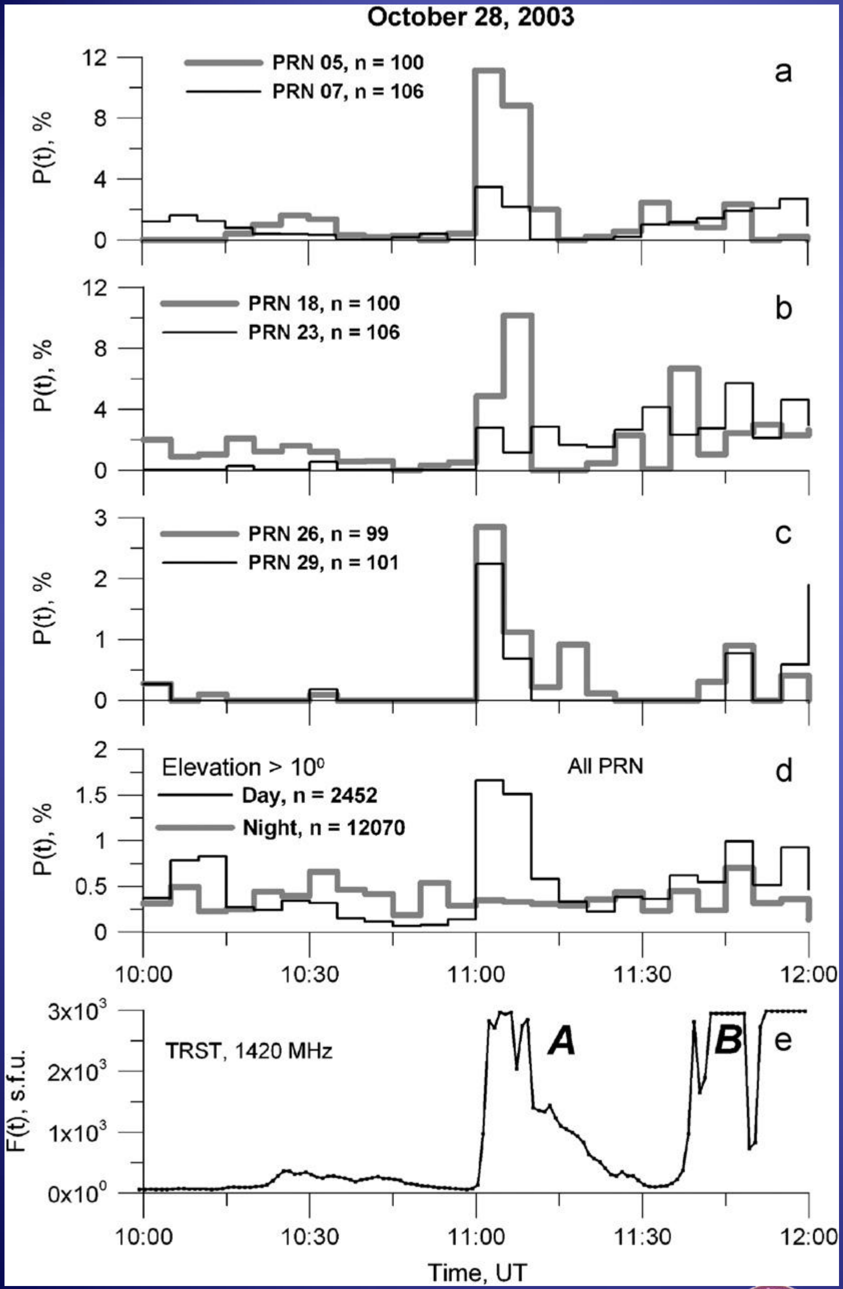

GPS phase slips during the solar flare on 28 October 2003 in the sunlit hemisphere. The relative density P(t) of L1–L2 phase slips for all (d) and individual GPS satellites (a), (b), and (c). The flux F(t) of RHCP radio emission (1420 M Hz) registered by the Trieste Solar Radio Spectrograph (e).

(Afraimovich et al., 2008)

Solar Radio Burst Impact on GPS on 6 Dec. 2006 (Courtesy of B. Murtagh, NOAA/SWPC)

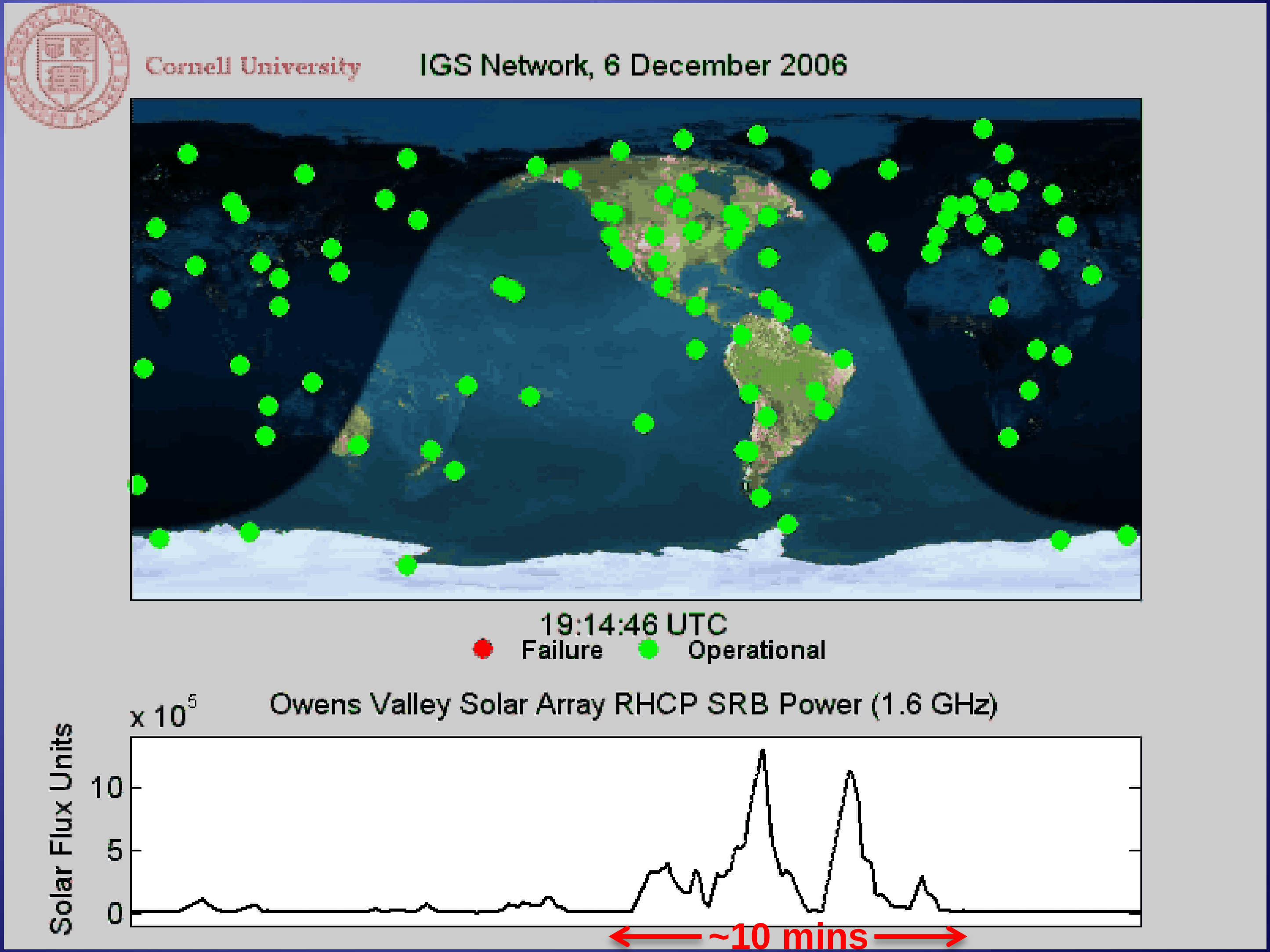

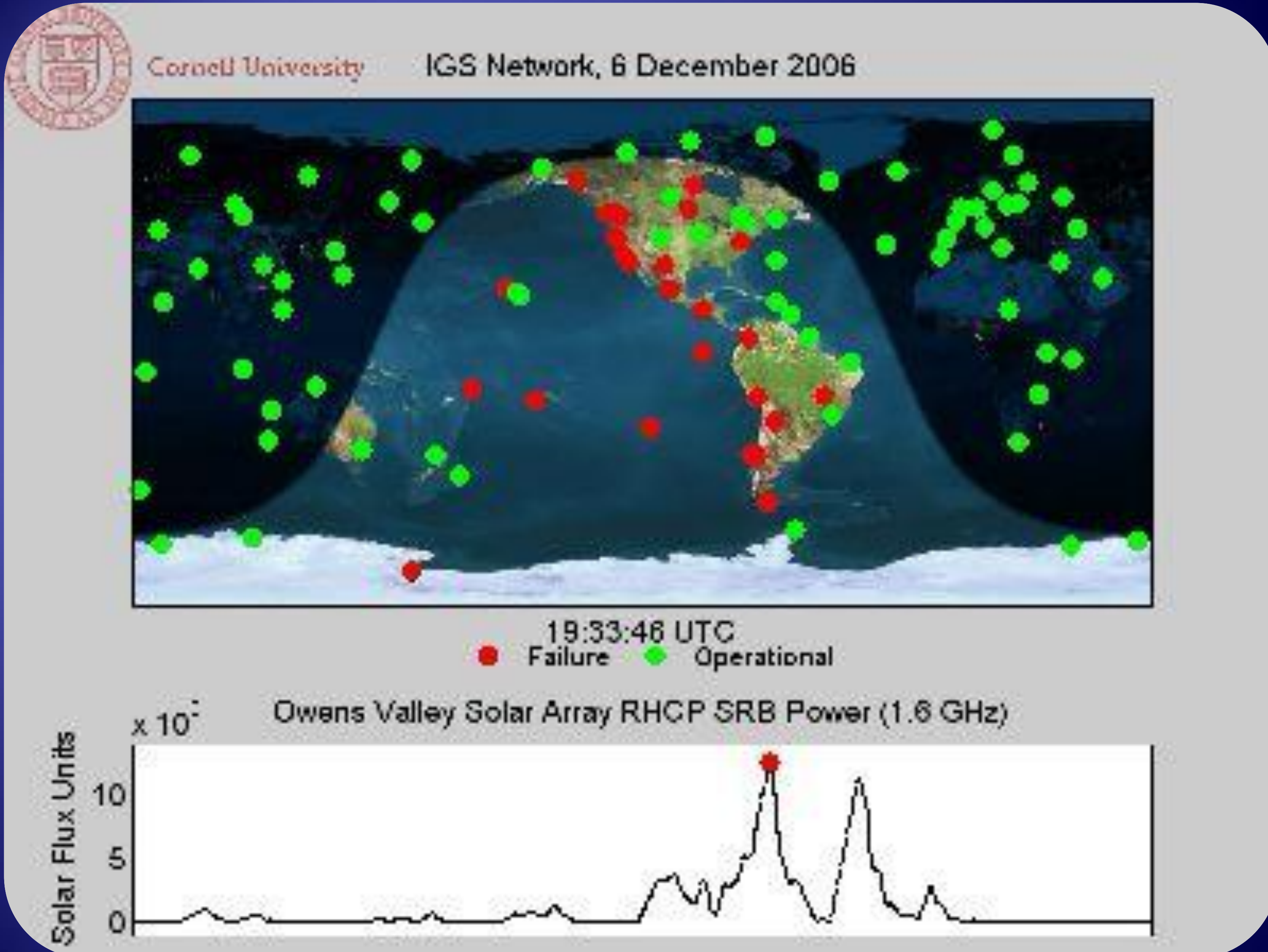
Cornell University
IGS Network, 6 December 2006
19:33:46 UTC
Failure
Operational
Owens Valley Solar Array RHCP SRB Power (1.6 GHz)
x 10
Solar Flux Units
10
5
0

Effects of SRBs on 5-6 December 2006

- P. Kintner (Cornell University):
  - Large number of receivers stopped tracking GPS signal over the entire sunlit side of the Earth
  - First quantitative measurement of the effect

- P. Doherty (Boston College):
  - The 6 Dec SRB was <u>the first one ever detected on the civil air navigation system</u> (WAAS, Wide Area Augmentation System)

[see Cerruti et al., 2006]

Source: GPS Daily (http://www.gpsdaily.com)

WAAS Affected by Ionospheric Storm on 29 and 30 Oct. 2003: Acceptable Limits Exceeded by 15- and 11-hour Periods (Courtesy B. Murtagh, NOAA/SWPC)

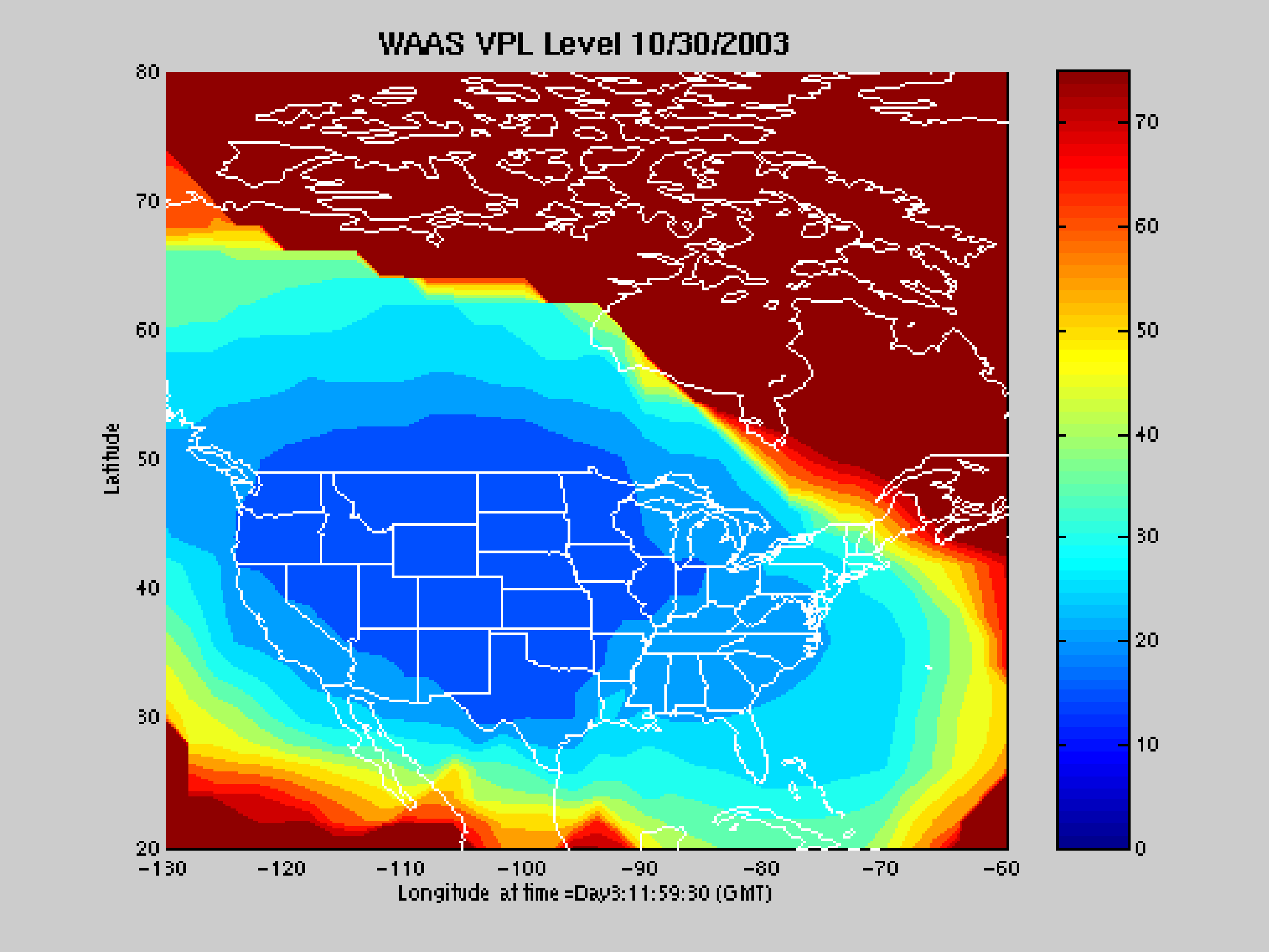

PEAK INTERFERENCE ON WAAS

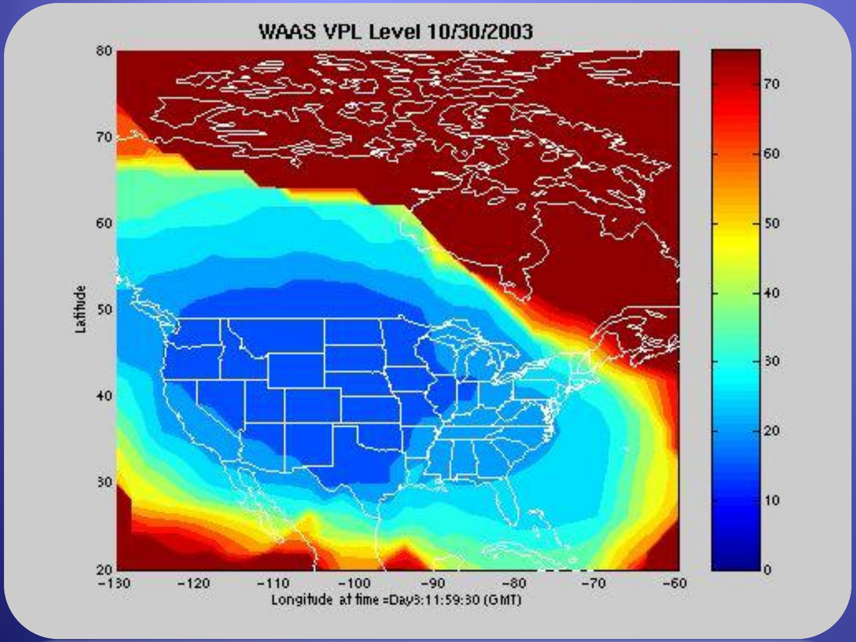

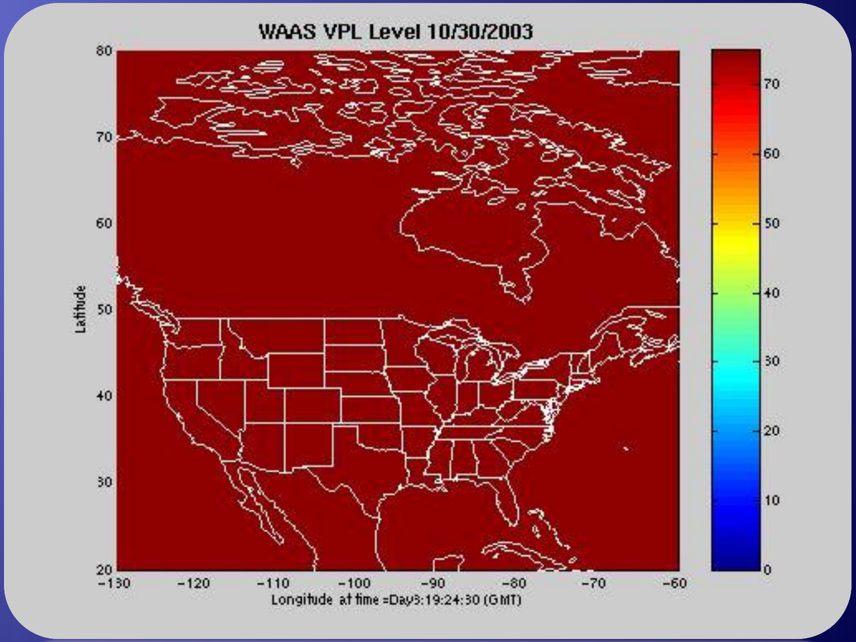

The Trieste Solar Radio System (TSRS) Data Products for SpW

Multichannel Synoptic Graph

- - 1 s downsampled data
- - updated every 10 minutes

Solar Radio Indices Graphs

- - 1-min-average values
- - 1-min-max values
- - 1-min-ahead forecast
- - updated every 10 minutes

Solar Radio Indices Files

- - ASCII
- - Binary
- - FITS

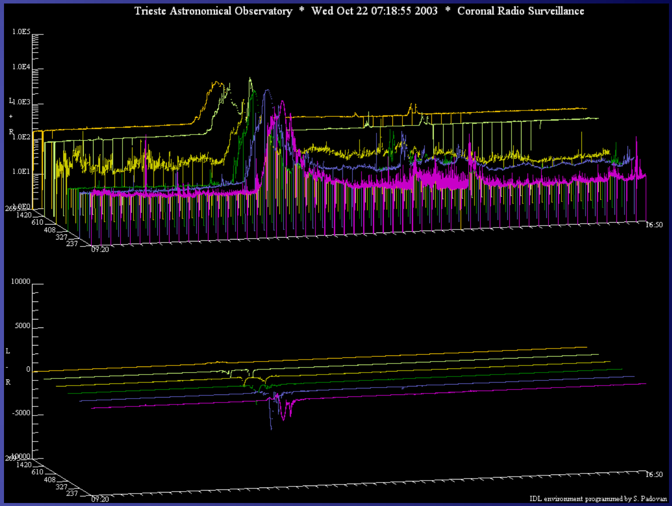

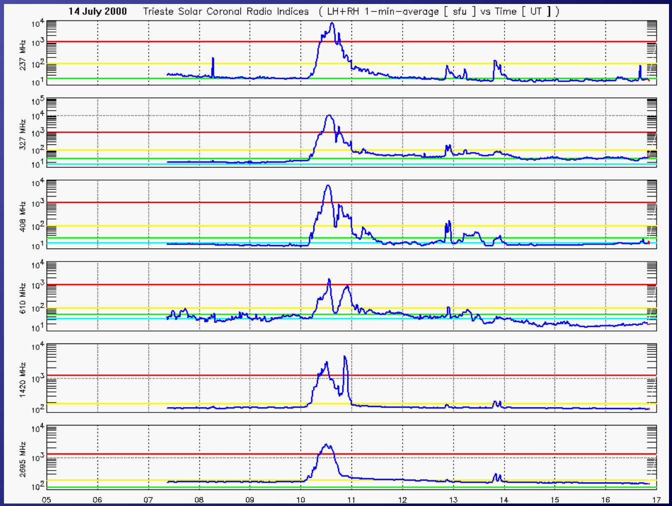

TSRS Data Products for SWENET

- 1-min-average and 1-min-max radio indices
- 237, 327, 408, 610, 1420, 2695 MHz
- FLUX DENSITY & CIRCULAR POLARIZATION
- [W / m^2 / Hz] & [dBm / Hz]
- Observed and 1-min-ahead Predicted Values
- Single polarization channels & sum of channels

GOES SXR Lightcurve 2006.12.05

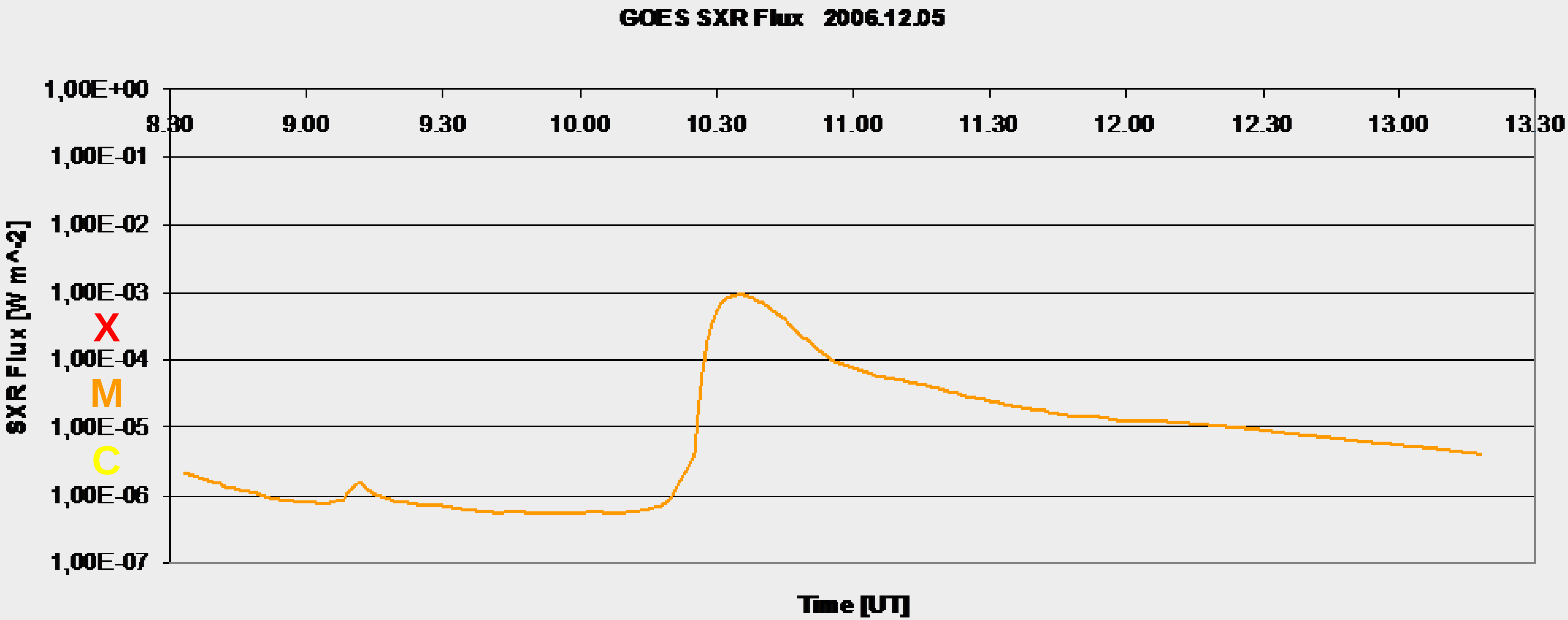

Date	Time Start	Time Max	Time End	AR	Latitude	Longitude	SXR Class	OPT Class
05/12/2006	10.18.00	10.35.00	10.45.00	10930	-7	-79	X9.0	2n

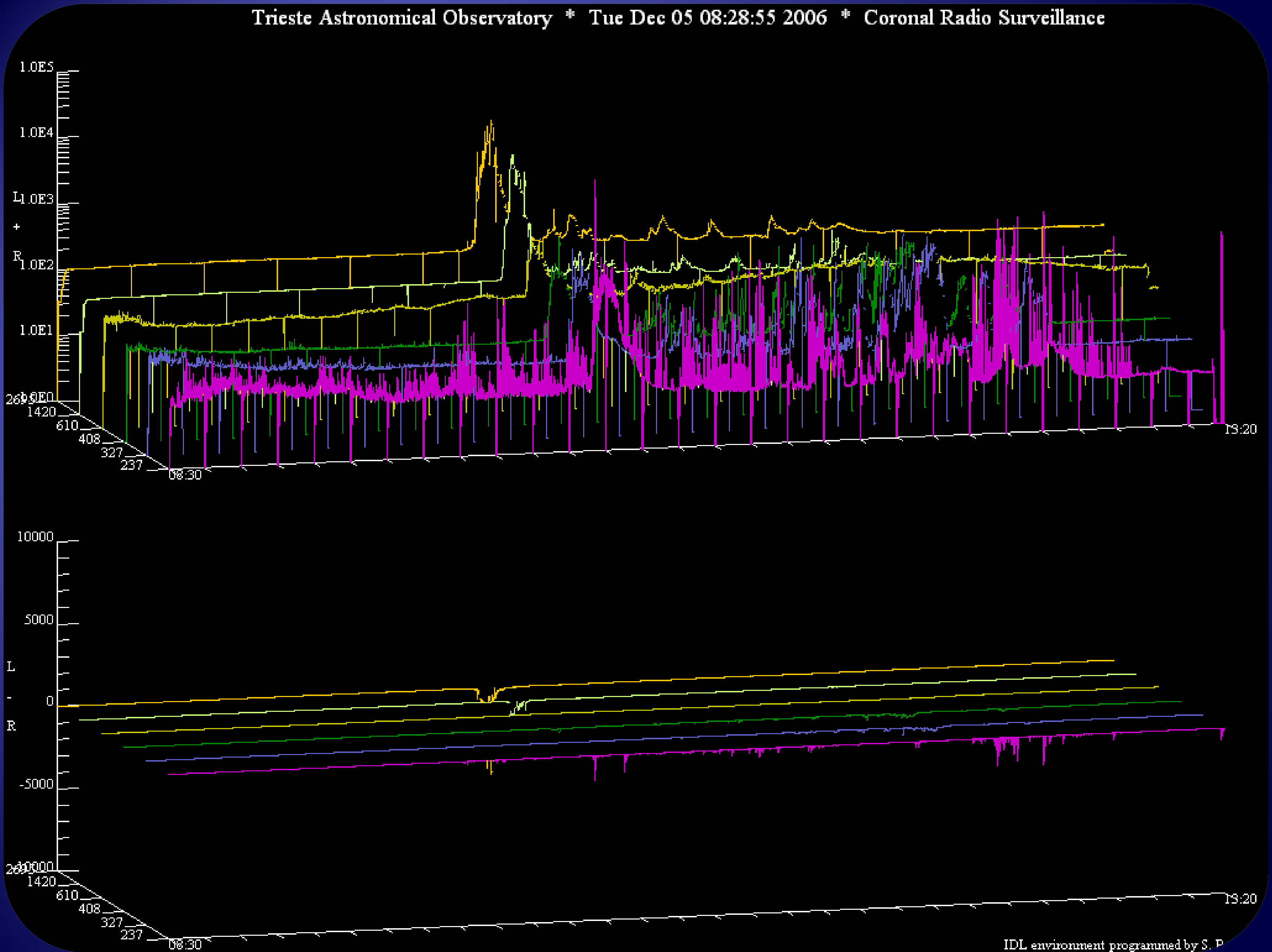
Trieste Astronomical Observatory * Tue Dec 05 08:28:55 2006 * Coronal Radio Surveillance
1.0E5
1.0E4
L 1.0E3
+
R 1.0E2
1.0E1
1.0E0
2695
1420
610
408
327
237
08:30
13:20
10000
5000
L
0
-
R
-5000
-10000
IDL environment programmed by S. P

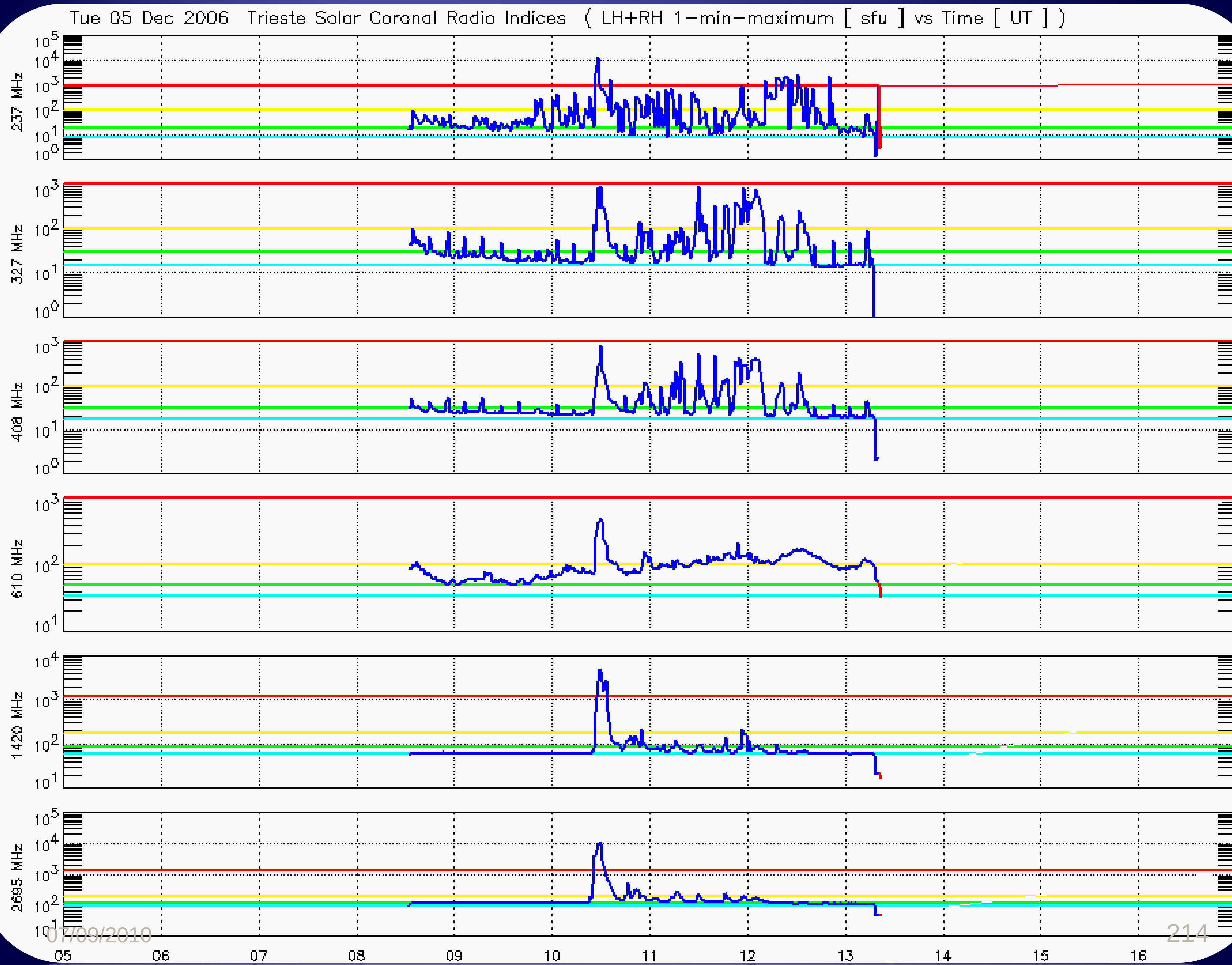
Tue 05 Dec 2006 Trieste Solar Coronal Radio Indices (LH+RH 1-min-maximum [sfu] vs Time [UT])
237 MHz
327 MHz
408 MHz
610 MHz
1420 MHz
2695 MHz
05
06
07
08
09
10
11
12
13
14
15
16

TSRS 1420 MHz
1-min Radio Index

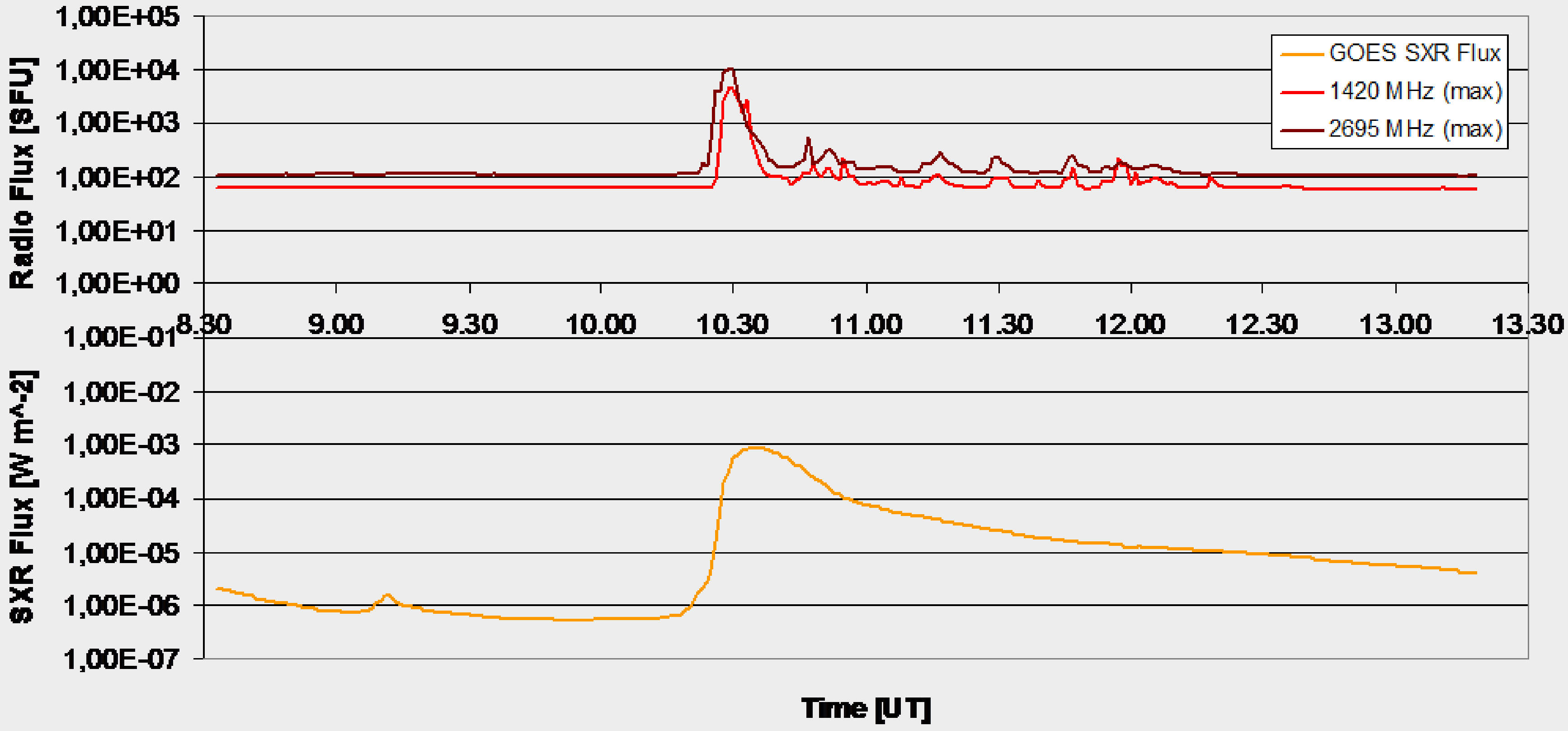

TSRS observed maximum radio flux density significantly exceed reported levels:

$S2695_{max}$ = 10,391 SFU $S1420_{max}$ = 4,870 SFU

TSRS 1420 and 2695 MHz CP Graph

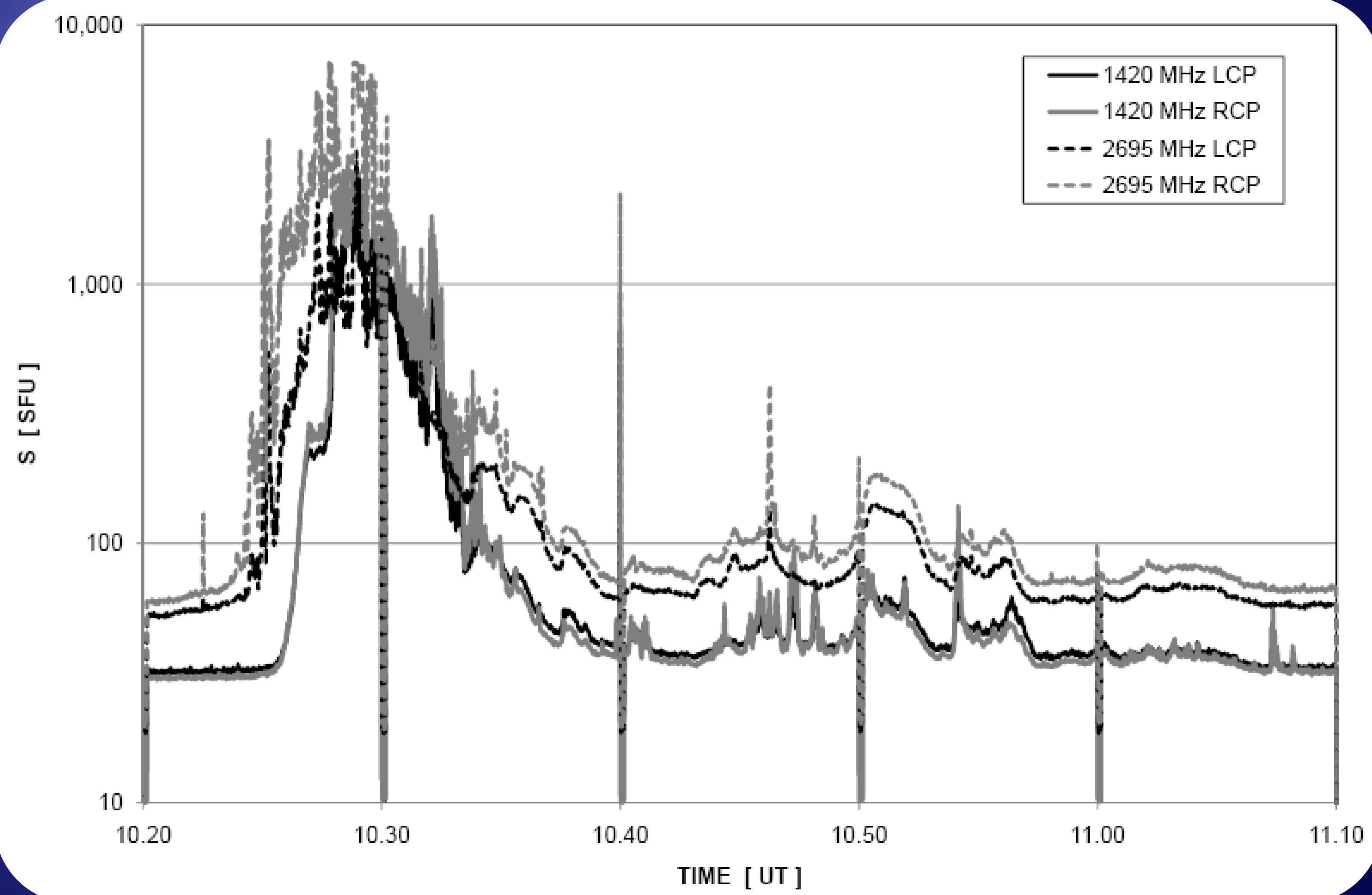

Timing of SRB with respect to SXR

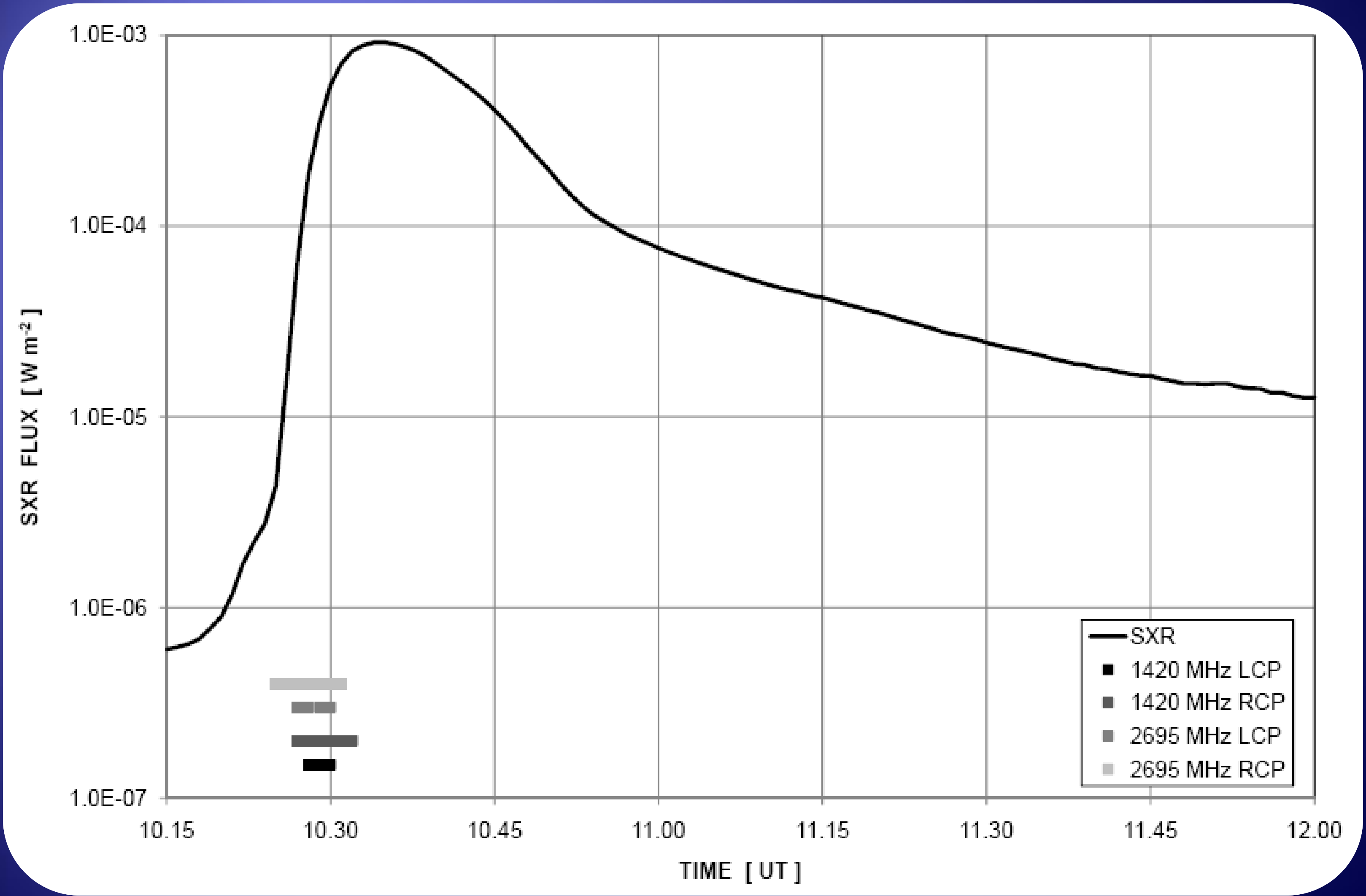

Sampling Time is a Key Issue

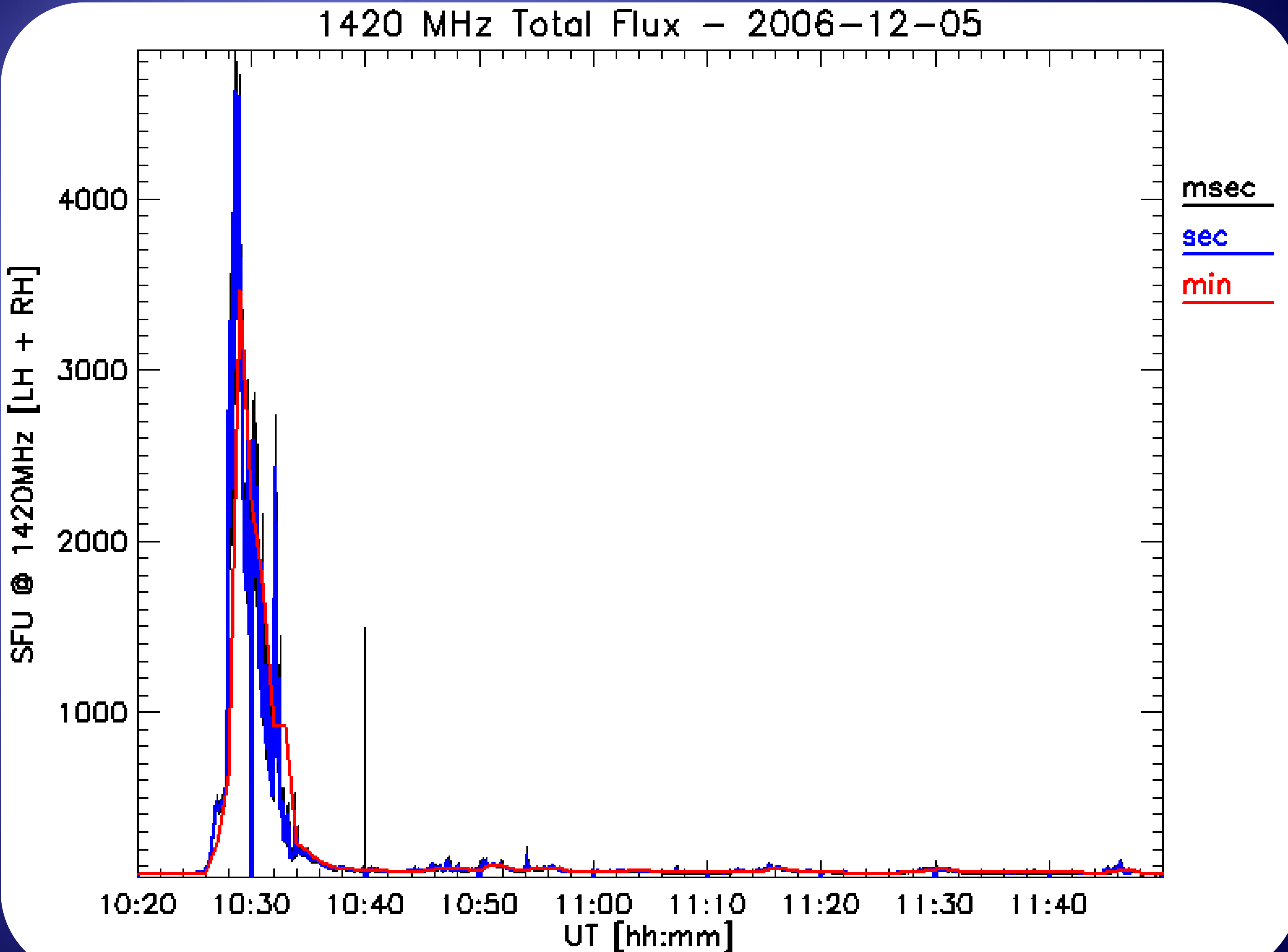

IDEAL SCHEME OF AN OPERATIONAL SERVICE FOR SRB MONITORING AND PREDICTION

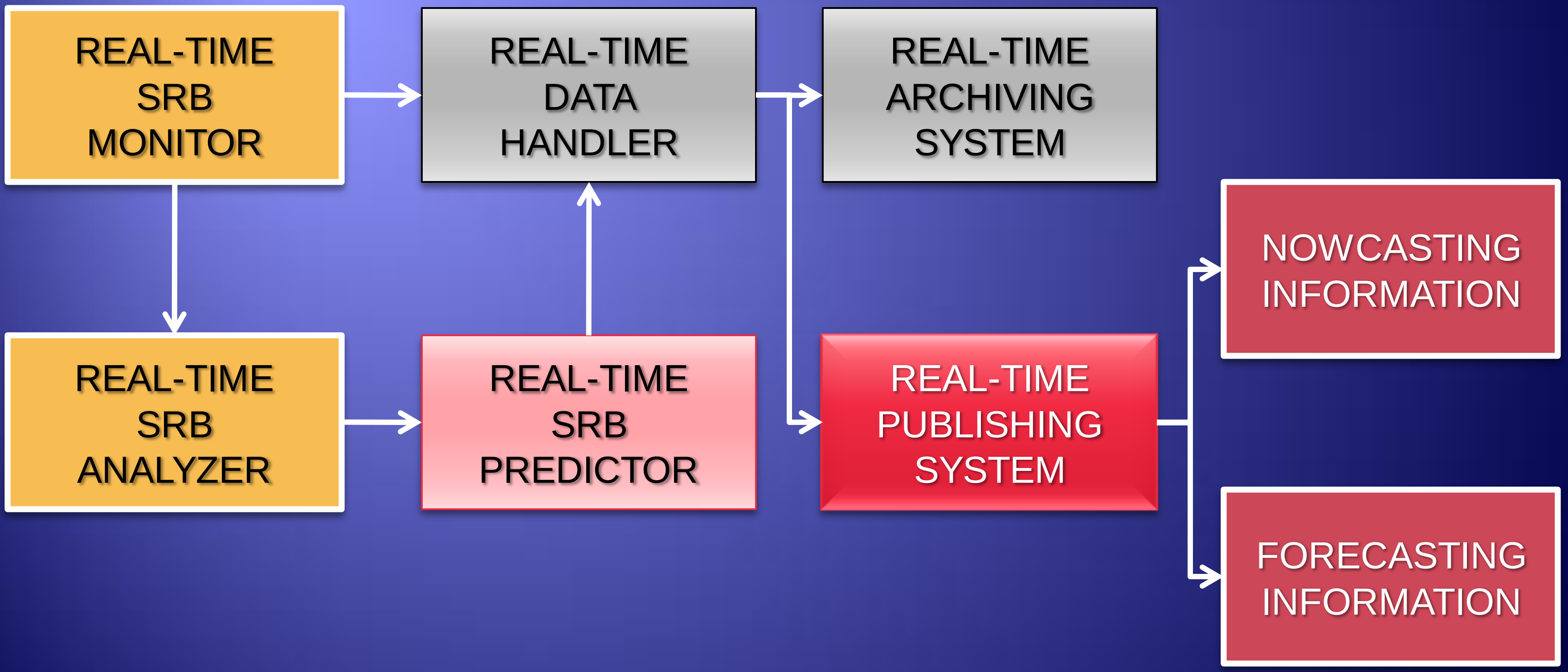

ROADMAP TO THE DEVELOPMENT

- Post-event analysis of a comprehensive set of SRB-GPS events to define geoeffective SRBs peculiar characteristics (time evolution of intensity and intensity thresholds for geoeffectivity)
- Development of a SRB analyzer capable of fully characterizing SRBs via a parameterization based on geoeffectivity features derived from post-event analysis
- Development of a SRB predictor system

CONCLUSIONS 1

- The interfering capability of SRBs for SATCOM, GPSs and WAAS is a matter of fact, and **it is of great relevance to NATO operations**

- **High time resolution** and **polarisation** information are key features in nowcasting to evaluate the geoeffectiveness of the phenomena

- An **extensive post-event analysis** is needed to assess the impact levels (TSRS catalogue 2000-2009, in preparation)

CONCLUSIONS 2

- SRB effects can be a **signifcant risk** for civil radio-based systems and can play a **mission-critical role** in military applications (→ Carrington event!)

- There is **no specific mention in ESA SSA**

- **US STRATCOM properly addresses it in SSA**

- **It has to be properly considered in NATO SSA**

DIRECT EFFECTS OF SOLAR RADIO WEATHER

OVERALL CONCLUSIONS

CONCLUSIONS

- SOLAR-ORIGINATE RADIO FREQUENCY INTERFERENCES CAN ACHIEVE VERY HIGH LEVELS ON A SPORADIC BASIS
- TO DATE, THEY ARE UNPREDICTABLE
- MOBILE COMMUNICATIONS ARE AFFECTED WITH A CERTAIN LEVEL OF SEVERITY DEPENDENT ON THE PHASE OF THE SOLAR ACTIVITY CYCLE
- GPS AND GNSS CAN BE SIGNIFICANTLY AFFECTED. THE IMPORTANCE OF THE IMPACT IS DEPENDENT ON THE OPERATIONAL FRAMEWORK, AS L.O.L. FOR TENS OF MINUTES CAN BE MISSION CRITICAL
- NO EFFECTIVE MITIGATION TECHNIQUES FOR THE MOST SIGNIFICANT EVENTS EXIST TO DATE

References (and Ref.'s therein)

Messerotti, M., Observing, modeling and predicting the effects of solar radio bursts on radio communications, AIP Conf. Proc. 1043, 277-283 (2008)

Messerotti, M., TSRS as a Solar Radio Noise Monitor for Communication and Navigation Systems, Earth, Moon and Planets 104, 1-4, 51-54 (2009)

Messerotti, M., et al., Solar Weather Event Modelling and Prediction, Space Sci. Rev. 147, 3-4, 121-185 (2009)

THANK YOU
FOR YOUR ATTENTION